CONF-800242--

MASTER

PROCEEDINGS OF THE GEOTHERMAL RESERVOIR WELL STIMULATION SYMPOSIUM

San Francisco, California
February 7, 1980

DISCLAIMER

PROCEEDINGS OF THE GEOTHERMAL RESERVOIR WELL STIMULATION SYMPOSIUM

February 7, 1980

UNITED STATES DEPARTMENT OF ENERGY

Conducted under Contract
No. DE-AC32-79AL01563

with Republic Geothermal, Inc.

PROCEEDINGS

GEOTHERMAL RESERVOIR WELL STIMULATION SYMPOSIUM

Edited by

Henry B. Crichlow
Petroleum Training and
Technical Services

Sponsored by

United States Department
of Energy

Conducted under Contract
No. DE-AC32-79AL01563

with Republic Geothermal, Inc.

FEBRUARY 7, 1980

CONTENTS

PREFACE vii

SYMPOSIUM ORGANIZATION
SYMPOSIUM COMMITTEE ROSTER viii
SESSION COMMITTEES ix

SESSION ONE
OPENING REMARKS
Robert Hanold 1

CONTRACT STATUS REPORT
Donald Campbell 5

HIGH TEMPERATURE PROPPANTS AND FLUIDS
Richard Sinclair 23

SESSION TWO
PROPPANTS AND PROPPANT TRANSPORT
Ali Daneshy 41

FRACTURE DESIGN MODELLING
Henry Crichlow 50

MATHEMATICAL TREATMENT OF TRACER BEHAVIOR IN A FRACTURE
Ottomar Vetter 109

SESSION THREE
ACTIVE AND PASSIVE SEISMIC TECHNIQUES IN MAPPING FRACTURES
James Albright 110

STIMULATION CASE HISTORIES:
(I) RAFT RIVER: MECHANICAL DESIGN AND OPERATIONS
(II) RAFT RIVER EVALUATION
(III) EAST MESA STIMULATION
Charles Morris 111
Robert Nicholson 155
Robert Verity 140
Scott Keys 175

SESSION FOUR

THERMAL STABILITY OF FRAC FLUIDS IN AQUEOUS SYSTEMS
Donald Tyssee 203

MASSIVE HYDRAULIC FRACTURING
Ralph Veatch 214

EXPLOSIVE STIMULATION OF A GEOTHERMAL WELL AT THE GEYSERS
Robert Hanold 215

SYMPOSIUM PARTICIPANTS 222

PREFACE

The Geothermal Reservoir Well Stimulation Symposium is now history. The international gathering held on February 7, 1980, brought together experts from all over the world to discuss their views on the subject of geothermal reservoir well stimulation.

On behalf of the conference attendees, we would like to thank all those who participated, organized, and offered their services, both in the developmental stage and in finalizing this effort.

The authors are to be commended for their presentations, and the attendees for their participation in the discussions. Finally, we wish to thank the United States Department of Energy; the prime contractor - Republic Geothermal, Inc.; and the subcontractors - Maurer Engineering, Inc.; Petroleum Training and Technical Services; Vetter Research; and MAPCO, Inc. for helping to make this possible.

SYMPOSIUM ORGANIZATION

SYMPOSIUM COMMITTEE ROSTER

COORDINATOR
Thomas Strickland
Republic Geothermal, Inc.
Santa Fe Springs, California

COORDINATOR
Henry Crichlow
Petroleum Training and Technical Services
Norman, Oklahoma

COORDINATOR
Donna Vanderburg
Petroleum Training and Technical Services
Norman, Oklahoma

SESSION COMMITTEES

SESSION ONE:
Henry Crichlow, Petroleum Training and Technical Services
Donald Tyssee, Vetter Research

SESSION TWO:
Donald Campbell, Republic Geothermal, Inc.
Thomas Strickland, Republic Geothermal, Inc.

SESSION THREE:
Robert Emslie, AMINOIL, USA
Stephen Pye, Union Oil company

SESSION FOUR:
Viv Kandarpa, Vetter Research
Robert Hanold, Los Alamos Scientific Laboratory

SESSION ONE

OPENING REMARKS
Robert Hanold
LOS ALAMOS SCIENTIFIC LABORATORY

CONTRACT STATUS REPORT
Donald Campbell
REPUBLIC GEOTHERMAL, INC.

HIGH TEMPERATURE PROPPANTS AND FLUIDS
Richard Sinclair
MAURER ENGINEERING, INC.

GEOTHERMAL WELL STIMULATION PROGRAM - - OPENING REMARKS

R. J. Hanold
Los Alamos Scientific Laboratory
Los Alamos, New Mexico

For over thirty years, well stimulation techniques of one form or another have been employed to enhance production from marginal or submarginal oil and gas wells. The formal introduction of well stimulation as a pseudo-science can probably best be tied to the introduction of hydraulic fracturing as an effective method for providing better communication between the producing reservoir horizon and the wellbore. Prior to this, independent operators were sometimes known to drop sticks of dynamite into unproductive wells initiating the era of "homegrown" stimulation techniques. What they lacked in sophistication, they sometimes made up for in increased production as these attempts were apparently more than casually successful.

Technical developments during the last decade on the application of well stimulation methods to oil and gas wells have been particularly significant. During this same time interval, the number of available geothermal wells that could benefit from effective stimulation treatments has become quite large. In response to this situation, the Department of Energy/Division of Geothermal Energy (DOE/DGE) elected to fund an extensive program in geothermal well stimulation technology. The basis for the program was the hardware, experience, and technology developed from the stimulation of hydrocarbon wells. The objective was clear - - extend this hardware and technology to the very specific requirements associated with the stimulation of geothermal wells.

The stimulation of geothermal wells presents some new and challenging problems in addition to the ones currently being faced in oil and gas well stimulation treatments. Formation temperatures will be in the 150-300C range and the behavior of frac fluids and proppants at these temperatues in a hostile brine environment will have to be carefully evaluated before

performance expectations can be determined. In order to avoid possible damage to the producing horizon of the formation, the high-temperature chemical compatibility between the in situ materials and the frac fluids, fluid additives, and proppants must be verified. In trying to assess the probability for a successful stimulation treatment, the response of formation rocks with entirely different physical characteristics must be predicted. Perhaps most significant of all, in geothermal wells the required techniques must be capable of bringing about the production of very large amounts of fluid. This necessity for high flow rates represents a significant departure from conventional oil field stimulation and demands the creation of fractures with very high flow conductivity or very large fracture surface areas in the case of matrix permeability dominated formations.

My involvement in the formulation of this program began with visits to a large number of industrial organizations with a firm commitment or vested interest in the development of geothermal energy. The technical discussions during these visits centered on the question - - - in what areas could the injection of Federal dollars be most productive in developing commercial geothermal well stimulation techniques applicable to the growing number of unproductive or marginal geothermal wells. Many of the people attending this first symposium on Geothermal Well Stimulation are people I contacted during those formative stages of this program. The end result of this effort was a document called a Request for Proposal (RFP) in which the DOE solicited proposals for formulating, managing, and implementing an extensive geothermal well stimulation program designed to assess, develop, and field test methods for increasing and prolonging the productivity of geothermal wells. This document was published by the Los Alamos Area Office of the DOE and was mailed to prospective industrial participants. Additional publicity for the program was sought by advertising in such prominent journals as The Oil and Gas Journal.

After publication of the Request for Proposal, a pre-proposal conference was held in Denver to answer questions related to the proposed program, DOE's ultimate intentions in this area, and the desired magnitude and scope of the program. By the required deadline date, five significant proposals were received from industrial organizations. It is interesting to

note that each proposal represented a consortium of organizations, apparently in response to the large magnitude and scope of the desired program. While a large segment of the geothermal community was enjoying the scenic wonders of Hilo at the Geothermal Resources Council annual meeting, another small group was tolerating the delights of downtown Washington in August while these proposals were being thoughtfully reviewed. This process was concluded with the announcement that the proposal submitted by Republic Geothermal had been selected as the winner.

The organizational structure under Republic Geothermal will be presented in detail by Don Campbell. I would like to point out that this program is under the technical cognizance of Cliff McFarland within the Division of Geothermal Energy at DOE. My capacity within this program is to serve as a technical advisor to the DOE.

Numerous geothermal wells have been drilled on the more obvious thermal anomalies with respectable success ratios. Dry holes or marginal producers, however, do occur in the development of every field. While some of these unproductive wells are on or outside the boundaries of the established reservoir, others are within the reservoir boundaries but have just not intersected a good portion of the producing horizon. These are the wells that become prime candidates for stimulation treatments. The goal of this program is to identify specific geothermal wells of marginal or submarginal value and to develop and test the necessary hardware and techniques to perform successful stimulation treatments on these wells. The ultimate goal of the program is to ensure that these products and techniques become available in the commercial marketplace for use by all well owners and operators.

The Statement of Work contained in the RFP set out very specific emphasis areas that were to be followed throughout the conduct of this program. The geothermal well stimulation program is limited to hydrothermal convective systems with a strong emphasis on hot water dominated reservoirs in the 150-300C range. The RFP was worded in such a way that nothing has been absolutely excluded but strong attention is directed toward the use of hydraulic fracturing and/or chemical treatments in hot water wells in developed reservoirs. High drilling costs associated with drilling in hot, fractured, and unpredictable geothermal formations provides the major

economic incentive for this program. The cost of drilling and completing a geothermal well can frequently be higher by a factor of 2 or 3 over the cost of a conventional oil or gas well to the same depth.

Stimulation treatments will be conducted in formations which produce hot water as a result of both matrix permeability and from natural existing fracture systems. The following targets of opportunity are of particular interest to this program:

- Wells that require additional drainage area because of insufficient formation permeability.
- Wells that did not intersect major fracture systems that are presumed to exist nearby.
- Wells that suffered man made damage during drilling or completion operations including mud or cement invasion.
- Wells that require periodic remedial treatment as a result of fluid production related damage.

Although numerous criteria have been established for the selection of candidate wells, perhaps the most significant is definite proof of a good producing reservoir. This data will normally be obtained from offset well production.

I would like everyone in the geothermal community to be aware of the existence of this program and the fact that we are continually reviewing well data as part of the selection process in picking our next candidate wells for stimulation treatments. Invitations to the stimulation team to review data for a potential candidate well are always in order.

GEOTHERMAL RESERVOIR WELL STIMULATION PROGRAM OVERVIEW AND STATUS REPORT

D. A. Campbell
Republic Geothermal, Inc.

INTRODUCTION

The principal purpose of this discussion is to review the status of the Geothermal Reservoir Well Stimulation Program (GRWSP) contract effort, including the accomplishments of the first ten months. First, however, a brief overview of the program is in order as an introduction.

The program is divided into two phases. Phase 1 is basically the engineering and laboratory studies, and Phase 11 mostly covers the field experiments. Phase 1 has received most of the project's attention during the first 10 months, but the future emphasis will be on the field activities. The main Phase 1 tasks are summarized on Table 1. Assessment of the state-of-the-art is the objective, i.e., to review the oil and gas industry stimulation technology and see how it may be applied to geothermal wells, to determine what additional technology is needed, and to conduct laboratory and engineering work to both evaluate and fill the needs for additional technology.

As shown on Table 2, the first Phase 11 task is to logically select and propose geothermal reservoirs and specific well candidates for stimulation experiments. The jobs are to be planned, conducted, and then evaluated. The first field experiment was originally intended to be a conventional hydraulic fracture treatment in a relatively low temperature geothermal reservoir. Thus, techniques on the margins of the upper temperature limit of what is currently being done in oil and gas industry could be used. Increasing the temperature and complexity of successive experiments was intended, along with the inclusion of a variety of lithologies. The scope of work was not intended to include explosives, and the emphasis was to be on hot water reservoirs, not vapor dominated reservoirs. The last task of this phase will be to disseminate the results of the work with project reports and symposiums. A second symposium covering the project will be held next year to summarize the results of work performed under the first contract.

An organization chart for the contract is shown on Figure 1. Cliff McFarland, from Washington's Department of Energy/Division of Geothermal Energy (DOE/DGE), is the Program Manager. Bob Hanold from the Los Alamos Scientific

Laboratory (LASL) is the technical advisor for the DOE, and Don Campbell is the Project Manager for the prime contractor, Republic Geothermal, Inc. (RGI). Charles Morris of Republic is in charge of Phase 1 activities, and in that capacity coordinates the work of two of the major subcontractors. Robert Verity, also of Republic, has a like position for Phase 11. Otto Vetter of Vetter Research is the subcontractor who deals mostly with the high pressure/temperature, chemical aspects of the program, along with tracer studies. Henry Crichlow, of Petroleum Training and Technical Services (PTTS), is responsible for the mathematical modeling efforts. Richard Sinclair of Maurer Engineering, also a subcontractor, is responsible for some of the basic material properties laboratory testing and the recommendation of frac fluids and proppants for dealing with the high temperature environment of geothermal wells. Maurer's main functions are, however, the hydraulic fracture mechanics and design for each experiment. Dan Slagle of MAPCO is responsible for some of the actual field work. Robert Nicholson, although not shown on the organization chart, is a consultant with Terra Services and as such primarily assists Republic in field work associated with the experiments. He was very instrumental in formulating the overall program initially, and will continue to be involved in a number of ways.

The reservoir selection process task, technology transfer task, and some of the reports that will be available from the program are discussed below in some detail, along with future experiments and the program schedule. The laboratory and computer work by the subcontractors and the two field experiments completed to date are discussed in detail in other Symposium reports.

RESERVOIR SELECTION TASK

The reservoir selection task was one of the first efforts of the contract. The task is nearly complete, and was begun by soliciting expressions of interest in participation from all geothermal operators and developers known to the general contractor. Those who responded positively are listed on Table 3. One of the prerequisites for participation was that the owner/operator be willing to release data to the public domain and also be willing to cost share in the sense the owner accepts the risk to wells and facilities. The project cannot assume liability for damage even though stimulation jobs are high risk operations in general. The developers were not required to put up out-of-pocket money. However, as the program is extended beyond this first contract, a true cost sharing mode of operation is probable.

Some of the reservoirs proposed as possible stimulation candidates are shown in Figure 2. Roosevelt Hot Springs in

Utah has a reservoir temperature of about 500 degrees F and produces mainly from a fractured granidiorite. The Geysers is the only vapor-dominated reservoir on the list, at about 450-470 degrees F, producing from fractured metamorphics (graywacke, primarily). Desert Peak in Nevada is around 400 degrees F, and produces from volcanics, mostly fractured. Chandler in Arizona is about 350 degrees F, and is a low porosity-permeability volcanic reservoir. Raft River, at around 290 degrees F, produces from a fractured quartz monzonite. East Mesa is shown to be around 350 degrees F. It has a matrix permeability and porosity that is good in general, but suffers local degradations. Westmorland is similar to East Mesa, but is about 450 degrees F. Brawley is near 500 degrees F and is a fractured medisediment of sandstone and siltstone with some matrix porosity and permeability. Baca is the hottest of all at about 530 degrees F, and produces principally from fractured volcanic tuff. Thus, a variety of lithologies and a wide range of temperatures are available for possible stimulation experiments.

Table 4 lists the main reservoir selection criteria that were used. The candidates were quantified on a scale of 1 to 10, considering such parameters as temperature, amount of data available, different lithology, etc. The volunteered candidates were then ranked. Table 5 shows the rank order. East Mesa was at the top with the highest total score; Westmorland (Salton Sea area) was next; then Baca, Brawley, Raft River, The Geysers, Roosevelt, Desert Peak, and Chandler. The program sequence will not necessarily proceed in the rank order shown. A reservoir of 500 degrees F could probably not be stimulated today effectively with conventional materials and hardware; so the lower temperature wells will be considered first while Phase 1 progresses. Furthermore, the order is subject to continual review as the field experiments proceed and additional candidates of opportunity are submitted for consideration. In the current contract, there is enough money to do only six experiments at four different sites, but an extension is probable.

RAFT RIVER EXPERIMENTS

The first two experiments were performed at Raft River, Idaho and are summarized on Table 6. Raft River RRGP-4 was the initial stimulation candidate and a Kiel dendritic type frac was used, employing conventional oil and gas technology. This is a 290-300 degree reservoir. The job was about 8,000 bbls and cost about $450,000, including a substantial amount of preparatory well work. The second experiment was in Raft River RRGP-5 and was a conventional planar frac. It was again about 8,000 bbls, but used a much higher concentration of sand--about 400,000 lbs. It cost about $500,000. These two jobs constitute a large part of the effort of the first ten months. The first job was done earlier than

originally planned at the DOE's request. A second stimulation treatment wasn't even in the first year plan of the original program. Their acceleration has interfered somewhat with completion of some of the Phase 1 tasks originally planned during this period. The details of the two experiments are discussed in other Symposium reports.

TECHNOLOGY TRANSFER

One of the major tasks in Phase 1 was the compilation of the Technology Transfer reports. The data sources were extensive literature reviews, the personal experience of those involved in the contract, and interviews with most of the service companies, operators, and researchers having expertise in the area. The principal aspects covered are summarized on Table 7. Basically, the reports constitute a comprehensive state-of-the-art summary with respect to hydraulic fracturing and chemical stimulation at this stage. They also provide a number of stimulation case histories in oil and gas reservoirs having relatively high temperatures. A selected bibliography of several hundred pertinent papers on the subject is included. It should be noted that there are a number of unsolved problems in the well stimulation area, even for oil and gas reservoirs. Failures are common, and little data on high temperature applications exists. Extending this technology to the geothermal environment poses a serious challenge. Not all attempts will be successful. There are a variety of reasons for failures, but in many cases they aren't well understood because of inadequate evaluation techniques.

GRWSP REPORTS

Table 8 lists the reports that are planned during the next year of the project. The Reservoir Selection Task, at least for the initial submittals, is complete, and the report is available now. The Technology Transfer reports will be available by the end of February. There are two volumes available on all the frac fluid properties at elevated temperatures that have been measured thus far. Proppants and their observed properties at high temperatures will soon be available in report form also. Surface Equipment and Downhole Equipment and Hardware reviews will be ready about April. Recent Stimulation and Technology Development Analyses, both physical and chemical, are basically recommendations of what needs to be done for geothermal applications.

It is hoped that enough physical and chemical data will be available by the middle of the summer to proceed with some of the higher temperature jobs anticipated. The Numerical Fracture Prediction Model is available now; the Numerical Fracture Response Reservoir Model should be ready in March, and the final reports on each field experiment will

come out as the program progresses. The first report on both of the Raft River experiments will be out in early March. The "First-Year Progress Report" will be out by the end of February, and the final project report will be completed in March of 1981. (Interested parties are invited to request copies of these reports.)

FUTURE EXPERIMENTS

Table 9 summarizes the experiments planned for the future. This is the current plan for the four future field experiments, but is subject to change. The first one shown will get two experiments out of the way. One is a multi-stage frac deep in the reservoir in low permeability sandstones and shales, just to enhance natural productivity. The other is a shallower zone frac in sandstones that have good theoretical productivity based on log analyses, but have been damaged by drilling fluid. This experiment will probably be performed at East Mesa with temperatures near 350 degrees F Assuming materials are available for 500 degrees F. jobs by late summer, an advanced type of stimulation treatment--perhaps an acid frac--will be attempted. This probably will be at Baca, although that would be the most difficult in terms of temperature. If Baca is precluded because of weather, then Brawley or Roosevelt Hot Springs or The Geysers will be the next choice. The last experiment planned under this contract is a multi-stage hydraulic fracture treatment with scale inhibitor tailed in after the fracture fluids. The idea is to have the scale inhibitor absorb on the formation rock and then de-absorb as the well is produced. This would be a cyclic process done repetitively in order to continue to produce the well. There are a number of wells that have downhole scaling problems and also require stimulation to increase productivity. Likely candidates are perhaps Westmorland or Brawley.

SCHEDULE

Figure 3 shows the schedule planned at this time. The reports previously referred to are indicated on the schedule by the small triangles. The Technology Review Task is shown to be finished in April, and the Stimulation Materials Evaluation will be finished by the fall, with most of the work in place by early summer. The Numerical Simulation work is essentially done as far as formulating the models, with the long tail-end shown on the schedule being for analysis work on the various experiments. Planning for each field experiment is shown to be followed by DOE approval indicated by the small squares. The schedule for field experiments spans a period from the experiment at the beginning of the line to a small diamond indicating the point at which evaluation reports will be issued. The project management reporting will continue throughout the contract. The project is currently at the point at which there is a

symposium and the First-Year Review report is submitted. Termination of the contract is scheduled for March of 1981, at which time another symposium will be held and, hopefully, successful experiments in 400-500 degrees F environments can be reported at that time.

FIGURE 1

PROJECT ORGANIZATION
GEOTHERMAL RESERVOIR WELL STIMULATION PROGRAM

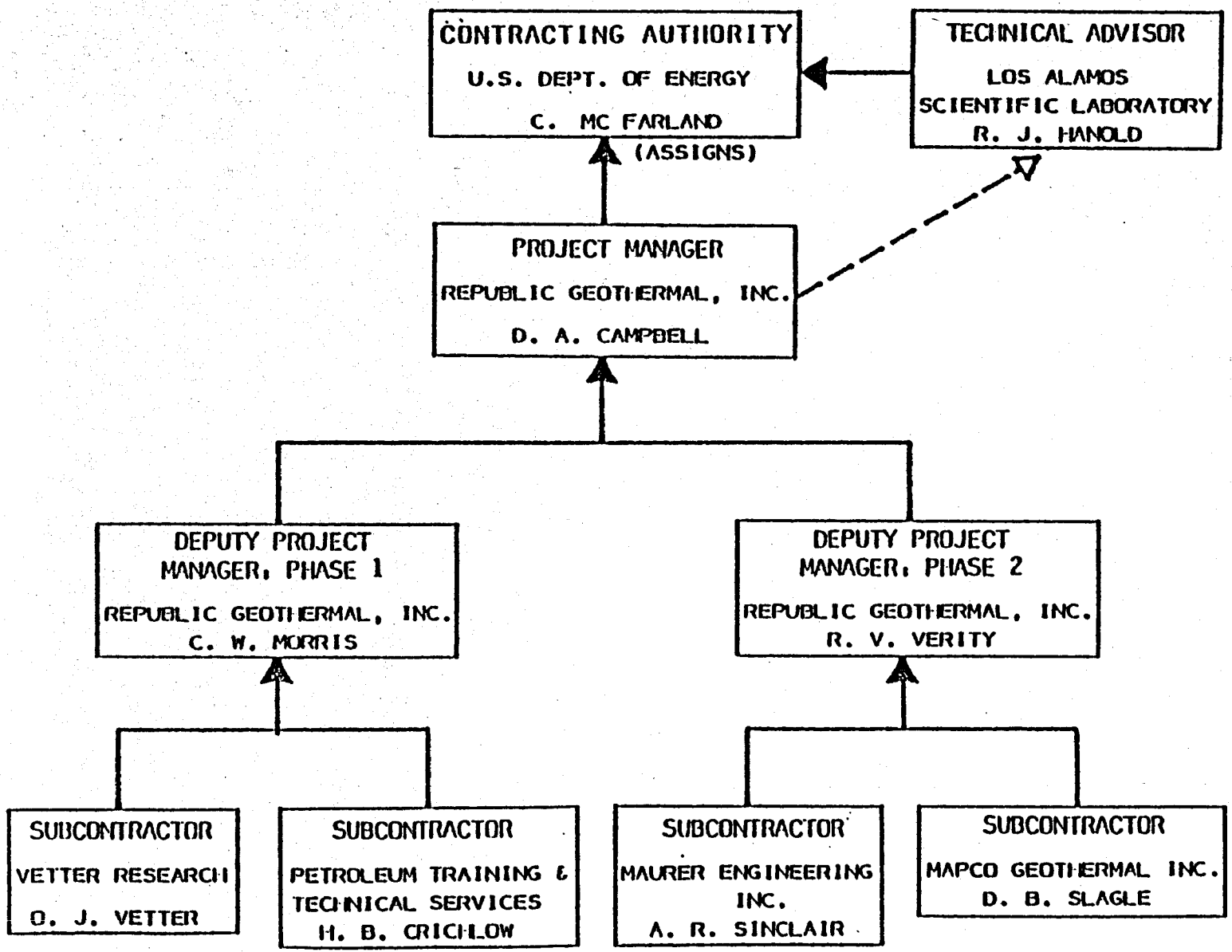

FIGURE 2

LOCATIONS OF GEOTHERMAL AREAS STUDIED FOR STIMULATION EXPERIMENTS

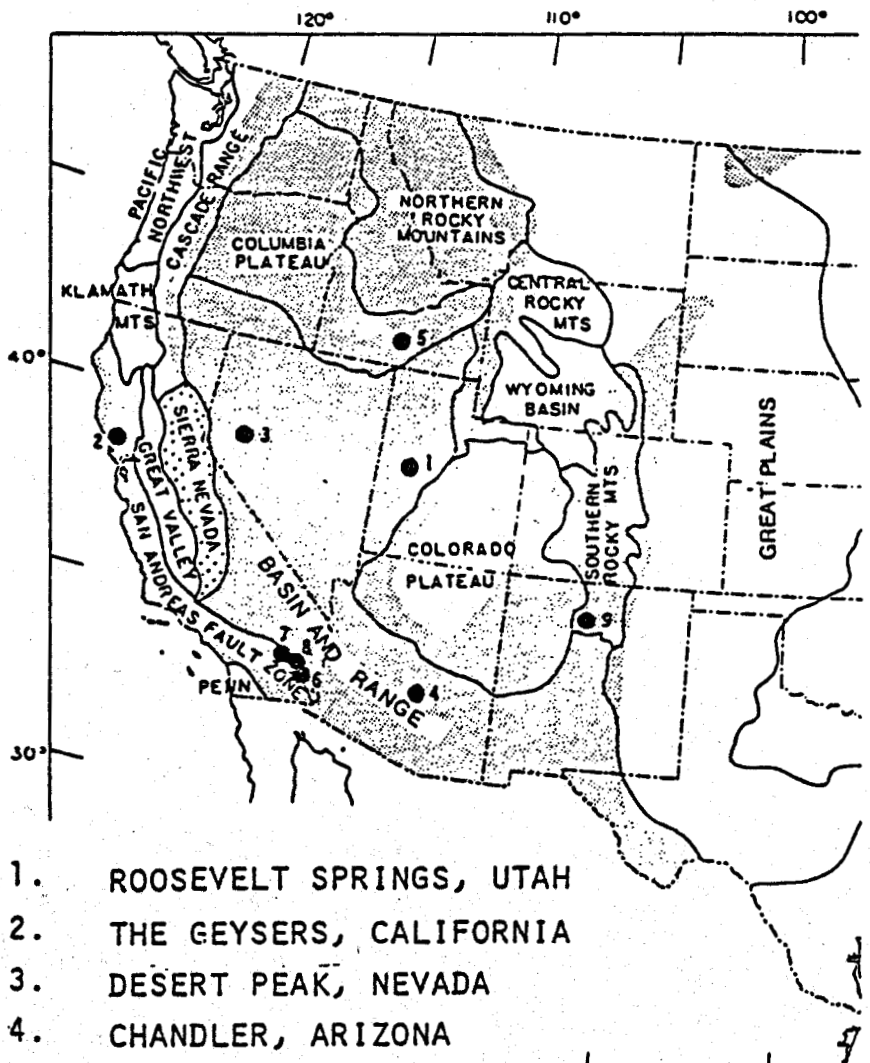

1. ROOSEVELT SPRINGS, UTAH
2. THE GEYSERS, CALIFORNIA
3. DESERT PEAK, NEVADA
4. CHANDLER, ARIZONA
5. RAFT RIVER, IDAHO
6. EAST MESA, CALIFORNIA
7. WESTMORLAND, CALIFORNIA
8. BRAWLEY, CALIFORNIA
9. BACA, NEW MEXICO

FIGURE 3

GRWSP SCHEDULE

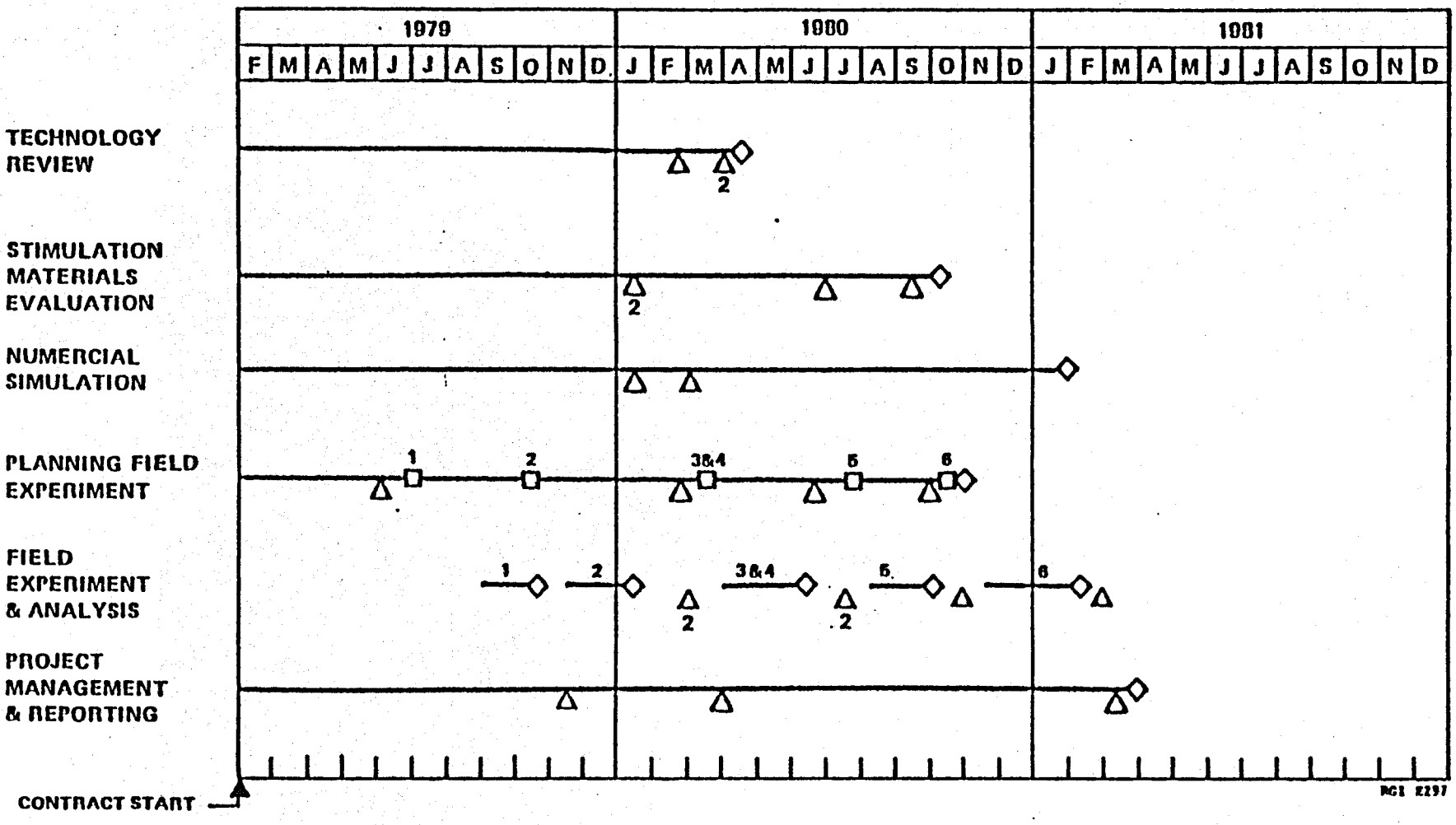

△ REPORT
□ CONTRACTING AGENCY APPROVAL
◇ COMPLETED ACTIVITY

TABLE 1

MAJOR TASKS - PHASE 1

- TECHNOLOGY REVIEW
  - TECHNOLOGY TRANSFER
  - EQUIPMENT REVIEW - SURFACE
  - EQUIPMENT REVIEW - DOWNHOLE
- STIMULATION MATERIALS EVALUATION
  - FRACTURE FLUID EVALUATION
  - FRACTURE PROPPANT EVALUATION
  - RECENT STIMULATION TECHNOLOGY DEVELOPMENT ANALYSIS
  - CHEMICAL STIMULATION ANALYSIS
- NUMERICAL SIMULATION
  - NUMERICAL MODEL DEVELOPMENT
  - NUMERICAL ANALYSIS

TABLE 2

MAJOR TASKS - PHASE II

- PLANNING FIELD EXPERIMENTS
  - RESERVOIR IDENTIFICATION, EVALUATION AND QUALIFICATION
  - WELL IDENTIFICATION, EVALUATION AND QUALIFICATION
  - PREPARE SPECIFIC WELL EXPERIMENT
  - ENVIRONMENTAL AND PERMITTING
  - FIELD EXPERIMENT ADMINISTRATION PLANNING
  - SPECIFICATIONS AND SUBCONTRACTING
- FIELD EXPERIMENT AND ANALYSIS
  - DESIGN AND PROVIDE SURFACE PRODUCTION FACILITIES
  - FIELD EXPERIMENT AND PRODUCTION TESTING
  - MONITORING AND DATA COLLECTION
  - DATA ANALYSIS AND INTERPRETATION
  - RADIOACTIVE TRACERS
- PROJECT REPORTING AND MANAGEMENT
- GEOTHERMAL WELL STIMULATION SYMPOSIUM

TABLE 3

RESOURCE DEVELOPERS EXPRESSING INTEREST IN PARTICIPATING IN PHASE II

- AMINOIL
- GEOTHERMAL KINETICS, INC.
- GETTY OIL CO.
- MAPCO, INC.
- PHILLIPS PETROLEUM CO.
- REPUBLIC GEOTHERMAL, INC.
- THERMOGENICS, INC.
- UNION OIL CO. OF CALIFORNIA
- U.S. DEPT. OF ENERGY, DGE/IDAHO

TABLE 4

RESERVOIR SELECTION CRITERIA

1. DEVELOPER PARTICIPATION
2. TEMPERATURE
3. AVAILABLE RESERVOIR DATA
4. NUMBER OF WELLS IN FIELD
5. PRODUCTION AND DISPOSAL FACILITIES
6. MECHANICAL CONDITION OF WELL
7. ROCK PROPERTIES
8. SCALING PROBLEMS
9. MONITORING CAPABILITY
10. PERMITTING AND ENVIRONMENTAL CONSIDERATIONS
11. LOGISTICS
12. SUBJECTIVE EVALUATION OF OVERALL STIMULATION POTENTIAL

TABLE 5

CANDIDATE RESERVOIR RANKING

1. EAST MESA, CA
2. WESTMORLAND (SOUTH SALTON SEA), CA
3. BACA, NM
4. BRAWLEY, CA
5. RAFT RIVER, CA
6. THE GEYSERS, CA
7. ROOSEVELT HOT SPRINGS, UT
8. DESERT PEAK, NV
9. CHANDLER, AZ

PROGRAM SEQUENCE REQUIRES INCREASING TEMPERATURE AND COMPLEXITY

SUBJECT TO CONTINUAL REVIEW

TABLE 6

GEOTHERMAL RESERVOIR WELL STIMULATION PROGRAM
FIELD EXPERIMENT SUMMARY

No. 1	A DENDRITIC ("KIEL") HYDRAULIC FRACTURE TREATMENT INTENDED TO IMPROVE COMMUNICATION WITH THE NATURAL FRACTURE SYSTEM IN A LOW TEMPERATURE GEOTHERMAL RESERVOIR - RAFT RIVER WELL RRGP-4, COMPLETED AUGUST 1979
No. 2	A CONVENTIONAL MASSIVE PLANAR HYDRAULIC FRACTURE TREATMENT INTENDED TO IMPROVE COMMUNICATION WITH THE NATURAL FRACTURE SYSTEM IN A LOW TEMPERATURE RESERVOIR - RAFT RIVER WELL RRGP-5, COMPLETED NOVEMBER 1979

TABLE 7

TECHNOLOGY TRANSFER

- TYPES OF STIMULATION TECHNIQUES
- PROCESS VARIABLES
- HYDRAULIC FRACTURING DESIGN
- TEMPERATURE EFFECTS
- FLUID INTERACTIONS
- FRACTURE EVALUATION
- FRACTURE MAINTENANCE
- FRACTURING PROBLEMS AND THEIR RESOLUTION
- CHEMICAL STIMULATION
- NUMERICAL MODELING
- STIMULATION CASE HISTORIES
- SELECTED BIBLIOGRAPHY

TABLE 8

GEOTHERMAL RESERVOIR WELL STIMULATION PROGRAM REPORTS

RESERVOIR SELECTION FOR FIELD EXPERIMENTS

TECHNOLOGY TRANSFER FROM PREVIOUS STIMULATION OPERATIONS

AVAILABLE DATA ON FRAC FLUIDS FOR GEOTHERMAL WELL STIMULATION (2 VOLUMES)

FRACTURING PROPPANTS AND THEIR PROPERTIES

SURFACE EQUIPMENT REVIEW

DOWNHOLE EQUIPMENT REVIEW

RECENT STIMULATION TECHNOLOGY DEVELOPMENT ANALYSIS (PHYSICAL AND MECHANICAL)

RECENT STIMULATION TECHNOLOGY DEVELOPMENT ANALYSIS (CHEMICAL)

NUMERICAL FRACTURE PREDICTION MODEL

NUMERICAL FRACTURE RESPONSE RESERVOIR MODEL

FINAL REPORTS ON EACH FIELD EXPERIMENT (1-6)

FIRST-YEAR PROJECT REPORT

FINAL PROJECT REPORT

TABLE 9

GEOTHERMAL RESERVOIR WELL STIMULATION PROGRAM
FUTURE FIELD EXPERIMENTS SUMMARY

Nos. 3 & 4	A COMBINED MULTI-STAGED HYDRAULIC FRACTURE TREATMENT INTENDED TO ENHANCE THE PRODUCTIVITY OF DEEP, LOW PERMEABILITY ZONES AND A MINI-FRAC INTENDED TO PENETRATE NEAR-WELLBORE IMPAIRMENT IN MORE SHALLOW, HIGH PERMEABILITY SANDS. MODERATE TEMPERATURE SANDSTONE-SHALE RESERVOIR WITH MATRIX PERMEABILITY AND POROSITY PROBABLY EAST MESA 58-30
No. 5	AN ADVANCED TYPE OF STIMULATION TREATMENT (ACID FRAC OR ....?) INTENDED TO IMPROVE COMMUNICATION WITH THE NATURAL FRACTURE SYSTEM IN A HIGH TEMPERATURE RESERVOIR PROBABLY BACA - POSSIBLY BRAWLEY, ROOSEVELT HOT SPRINGS, OR THE GEYSERS
No. 6	A MULTI-STAGED HYDRAULIC FRACTURE TREATMENT WITH SCALE INHIBITOR INTENDED TO ENHANCE PRODUCTIVITY, REDUCE NEAR WELLBORE PRESSURE DROP, AND CONTROL SCALE FORMATION. HIGH TEMPERATURE SANDSTONE-SHALE RESERVOIR WITH MATRIX PERMEABILITY AND POROSITY, AND A HISTORY OF DOWNHOLE AND FORMATION SCALING. PROBABLY WESTMORLAND (SOUTH SALTON SEA)

High Temperature Proppants and Fluids for Geothermal Well Stimulation

by

A. R. Sinclair
Maurer Engineering, Inc.
Houston, TX

January 25, 1930

TR80-5

High Temperature Proppants and Fluids for Geothermal Well Stimulation

1. ABSTRACT:

All available data on proppants and fluids were examined to determine deficient areas in technology as required by 300 to 500 degrees F. (150 degrees to 265 degrees C.) geothermal wells. While fluid properties have been examined well into the 450 degree F. range, proppants have not been tested at elevated temperatures except in a few instances. This paper presents the latest proppant test data at geothermal temperatures. It also shows some physical properties of possible fluid systems and discusses various techniques that can be worthwhile in geothermal wells.

2. INTRODUCTION

The Geothermal Well Stimulation Management Program began early in 1979. Its intent was to gather available data from the service companies, oil companies and research centers on what were the best techniques, materials, and ideas in the oil and gas industry to stimulate producing wells. During April of 1979, all service companies were visited and interviewed to that they could be briefed on our program and on special problems of higher temperature wells.

The major objective is to produce workable, economic techniques of stimulation for hot water geothermal wells. Geothermal energy has a great potential for tomorrow's energy supply; however, many highly productive geothermal hot water wells tend to damage themselves by virtue of their high productivity. The hot water can carry dissolved solids which are easily precipitated or plated out by a slight change in temperature or pressure. The water also contains carbon dioxide which can flash when the pressure is reduced. Both carbon dioxide and water can change phases in these wells. If any phase change or precipitation occurs in the formation, then damage is possible. With high drawdown rates, it is likely that one of these mechanisms can be triggered. When the formation becomes damaged, the producing zone is eventually plugged and becomes non-producing. The damage zone may be only a few feet around the wellbore or it may extend up to 100 feet away from the wellbore. So, one objective is merely to remove near wellbore damage to restore earlier production. An effective way to do this is to hydraulically fracture the damaged zone. A vertical fracture can easily break through the wellbore skin and damaged area. With larger fracture jobs it is possible to change the flow pattern to a more linear one (versus radial flow in a non-fractured well). If the pressure gradient is decreased by the fracture, then the tendency for the well to redamage itself is also decreased. An increase in stimulated production over initial production is not always required although sometimes that is the object of the treatment for reservoir stimulation where tight zones can be interconnected to more permeable or hotter zones.

In our experience to date, we find that present geothermal wells present a hostile temperature environment up to well above 500 degrees F. (265 degrees C.) but only a semi-hostile stress environment with fracture gradients up to 0.8 and closure stresses well below 6000 psi. With these conditions in mind let us look at the proppants, fluids and techniques that we have available to stimulate the hot water geothermal wells.

3. PROPPANTS

Sand

While sand is generally used as a proppant today and it has been the most widely used in the past, it may not be strong enough to withstand the hot water in geothermal wells at elevated temperatures. Only resin coated sand (1), sintered bauxite (2), and resin coated bauxite were found to be temperature insensitive.

Sand is definitely affected by temperature, particularly when tested in hot water at various closure stresses. Fig. 1 shows the effect of temperature on common frac sand (20/40 mesh). These results are short term results and only suggest the severity of long term field results. There are Ottawa, Brady and Colorado sands presented in their order of strength from high strength to low strength, respectively. Fig. 2 shows how these three sands retain their permeability under varying closure stress. A limited supply of Ottawa has caused widespread use of Brady and Colorado sands.

There are several mechanisms that can destroy sand grains in the fracture. First, the sand is brittle and point-to-point loading occurs which causes brittle failure. Second, sand is full of microfractures and faults which weaken the sand. Finally, when sand is stressed in a corrosive medium like hot water, stress corrosion cracking (3) appears to destroy the sand at low closure stresses. High temperatures and high stresses combine to bring out the worst in sand and emphasize the inadequacies of sand as a proppant under high temperature conditions.

Resin Coated Sand (Super Sand) and Resin Coated Bauxite (Super Bauxite)

The strongest proppant tested to date is the Resin coated bauxite (4). It shows no temperature sensitivity or permeability decrease under load. Also, the resin coated sand is not temperature or load sensitive but does have a slightly less permeability at any closure stress due to a slightly different distribution of particle sizes. Fig. 3 shows the permeability of Super Bauxite and Super Sand II under varying closure stress to 10,000 psi at 350 degrees F. No temperature differences or sensitivities were found so tests at all temperatures gave about the same results shown in Fig. 3 within experimental scatter.

Sintered Bauxite

Shortly after the resin coated sand was patented (9) sintered bauxite (2) came into being. Although slightly crushable, the sintered Bauxite is much stronger than sand and effectively inert in hot brines. Fig. 3 also shows how

Bauxite permeability behaves under increasing closure stress. It exceeds resin coated sand at lower closure stress but drops below resin coated sand at 10,000 psi. It does not appear to be temperature sensitive but the data scatter appears to be greater than the resin coated materials because of variations in packing density and due to slight crushing of some particles.

Glass Beads

During the 1960's, glass beads became popular, and besides looking good, the tests in air at room temperature showed them to be very strong. However, field data indicated that a well treated with these expensive beads was likely to perform about the same as with the proppant, sand. During the 1970's, tests conducted in warm brine showed that glass beads failed catastrophically. The main reasons for failure were similar to sand: brittle material (point-to-point loading) and stress corrosion cracking. Because of the uniformity of particle size and shape, glass beads usually fail all at once. Fig. 4 shows the extreme loss of permeability under load and the adverse temperature effects which makes glass beads unusable in any geothermal environment.

4. FLUIDS

Many fluids and fluid systems have been tested for the geothermal wells. Water soluble polymers are the main viscosifiers for application in geothermal wells. Above 250 degrees F. (120 degrees C.) almost all polymer systems show decline in viscosity as shown for hydroxypropyl guar in Fig. 5. There are many techniques that can be used to delay this decline or degradation in properties. One such technique is the addition of 5% of methanol to the polymer water solutions. This has a stabilizing effect on the fluid. Other proprietary products are available which are added as high temperature stabilizers.

Polymer degradation is also speeded by dissolved oxygen in hot water. This effect is minimized by adding an oxygen scavenger to the water. The type and amount of polymer determines the speed and extent of degradation.

Previously, polymers used in fracturing were of these basic types: polysaccharides, modified celluloses and polyacrylamides. Representative generic names for these are guar gum, hydroxyethyl cellulose, and nonionic polyacrylamide. These particular polymers were chosen because of their ability to viscosify water, friction reduction effects, cost, ease of handling and tolerance to brine.

An ideal frac fluid (6) would have the properties of high viscosity for sand carrying, low pumping friction, wide

chemical compatibility, and low cost. In the case of geothermal hot water wells, an ideal frac fluid would retain its desirable properties at the high temperature until it has done its job of placing the proppant in the fracture.

Typical high temperature fluids are shown in Figs. 6 through 9. Each fluid's viscosity is plotted versus temperature to show how the high temperature degrades the fluids. Each set of data has been tested by different companies using different conditions and should not be compared directly.

5. STIMULATION TECHNIQUES

A stimulation technique requires 4 different technologies to interact to provide the completed result. These are:

* Fluids
* Proppants
* Equipment
* Engineered Technique

While there are many good fluid systems and proppants, only judicious combinations and a well thought out schedule which uses all of these materials and available equipment to best advantage is an optimum stimulation technique.

Many types of hydraulic fracturing have been proposed and considered for geothermal well stimulation. In Table I some of these techniques are shown and discussed as to advantages and disadvantages. In general, the categories of hydraulic fracture can be considered "Planar Fracturing" or "Dendritic Fracturing."

Planar Fracturing

All conventional fracturing (7) is an attempt to make a planar, vertical fracture in the producing formation. This occurs when the pressure and fluid flow is sufficient to break the formation in its plane of weakness. After the planar fracture is created, a proppant is carried into the fracture to keep it open and conductive for subsequent production.

In geothermal wells, large tubular goods are available and the producing formations are at reasonably shallow depths so that high flow rates can be used to create the planar fractures. Along with efficient fracture creation, convective cooling can be achieved to keep the working fluid much cooler than the ambient formation temperature. In the

space of 4 hours cooldown by convection can reach several hundred feet from the wellbore with volumes up to 25,000 bbls of fluid injected. Reheating of the fracture area is mainly by conduction so the time for complete reheating is measured in days. Fluid systems that compliment the high flow rate fracs will be chosen for each particular application. Each formation's permeability, porosity and temperature also affects the selection of the fluid system's physical properties such as its viscosity. The complex chemistry caused by the high temperature water will require complete chemical compatability testing.

Dendritic Fracturing

Branched fractures can be caused by several techniques. The main proponent of dendritic fracturing has been Kiel (8). An estimate of over 750 Kiel Fracs have been run to date. Dendritic fractures are caused by pulsing the formation slowly which causes formation spalling and diversion of the fracture wings by downhole stress modification. Methods to predict the extent and direction of the fractures are still being worked upon; however, the best results have been reported in naturally fractured formations where major and minor fracture systems already exist but may not have flow capabiity. Usually 5 or more stages of fluids are used with each stage utilizing a low viscosity fluid, sand slugs, and several flow back periods. High flow rates and high friction reduction are used to advantage on these treatments.

Other types of dendritic fracturing have been employed by LASL and other service companies where a pulsed frac technique is used. Also, low or high density particles have been used to limit fracture growth in one or more direction and cause the fracture to grow in a preferential direction.

6. CONCLUSIONS

An engineered combination of a fluid system, a highly conductive proppant, and reliable equipment is required to effectively stimulate hot water geothermal wells. Generally, high flow rates and heat blockage will be used to advantage with either conventional/planar fracturing or with a dendritic fracturing technique.

Many of today's fluid systems have been tested to above 400 degrees F. Some fluids have survived quite well. Current test on proppants have shown temperature sensitivities in sand and glass beads; however, there are resin coated materials and sintered bauxite which are not temperature sensitive. Much more work is required in the specific application of fluid systems and proppants to the actual geothermal wells since the temperature, water chemistry and formation properties vary greatly.

7. REFERENCES

1 Sinclair, A. R. and J. W. Graham:
"A New Proppant for Hydraulic Fracturing", ASME Paper 78-Pet-34 presented Nov. 1978, in Houston, TX.

2 Cooke, C. E., et al:
"Hydraulic Fracturing Method Using Sintered Bauxite Propping Agent" Issued to Exxon Production Research Co., U. S. Patent No. 4068718, Jan. 1978.

3 Cooke, C. E.:
"Conductivity of Fracture Proppants in Multiple Layers," Journal of Petroleum Technology, Sept. 1973, pp 1101-1107.

4 Sinclair, A. R. and J. W. Graham:
"An Effective Method of Sand Control", SPE Paper 7004, Third Symposium on Formation Damage, Lafayette, LA, Feb. 1978.

5 Cooke, C. E.:
"Hydraulic Fracturing with a High Strength Proppant", SPE Paper 6213, 1976 Fall AIME-SPE Meeting in New Orleans, LA, Oct. 1971.

6 Sinclair, A. R., et al:
"Polymer Emulsion Fracturing", Journal of Petroleum Technology, July 1974, pp 731.

7 Howard, G. C. and Fast, C. R.:
"Hydraulic Fracturing", Monograph Series Society of Petroleum Engineers of AIME, Dallas, TX, 1970.

8 Kiel, O. M.:
"Hydraulic Fracturing Process Using Reserve Flow", U.S. Patent No. 3,933,205, Jan. 20, 1976.

9 Graham, J. W., et al:
"Method for Treating Subterranean Formation", Assigned to Exxon Production Research Co., U.S. Patent No. 3,939,191, Dec. 1975.

Potential Type of Stimulation Treatment	Brief Description of Treatment	Removes Wellbore Damage	Provides Reservoir Stimulation	Viscosity, Sand Carrying, and Fluid Properties	Type of Proppant
Water Frac	Planar Frac with water as the fluid, sand as the proppant. Usually high rate jobs.	Yes	Slight, because fractures are too short.	Poor to Fair	Usually sand at low concentrations of up to 1 lb/gal.
Kiel-Dendritic Frac	Pump in/flow back multiple stages to create branched fracture in formation, uses various fluids and proppants.	Yes	Yes, Twice the average planar fracture.	Good because of sand slugs carried at high turbulent rates.	Usually flow to 20/40 mesh sand in slugs at high concentrations 2 to 8 lb/gal.
Pressure Cycling Fracturing	Uses low cycle fatigue of formation to enhance fracturing.	Yes	Yes	Fair to Good	Usually sand at low to medium concentrations, maybe slugs of sand.
Gelled Frac	Planar Frac using Polymer water and sand	Yes	Yes, Size Sensitive	Fair to Good	Sand usually at low concentrations 1 to 3 lb/gal.
Cross-linked Gel Frac	Cross-linked polymers to fully suspend sand or proppant in a planar frac.	Yes	Yes, Size Sensitive	Excellent	Sand, Super Sand or Bauxite at any concentration to 10 lb/gal.
Foam Frac	Nitrogen/water mixture with a foaming agent to credit a planer fracture.	Yes	Yes, Size and rate sensitive	Excellent	Sand at low average concentration because sand only added to liquid.
Emulsion Frac	Polymer water in oil emulsion carrying sand and other proppant to make a planar frac.	Yes	Yes	Excellent Viscosity tailored to job.	Sand, Super Sand or Bauxite at any concentration to 8 lb/gal.
Cool Frac	High rate water or polymer frac to create a planar water fracture in a hot formation.	Yes	Yes	Fair to Good	Sand at low concentrations (small sand to 20/40 mesh).
Super Sand Frac	Use of a cohesive proppant to prevent sand movement and loss of fracture conductivity at high closure stress-uses any fluids to make a planar frac.	Yes	Yes	Good, Size sand for job	Super Sand - a cohesive proppant retains permeability under high closure.
Bmundmd/Gravity Frac	Use of various densities of fluids, diverting agents, spacers, and proppant to control fracture vertical height and create a long planar frac.	Yes	Yes Height control	Fair to Good	Varies from Nylon, Plastics to sand, Super Sand to Bauxite and steel shot. Also diverting agents, spacers, & sealant.
Matrix Acidize	Low rate acid injection	Yes	No	Poor to None	None
Acid Frac	High rate acid injection to create an unpropped planar frac.	Yes	No	Poor	Usually only 100 mesh sand low concentrations.
Chemical Inhibitor	Injection of special chemicals & surfactants to control corrosion, inhibit reactions and to lower surface tension.	Yes	No, unless large or combination treatments.	Fair to Poor	Sand at low concentrations.
Erosion Frac	Injection of various fluids at high rates to help clean damage and fine away from wellbore. Makes a planar frac.	Yes	Yes, if also large volumes	Fair to good.	Any abrasive proppant material 1 to 4 lb/gal usual concentration.

Chemical Effects	Fluid Compatibility	Formation Damage	Application to Geothermal Reservoirs	Comments
Minimal	Water has to be compatible.	Minimal if water is compatible w/formations.	Yes, in certain areas to overcome wellbore damage by scale and to reduce pressure drop.	Plain water will not be as widely used as gelled water since it has no limit in safety factors.
Minimal	Water has to be compatible.	Minimal if water is compatible w/formations.	Yes, for increased production fractures and fractured zones.	Good potential technique for fractured formations.
Minimal	Water has to be compatible.	Minimal if water is compatible w/formations.	Yes, for increased production fractures and fractured zones.	Good potential technique for fractured formations.
Water Analysis + Polymer Chemistry.	Water has to be compatible	Polymer debris can damage, check w/core tests.	Yes, standard method.	Good potential in general geothermal work.
Water Analysis + Polymer Chemistry.	Water has to be compatible.	Check for damage, cross-link breakage, polymer breakage, residue.	Yes, but temperature sensitivity and cost may moderate or minimize use.	Fair potential in special geothermal work.
Surfactants have complex chemistry	Water compatible	Minimal with water & chemistry checked.	No, cost and temperature sensitivity minimize effectiveness.	Poor potential because major attribute of quick clean up required.
Oil, Water & surfactant chemistry check	Complex compatibilities	Usually minimal if checked out thoroughly with reservoir.	No, oil is not wanted in a geothermal well.	Not under consideration for geothermal, widely used in oil and gas wells.
Minimal short-time fractures, quick trtmt.	Water compatible	Usually minimal.	Yes, high rates give good margin for error-extend fracture into very hot reservoir.	Good potential for long planar fracs in all types of geothermal reservoirs.
Minimal phenolic formaldehyde resin.	Water compatible	Minimal because no fines movement Super Sand is good downhole filter.	Yes, no sand flow back permanent stimulation.	Good potential in combination with cool, gelled and kiel-dendritic fractures techniques.
Check heavy & Lt. fluids because density is modified chemically-salts, etc.	Check any fluids used.	Intentional damage on top or bottom of fracture.	Possible, special situation.	Complex technique may be required in areas of low data input.
HCL or HF extreme	Before & After Reaction.	Possible and Temp. Effects	Possible, but not likely.	High-Temperature effects unknown.
HCL, HF, or organic acid extreme.	Before & After reaction.	Possible and Temp. Effects.	Possible in certain applications.	High-Temperature effects unknown.
Each chemical might have an effect.	Check overall system for compatibility	Could have damage capability, ch.	Maybe required in certain reservoir for long-term production.	Potential and need unknown at this time.
Minimal but check any new fluid.	Water Compatible	Minimal by high rate.	Yes, may be necessary for maximum flow conditions and scale removal.	Potential appears good, needs more evaluation.

Fig.1 Temperature Effects on 20/40 Brady Texas Sand

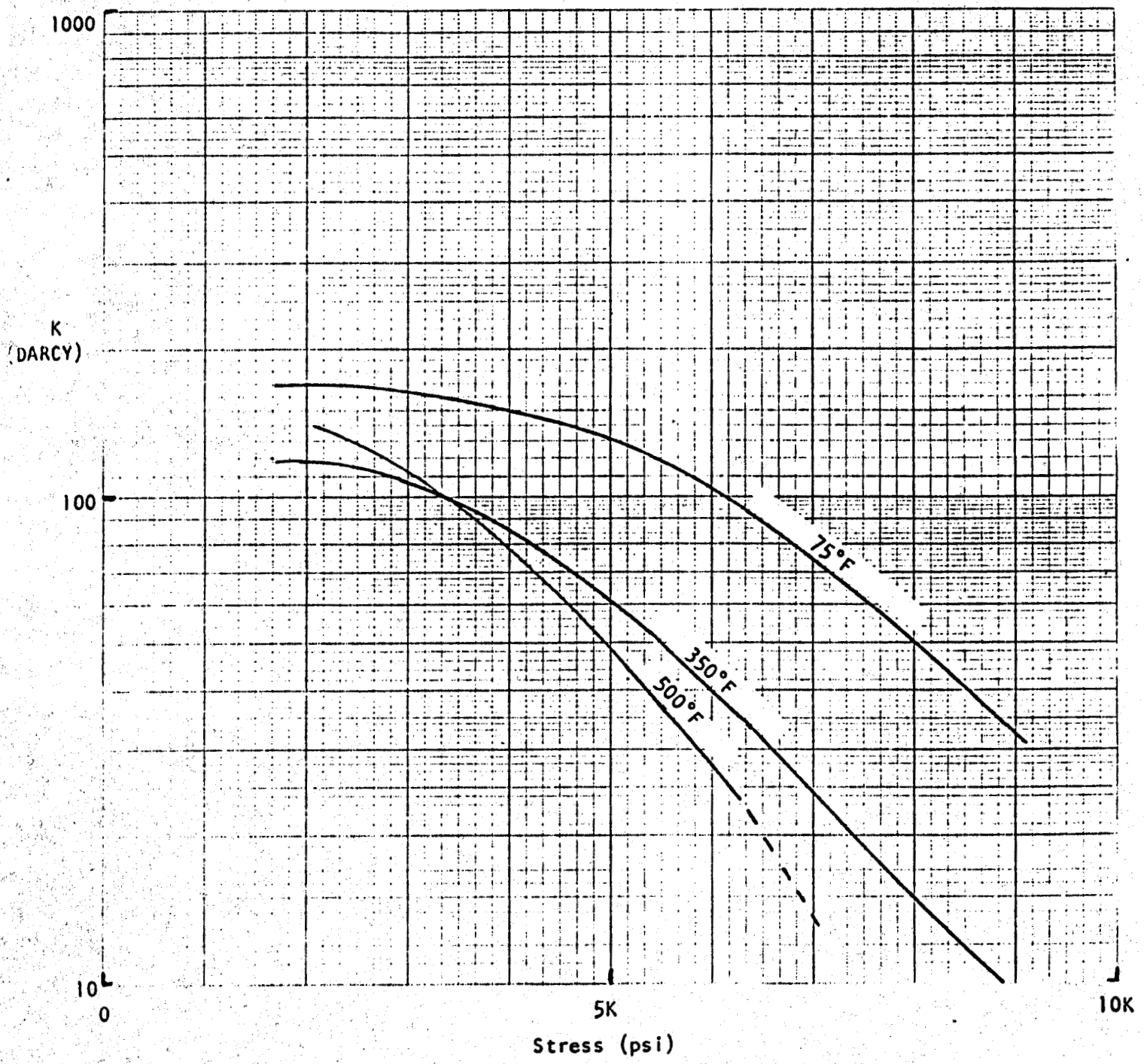

Fig. 2 Loss of Permeability with Increasing Closure Stress and Temperature for Three Frac Sands.

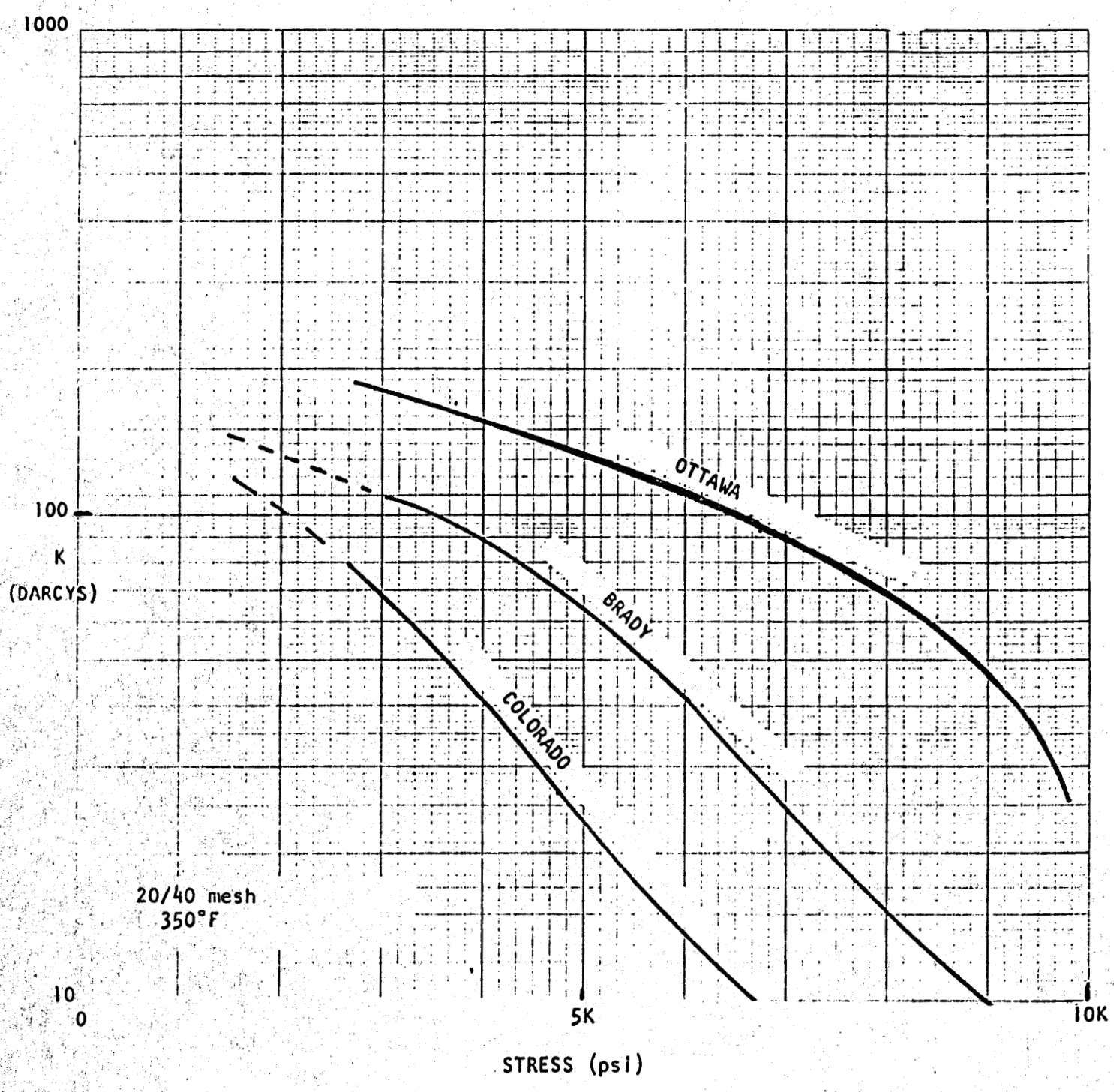

Fig. 3 Permeability versus Closure Stress Temperature Insensitive Proppants.

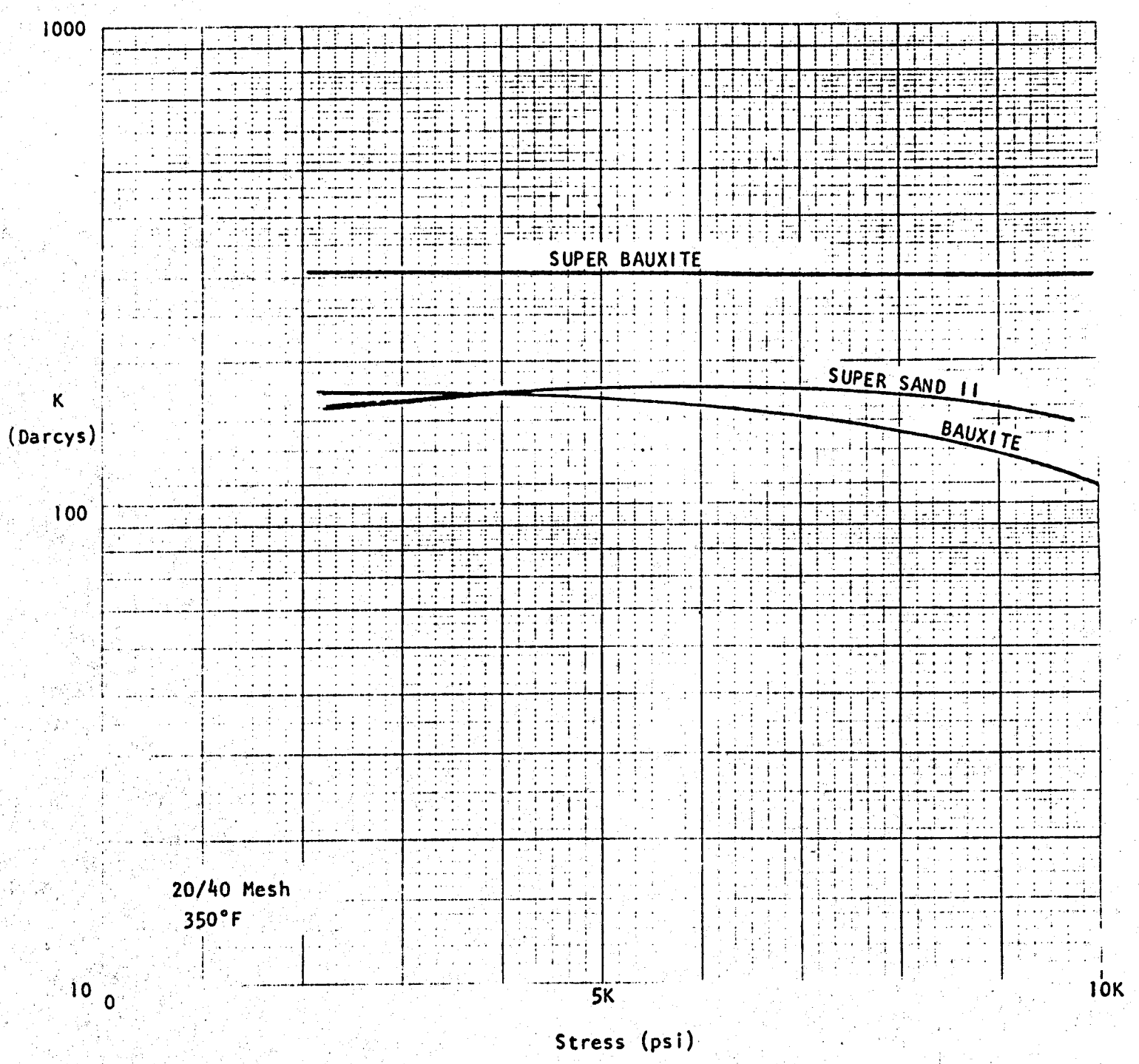

Fig. 4 Permeability of Glass Beads Versus Closure Stress and Temperature.

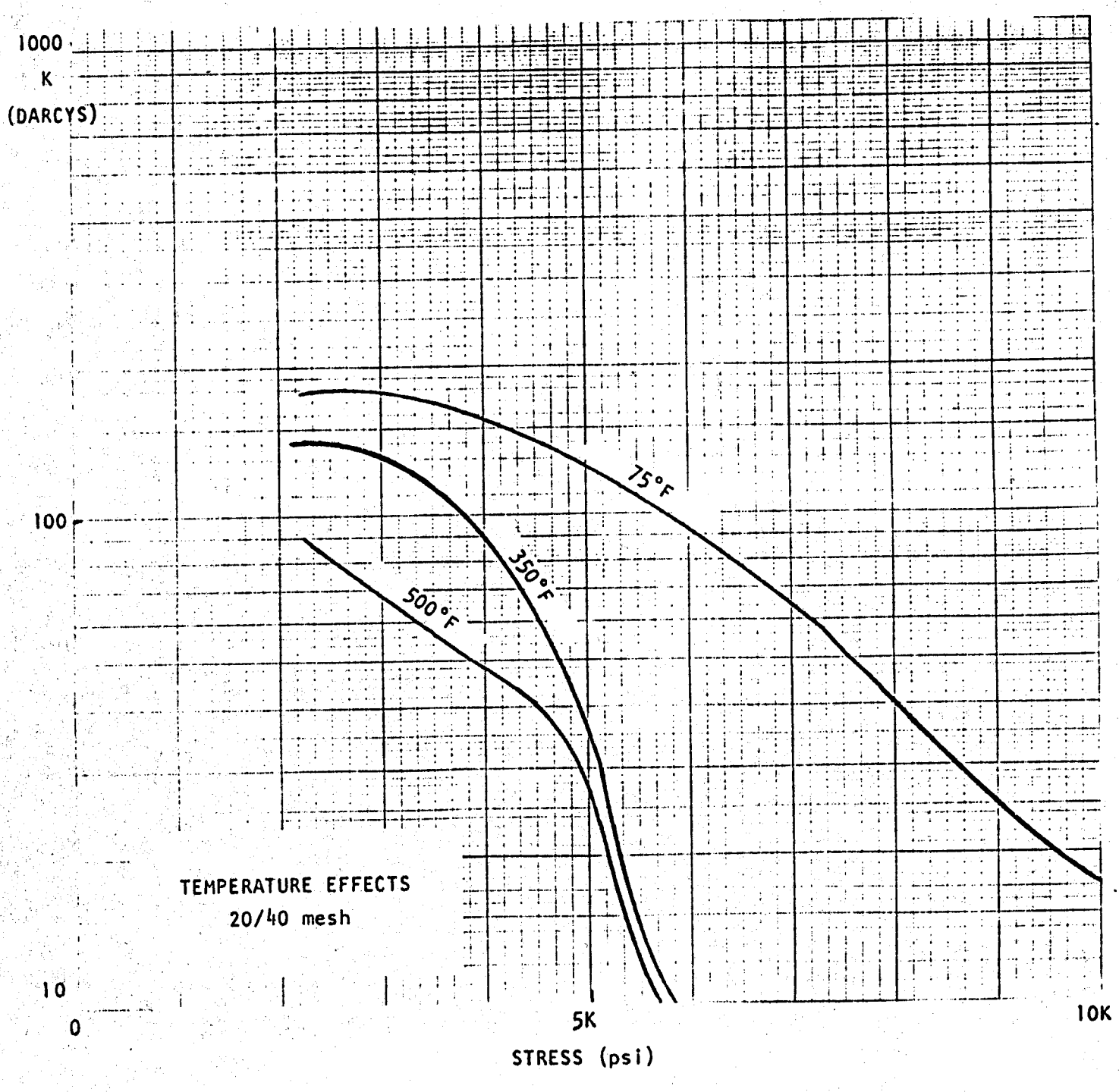

Fig. 5

VISCOSITY ($170\ SEC^{-1}$) VERSUS TEMPERATURE OF H P GUAR (1%) AND METHYL ALCOHOL, (5%)

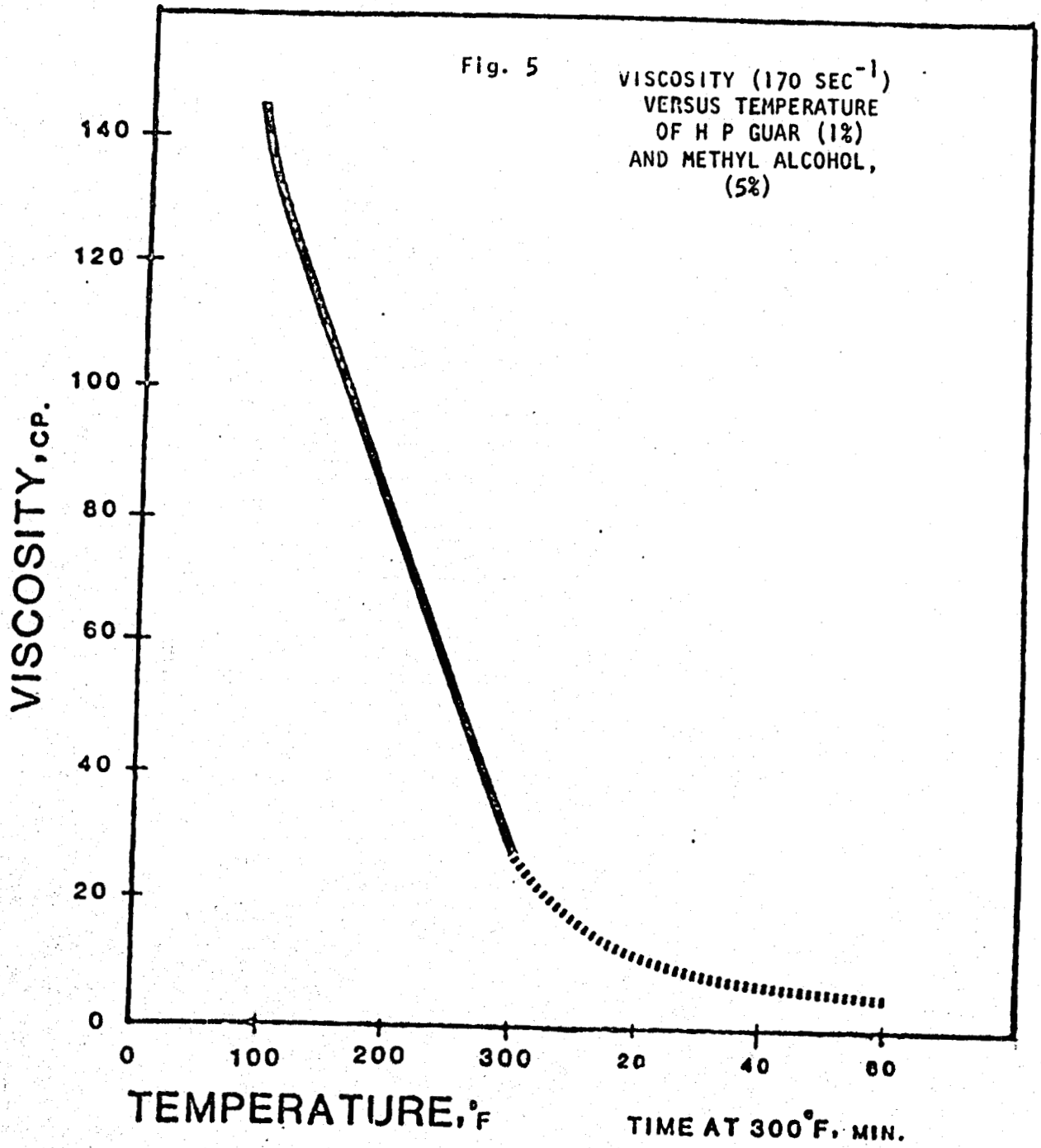

Fig. 6 POLYMER A VISCOSITY VERSUS TEMPERATURE WITH AND WITHOUT METHANOL

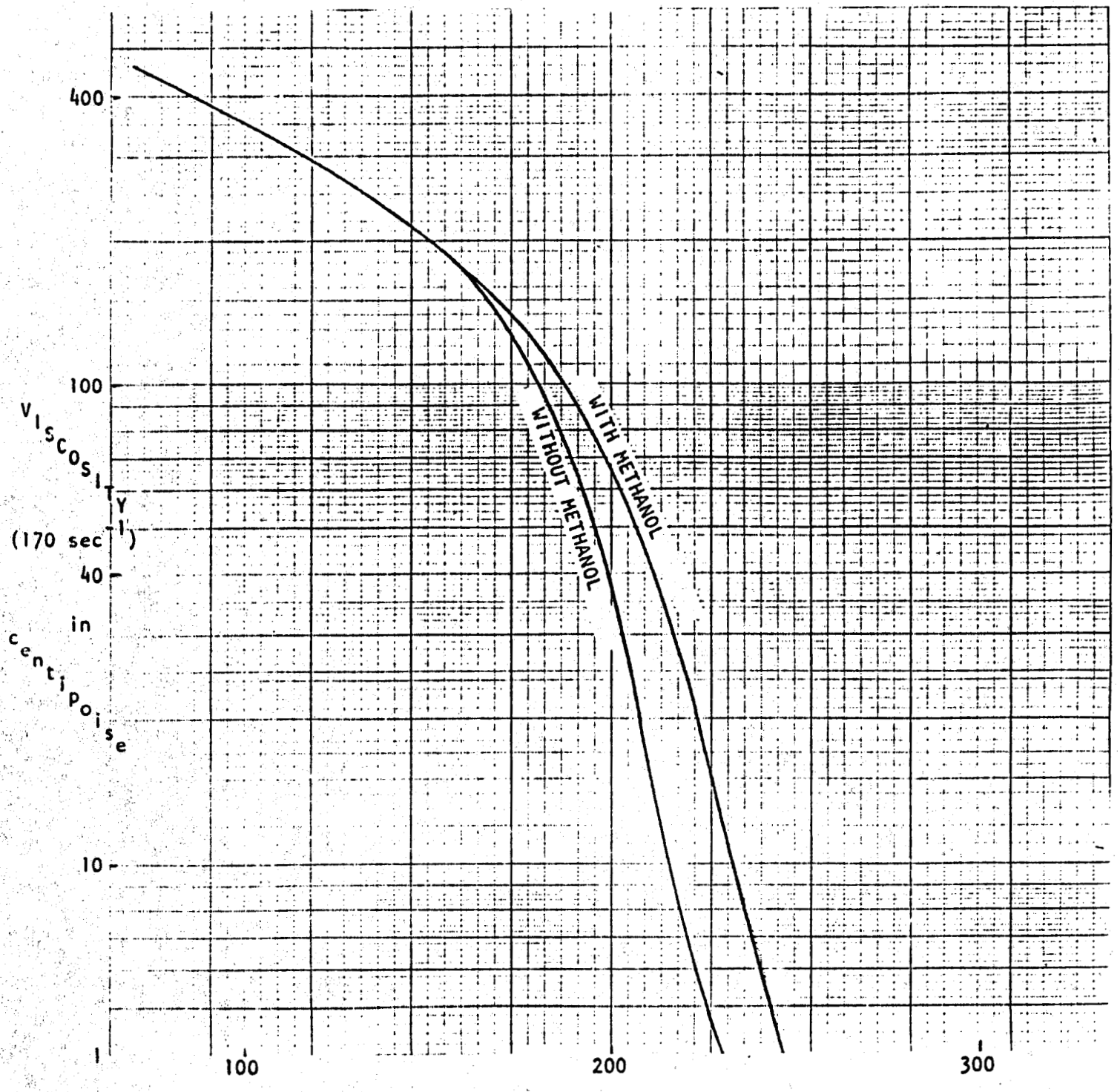

FIGURE 7 VISCOSITY vs. TEMPERATURE FOR POLYMER B

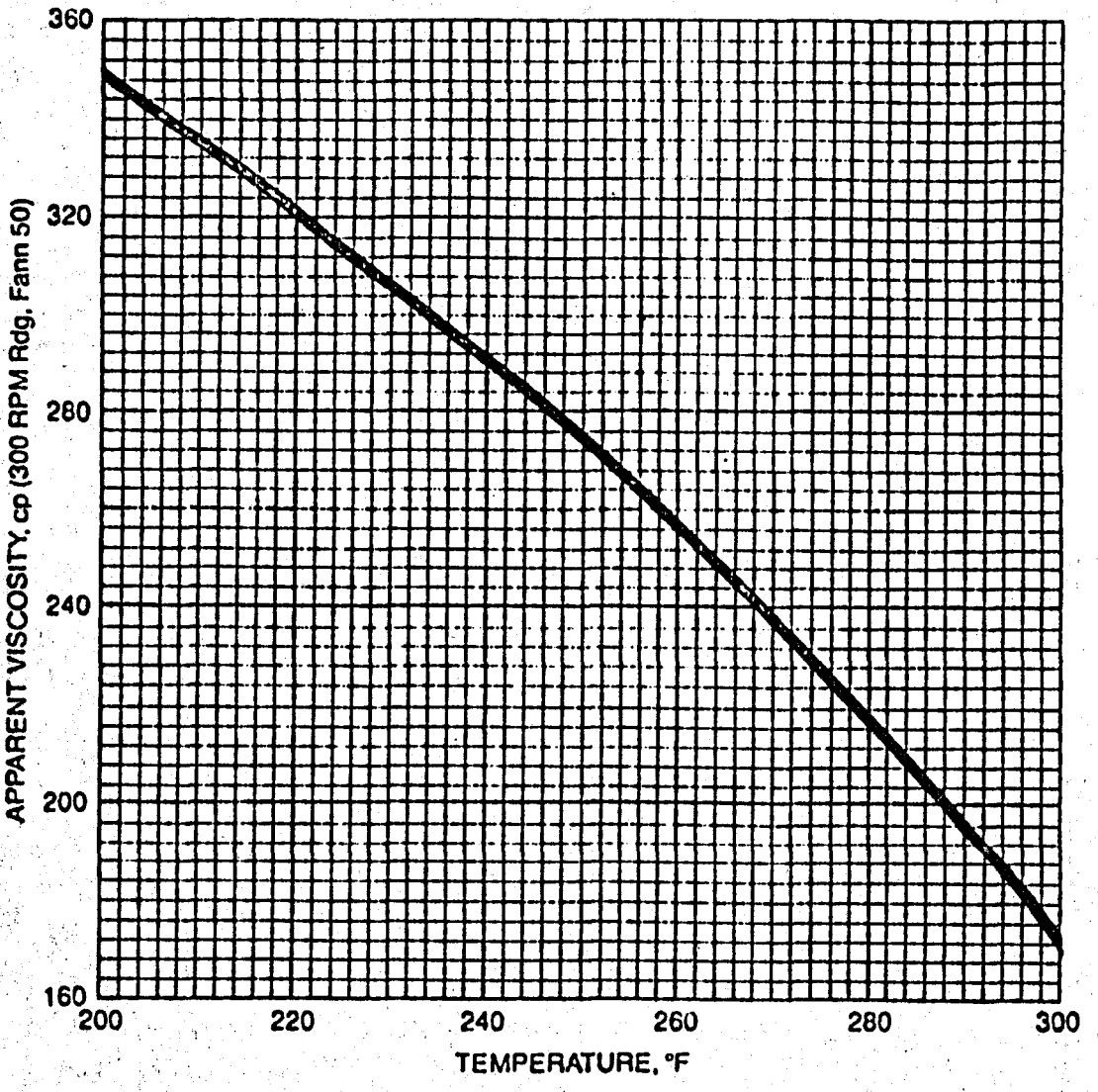

FIGURE 8 VISCOSITY vs. TEMPERATURE FOR POLYMER C

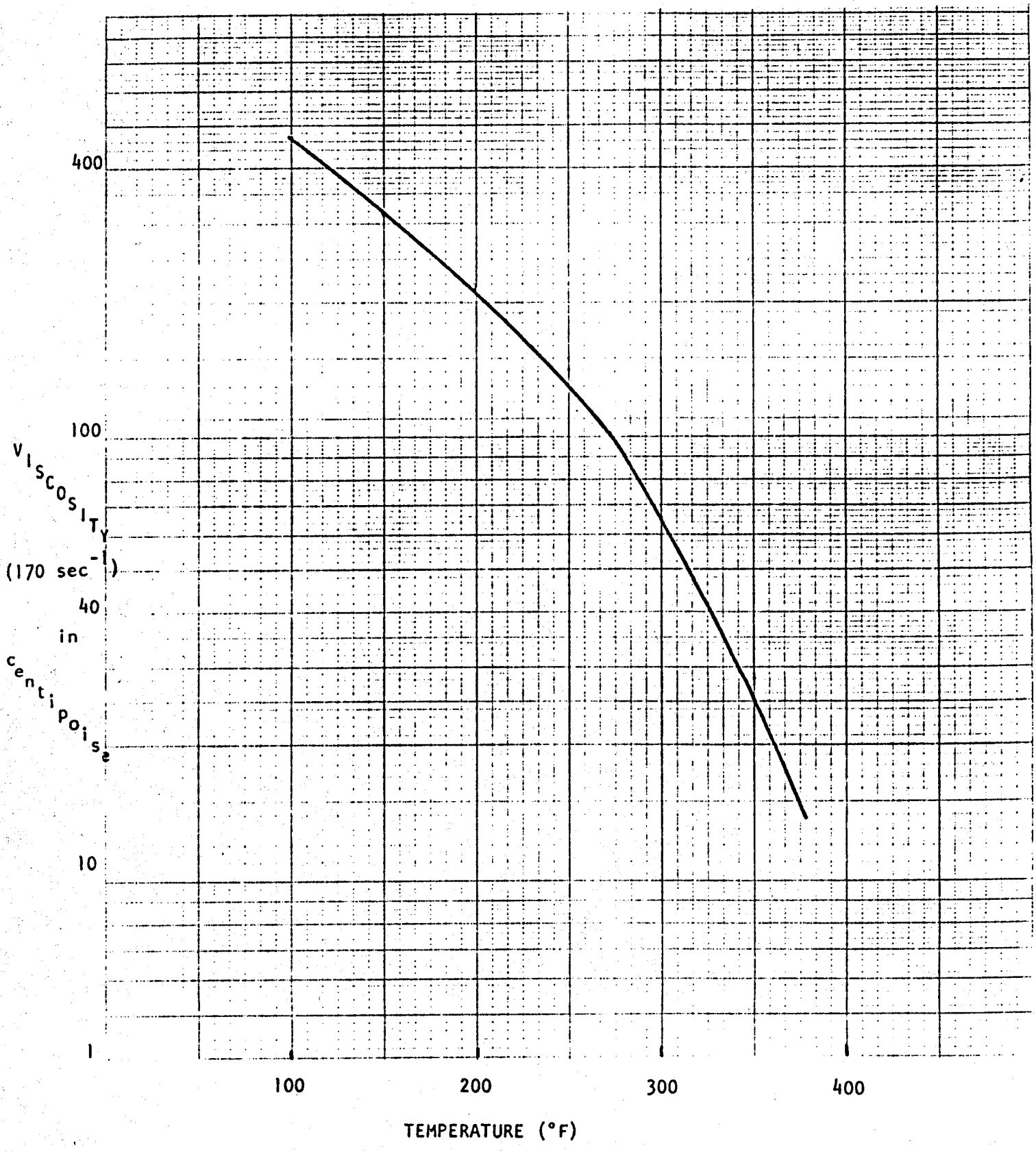

FIGURE 9 VISCOSITY vs. TEMPERATURE FOR POLYMER D

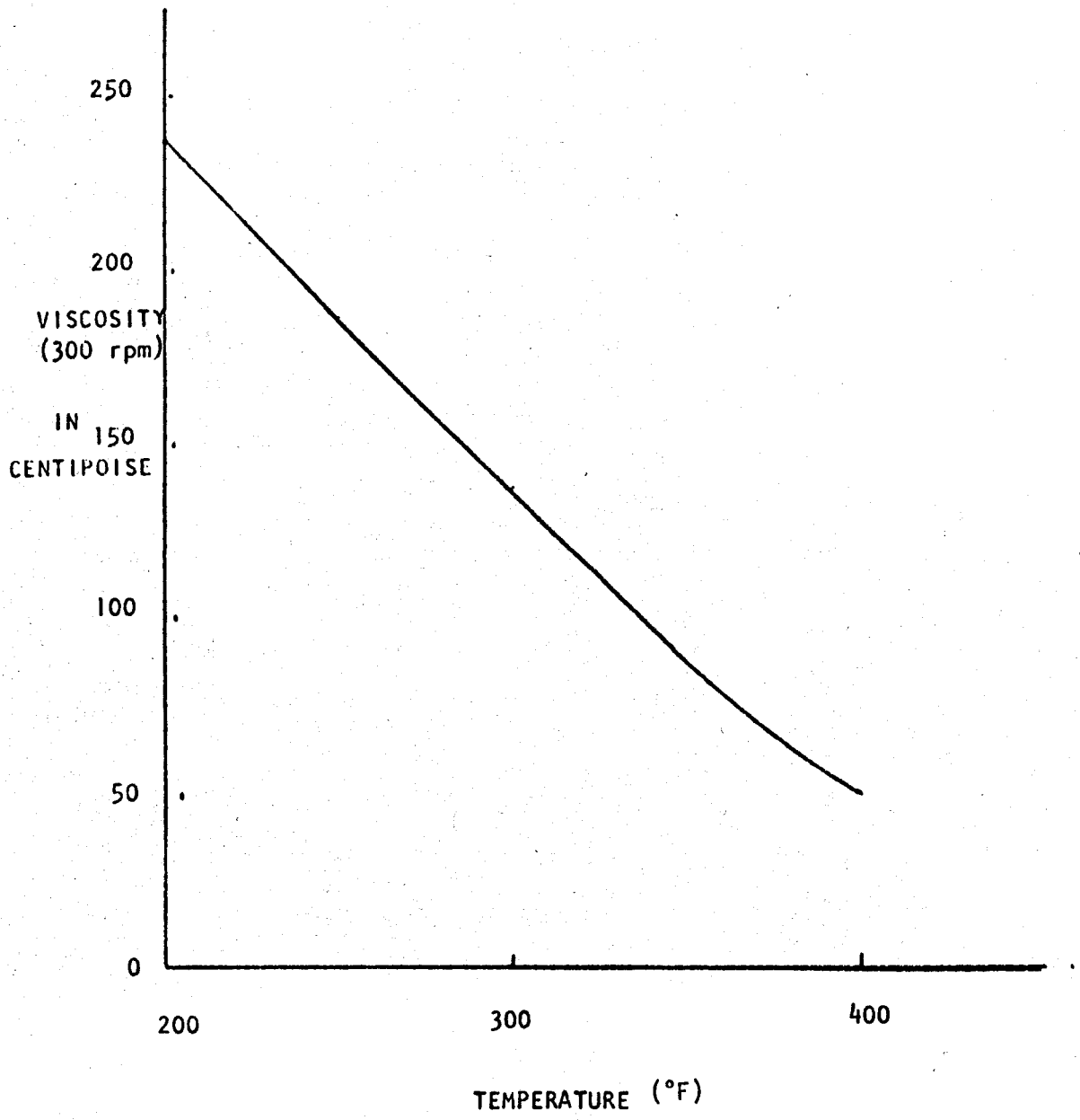

SESSION TWO

PROPPANTS AND PROPPANT TRANSPORT
Ali Daneshy
HALLIBURTON SERVICES

FRACTURE DESIGN MODELLING
Henry Crichlow
Petroleum Training and Technical Services

MATHEMATICAL TREATMENT OF TRACER BEHAVIOR IN A FRACTURE
Ottomar Vetter
VETTER RESEARCH

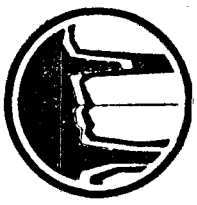

Published by permission of
SPE of AIME

Numerical Solution of Sand Transport in Hydraulic Fracturing

A. A. Daneshy, SPE-AIME, Halliburton Services

Introduction

Most hydraulic fracturing treatments are performed with a slurry composed of a fracturing fluid mixed with a propping agent. The propping agent usually consists of sand particles varying in size from 4 to 60 mesh. High-strength glass beads of the same sizes also are used occasionally. The dominant use of sand as a propping agent has resulted in frequent substitution of the term "sand" for propping agent. The two terms will be used interchangeably in this paper.

The reason for using a propping agent is simple. At the end of a fracturing treatment, the hydraulic fracture has to be kept open so that the reservoir fluid can flow through it. A propping agent serves this purpose and has to meet certain requirements. A proppant must be introduced in sufficient amounts, and individual particles should be strong enough so that they will not be crushed by the action of the in-situ stresses. Furthermore, the sand bed should be conductive enough to transmit the reservoir fluid flowing into it.

Although particle transport is well established in chemical engineering, most research has been conducted on flow through cylindrical pipes. The available research for particle transport through parallel plates is scarce. One of the first investigations of proppant transport in hydraulic fractures was conducted by Kern *et al.*,[1] who considered bed buildup for vertical fractures. After several studies of proppant movement in horizontal fractures,[2-4] bed buildup in vertical fractures was treated by Babcock *et al.*[5] In their comprehensive study, these authors conducted a theoretical and experimental investigation of the proppant movement and deposition between two parallel plates with limited vertical extent. Schols and Visser[6] investigated the mechanics of bed buildup and related it to particle size. Van Domselaar and Visser[7] considered proppant concentration in a fracture created by a viscous gel in which there is no particle settlement.

An attempt is made to consider proppant settlement in hydraulic fractures with conditions similar to those encountered in the field. Allowing for a change in either the proppant type or concentration during treatment, this study includes (1) the influence of fluid leak-off on fracture geometry and the concentration of the proppant in it, and (2) consideration of pseudoplastic as well as Newtonian fluids. The results were obtained by numerical computations carried out with a computer.

0149-2136/78/0001-5636$00.25

Proppant Deposition in Hydraulic Fractures

The determination of a proppant schedule usually involves the fracture geometry.

Suppose L denotes the length, ω_{max} the wellbore width, and h the height of an induced vertical hydraulic fracture. Assuming that q, the fluid injection rate, stays constant during treatment, that the treatment fluid does not change, and that h is constant, then the variations of L and ω_{max} with treatment time, t, can be expressed as[8]

$$L = A_1 t^{m_1}, \quad \ldots\ldots\ldots\ldots\ldots\ldots\ldots\ldots (1)$$

$$\omega_{max} = A_2 t^{m_2}, \quad \ldots\ldots\ldots\ldots\ldots\ldots\ldots\ldots (2)$$

A numerical solution is developed for the deposition of a propping agent inside a hydraulic fracture. Such parameters as fluid leak-off into the formation, increase in sand concentration caused by leak-off, non-Newtonian fracturing fluids, hindered settling velocity, and an up-to-date geometry are taken into consideration. Three examples investigate the proppant deposition for low-, medium-, and high-viscosity fracturing fluids.

where A_1, A_2, m_1, and m_2 are constants whose values depend on the treatment parameters. (A_1 is usually a number in tens, while A_2, m_1, and m_2 are in tenths.) The time (t) is related to the injected volume (V) and rate (q) by

$$V = qt. \quad \ldots\ldots\ldots\ldots\ldots\ldots\ldots\ldots\ldots\ldots (3)$$

Generally, the first fluid pumped inside the fracture does not contain any propping agent. This fluid is called "pad" and its volume is called "pad volume." The pad volume serves several purposes in fracturing. Two of these purposes are particularly important in sand transport. When the first proppant particles enter the fracture, the fracture width must be wider than the particle diameter. To avoid any particle bridging, a fracture width must be at least two or three times larger than the particle diameter. This gives a lower limit for the pad volume whose value can be computed from Eqs. 2 and 3 as $1/m_2$, giving

$$V_p > q\left(\frac{\alpha\omega_{max}}{A_2}\right)^{1/m_2}, \quad \ldots\ldots\ldots\ldots\ldots\ldots (4)$$

where V_p denotes the pad volume and α normally has a value of 2 or 3. The pad volume sometimes serves another purpose, too. As the proppant moves along the fracture length, its concentration continually increases because of fluid loss into the formation. If the fracturing fluid is viscous enough, the proppant may approach the fracture tip and still be suspended in the fluid. In such instances, the proppant becomes immobile inside the fracture because either (1) fluid loss is so high that the slurry is essentially a packed sand column, or (2) the local fracture width is so small that the sand is trapped in the fracture and the fluid moves through, leaving the sand behind. Both instances result in unusually high, undesirable treatment pressures. This problem is overcome by increasing the pad volume, which keeps the proppant away from the fracture tip.

A propping agent usually is introduced in small concentration and size. As treatment progresses, the sand concentration increases and also may consist of coarser particles. The proppant motion inside the fracture occurs horizontally, caused by fluid flow, and vertically (downward), caused by gravity. The horizontal velocity of the proppant is observed experimentally to equal the average fluid velocity; that is, the sand moves in the same column of fluid. The vertical sand velocity (usually referred to as "settling velocity") is governed by fluid properties as well as particle size and specific gravity (Appendix A).

As the proppant/fracturing-fluid slurry moves in the fracture, sand concentration increases because of fluid loss into the formation. Increased sand concentration hinders sand settlement and, therefore, allows the sand to move farther into the fracture before being deposited at the fracture bottom. The mathematical expression for hindered settling velocity is presented in Appendix B. The increase in sand concentraton caused by leak-off is uniform along the fracture length. Initially, because of small leak-off rates at the wellbore, the sand concentration change is slow. As the sand moves closer to the fracture tip, the rate of concentration buildup increases. Near the fracture tip, the sand concentraton builds up rapidly and soon reaches critical values because of high leak-off rates.

Fig. 1 shows the free-motion settling velocities of various industrial proppants in fracturing fluids of different viscosities. For ease of comparison, the fracturing fluids are assumed to be Newtonian. There is a great difference among the settling velocities of the commonly used industrial propping agents. For example, in a fracturing fluid with 100-cp viscosity, 8-12 mesh sand has a settling velocity of about 0.145 ft/sec. This size sand takes about 11.5 minutes to drop from the top to the bottom of a 100-ft fracture. In the same fluid, 40-60 mesh sand has a settling velocity of about 0.004 ft/sec. This size of sand takes about 417 minutes to drop 100 ft. In other words, the 8-12 mesh sand settles approximately 36 times faster than the 40-60 mesh sand. If a 100-ft fracture

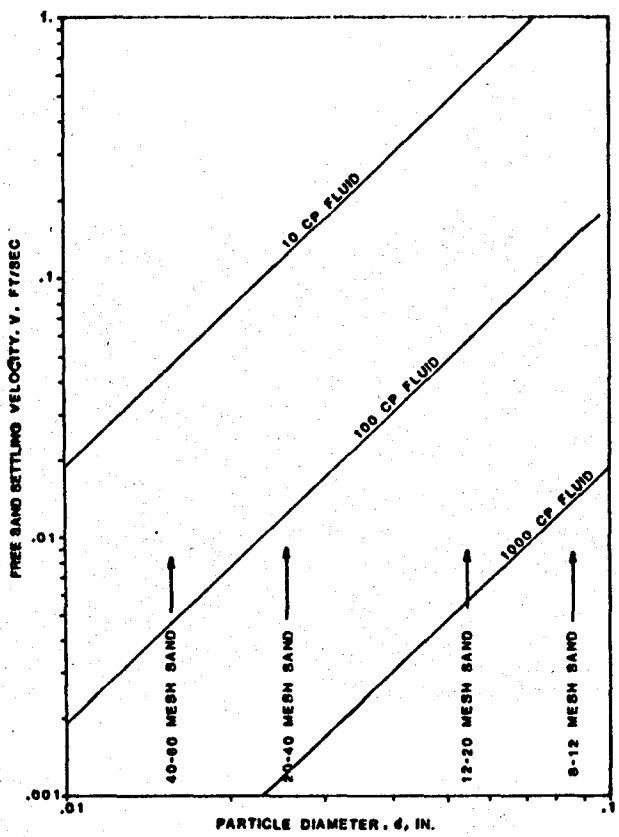

Fig. 1—Free-sand settling velocity vs sand diameter for three different viscosities of fluid.

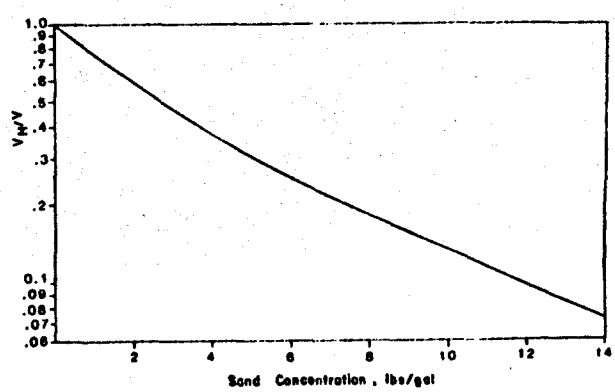

Fig. 2—Ratio of hindered vs free settling velocities for various sand concentrations.

is propped with 40-60 mesh sand and the treatment time is 2 hours (120 minutes), the maximum sand settlement will be about 29 ft. (The actual settlement will be smaller because of hindered settling that results from an increase in sand concentration.) Thus, the 100-cp fluid carries the 40-60 mesh sand to near perfect transport. However, if 8-12 mesh sand is used, most of the sand will settle at the bottom of the fracture. While a 100-cp viscosity fluid might be transporting the 40-60 mesh sand perfectly, this fluid cannot do so for 8-12 mesh sand.

Fig. 2 shows the effect of sand concentration on the settling velocity. It is a plot of the ratio of hindered settling velocity (actual settling velocity) vs the free-motion velocity for various sand concentrations. An increase in sand concentration greatly affects the settling velocity. For example, a 3-lb/gal concentrated sand settles at a rate of less than one-half that of the same sand in free motion.

An important point should be noted. From the discussion, one may conclude that it is always better to use finer sand to increase the propped area of the fracture. This is not always true. Coarser sands are more conductive and can transmit more fluid to the wellbore. Because the propping agent creates a conductive fracture, proppant selection should be based on optimizing well productivity.

Assume that all the propping agent used for a fracturing treatment is the same size. As this sand travels along the fracture length, a part of the sand settles to the fracture bottom and forms a bed. In time, this bed enlarges (Fig. 3a). The growth of the bed continues along the fracture length and height until the first sand particle introduced at the top of the fracture reaches the fracture bottom. Only then does the sand bed increase in height (Fig. 3b).

As the sand bed grows higher, it reduces the fracture area open to fluid flow. This results in an increase in fluid velocity. As fluid velocity increases with continued bed deposition, the velocity value becomes large enough to move the sand without depositing it. This velocity corresponds to a bed height designated the "equilibrium bed height," h_{eq}. The mathematics are presented in Appendix C. Once the bed height reaches h_{eq}, its growth tends to create a rectangular sand bed (Fig. 3c). The sand bed grows in this manner until angle θ (Fig. 3c) reaches the angle of repose (approximately 30°). Then the bed again begins to grow in length so that angle θ remains essentially constant.

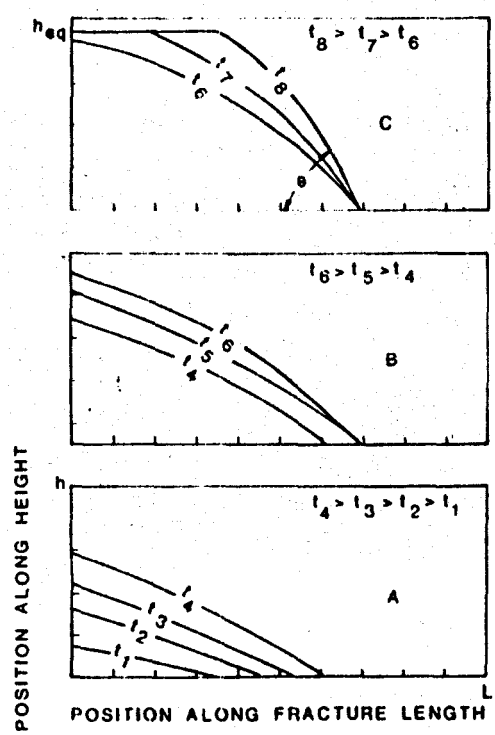

Fig. 3—Growth of the sand bed for uniformly sized particles.

Several points should be noted here. First, because most fracturing treatments usually begin with a finer sand and change to a coarser size during treatment, the sand bed seldom has a simple shape. Second, a viscosity low enough to deposit the sand in a bed is assumed. There are many cases where the fracturing-fluid viscosity is so high that it carries the sand in perfect transport. Therefore, the discussion of sand transport will be different. Third, the treatment time in some fracturing procedures may not be long enough to allow the bed deposition to experience all the stages. In such cases, three factors should be considered: (1) the deposited bed at the end of pumping, (2) the suspended sand at the end of pumping, and (3) the bed shape if all the sand is deposited into a bed, assuming that the fracture stays open long enough to allow the sand to be deposited after treatment.

Numerical Solution of Sand Transport

The numerical solution of sand transport uses a fracture geometry discussed in an earlier paper.[8] The fracture is divided into small elements. Treatment time also is divided into small increments. As the sand travels inside the fracture, sand condition is computed for each element length. This includes the calculation of the fluid volume loss, the resulting increase in sand concentration, the actual sand settlement velocity, the volume of deposited sand, the height of the deposited bed (based on the actual fracture width at that element), and the height of the sand in suspension. Integrating these parameters along the fracture length yields the sand-transport profiles at that time increment. As the time is increased continuously in the computation (until the treatment time is reached), the sand-transport profiles for various times during the treatment are obtained.

Final solution of the numerical computations gives the following sand-transport profiles:

1. Sand bed deposited at the end of pumping. A profile shows the position of the top of the sand bed deposited during fluid injection and along the fracture length.

2. Sand in suspension at the end of pumping. Some of the sand pumped inside the fracture does not have enough time to settle into a bed. The position of the top of this sand and its concentration along the fracture length are variables computed in the solution.

3. Bed shape after total sand deposition. Another profile shows the position of the top of the bed formed along the fracture length if all the pumped sand was deposited in a bed.

This information is sufficient for a complete analysis of the sand deposition. Sand-transport Profiles 1 and 3 give obvious results. Profile 2 shows the bed shape and the suspended sand concentration if the fracture

closes on the sand immediately. If the fracture stays open long enough for all sand to settle, Profile 3 results. For any time between these two situations, the bed shape is determined from the information already provided in Profile 2. From the concentration and the location of the sand in suspension, new profiles can be computed for various times with the equations given in Appendixes A and B. Significant aspects of the numerical results are demonstrated best through example solutions for various treatment conditions.

Low-Viscosity Fluids

The important features of sand transport in low-viscosity fluids are the rapid settling velocity of the proppant and the ease of building a bed to equilibrium height. Fig. 4 depicts a typical example. The treatment conditions are listed on the right side of the figure. The hydraulic fracture is represented by the rectangle. The base of this rectangle denotes position along fracture length, with base length indicating the final fracture length created. The height of the rectangle denotes the fracture height.

In this example, the sand bed near the wellbore has reached equilibrium height. This bed has a step-like shape that results because the 20-40 mesh sand has a slower settling velocity than the 10-20 mesh sand and, therefore, has traveled farther in the fracture before reaching bottom.

The transport profile has only one curve, which is the bed height after total sand deposition. This occurs because at the end of fluid pumping, the sand in suspension constitutes a small percentage of total sand and settles rapidly. Therefore, this sand can be ignored without loss. The carrying distance of the sand is about 2.8×10^2 ft, and the sand covers about 40 percent of the created fracture area.

Fig. 4 contains a graphical representation of fracture geometry changes with time, expressed by Eqs. 1 and 2. Because in most industrial treatments the size of a fracturing operation usually is defined by volume rather than time, Eqs. 1 and 2 are modified to show L and ω as functions of volume. This axis is used to read the variations of fracture length and maximum fracture width with volume. For any given injected volume, one can identify the point corresponding to that volume on the axis and can read the maximum fracture width from the divisions above the axis. (For example, for an injected volume of 2.1×10^4 gal, the maximum fracture width is slightly larger than 0.15 in.) To determine the corresponding fracture length, draw a line normal to the axis at the point under consideration. The intersection of this normal line with fracture length yields the length (2.8×10^2 ft for the example).

A graph (Fig. 4) is a compact but complete way of demonstrating the results of a fracture geometry and sand-transport computations.

Another fracture design is given in Fig. 5 to show the significance of the graphical display method. The amount of injected sand is small in this design, which results in a poor bed. This conclusion can be drawn rapidly by simply looking at Fig. 5. Note that the examples in Figs. 4 and 5 indicate the sand traveled about the same distance in the fracture.

The transport profiles consist of three curves in Fig. 5. The top curve, marked Δ, denotes the sand in suspension at the end of pumping. The bottom curve, marked x, denotes the deposited bed at the end of pumping. The curve marked * shows the bed shape if all the sand in

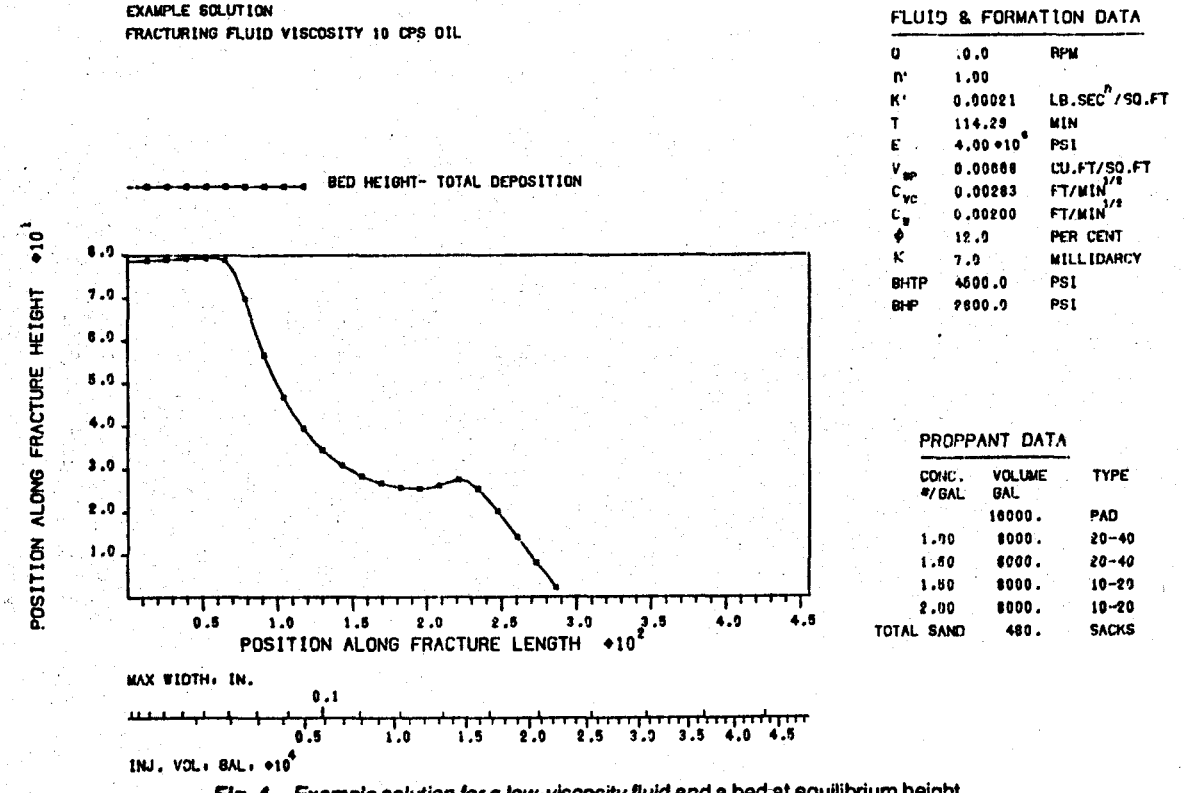

Fig. 4—Example solution for a low-viscosity fluid and a bed at equilibrium height.

suspension was deposited on top of the existing bed. The sand in suspension has two parts. One part is near the fracture tip and is mainly 20-40 mesh sand. The other part near the wellbore is 10-20 mesh sand. The concentrations of these sands are given at the top of the rectangle. The numbers on the axis give the sand concentrations. The location of the tick mark corresponds to position along the fracture length as indicated at the bottom of the rectangle. The 20-40 mesh sand in suspension is shown to have a concentration of 3.1 lb/gal at about 230 ft in the fracture, while the 10-20 mesh sand concentration is 2.2 lb/gal at about 40 ft in the fracture. Although the concentration of both sand types increases, the 20-40 mesh sand has a higher increase because this sand remains in the fracture longer.

Fig. 5 also shows the differences in the settling velocities of various sand sizes. After traveling about 80 ft in the fracture, the 10-20 mesh sand reaches the fracture bottom. The 20-40 mesh sand travels about 275 ft in the fracture and is still in suspension. This explains the irregular shape of the deposited bed.

Medium-Viscosity Fluids

Fluid viscosities ranging to about 200 cp fall in this category. The important characteristic of proppant transport for such fluids is the irregularity of resulting sand beds. While medium-viscosity fluids can carry finer particles for large distances, coarser sizes settle to the bottom much faster, yielding beds such as those in Fig. 6. In this example, the fracturing fluid is assumed to be Newtonian with 50-cp viscosity. The 20-40 mesh sand pumped at the beginning of sand injection is still in suspension inside the fracture, and its concentration has increased from 1.0 to 3.1 lb/gal and from 2.0 to 3.7 lb/gal, respectively. The 10-20 mesh sand pumped at 2.0 lb/gal has settled completely in the fracture near the wellbore. The 10-20 mesh sand pumped at 3.0 lb/gal has settled partially. The shape of the deposited bed near the wellbore shows the smaller carrying distance of the 10-20 mesh sand at 2.0 lb/gal (compared with 3.0 lb/gal). This shape is caused by the sand's higher hindered settling velocity (lower concentration).

The curve indicating bed shape after total sand deposition is irregular in shape and consists of two higher beds joined by a narrow one in the middle. If such bed shapes are undesirable for a specific treatment, the problem can be overcome easily by selecting one size of proppant.

Fig. 6 clearly demonstrates the effect of sand size and concentration on the bed deposition. Such cases usually are encountered with medium-viscosity fluids.

High-Viscosity Fluids

This range covers viscosities that are sufficient to carry the sand in perfect transport. An example of such a fluid is shown in Fig. 7. The deposition profiles have two curves — sand in suspension and bed height at the end of pumping. As Fig. 7 indicates, the deposited sand at the end of pumping constitutes a minor part of the injected sand. Nearly all the injected sand is in suspension and has an almost rectangular shape. The minor irregularity in the shape is caused by variations in settling velocities resulting from particle diameter and differences in proppant concentration. Fig. 7 also shows the changes in sand concentration resulting from leak-off. For example, the initial sand pumped at 1.0 lb/gal is occupying the tip of the fracture and has a concentration of 2.0 lb/gal.

One of the difficulties normally encountered in the design of hydraulic fractures with high-viscosity fluids is

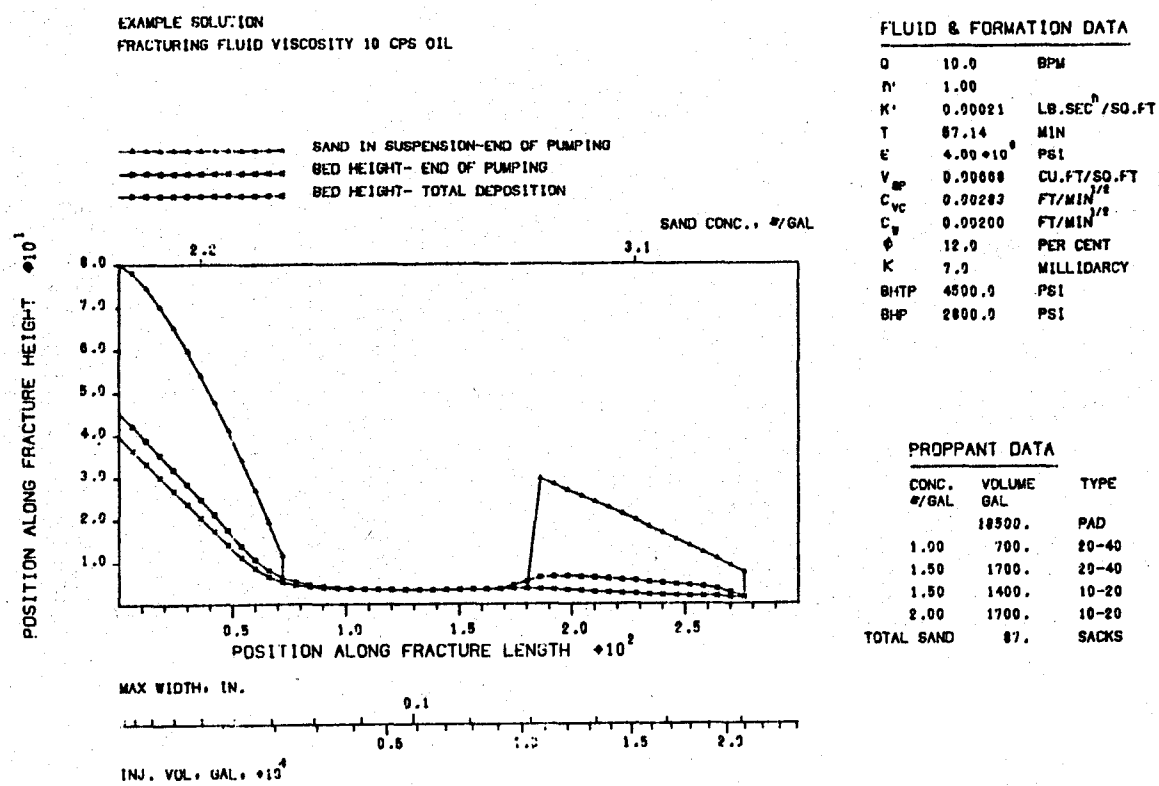

Fig. 5—Example solution for a low-viscosity fluid with insufficient sand.

computation of the pad volume. An optimum pad volume is usually large enough so that the sand does not reach high concentration at the fracture tip, yet is small enough to let the sand approach the fracture tip at acceptable concentrations. This problem can be overcome by using the numerical method presented in this paper. If the assumed pad volume does not satisfy the required conditions, the computer can be programmed to find the optimum value by a trial-and-error method, and carry out the calculations with the computed pad volume. The example in Fig. 7 shows such an optimization. This fracture is covered almost totally with sand.

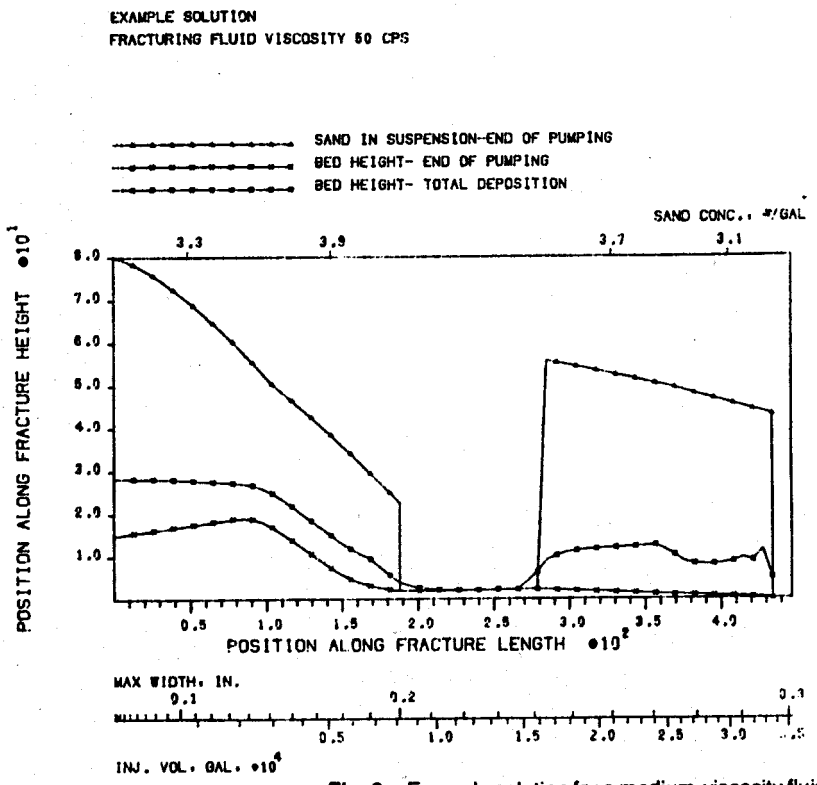

FLUID & FORMATION DATA

Q	10.0	BPM
n'	1.00	
K'	0.00104	LB.SEC^n/SQ.FT
T	83.33	MIN
E	4.00 •10^6	PSI
V_{SP}	0.00267	CU.FT/SQ.FT
C_{VC}	0.00258	FT/MIN$^{1/2}$
C_w	0.00150	FT/MIN$^{1/2}$
ϕ	12.0	PER CENT
K	7.0	MILLIDARCY
BHTP	4500.0	PSI
BHP	2800.0	PSI

PROPPANT DATA

CONC. #/GAL	VOLUME GAL	TYPE
	20000.	PAD
1.00	2400.	20-40
2.00	3200.	20-40
2.00	3900.	10-20
3.00	6500.	10-20
TOTAL SAND	331.	SACKS

Fig. 6—Example solution for a medium-viscosity fluid.

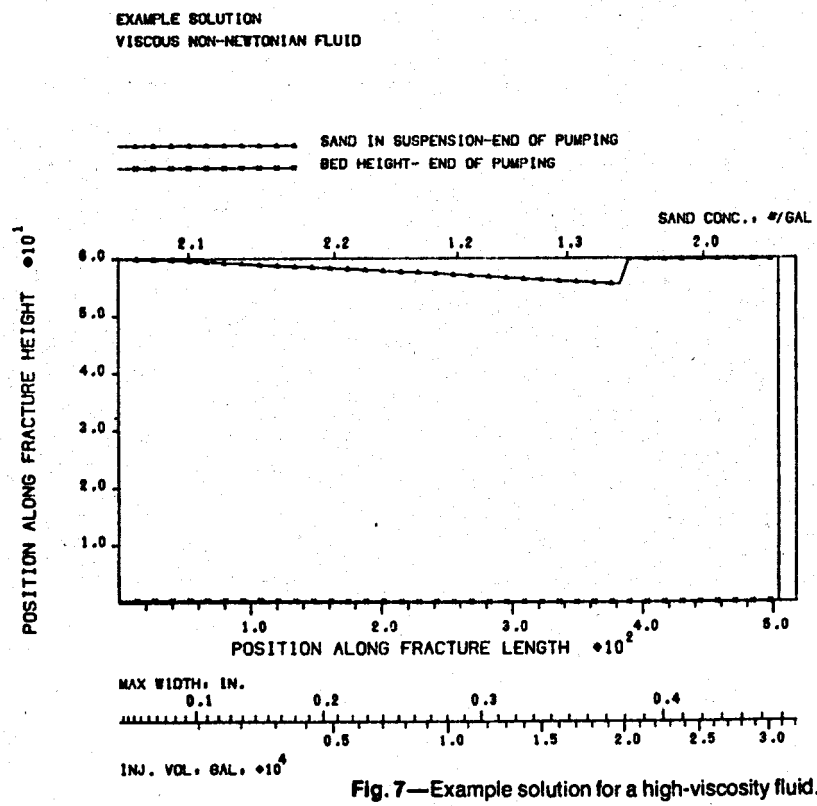

FLUID & FORMATION DATA

Q	10.0	BPM
n'	0.31	
K'	0.08200	LB.SEC^n/SQ.FT
T	76.19	MIN
E	3.70 •10^6	PSI
V_{SP}	0.00668	CU.FT/SQ.FT
C_{VC}	0.00416	FT/MIN$^{1/2}$
C_w	0.00100	FT/MIN$^{1/2}$
ϕ	18.0	PER CENT
K	12.0	MILLIDARCY
BHTP	4800.0	PSI
BHP	2900.0	PSI

PROPPANT DATA

CONC. #/GAL	VOLUME GAL	TYPE
	14000.	PAD
1.00	4000.	20-40
1.00	6000.	10-20
2.00	8000.	10-20
TOTAL SAND	260.	SACKS

Fig. 7—Example solution for a high-viscosity fluid.

Summary

1. A numerical method is developed for the solution of sand transport in hydraulic fractures. This solution includes such factors as fluid leak-off, the resulting increase in the sand concentration, and the subsequent decrease in the sand settling velocity.

2. The numerical method can be used to compute the sand transport with varying sand concentrations and types, similar to actual field practice.

3. The numerical method allows the computation of an optimum pad volume for fracturing treatments conducted with high-viscosity fluids.

4. This paper recommends the use of sand-transport profiles when considering particle transport in hydraulic fracturing.

Nomenclature

A_1, A_2 = constants
C_w = fluid loss coefficient
d = particle diameter
E = Young's modulus
f_{vsl} = volume fraction of slurry occupied by the fluid
F = drag coefficient
g = gravity acceleration
h = fracture height
h_{eq} = equilibrium bed height
k = formation permeability
K = absolute fluid consistency
K_n = fluid consistency for flow between two infinite parallel plates
L = fracture length
m_1, m_2 = constants
n = fluid flow behavior index
N_{Re} = Reynold's number
q = fluid injection rate
r_H = hydraulic radius
t = fracturing treatment time
t_{eni} = the exposure time to fluid of point x_i at $t = t_n$
t_i = time at which fracture tip has reached point x_i
t_n = treatment time after n time increments
t_{sp} = spurt time
v = particle settling velocity
v_{eq} = equilibrium velocity
v_h = hindered settling velocity
$(v_w)_{eq}$ = friction velocity
V = volume injected inside the fracture
V_{fni} = volume of fracture in the ith element at t_n
V_{lni} = volume of fluid lost in the ith element at t_n
V_n = fluid volume injected during nth time increment
V_p = pad volume
V_{sp} = spurt volume
x_i = position of a point in the fracture
Y_{ni} = distance the leak-off fluid has penetrated the formation at x_i at t_n
α = constant
Δt_n = duration of a treatment time increment
Δh_s = change in the height of the suspended sand caused by settling
Θ = angle of repose of a sand bed
ϕ = formation porosity
ρ_{sd} = sand density
ρ_f = fluid density
ρ_{sl} = slurry density
v_{lmn} = fluid lost or leak-off between t_m and t_n
ω_{max} = fracture width at the wellbore
ω_i = fracture width at x_i

Acknowledgments

The author thanks the management of Halliburton Services for permission to publish this paper and is grateful for the many helpful suggestions provided by Jim Williams during this investigation.

References

1. Kern, L. R., Perkins, T. K., and Wyant, R. E.: "The Mechanics of Sand Movement in Fracturing," *Trans.*, AIME (1959) **216**, 403-405.
2. Wahl, H. A. and Campbell, J. M.: "Sand Movement in Horizontal Fractures," *J. Pet. Tech.* (Nov. 1963) 1239-1246; *Trans.*, AIME, **228**.
3. Wahl, H. A.: "Horizontal Fracture Design Based on Propped Fracture Area," *J. Pet. Tech.* (June 1965) 723-731; *Trans.*, AIME, **234**.
4. Lowe, D. K. and Huitt, J. L.: "Propping Agent Transport in Horizontal Fractures," *J. Pet. Tech.* (June 1966) 753-764; *Trans.*, AIME, **237**.
5. Babcock, R. E., Prokop, C. L., and Kehle, R. O.: "Distribution of Propping Agents in Vertical Fractures," *Prod. Monthly* (Nov. 1967) 11-18.
6. Schols, R. S. and Visser, W.: "Proppant Bank Buildup in a Vertical Fracture Without Fluid Loss," paper SPE 4834 presented at the SPE-AIME European Spring Meeting, Amsterdam, May 29-30, 1974.
7. Van Domselaar, H. R. and Visser, W.: "Proppant Concentration in and Final Shape of Fractures Generated by Viscous Gels," *Soc. Pet. Eng. J.* (Dec. 1974) 531-536.
8. Daneshy, A. A.: "On the Design of Vertical Hydraulic Fractures," *J. Pet. Tech.* (Jan. 1973) 83-93; *Trans.*, AIME, **255**.
9. Steinour, H. H.: "The Rate of Sedimentation," *Ind. Eng. Chem.* (1944) **36**.
10. Brown, G. G.: *Unit Operations*, John Wiley & Sons, Inc., New York (1951).

APPENDIX A

Settling Velocity

The rate of proppant bed deposition in hydraulic fractures depends on the settling velocity of the proppant inside the fracture. For a spherical particle in a power-law model fluid, the drag coefficient F is given by Stoke's law as

$$F = \frac{4}{3} \frac{\rho_{sd} - \rho_f}{\rho_f} \frac{gd}{v^2} \quad \ldots\ldots\ldots\ldots\ldots\ldots (A\text{-}1)$$

The drag coefficient is related to the Reynold's number, N_{Re}, by

$$N_{Re} = \frac{24}{F} \quad \ldots\ldots\ldots\ldots\ldots\ldots\ldots\ldots (A\text{-}2)$$

The Reynold's number is given by

$$N_{Re} = \rho_f \frac{v^{2-n} d^n}{K(3)^{n-1}}, \quad \ldots\ldots\ldots\ldots\ldots\ldots (A\text{-}3)$$

where n and K are the flow behavior index and the absolute consistency of the power-law model. Eqs. A-1 through A-3 can be combined to yield the particle settling velocity:

$$v = \left[\frac{(\rho_{sd} - \rho_f) g d^{n+1}}{18K(3)^{n-1}}\right]^{1/n}. \quad \ldots\ldots\ldots\ldots (A\text{-}4)$$

For hydraulic fracturing use, the fluid consistency for

flow between two infinite parallel plates, K_a, is preferred to K. These factors are related by

$$K = K_a\left(\frac{3n}{2n+1}\right)^n \quad \ldots\ldots\ldots\ldots\ldots\ldots \text{(A-5)}$$

Also, using engineering units of feet per second for v, inches for d, pound-seconds^n per square foot for K_a, pounds per cubic foot for ρ_{sd} and ρ_f, and substituting $g = 32.2$ lbf-ft/sec^2, Eq. A-4 becomes

$$v = \frac{(2n+1)d}{108n}\left[\frac{(\rho_{sd}-\rho_f)d}{72K_a}\right]^{1/n}. \quad \ldots\ldots \text{(A-6)}$$

APPENDIX B
Hindered Settling Velocity

The settling velocity, v, given by Eq. A-6, is for the free motion of a single particle. In hydraulic fracturing, the mixture of the fluid and the propping agent is usually a slurry. To compute the particle settling velocity in a slurry, one has to correct the free-motion velocity to account for two factors. First, the viscosity considered for particle settlement should be the viscosity of the slurry.[9] Second, the fluid density should be replaced by the slurry density. Both these corrections can be calculated by using the volume fraction of the slurry, f_{vsl}, occupied by the fluid. The necessary calculations have been developed for spherical particles.[10] The corrected hindered settling velocity, v_h, can be derived from

$$v_h = v\,\frac{f_{vsl}^{\,2}}{10^{1.82(1-f_{vsl})}}. \quad \ldots\ldots\ldots\ldots\ldots \text{(B-1)}$$

APPENDIX C
Equilibrium Bed Height

Equilibrium bed height, h_{eq}, is the maximum height a sand bed can have in a given hydraulic fracture. Babcock *et al.*[5] indicate

$$v_{eq} = \frac{1.12\,q}{\omega\,h_{eq}}. \quad \ldots\ldots\ldots\ldots\ldots\ldots \text{(C-1)}$$

In Eq. C-1 ω is given in inches, h_{eq} in feet, and q in barrels per minute. To calculate h_{eq} from Eq. C-1, one needs to know v_{eq}. This is found by the following method.[5]

Let $(v_w)_{eq}$ denote the friction velocity of the particle at equilibrium bed height. This is related to other sand-transport parameters by

$$(v_w)_{eq} = \frac{3.46\,v_{eq}\left(\frac{\rho_f}{\rho_{sl}}\right)^{1/2}}{\left(\frac{4v_{eq}r_H\rho_f}{\mu}\right)^{1/2}} \text{ (laminar flow)}, \quad \ldots \text{(C-2)}$$

$$(v_w)_{eq} = \frac{0.2\,v_{eq}\left(\frac{\rho_f}{\rho_{sl}}\right)^{1/2}}{\left(\frac{4v_{eq}r_H\rho_f}{\mu}\right)^{1/8}} \text{ (turbulent flow)}. \quad \ldots \text{(C-3)}$$

$$v/(v_w)_{eq} = 0.54\left(\frac{v\,d\,\rho_f}{\mu}\sqrt{\frac{4r_H}{d}}\right)^{1/2}. \quad \ldots\ldots \text{(C-4)}$$

All parameters in Eq. C-4 are known except $(v_w)_{eq}$ and r_H. The value of r_H is given by

$$4r_H = 4\,\frac{\omega h}{2(\omega+h)} \simeq 2\omega. \quad \ldots\ldots\ldots\ldots \text{(C-5)}$$

Thus, $(v_w)_{eq}$ can be derived from Eq. C-4. Since Eq. C-4 is basically for Newtonian fluids, to use it for non-Newtonian fluids, μ should be replaced by an apparent viscosity based on the shear stress around the particle. With $(v_w)_{eq}$ known, one can calculate v_{eq} from Eqs. C-2 or C-3, based on whether the fluid is in laminar or turbulent flow. With v_{eq} known, h_{eq} can be computed from Eq. C-1.

APPENDIX D

Consider a hydraulic fracture with length L, maximum width ω_{max}, and height h. Suppose the fracture is divided into small elements, with x_i denoting the distance between each nodal point and the wellbore, and ω_i denoting the fracture width at x_i (Fig. 8).

As the fracture propagates away from the borehole, it reaches x_i at time t_i. From Eq. 1 we derive

$$x_i = A_1 t_i^{m1},$$

or

$$t_i = (x_i/A_1)^{1/m1}. \quad \ldots\ldots\ldots\ldots\ldots\ldots \text{(D-1)}$$

The treatment time can be divided into small increments, Δt_n, so that at any time $t = t_n$,

$$t_n = \Sigma\,\Delta t_n.$$

At each time, t_n, the volume of each increment of fracture length, V_{fni}, is computed from

$$V_{fni} = \frac{1}{2}(\omega_{i+1}+\omega_i) \;\Big|_{t=t_n}\; (x_{i+1}-x_i)h. \quad \ldots \text{(D-2)}$$

At time $t = t_n$, the point x_i has been exposed to fluid for t_{eni}, where

$$t_{eni} = t_n - t_i.$$

The leak-off volume, V_{lni}, at $t = t_n$ in element i is given by

$$V_{lni} = (x_{i+1}-x_i)\left[f(t_{eni}) + f(t_{en(i+1)})\right]h. \quad \ldots \text{(D-3)}$$

The leak-off function, $f(t)$, is usually determined experimentally and has a shape similar to the curve in Fig.

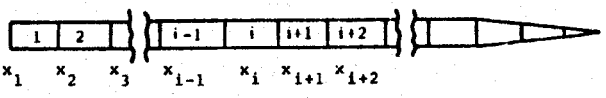

Fig. 8—Division of the fracture into small elements.

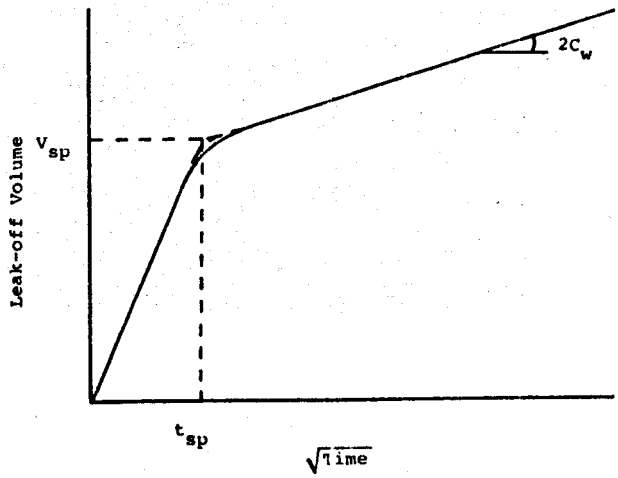

Fig. 9—Fluid leak-off curve.

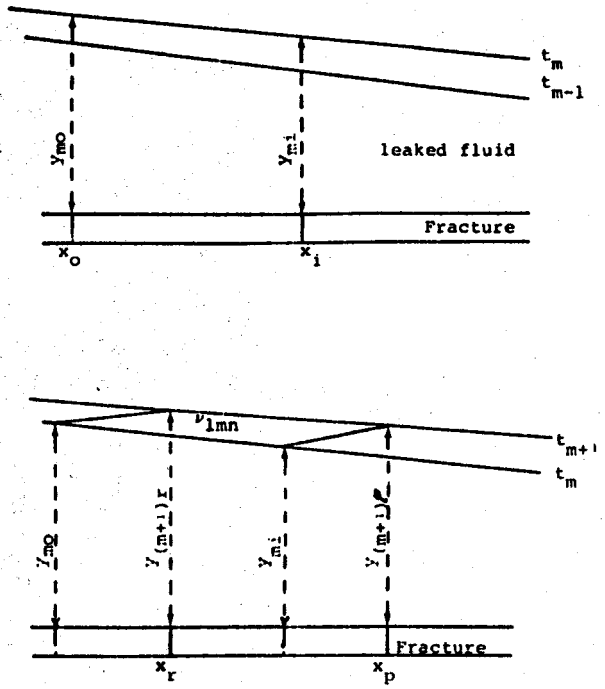

Fig. 10—Schematics of fluid leak-off in the fracture.

9. The mathematical form of $f(t)$ is

$$f(t) = \begin{cases} V_{sp}\sqrt{t/t_{sp}} & t < t_{sp} \\ V_{sp} + 2C_w\sqrt{t - t_{sp}} & t > t_{sp}. \end{cases}$$

As the fluid leaks into the formation, it travels away from the borehole wall. The distance, y_{ni}, that leak-off fluid travels in the formation at $t=t_n$ and $x=x_i$ is

$$Y_{ni} = f(t_{eni})/\phi.$$

During each Δt_n the volume of fluid, V_n, injected into the fracture is

$$V_n = q\ \Delta t_n,$$

where q is the injection rate. The volume is divided into two components -- one occupies the fracture and the other is lost as leak-off. Referring to Fig. 10, the volume lost from V_n as leak-off between t_{m-1} and t_m is given by

$$v_{lmn} = 1/4\left[(x_p - x_r) + (x_i - x_o)\right]\left[f\left(t_{e(m+1)}\right) - f\left(t_{emo}\right) + f\left(t_{e(m+1)}\right) - f\left(t_{emi}\right)\right]h. \quad \ldots\ldots\ldots \text{(D-4)}$$

where v_{lmn} denotes the volume lost from V_n during Δt_m. From mass balance,

$$V_n = \sum_{n}^{m} v_{lmn} + \sum_{o}^{i} V_{fmi}. \quad \ldots\ldots\ldots\ldots \text{(D-5)}$$

Eq. D-5 allows several sets of computations.

1. The location of each fluid increment in the fracture can be calculated. This is done by successively increasing i from an initial value of 0 until Eq. D-5 is satisfied. Starting with the last increment of injected fluid, one tries to determine the location of the leading front of each fluid increment. Successive use of Eq. D-5 for preceding fluid increments allows the determination of each fluid increment's location in the fracture.

2. The percent of each fluid increment left in the fracture can be found. If V_n consists of both solid and liquid components (slurry), then Eq. D-5 allows calculation of the increase in the solid concentration as a result of liquid leak-off.

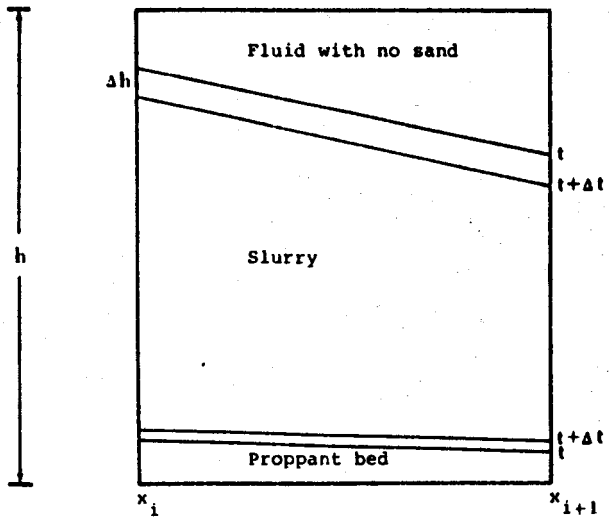

Fig. 11—Schematic of sand settlement in the fracture.

Consider an element of fracture at time t, containing a slurry and a sand bed (Fig. 11). At $t + \Delta t$, the top of the slurry column moves down, while the sand bed rises because of particle settlement. The height Δh is found from

$$\Delta h_s = v_h\,\Delta t. \quad \ldots\ldots\ldots\ldots\ldots\ldots \text{(D-6)}$$

The fluid volume that has lost its sand is $(\omega_{i+1} + \omega_i)(x_{i+1} - x_i)\Delta h/2$, which is deposited above the bed during Δt. One can compute the increase in bed height, as well as the location of the slurry in the fracture during the treatment. Although the fluid does not remain stationary in the fracture during Δt, the movement basically replenishes the element. As long as Δt is selected so that during this period the element contains the same kind of slurry, the fluid inside can be assumed stationary for bed height computations.

The position of sand in suspension in the fracture is determined best by considering the volume element, V_n. If Δt_n is selected so that V_n contains the same concentration and type of sand, then Eq. D-5 yields the location of V_n in the fracture. Eq. D-6 then is used to compute how much the sand settles at various x_i. The bed-height/total-deposition profile is found by settling all of the sand in suspension above the existing bed at the end of the treatment.

The numerical solution is performed by dividing the fracture into small elements. The treatment time also is divided into small increments so that each increment contains the same slurry.

At a given time $t=t_n$, the location and sand concentrations of each of the previous fluid increments in the fracture are calculated using the equations presented in this appendix. Repeating these computations for successive time increments allows the study of sand placement with time. **JPT**

Original manuscript received in Society of Petroleum Engineers office Sept. 10, 1975. Paper accepted for publication Oct. 4, 1977. Revised manuscript received Aug. 31, 1977. Paper (SPE 5636) was presented at the SPE-AIME 50th Annual Fall Technical Conference and Exhibition, held in Dallas, Sept. 28-Oct. 1, 1975.

FRACTURE DESIGN MODELLING

By

HENRY B. CRICHLOW

Petroleum Training and Technical Services

Norman, Oklahoma

ABSTRACT

In this study a design tool is discussed whereby the various components that enter the design process of a hydraulic fracturing job are combined to provide a realistic appraisal of a stimulation job in the field. An interactive computer model is used to solve the problem numerically to obtain the effects of various parameters on the overall behavior of the system.

INTRODUCTION

A design model offers the engineer a quantitative tool for evaluating his alternatives by considerably widening his scope in the evaluation of complex problems. In addition, the formulation of a design model presents a clearer picture of the process to the engineer and this sometimes reveals the interrelationships between variables which were not immediately apparent. The concept of the design model embodies the formulation of a solution technique to the problem, which is fast, efficient, economic and understandable by the engineer and reproduces adequately the physical behavior of the process. This model could then be used to predict.

The interactive fracture design involves the development of and synthesis of three basic elements:

(1) Fracture Generation Model - This model would calculate the fracture parameters based on the design input. This model was developed by Maurer Engineering.

(2) Heat Transfer Model - This model allows the determination of temperature dependent viscosity data within the fracture by including conduction and convection heat loss.

(3) Wellbore Hydraulics Model - This allows the computation of temperature profiles within the wellbore for various geometries and flow rates.

DESIGN METHODOLOGY

Fracture design modelling is based on a modular approach. Each element of the total system is considered independently and connected to the others by the information flow stream shown in Fig. 1. Once the information flow has been determined the "natural order" of the system is easy to establish. In other words, what the "cause and effect" relations are and how the equations which govern the system are coupled.

A primary objective of this model is to allow the engineer to design a stimulation treatment that would include the effects of temperature changes within the fracture itself and incorporate these changes into the design of the stimulation job.

THE FRACTURE ENVIRONMENT

The classical representation of the fracture geometry is shown in Fig. 2. The important features are:

(1) The fracture is symmetric to the wellbore and extends along the x-axis to a distance L.

(2) Leakoff occurs in the y-axis in a direction normal to the fracture face.

(3) This leakoff fluid is flowing counter to the heat flux and provides a substantial cooling effect referred to as heat blockage.

(4) The temperature distribution in the fracture T(x) varies according to the assumed leakoff rate and fracture parameters.

(5) The temperature in the fracture T(x) always approaches the undisturbed reservoir temperature at a large enough distance.

(6) The temperature profile in the formation rock T(y) varies with distance from the fracture face and always approaches undisturbed reservoir temperature at large 'y'.

At different times the fracture length increases and all temperature distributions will then vary and as a result, the consequent change in viscosity-distance relationship will cause variations in the fracture geometry.

MODELLING OF DESIGN ELEMENTS

1. Wellbore Temperature Model:

The fracture fluid enters the formation at a temperature different from the surface injection temperature. Because of this temperature change, the fluid viscosity is not the same as that measured at the surface. The proper fracture design calls for a realistic determination of the fracture fluid viscosity. The solution technique proposed by Juarez (1) has been used to calculate the temperature profile within the flowing stream and to allow the determination of sand-face viscosity of the fracture fluid. The equation system for solving the temperature model is incorporated into the overall fracture model.

The governing equations are:

$$T(z,t) = g_e Z + T_{es} - g_e A + (T_{fs} + G_e A - T_{es})\, e^{-z/A} \qquad (1)$$

where

$$A = \frac{Wc_f[k_{he} + r_{ti} Uf(t)]}{2\pi r_{ti} k_{he} U} \qquad (2)$$

The work reported by Romero-Juarez (1) is designed for a specific application to a well with 7 5/8-inch casing and 4 1/2-inch tubing and a pumping time of one hour.

In order to generalize this model to any possible system the following changes were incorporated into the design:

(1) The original unsimplified equations were used.

(2) A multiple linear regression analysis on the Ramey time function (2) was made to relate this transient time function to pumping time and casing OD. The data given in Fig. 3 reference 3 was fitted to a regression curve. A typical form of the data is shown in Fig. 3, and the regression analysis is shown in Appendix A.

The temperature profile can be determined in any well geometry at any time.

The viscosity of the injected fluid at the formation face is then determined.

2. Fracture Generation Model:

The fracture generation model utilizes the Geertsma and de Klerk approach. This model requires the following input:

(1) Injection rate

(2) Viscosity

(3) Fracture height

(4) Rock shear modulus

(5) Spurt loss

Output consists of the following:

(1) Fracture width

(2) Fracture length

(3) Fracture volume

(4) Efficiency

all as functions of time.

The basic equations for the width and length of the fracture are:

$$W_w = 2.1 \sqrt[4]{\frac{\mu Q L^2}{Gh}} \qquad (3)$$

and

$$L = \frac{Q}{32\pi hc^2} (\pi W_{we} + 8S_p) \left(\frac{2\alpha_L}{\sqrt{\pi}} - 1 + e^{\alpha_L^2} \operatorname{erfc} \alpha_L \right)$$

For a complete derivation and definition of symbols the reader is referenced to the original paper by Geertsma and de Klerk (3).

3. Fracture Fluid Temperature Determination Model:

There are two published techniques which allow the engineer to determine the temperature in the fracture. These are published by Sinclair (4) and by Whitsitt and Dysart (5).

The details of each technique are shown later, but the major differences are based on the way in which the leakoff rate is handled in each case. Fig. 4 shows the leakoff rate representations for each technique.

4. Sinclair Temperature Model:

The heat transfer model is based on the Sinclair (4) equations.

$$T_{Db} = \frac{1}{2} U(\tau - \delta M_D)\left\{\exp[2\alpha(\delta + \xi)] \operatorname{erfc}\left(\frac{\delta + \xi}{2\sqrt{\tau - \delta M_D}} + \alpha\sqrt{\tau - \delta M_D}\right)\right.$$

$$\left. + \operatorname{erfc}\left(\frac{\delta + \xi}{2\sqrt{\tau - \delta M_D}} - \alpha\sqrt{\tau - \delta M_D}\right)\right\}$$

where

$$\tau = \frac{k_1 t}{H^2 M_1} \qquad \delta = \frac{1}{2\alpha} \ln\left|\frac{i_D}{i_D - 2\alpha x_D}\right|$$

$$M_D = \frac{M_{fA} W}{24 M_1 H} \qquad i_D = \frac{i_{st} \rho_{st} C_{fF}}{4 H k_1}$$

$$\alpha = \frac{M_f \mu H}{2k_1} \qquad \xi = \frac{|y| - \frac{1}{2}W}{H}, \quad |y| > \frac{1}{2} W$$

$$x_D = |x/H| \qquad = 0 \qquad |y| \leq \frac{1}{2} W$$

5. Whitsitt-Dysart Model:

The Whitsitt-Dysart (5) temperature profile model has been derived using a combination of a mass energy balance in the fracture zone and an energy balance in the formation zone.

Within the formation there is conductive and convective heat loss away from the fracture face. The conductive heat loss is derived from the heat flux in the rock matrix while the convective heat loss is produced by the flow of leakoff fluid into the rock matrix.

For the typical fracture operation, only the temperature gradient and the associated heat flux at the fracture face is needed.

An energy balance on the fluid flowing in the fracture produces the following governing equation:

$$\frac{dT}{dx} = \frac{2h}{W_t[1 - (x/L)^2]C_f} \sqrt{\frac{Mk}{\pi t}} (T_i - T)\, \psi(\eta)$$

$$\psi(\eta) = e^{-\eta^2} - \sqrt{\pi}\, \eta \operatorname{erfc}(\eta)$$

$$\eta = \frac{W_t x C_f}{hL^2(1 - \phi)} \sqrt{\frac{t}{Mk}}$$

RESULTS

The model was utilized to interactively design several stimulation treatments. The sample data and results are shown in Fig. 5 through Fig. 10. The data presented is fully annotated and self-explanatory.

CONCLUSIONS

A simple effective tool for designing stimulation treatments in geothermal wells has been developed. The design procedure facilitates a broader analysis by the engineer/analyst in determining the optimum design factors within a given set of design criteria. The tool is useable at the field level by operations personnel.

6. References

1 Romero-Juarez, A:
"A Simplified Method for Calculating Temperature Changes in Deep Wells", SPE-AIME, Petroleos Mexicanos, June 1979.

2 Ramey, H. J., Jr.:
"Wellbore Heat Transmission", Trans. AIME (1962) 225, 427-435.

3 Geertsma, J. and DeKlerk, R.:
"A Rapid Method of Predicting Width and Extent of Hyrdraulically Induced Fractures", Journal of Petroleum Technology, December 1969, p. 1571.

4 Sinclair, A. Richard:
"Heat Transfer Effects in Deep Well Fracturing", Journal of Petroleum Technology, December 1971, p. 1634.

5 Whitsitt, N. F., and Dysart, G. R.:
"The Effect of Temperature on Stimulation Design", Journal of Petroleum Technology, April 1970, pp. 493-502.

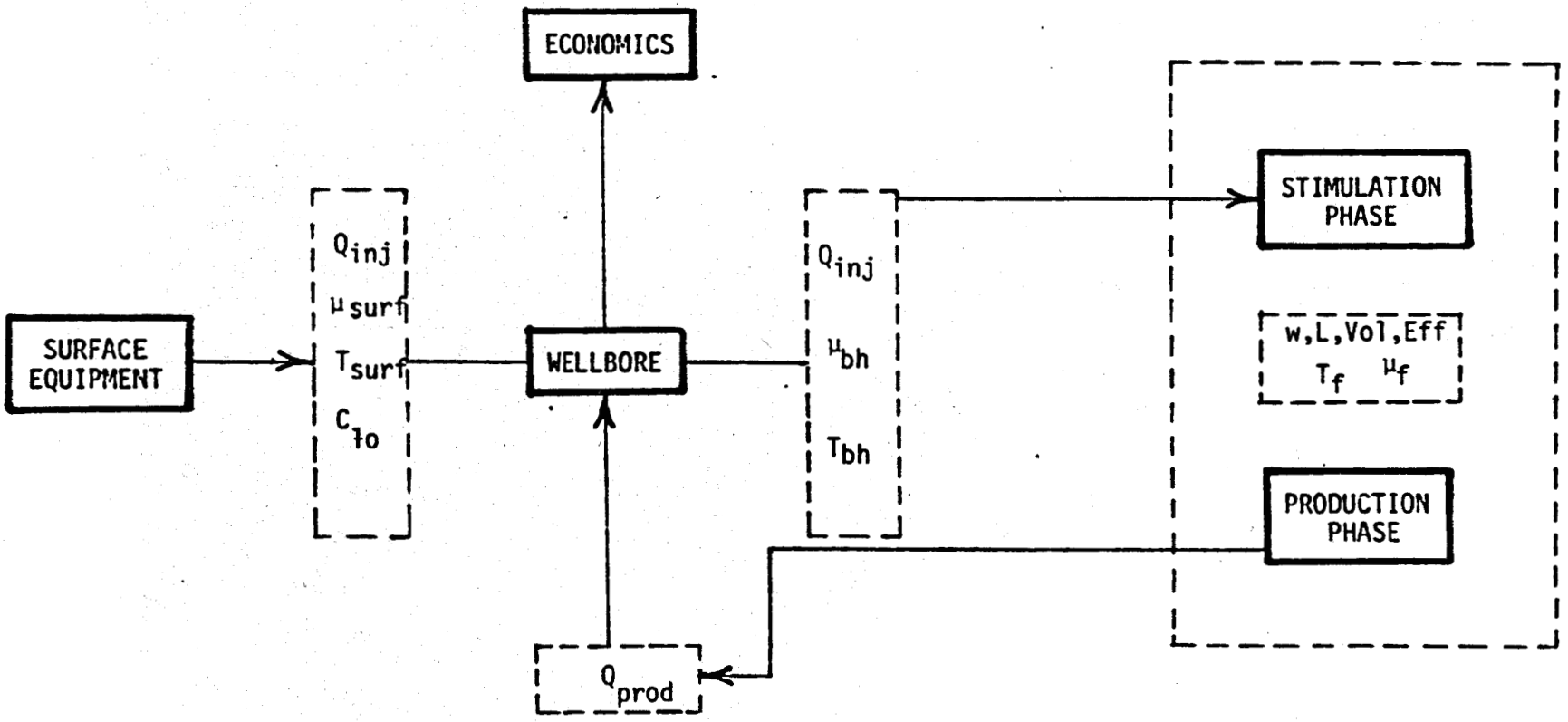

Fig 1 Information Flow

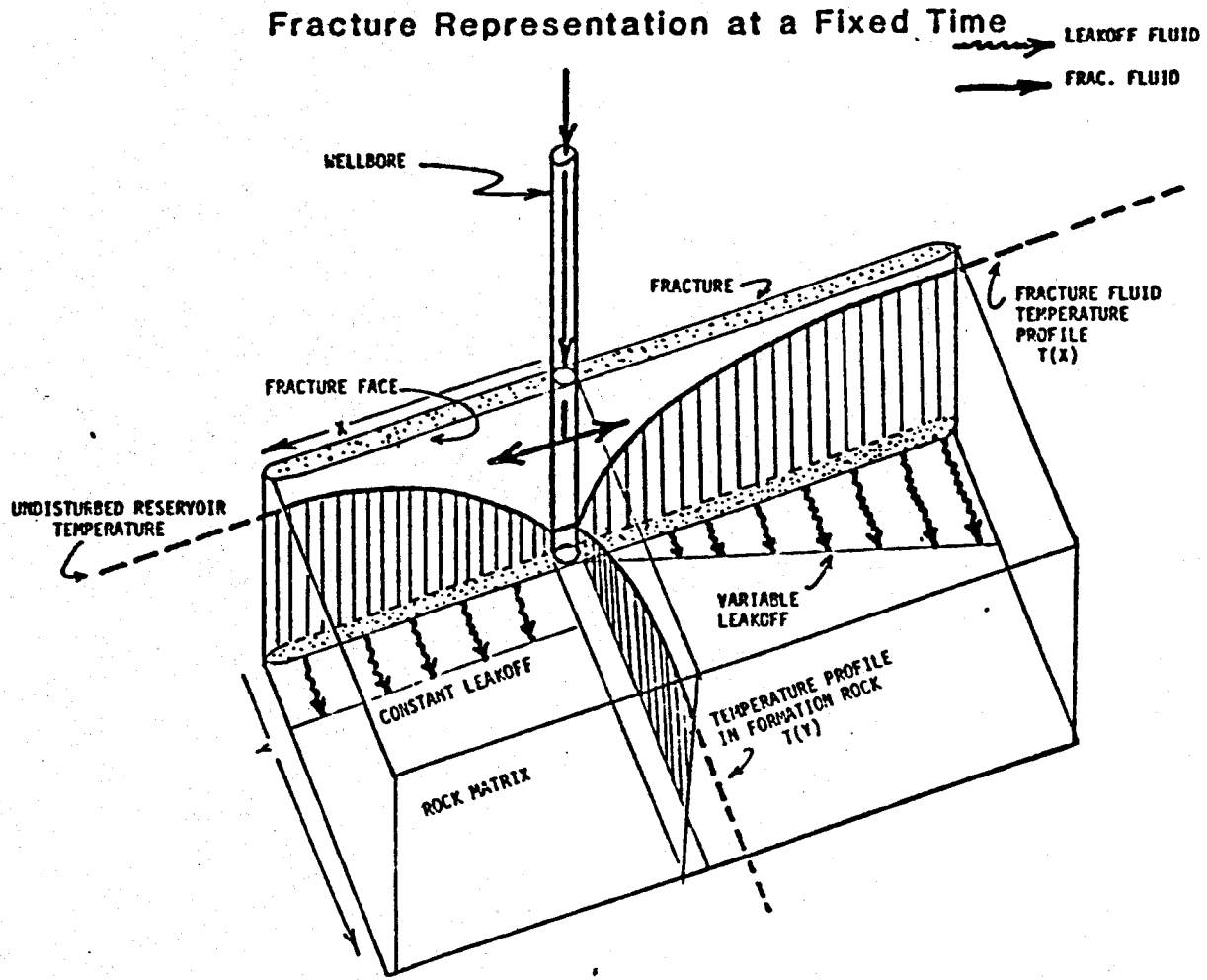
Fracture Representation at a Fixed Time
LEAKOFF FLUID
FRAC. FLUID
WELLBORE
FRACTURE
FRACTURE FLUID TEMPERATURE PROFILE T(X)
FRACTURE FACE
UNDISTURBED RESERVOIR TEMPERATURE
VARIABLE LEAKOFF
CONSTANT LEAKOFF
TEMPERATURE PROFILE IN FORMATION ROCK T(Y)
ROCK MATRIX

Fig.2

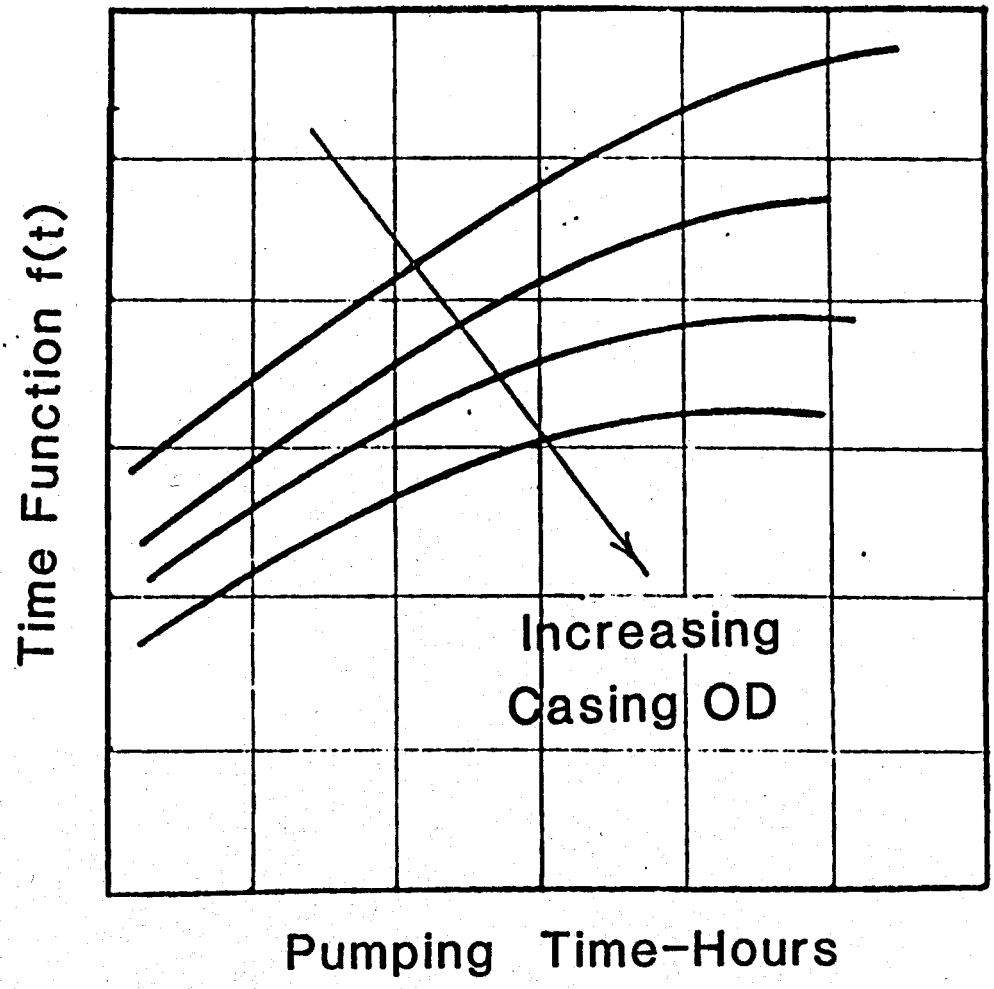

Fig.3 Time function for wellbore heatloss

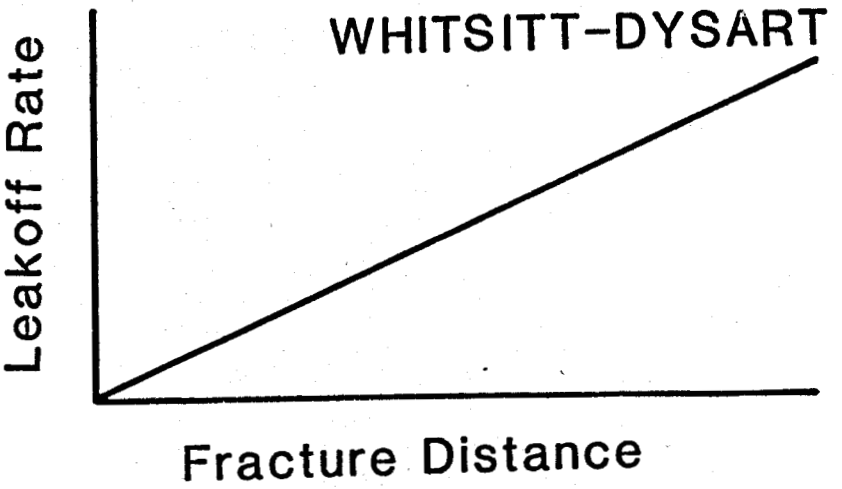

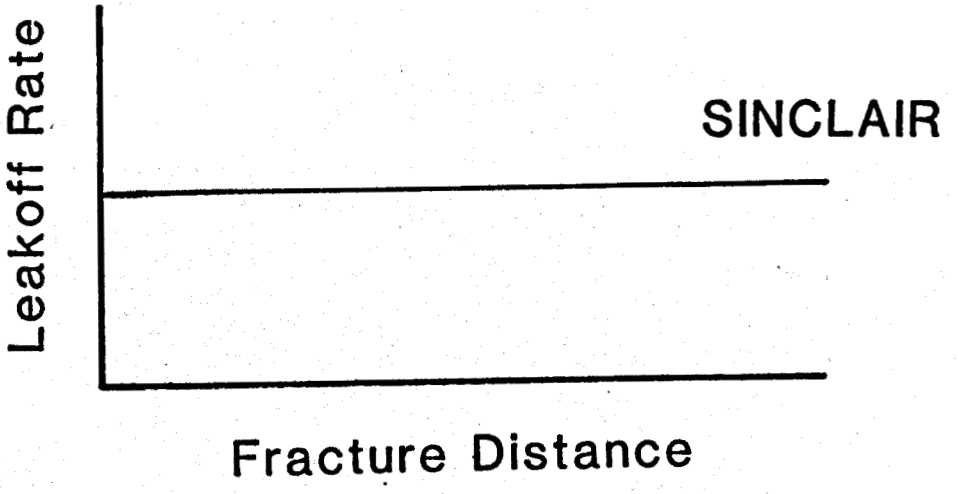

Fig.4 Fluid Leakoff Models

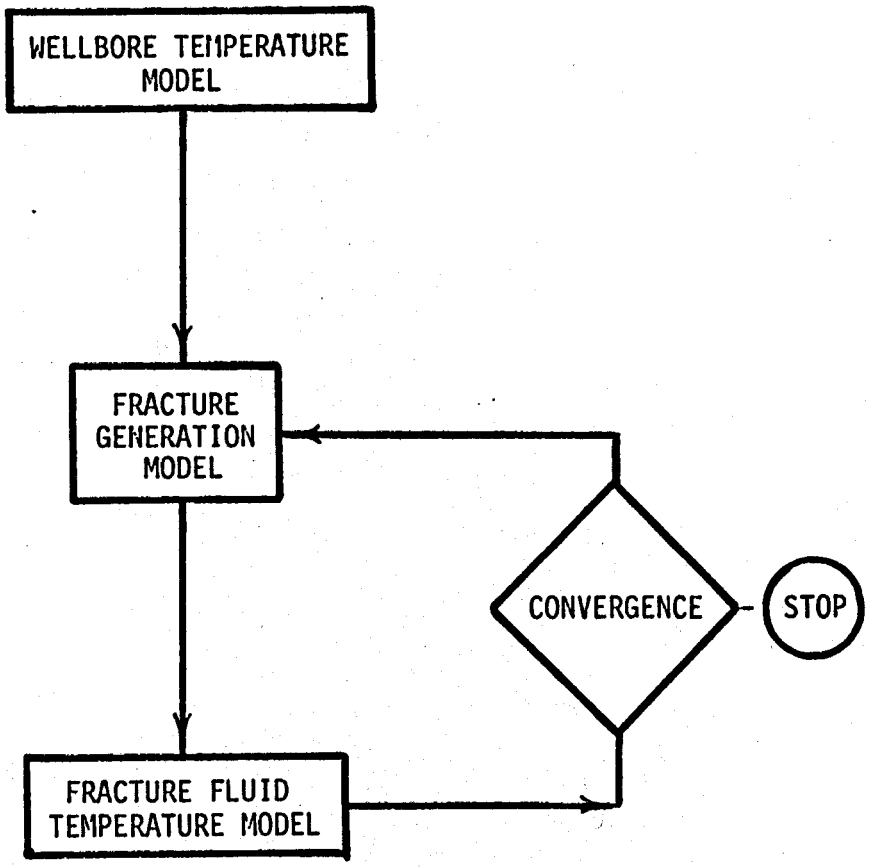

Fig.5 Generalized Flow Chart

Combination of Fracture Design

and

Temperature Model

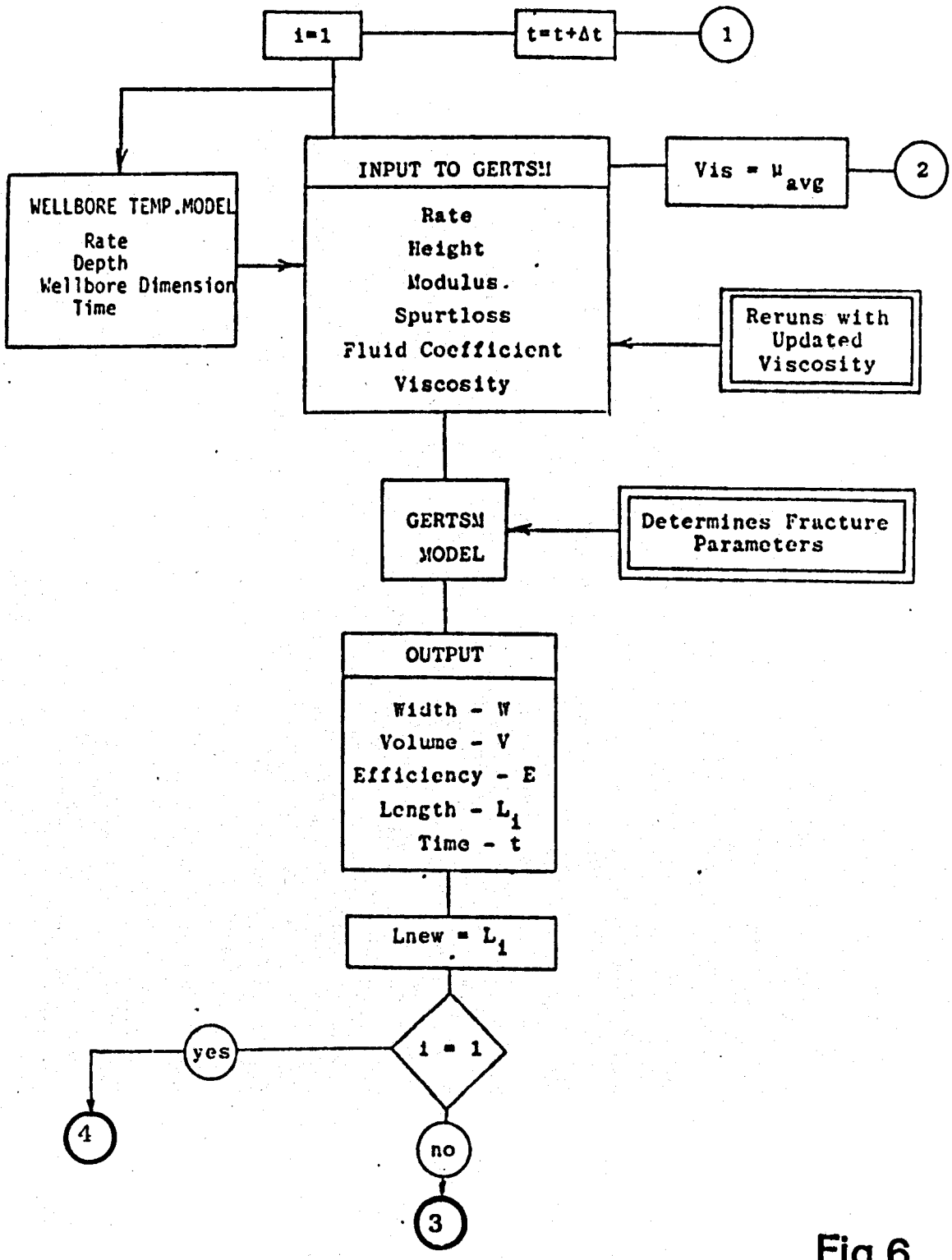

Fig.6

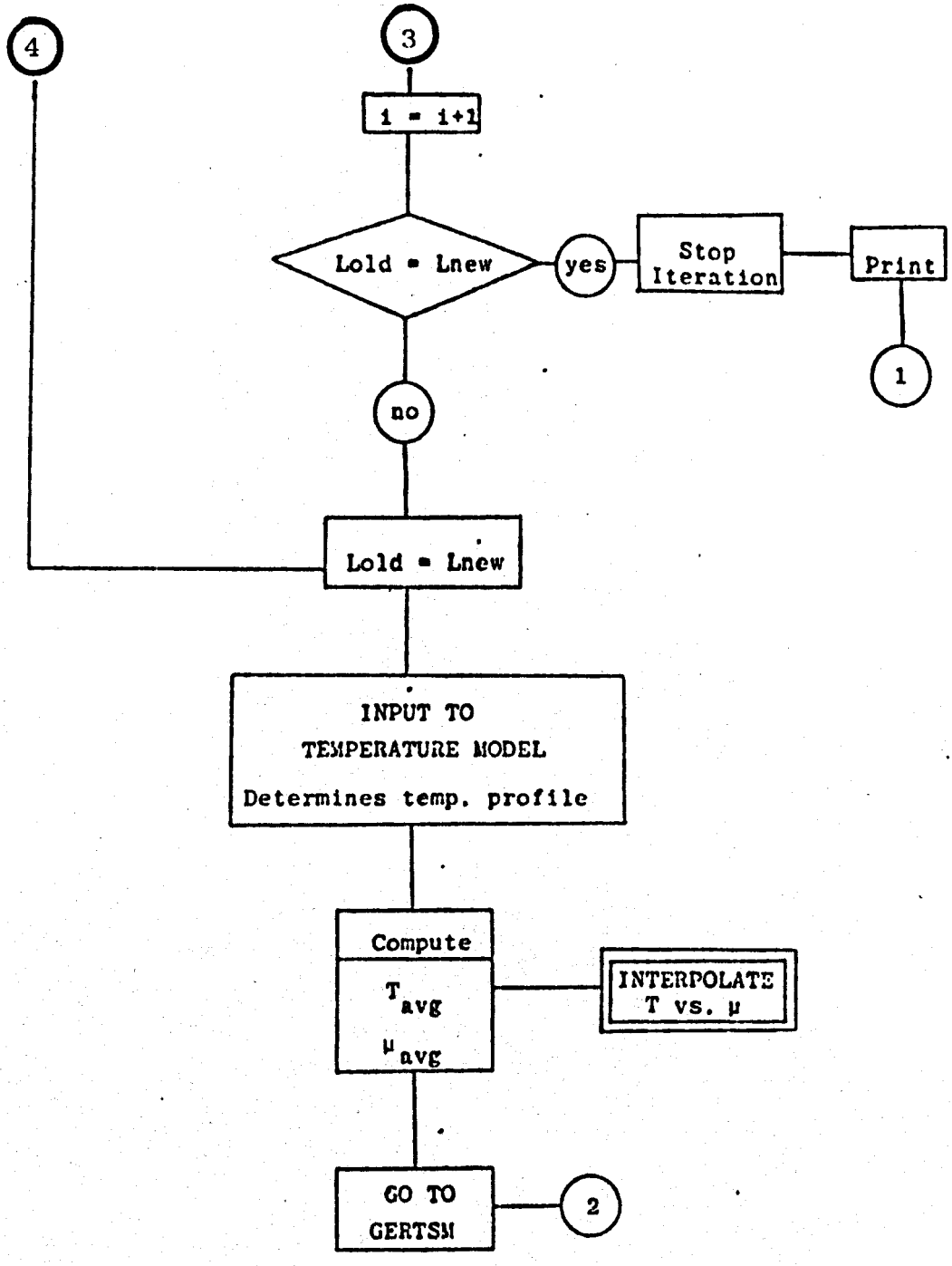
4
3
i = i+1
Lold = Lnew
yes
Stop Iteration
Print
1
no
Lold = Lnew
INPUT TO
TEMPERATURE MODEL
Determines temp. profile
Compute
T_{avg}
μ_{avg}
INTERPOLATE T vs. μ
GO TO GERTSM
2

Fig 6 (cont,d)

Data

```
00010 NO          (DO YOU WANT TO ECHO THE INPUT? )
00020 YES         (DO YOU WANT TO SEE THE TEMPERATURE PLOT?)
00030 YES         (DO YOU WANT TO SEE THE VISCOSITY PLOT?)
00040 YES         (DO YOU WANT TO USE SINCLAIR MODEL?)
00050 NO          (DO YOU WANT TO CALL WELTEM ?)
00060  INITIAL TIME (SEC.)
00070  0.0
00080  MAX TIME      (SEC.)
00090  2700.0
00100  TIME INCREMENT (SEC.)
00110  300.0
00120  INJECTION RATE (BPM)
00130  15.
00140  VISCOSITY (CP)
00150  200.
00160  RHO
00170 62.4
00180  ROCK SHEAR MODULUS (PSI)
00190  2600000.
00200  FRACTURING FLUID COEFF. (FT/MIN**(1/2) )
00210  0.002
00220  SPURT LOSS (FT3/FT2=FT)
00230  0.0
00240 FRACTURE HEIGHT, FT.
00250 100.
00260 SPEC. HEAT OF FRACTURE FLUID, BTU/LB  F
00270  1.
00280 VOL.HEAT CAP.(FLUIDS),BTU PER CU.FT.  F
00290 62.4
00300  VOL.HEAT CAP.(ROCK), BTU PER CU.FT.  F
00310   51.6
00320 THERMAL CONDUCTIVITY, BTU/FT SEC  F
00330  0.000417
```


Table 1

```
00340 POROSITY, DECIMAL
00350 0.22
00360 INITIAL TEMPERATURE
00370 80.0
00380  RESERVOIR TEMP.
00390    300.
00400 DEPTH
00410 5000.
00420 PERMEABILITY
00430 0.1
00440 PRESSURE
00450 2500.
00460  LEAKOFF COEF. = ZERO
00470  0.0
00480  LEAKOFF COEF. #1
00490  0.1
00500 DENSITY OF ROCK,LB PER CU.FT.
00510  165.0
00520   TUBING ID (INCHES)
00530   4.0
00540   TUBING OD (INCHES)
00550   4.5
00560   CASING ID (INCHES)
00570   7.675
00580   GEOTHERMAL GRADIENT (DEG F/FT)
00590   0.01
00600   TIME FUNCTION
00610   0.7
00620   FORMATION SURFACE TEMP. (DEG F)
00630   70.
00640   FLUID SURFACE TEMP.  (DEG F)
00650   70.
00660  LOW  TEMP. VALUE     (DEG.F)
00670  100.
00680  VISCOSITY AT LOW  TEMP.  (CP)
00690  150.
00700  HIGH TEMP. VALUE     (DEG.F)
00710  300.
00720  VISCOSITY AT HIGH TEMP.  (CP)
00730  10.
00740 FLUID TYPE
00750 WATER GEL
END OF DATA
```

Table 1 (cont,d)

***** KURVE # 1 *****

IN GERTSM: MU = 200.00

Initial Output from Fracture Generation Model

WIDTH	LENGTH	VOLUME	EFF.	TIME
0.129	98.2	210.4	50.0	5.0

DARCY VELOCITY IS 0.03 FT PER DAY

FRACTURE LENGTH IS 98.21 FT

TEMPERATURE RATIO	DISTANCE RATIO
0.0000	0.0
0.1562	0.0500
0.3106	0.1000
0.4569	0.1500
0.5891	0.2000
0.7031	0.2500
0.7961	0.3000
0.8677	0.3500
0.9194	0.4000
0.9543	0.4500
0.9760	0.5000
0.9885	0.5500
0.9950	0.6000
0.9981	0.6500
0.9993	0.7000
0.9998	0.7500
0.9999	0.8000
1.0000	0.8500
1.0000	0.9000
1.0000	0.9500
1.0000	1.0000

Initial Temperature Ratio Data from SINCLAIR Model

Intermediate Calculations

Table 2

DISTANCE	TEMPERATURE	VISCOSITY
0.0	80.00	196.65
4.91	114.37	123.47
9.82	148.34	77.96
14.73	180.52	50.42
19.64	209.60	34.01
24.55	234.68	24.22
29.46	255.13	18.36
34.37	270.90	14.83
39.28	282.27	12.71
44.19	289.94	11.46
49.10	294.73	10.74
54.01	297.47	10.35
58.92	298.90	10.15
63.84	299.57	10.06
68.75	299.85	10.02
73.66	299.96	10.01
78.57	299.99	10.00
83.48	300.00	10.00
88.39	300.00	10.00
93.30	300.00	10.00
98.21	300.00	10.00

Temperature Viscosity within the Fracture

IN GERTSM: MU = 18.38

Updated Viscosity

WIDTH	LENGTH	VOLUME	EFF.	TIME
0.077	114.9	146.7	34.9	5.0

New Fracture Parameters

Table 3

HYDRAULIC FRACTURE DESIGN PROGRAM

USING

TEMPERATURE DEPENDENT FRACTURE FLUID PROPERTIES

FRACTURE PARAMETERS

TIME (MINS)	WIDTH (IN)	LENGTH (FT)	VOLUME CU.FT	EFF. %	AVG.FLUID TEMP. DEG.F
0.0	0.0	0.0	0.0	0.0	300.0
10.0	0.146	299.6	727.3	43.2	257.8
20.0	0.176	443.4	1301.2	38.7	259.6
30.0	0.197	556.4	1824.1	36.1	260.5
40.0	0.213	653.1	2315.1	34.4	261.0
50.0	0.226	739.1	2783.1	33.1	261.4
60.0	0.237	817.4	3233.5	32.0	261.7

Table 4

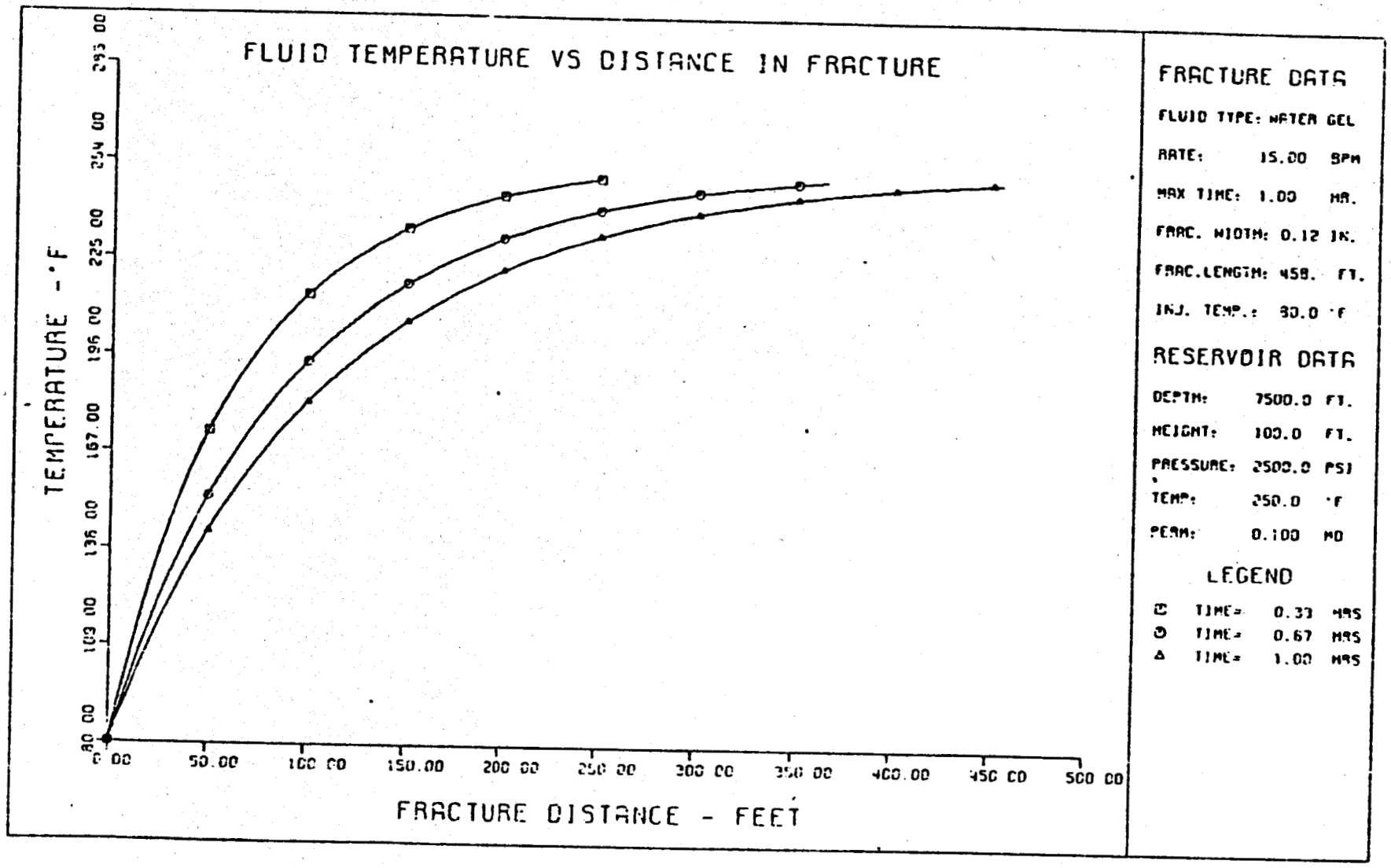
FLUID TEMPERATURE VS DISTANCE IN FRACTURE
TEMPERATURE - °F
80.00
109.00
136.00
167.00
196.00
225.00
254.00
283.00
0.00
50.00
100.00
150.00
200.00
250.00
300.00
350.00
400.00
450.00
500.00
FRACTURE DISTANCE - FEET
FRACTURE DATA
FLUID TYPE: WATER GEL
RATE: 15.00 BPM
MAX TIME: 1.00 HR.
FRAC. WIDTH: 0.12 IN.
FRAC.LENGTH: 458. FT.
INJ. TEMP.: 80.0 °F
RESERVOIR DATA
DEPTH: 7500.0 FT.
HEIGHT: 100.0 FT.
PRESSURE: 2500.0 PSI
TEMP: 250.0 °F
PERM: 0.100 MD
LEGEND
TIME= 0.33 HRS
TIME= 0.67 HRS
TIME= 1.00 HRS

Fig 7

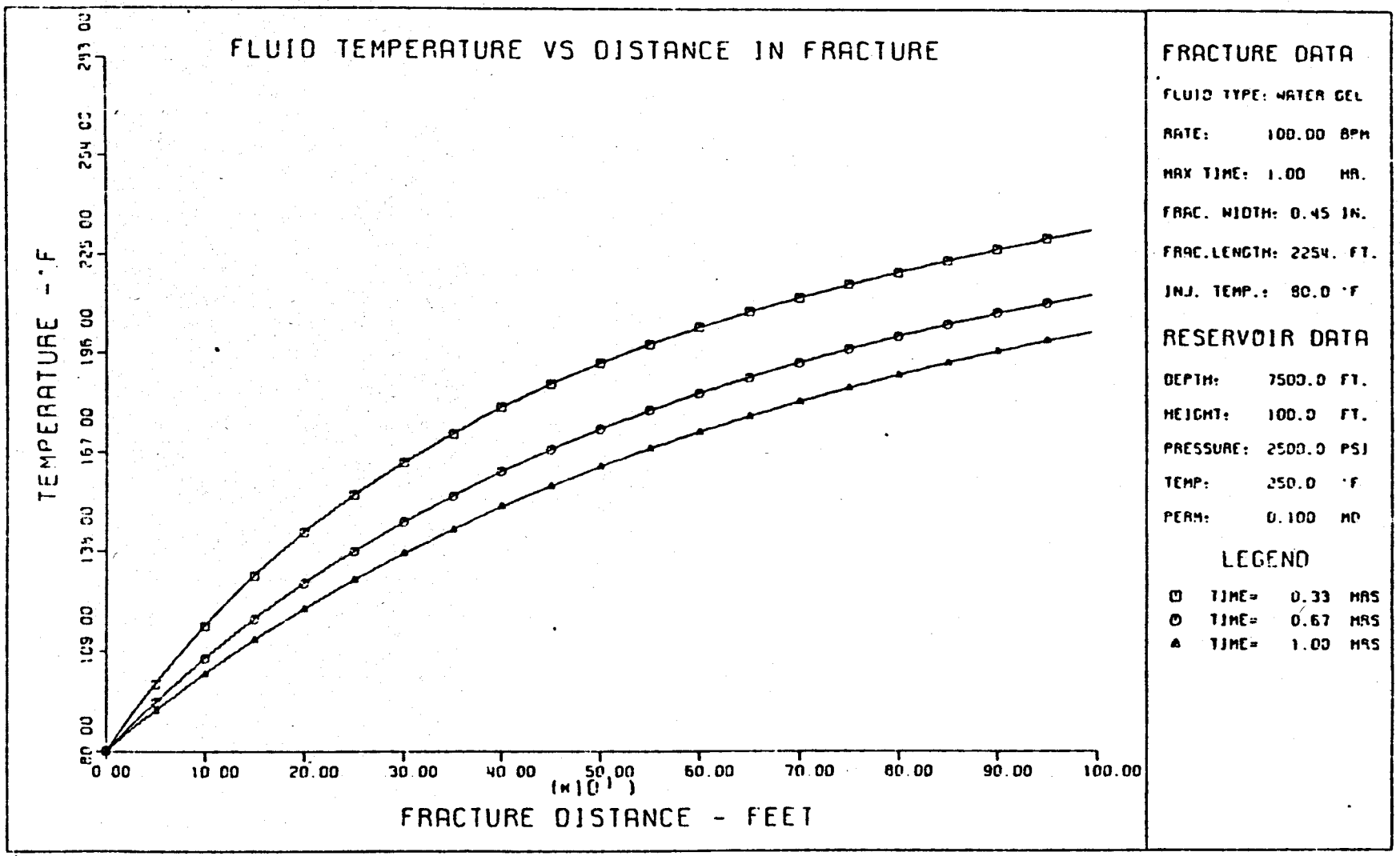
FLUID TEMPERATURE VS DISTANCE IN FRACTURE
TEMPERATURE - °F
80.00
109.00
138.00
167.00
196.00
225.00
254.00
283.00
0.00
10.00
20.00
30.00
40.00
50.00
60.00
70.00
80.00
90.00
100.00
(X10¹)
FRACTURE DISTANCE - FEET
FRACTURE DATA
FLUID TYPE: WATER GEL
RATE: 100.00 BPM
MAX TIME: 1.00 HR.
FRAC. WIDTH: 0.45 IN.
FRAC.LENGTH: 2254. FT.
INJ. TEMP.: 80.0 °F
RESERVOIR DATA
DEPTH: 7500.0 FT.
HEIGHT: 100.0 FT.
PRESSURE: 2500.0 PSI
TEMP: 250.0 °F
PERM: 0.100 MD
LEGEND
TIME= 0.33 HRS
TIME= 0.67 HRS
TIME= 1.00 HRS

Fig 8

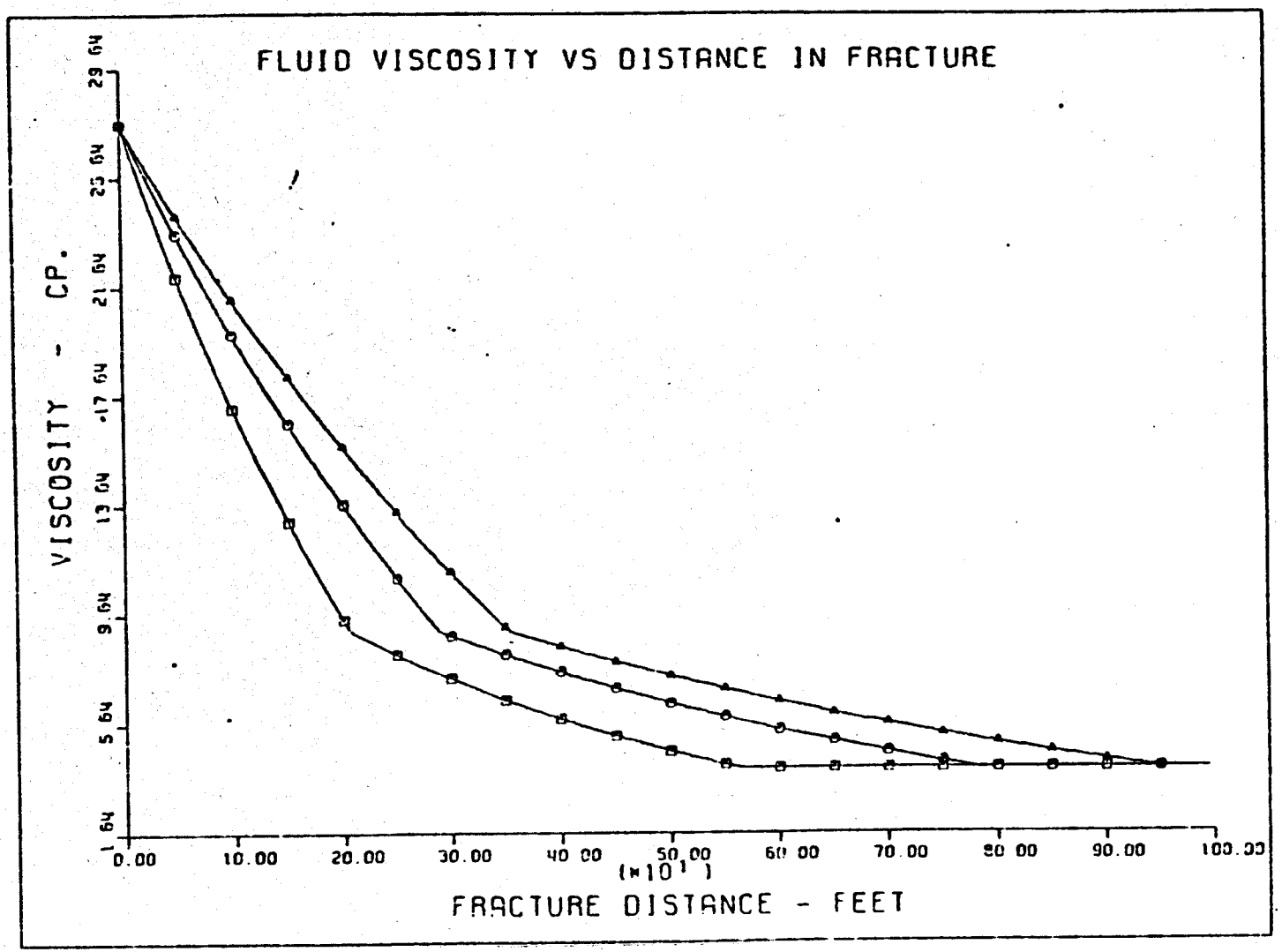
FLUID VISCOSITY VS DISTANCE IN FRACTURE
VISCOSITY - CP.
29.6M
25.6M
21.6M
17.6M
13.6M
9.6M
5.6M
1.6M
0.00
10.00
20.00
30.00
40.00
50.00
60.00
70.00
80.00
90.00
100.00
(*10^1)
FRACTURE DISTANCE - FEET

Fig 9

Input

```
03460       SUBROUTINE INPUT
03470       DIMENSION FLTYPE(5)
03480       COMMON/C05/ JC(10,36),ECKVAL(36),JF(10)
03490       COMMON/C10/ WORK(2,9),H,RINJ,C,FM,FK,TIME,PHI,LENGTH,TEMP,W,TRE
03500       COMMON/C20/IN,OUT,X,DX
03510       COMMON/CLAIR/Q,MU,FH,G,CB,SP
03520       COMMON/C40/FLTYPE,DEPTH,PERM,PRESS,WIDTH
03530       COMMON/VJ10/CZERO,C1,C2,RHO,HKF
03540       COMMON/CAUG1/TINIT,TMAX,TINCR
03550       COMMON/COCT10/ DENROK,RHOFCF
03560       COMMON/ROCT11/DTI,DTE,DCI,DCE,GE,SFT,TES,TFS
03570       COMMON/TERCON/A,B,TLOW,THIGH,VLOW,VHIGH
03580       COMMON/INTTAB/NR,TEMINT(10),VISINT(10)
03590       DATA NW/10/
03600       INTEGER OUT,FLTYPE
03610       REAL LENGTH,MU
03620       READ(IN,20) (JF(K),K=1,NW)
03630       READ(IN,32) FLTYPE
03640       READ(IN,20) (JC(K,1),K=1,NW)
03650       READ(IN,4) TINIT
03660       ECKVAL(1) = TINIT
03670       READ(IN,20) (JC(K,2),K=1,NW)
03680       READ(IN,4) TMAX
03690       ECKVAL(2) = TMAX
03700       READ(IN,20) (JC(K,3),K=1,NW)
03710       READ(IN,4) TINCR
03720       ECKVAL(3) = TINCR
03730       READ(IN,20) (JC(K,4),K=1,NW)
03740       READ(IN,4) Q
03750       ECKVAL(4) = Q
03760       RINJ = Q
03770       READ(IN,20) (JC(K,5),K=1,NW)
03780       READ(IN,4) MU
03790       ECKVAL(5) = MU
03800       READ(IN,20) (JC(K,6),K=1,NW)
03810       READ(IN,4) RHO
03820       ECKVAL(6) = RHO
03830       READ(IN,20) (JC(K,7),K=1,NW)
03840       READ(IN,4) G
03850       ECKVAL(7) = G
03860       READ(IN,20) (JC(K,8),K=1,NW)
03870       READ(IN,4) CB
03880       ECKVAL(8) = CB
03890       READ(IN,20) (JC(K,9),K=1,NW)
03900       READ(IN,4) SP
03910       ECKVAL(9) = SP
03920       READ(IN,20) (JC(K,10),K=1,NW)
03930    20 FORMAT( 18A4 )
03940    25 FORMAT( 2X, 18A4 )
03950       READ(IN,4) H
03960       ECKVAL(10) = H
```

Program Listing

```
03970        FH = H
03980      4 FORMAT( F10.2)
03990     30 FORMAT( 2X, F10.2 )
04000     31 FORMAT( 2X, F10.4 )
04010        READ(IN,20) (JC(K,11),K=1,NW)
04020        READ(IN,4) C
04030        ECKVAL(11) = C
04040         READ(IN,20)(JC(K,12),K=1,NW)
04050          READ(IN,4) RHOFCF
04060           ECKVAL(12) = RHOFCF
04070        READ(IN,20) (JC(K,13),K=1,NW)
04080        READ(IN,4) FM
04090        ECKVAL(13) = FM
04100        READ(IN,20) (JC(K,14),K=1,NW)
04110        READ(IN,4) FK
04120        ECKVAL(14) = FK
04130        READ(IN,20) (JC(K,15),K=1,NW)
04140        READ(IN,4) HKF
04150        ECKVAL(15) = HKF
04160        READ(IN,20) (JC(K,16),K=1,NW)
04170        READ(IN,4) PHI
04180        ECKVAL(16) = PHI
04190        READ(IN,20) (JC(K,17),K=1,NW)
04200        READ(IN,4) TEMP
04210        ECKVAL(17) = TEMP
04220        READ(IN,20) (JC(K,18),K=1,NW)
04230        READ(IN,4) TRES
04240        ECKVAL(18) = TRES
04250        READ(IN,20) (JC(K,19),K=1,NW)
04260        READ(IN,4) DEPTH
04270        ECKVAL(19) = DEPTH
04280        READ(IN,20) (JC(K,20),K=1,NW)
04290        READ(IN,4) PERM
04300        ECKVAL(20) = PERM
04310     34 FORMAT(2X,F10.5 )
04320        READ(IN,20) (JC(K,21),K=1,NW)
04330        READ(IN,4) PRESS
04340        ECKVAL(21) = PRESS
04350        READ(IN,20) (JC(K,22),K=1,NW)
04360        READ(IN,4) CZERO
04370        ECKVAL(22) = CZERO
04380        READ(IN,20) (JC(K,23),K=1,NW)
04390        READ(IN,4) C1
04400        ECKVAL(23) = C1
04410        READ(IN,20) (JC(K,24),K=1,NW)
04420        READ(IN,4) DENROK
04430        ECKVAL(24) = DENROK
04440        READ(IN,20) (JC(K,25),K=1,NW)
04450        READ(IN,4) DTI
04460        ECKVAL(25) = DTI
04470        READ(IN,20) (JC(K,26),K=1,NW)
```

```
04480        READ(IN,4) DTE
04490        ECKVAL(26) = DTE
04500        READ(IN,20) (JC(K,27),K=1,NW)
04510        READ(IN,4) DCI
04520        ECKVAL(27) = DCI
04530        READ(IN,20) (JC(K,28),K=1,NW)
04540        READ(IN,4) DCE
04550        ECKVAL(28) = DCE
04560        READ(IN,20) (JC(K,29),K=1,NW)
04570        READ(IN,4) GE
04580        ECKVAL(29) = GE
04590        READ(IN,20) (JC(K,30),K=1,NW)
04600        READ(IN,4) TES
04610        ECKVAL(30) = TES
04620        READ(IN,20) (JC(K,31),K=1,NW)
04630        READ(IN,4) TFS
04640        ECKVAL(31) = TFS
04650        IF (NR.GT.0) GO TO 51
04660        READ(IN,20) (JC(K,32),K=1,NW)
04670        READ(IN,4) TLOW
04680        ECKVAL(32) = TLOW
04690        READ(IN,20) (JC(K,33),K=1,NW)
04700        READ(IN,4)  VLOW
04710        ECKVAL(33) = VLOW
04720        READ(IN,20)  (JC(K,34),K=1,NW)
04730        READ(IN,4)  THIGH
04740        ECKVAL(34) = THIGH
04750        READ(IN,20) (JC(K,35),K=1,NW)
04760        READ(IN,4) VHIGH
04770        ECKVAL(35) = VHIGH
04780     32 FORMAT( 5A4 )
04790        GO TO 41
04800     51 READ(IN,20) (JC(K,32),K=1,NW)
04810        DO 40 JR=1,NR
04820     40 READ(IN,39) TEMINT(JR),VISINT(JR)
04830     39 FORMAT(2F10.3)
04840     41 CONTINUE
04850        RETURN
04860        END
```

```
12630 C       THIS IS THE MAIN ROUTINE
12640        COMMON/C10/ WORK(2,9),H,RINJ,C,FM,FK,TIME,PHI,LENGTH,TINJ,W,TRES
12650        COMMON/C20/IN,OUT,X,DX
12660        COMMON/C40/FLTYPE,DEPTH,PERM,PRESS,WIDTH
12670        COMMON/C50/ SAVAVT(10), NUMPTS(9),NPASS
12680        COMMON/C60/KURVE
12690        COMMON/CLAIR/Q,MU,FH,G,CB,SP
12700        COMMON/CAUG1/TINIT,TMAX,TINCR
12710        COMMON/CMG/MODELS
12720        COMMON/FRACV/WS(10),XLS(10),VOLS(10),EFFS(10),TIM(10)
12730        COMMON/TERCON/A,B,TLOW,THIGH,VLOW,VHIGH
12740        COMMON/BXOCT/ BXLEN
12750        COMMON/NEWINT/KALINT
12760        COMMON/INTTAB/NR,TEMINT(10),VISINT(10)
12770        DATA MAXROW/10/,IOUT/3/
12780        INTEGER OUT,YES/'Y'/
12790 C      TINIT = INITIAL TIME,TMAX=MAX TIME,TINCR=TIME INCRMT.
12800 C      TIME UNITS ARE READ IN SUBROUTINE INPUT, UNITS: SECONDS.
12810        REAL LENGTH,MU
12820 C       DO YOU WANT TO ECHO THE INPUT?
12830        READ(IN,4) JIN
12840      4 FORMAT( A1 )
12850 C       DO YOU WANT TO SEE THE TEMPERATURE PLOT?
12860        READ(IN,4) JPLOTT
12870 C       DO YOU WANT TO SEE THE VISCOSITY PLOT?
12880        READ(IN,4) JPLOTV
12890 C       DO YOU WANT TO USE SINCLAIR MODEL?
12900        READ(IN,4) MODELS
12910 C       DO YOU WANT TO CALL WELTEM ?
12920        READ(IN,4) KALLW
12930 C       DO YOU WANT TO READ IN VISCOSITY TABLE?
12940         READ(IN,6) KALINT,NR
12950      6 FORMAT(A1,4X,I2)
12960        IF (KALINT.LE.MAXROW) GO TO 17
12970        WRITE(6,16) KALINT,MAXROW
12980     16 FORMAT(/,3X,'*** INPUT ERROR. VALUE GIVEN FOR NUMBER OF ROWS',
12990       ? ' IN VISCOSITY TABLE',/,8X,'IS TOO LARGE. IT WAS READ AS ',
13000       ?  I2,'  MAXIMUM ALLOWABLE IS ',I2,'.',/,
13010       ?  8X,'PLEASE CORRECT AND RESUBMIT. JOB TERMINATED.')
13020         STOP
13030     17 CONTINUE
13040        CALL INPUT
13050        IF ( (TMAX/TINCR).LE.9.) GO TO 19
13060        WRITE(6,18)
13070     18 FORMAT(///,4X,'***** INPUT ERROR.  MAX TIME STEPS IS NINE. ',
13080       ? /,11X,'YOU MUST ADJUST INPUT VALUES "MAX TIME" AND ',
13090       ? '"TIME INCREMENT" SUCH THAT:',/,11X,'MAX TIME DIVIDED BY',
13100       ? ' TIME INCREMENT IS LESS THAN OR EQUAL TO 9. ',
13110       ?  /,11X,'JOB TERMINATED.  ')
13120     19 CONTINUE
13130        IF (NR.GT.0) GO TO 30
13140        A =(ALOG10(VLOW)-ALOG10(VHIGH))/(TLOW-THIGH)
13150        B =  VLOW / (10.**(A*TLOW))
13160 C      A AND B ARE USED IN SUBROUTINE TERP.
```

```
13170     30 IF (JIN.EQ.YES) CALL ECHO
13180        T = TINIT
13190        TMAXPL = TMAX + 1.
13200        IF (KALLW.EQ.YES) CALL WELTEM(TINJ,MU)
13210      5 T = T + TINCR
13220        IF (T.GT.TMAXPL) GO TO 40
13230 C     T IS TIME IN SECONDS.
13240        CALL GERTSM(T,TINJ)
13250        GO TO 5
13260     40 WRITE(6,55)
13270     55 FORMAT(//,'       MAX TIME REACHED IN MAIN.    ',//)
13280        WRITE(IOUT,502)
13290    502 FORMAT(5(/))
13300        WRITE(IOUT,503)
13310    503 FORMAT(1X,78('*'))
13320        WRITE(IOUT,504)
13330    504 FORMAT(1X,'*',76X,'*')
13340        WRITE(IOUT,504)
13350        WRITE(IOUT,505)
13360    505 FORMAT(1X,'*',20X,'HYDRAULIC  FRACTURE  DESIGN  PROGRAM',T79,'*')
13370        WRITE(IOUT,504)
13380        WRITE(IOUT,506)
13390    506 FORMAT(1X,'*',36X,'USING',T79,'*')
13400        WRITE(IOUT,504)
13410        WRITE(IOUT,507)
13420    507 FORMAT(1X,'*',12X,'TEMPERATURE  DEPENDENT  FRACTURE  FLUID',
13430       ?  '  PROPERTIES',T79,'*')
13440        WRITE(IOUT,504)
13450        WRITE(IOUT,503)
13460        WRITE(IOUT,504)
13470        WRITE(IOUT,508)
13480    508 FORMAT(1X,'*',25X,'FRACTURE  PARAMETERS',T79,'*')
13490        WRITE(IOUT,504)
13500        KM1 = KURVE - 1
13510        DO 20 L=1,KM1
13520     20 SAVAVT(KURVE-L+1) = SAVAVT(KURVE-L)
13530        SAVAVT(1) = TRES
13540        WRITE(IOUT,21)
13550     21 FORMAT(1X,'*',5X,'TIME',6X,'WIDTH',6X,'LENGTH',6X,'VOLUME',
13560       ?  5X,'EFF.',4X,'AVG.FLUID TEMP.',T79,'*',
13570       ? /,1X,'*',4X,'(MINS)',6X,'(IN)',7X,'(FT)',8X,'CU.FT',6X,'%',
13580       ? 11X,'DEG.F',T79,'*')
13590        WRITE(IOUT,504)
13600        WRITE(IOUT,22) (TIM(MM),WS(MM),XLS(MM),VOLS(MM),EFFS(MM),SAVAVT(MM
13610       ?     ),MM=1,KURVE)
13620     22 FORMAT(1X,'*',F10.1,F10.3,2X,F10.1,2X,F10.1,F9.1,4X,F10.1,T79,'*')
13630        WRITE(IOUT,504)
13640        WRITE(IOUT,503)
13650        WRITE(IOUT,509)
13660    509 FORMAT( 10(/) )
13670        BXLEN = XLS(KURVE)
13680        IF (JPLOTT.EQ.YES)  CALL PLOTT(NUMPTS)
13690        IF (JPLOTV.EQ.YES)  CALL PLOTV(NUMPTS)
13700        IF (JPLOTT.EQ.YES.OR.JPLOTV.EQ.YES)  CALL PLOT(0.,0.,999)
13710        STOP
13720        END
```

Sinclr

```
      SUBROUTINE SINCLR(Q,TRES,TINJ,W,H,T,KK,L,VISC,RH1CV,EFFPER)
      DIMENSION TEMP(21),RATIO(21)
      COMMON/PLAY/DIST(202,9),TREAL(202,9),VISCOS(202,9)
      COMMON/C50/SAVAVT(10),NUMPTS(9),NPASS
      COMMON/COCT10/RHO1C1,RHOFCF
      COMMON/C60/KURVE
      COMMON/NEWINT/KALINT
      REAL LMAX,LMAX1,L,K,KK,M
      DATA EFF/0.5/
      INTEGER YES/'Y'/
      RHO1C1 = RH1CV
      EFF = EFFPER / 100.
      IF (KURVE.LE.9) GO TO 8
      WRITE(6,7)
    7 FORMAT(//,5X,'*** ERROR. ARRAY SUBSCRIPT TOO LARGE.  SEE KURVE ',
     ?  'IN SUBROUTINE SINCLR.  ',/,9X,'JOB TERMINATED.  ')
      STOP
    8 CONTINUE
      T = T / 60.
      K = KK * 3600.
      Q = Q * 60.*24.
      XI = 1.
      DXN = 0.01
      IF (EFF.EQ.1.) GO TO 20
   10 CONTINUE
      XNUM = XI * DXN
      F = EXP(-XNUM)+2.*EFF*XNUM-1.
      IF (F.GT.0.0) GO TO 30
      XI = XI + 1.
      GO TO 10
   20 XNUM = 0.0
   30 CONTINUE
      WRITE(6,11)
   11 FORMAT(//)
      VF = 2.*W*XNUM/T
      WRITE(6,14) VF
   14 FORMAT(2X,'DARCY VELOCITY IS',F6.2,2X,'FT PER DAY',/)
      WRITE(6,16) L
   16 FORMAT(2X,'FRACTURE LENGTH IS',F10.2,2X,'FT',//)
      RHOFCF = 43.
      ALPHA = RHOFCF*VF*H/(2.*K*24.)
      TAU = K*T/(H*H*RHO1C1)
      M = RHOFCF*W/(24.*RHO1C1*H)
      QQ = Q
      TEMP(1) = 0.0
      DO 100 I=1,21
      XI = I - 1
      RATIO(I) = .05*XI
      X = L*RATIO(I)
      DIST(I,KURVE) = X
      GAM = X/H
      Q = QQ*RHOFCF*5.61/(4.*H*K*24.)
      DEL = (1./(2.*ALPHA))*ALOG(Q/(Q-2.*ALPHA*GAM))
      RAD = SQRT(TAU-DEL*M)
      CRLS = DEL/2./RAD
      CRRS = ALPHA*RAD
```

```
15070        ARG1 = CRLS+CRRS
15080        ARG2 = CRLS-CRRS
15090        IF (ARG1.GT.1.0E01) GO TO 93
15100        XX1 = ERFC(ARG1)
15110        GO TO 94
15120     93 XX1 = 0.
15130     94 CONTINUE
15140        IF (ARG2.GT.1.0E01) GO TO 95
15150        XX2 = ERFC(ARG2)
15160        GO TO 96
15170     95 XX2 = 0.
15180     96 CONTINUE
15190        IF (XX1.LT.0.1E-10) XX1 = 0.1E-10
15200        IF (XX2.LT.0.1E-10) XX2 = 0.1E-10
15210        ZCR1 = (Q-2.*ALPHA*GAM)
15220        ZCR2 = Q / ZCR1
15230        ZCR3 = ZCR2 * XX1
15240        CRTPI = (ZCR3 + XX2) / 2.
15250        TEMP(I) = 1. - CRTPI
15260    100 CONTINUE
15270        TOT = 0.0
15280        DO 210 J=1,21
15290        TREAL(J,KURVE) = TINJ + TEMP(J) * (TRES-TINJ)
15300        IF (KALINT.NE.YES) GO TO 105
15310        CALL INTERP(TREAL(J,KURVE),VIS)
15320        GO TO 106
15330    105 CALL TERP(TREAL(J,KURVE),VIS)
15340    106 CONTINUE
15350        VISCOS(J,KURVE) = VIS
15360    210 TOT = TOT + TREAL(J,KURVE)
15370        AVGT = TOT / 21.
15380        SAVAVT(KURVE) = AVGT
15390        WRITE(6,21)
15400     21 FORMAT(6X,'TEMPERATURE',5X,'DISTANCE',/,8X,'RATIO',9X,'RATIO',/)
15410        DO 200 J=1,21
15420        WRITE(6,22) TEMP(J),RATIO(J)
15430     22 FORMAT(2X,F13.4,F14.4)
15440    200 CONTINUE
15450        IF (KALINT.NE.YES) GO TO 205
15460        CALL INTERP(AVGT,VISC)
15470        GO TO 206
15480    205 CALL TERP(AVGT,VISC)
15490    206 CONTINUE
15500        WRITE(6,23)
15510     23 FORMAT(///,'            DISTANCE     TEMPERATURE     VISCOSITY',/)
15520        T = T * 60.
15530        NUMPTS(KURVE) = 21
15540        NPASS = KURVE
15550        KN = KURVE
15560        WRITE(6,5566) (DIST(MB,KN),TREAL(MB,KN),VISCOS(MB,KN),
15570       ?   MB=1,21)
15580  5566 FORMAT( 3X,3F15.2)
15590        Q = QQ/(60.*24.)
15600        RETURN
15610        END
```

Dysart

```
00010       SUBROUTINE DYSART(TIME,LENGTH,WIDTH,EFF,VAVG)
00020 C      INCOMING:  TIME,LENGTH,WIDTH,EFF   PASSED OUT:  VAVG
00030 C      VAVG IS VISCOSITY CORRESPONDING TO AVG. TEMP.
00040       COMMON/C10/WORK(2,9),H,RINJ,C,FM,FK,OLDTIM,PHI,OLDLEN,TEMPV,W,TRES
00050       COMMON/C20/IN,OUT,X,DX
00060       COMMON/C30/YPRIME(1)
00070       COMMON/C40/FLTYPE,DEPTH,PERM,PRESS,OLDWID
00080       COMMON/C50/ SAVAVT(10), NUMPTS(9),NPASS
00090       COMMON/C60/KURVE
00100       COMMON/PLAY/ XP(202,9),YP(202,9),VISCOS(202,9)
00110       COMMON/NEWINT/KALINT
00120       DIMENSION TEMP(1),CAR(24),FLTYPE(5)
00130       DATA POS/0.1E-20/,MAX/200/,KPL/1/
00140       INTEGER OUT,ONE/1/,TWO/2/,FLTYPE,YES/'Y'/
00150       REAL LENGTH
00160       EXTERNAL CDTDX
00170       KEG = KURVE
00180       OLDTIM = TIME
00190       OLDLEN = LENGTH
00200       OLDWID = WIDTH
00210       NEQT = 1
00220       MSFLAG = 0
00230       WRITE(6,39) KPL
00240    39 FORMAT(/,5X,'CALL TO DYSART #',I2 )
00250       KPL = KPL + 1
00260       IF (KEG.LE.9) GO TO 42
00270       WRITE(OUT,46)
00280    46 FORMAT(/,3X,'*** VALUE OF KEG IN SUB.DYSART EXCEEDS ',
00290      ? 'ARRAY SIZE 9. JOB TERMINATED. ')
00300       STOP
00310    42 CONTINUE
00320       X = 0.0
00330       KOUNT = 1
00340       XP(1,KEG) = 0.0
00350       YP(1,KEG) = TEMPV
00360       IF (KALINT.NE.YES) GO TO 37
00370       CALL INTERP(TEMPV,V)
00380       GO TO 38
00390    37 CALL TERP(TEMPV,V)
00400    38 CONTINUE
00410       VISCOS(1,KEG) = V
00420 C     WRITE(6,41) EFF,TIME
00430 C  41 FORMAT(/,2X,' EFF=    ',E14.6,7X,'TIME = ',E14.6,'  SECONDS. ')
00440 C     WRITE(6,43) LENGTH,WIDTH
00450 C  43 FORMAT(2X,' LENGTH=',E14.6,' FT.',3X,'WIDTH =',E14.6,' IN.',/)
00460 C     WRITE(3,44) TIME
00470 C  44 FORMAT('TIME=',E15.7)
00480 C     WRITE(6,42)
00490 C     W = RINJ * 5.833333 * EFF / 100.
00500       W = RINJ * 5.833333 * 0.5
```

```
00510         TEMP(1) = TEMPV
00520         KNIT = 0
00530      40 CONTINUE
00540         KNIT = KNIT + 1
00550         IF (KNIT.GT.200) GO TO 79
00560         XEND = X + DX
00570         IF (ABS(LENGTH-XEND).LE.POS) GO TO 50
00580         ONE = 1
00590         CALL DVERK(NEQT,CDTDX,X,TEMP,XEND,0.01,ONE,CAR,TWO,WORK,KEM)
00600         ZTEMP = TEMP(1)
00610         XOL = X / LENGTH
00620 C       WRITE(OUT,45) X,XOL,TEMP(1),YPRIME(1)
00630 C    45 FORMAT(6X,F6.1,4X,3E15.6)
00640 C       WRITE(3,48) X,TEMP(1)
00650 C    48 FORMAT(F5.1,E15.7)
00660 C       WRITE(OUT,49) X,TEMP(1)
00670 C    49 FORMAT(2X,F5.1,2X,E14.6 )
00680 C......PLOT OPTIONS AND SELECT NEW TIME HERE.
00690         IF (KOUNT.LE.MAX) GO TO 58
00700         IF( MSFLAG.EQ.1) GO TO 55
00710         WRITE(OUT,57) MAX
00720      57 FORMAT(/,'  MAX ARRAY SIZE ',I3,' REACHED IN SUB.DYSART. ',
00730        ? ' NO MORE POINTS SAVED.',/,'  PROGRAM CONTINUES.',/)
00740         MSFLAG = 1
00750         GO TO 56
00760      55 CONTINUE
00770      58 KOUNT = KOUNT + 1
00780      56 CONTINUE
00790         XP(KOUNT,KEG) = X
00800         YP(KOUNT,KEG) = ZTEMP
00810         IF (KALINT.NE.YES) GO TO 59
00820         CALL INTERP(ZTEMP,V)
00830         GO TO 60
00840      59 CALL TERP(ZTEMP,V)
00850      60 CONTINUE
00860         VISCOS(KOUNT,KEG) = V
00870         IF (X.LT.LENGTH) GO TO 40
00880      50 WRITE(OUT,52)
00890      52 FORMAT(/,'  *** CONVERGENCE IN DVERK.  ')
00900         KOUNT = KOUNT - 1
00910         XKOUNT = KOUNT
00920         TOTT = 0.0
00930         DO 153 K=1,KOUNT
00940     153 TOTT = TOTT + YP(K,KEG)
00950         AVGTMP = TOTT / XKOUNT
00960         IF (KALINT.NE.YES) GO TO 61
00970         CALL INTERP(AVGTMP,VAVG)
00980         GO TO 62
00990      61 CALL TERP(AVGTMP,VAVG)
01000      62 CONTINUE
```

```
01010         SAVAVT(KURVE+1) = AVGTMP
01020 C       WRITE(6,76) AVGTMP,VAVG
01030 C    76 FORMAT(/,3X,'TRACE AVG.TEMP=',E14.6,4X,'& VISCOS=',E14.6,/)
01040         WRITE(6,75)
01050      75 FORMAT(5X,'LENGTH',7X,'TEMP',8X,'VISCOSITY',/)
01060          WRITE(OUT,72) (XP(KU,KEG),YP(KU,KEG),VISCOS(KU,KEG),
01070        ?  KU=1,KOUNT,20)
01080      72 FORMAT(2X,F6.1,5X,F8.3,5X,F8.3)
01090         KONTEV = KOUNT/20*20
01100         IF(KONTEV.NE.KOUNT) WRITE(OUT,72) XP(KOUNT,KEG),YP(KOUNT,KEG),
01110        ?  VISCOS(KOUNT,KEG)
01120         WRITE(OUT,73)
01130      73 FORMAT(/)
01140 C        SAVE KOUNT (# OF POINTS) PER EACH CURVE, FOR USE BY PLOT ROUTINES
01150         NUMPTS(KEG) = KOUNT
01160         NPASS = KEG
01170 C    42 FORMAT(/,T10,'X',T23,'X/L',T36,'TEMP',T51,'DT/DX')
01180 C    42 FORMAT(/,T6,'X',T16,'TEMP' )
01190 C       ENDFILE 3
01200 C       REWIND 3
01210         RETURN
01220      79 WRITE(6,80)
01230      80 FORMAT(///,5X,'*** UNABLE TO CONVERGE IN 200 ITERATIONS.',
01240        ?  /,9X,'JOB TERMINATED IN SUBROUTINE DYSART. ')
01250         STOP
01260         END
```

Cdtdx

```
01270       SUBROUTINE CDTDX(NEQT,X,TEMP,YPRIME)
01280       COMMON/C10/ WORK(2,9),H,RINJ,C,FM,FK,TIME,PHI,LENGTH,TEMPD,W,TRES
01290       COMMON/C20/IN,OUT,XX,DX
01300       COMMON/C30/YDUP(1)
01310       COMMON/VJ10/CZERO,C1,C2,RHO,HKF
01320       DIMENSION TEMP(NEQT),YPRIME(1)
01330       INTEGER OUT
01340       REAL LENGTH
01350       DATA PI/3.14159/,POS/0.1E-20/,SQRTPI/1.772453/
01360 C.....CALCULATE NU (ZU)
01370       DPR = FM * FK
01380       IF (ABS(DPR).GE.POS) GO TO 12
01390       WRITE(OUT,33)
01400    33 FORMAT(/'   *** ERROR. DIVIDE CHECK CALC. ZN. ')
01410       STOP
01420    12 PR = SQRT( TIME/DPR )
01430 C     WL = CZERO * X * X + C1 * X + C2
01440 C      COMPUTE LEAKOFF RATE IN LB/FT**2-SEC
01450 C      CZERO IS THE LEAKOFF VELOCITY AT THE BASE OF FRACTURE.
01460 C      C1 IS LEAKOFF VELOCITY IN FT/DAY
01470       WL = CZERO + X/LENGTH * (C1-CZERO)
01480       WL = WL * RHO / 14400.
01490       DPL = H * (LENGTH*LENGTH) * (1.0-PHI)
01500 C     TO CONVERT TO LB/FT*FT-SEC
01510       WL = WL * RHO / 14000.
01520       IF (ABS(DPL).GE.POS) GO TO 18
01530       WRITE(OUT,44)
01540    44 FORMAT(/,'  *** ERROR. DIVIDE CHECK CALC. DPL.  ')
01550       STOP
01560    18 PLN = W * X * C
01570       ZN = PLN / DPL * PR
01580 C.....CALCULATE PSI   (PSI)
01590       EN = ZN * ZN
01600       PSI = EXP(-EN) - SQRTPI * ZN * ERFC(ZN)
01610 C.....CALCULATE DT/DX  (DTDX)
01620       DPR3 = PI * TIME
01630       IF (ABS(DPR3).GE.POS) GO TO 28
01640       WRITE(OUT,55)
01650    55 FORMAT(/'  *** ERROR. DIVIDE CHECK CALC. DPR3.  ')
01660       STOP
01670    28 FR = SQRT(DPR / DPR3)
01680       TST = X / LENGTH
01690       ST = TST * TST
01700        ST = ST -1.0E-06
01710       D3 = W * (1.-ST) * C
01720       IF (ABS(D3).GE.POS) GO TO 24
01730       WRITE(OUT,66)
01740    66 FORMAT(/'  *** ERROR. DIVIDE CHECK CALC. D3.'  )
01750       STOP
01760    24 DTDX = (2.*H) / D3 * FR * ( TRES - TEMP(1) ) * PSI
01770       YPRIME(1) = DTDX
01780       YDUP(1) = DTDX
01790 C     WRITE(OUT,1111) D3,ST,W,TEMP(1),PSI,DTDX
01800 C1111  FORMAT(' INTERMED ..D3,ST,W,TEMP,PSI,DTDX..',6E15.7)
01810       RETURN
01820       END
```

Echo

```
      SUBROUTINE ECHO
      DIMENSION FLTYPE(5)
      COMMON/C05/ JC(10,36),ECKVAL(36),JF(10)
      COMMON/C10/ WORK(2,9),H,RINJ,C,FM,FK,TIME,PHI,LENGTH,TEMP,W,TRES
      COMMON/C20/IN,OUT,X,DX
      COMMON/CLAIR/Q,MU,FH,G,CB,SP
      COMMON/C40/FLTYPE,DEPTH,PERM,PRESS,WIDTH
      COMMON/VJ10/CZERO,C1,C2,RHO,HKF
      COMMON/CAUG1/TINIT,TMAX,TINCR
      COMMON/TERCON/A,B,TLOW,THIGH,VLOW,VHIGH
      COMMON/INTTAB/NR,TEMINT(10),VISINT(10)
      DATA NW/10/
      INTEGER OUT,FLTYPE
      REAL LENGTH,MU
      WRITE(OUT,6)
    6 FORMAT(//,5X,'INPUT VALUES ARE:  ',/)
      WRITE(OUT,7) (JF(L),L=1,NW)
      WRITE(OUT,7)  FLTYPE
      NT = 35
      IF (NR.GT.0) NT = 31
      DO 10 K=1,NT
      WRITE(OUT,7) (JC(L,K),L=1,NW)
    7 FORMAT( 2X, 18A4 )
      WRITE(OUT,8) ECKVAL(K)
    8 FORMAT(2X,F15.5)
   10 CONTINUE
      IF (NR.LE.0) GO TO 16
      WRITE(OUT,7) (JC(L,32),L=1,NW)
      DO 15 K=1,NR
   15 WRITE(OUT,14) TEMINT(K),VISINT(K)
   14 FORMAT(2X,2F10.3)
   16 CONTINUE
      WRITE(OUT,12)
   12 FORMAT(//)
      RETURN
      END
```

Weltem

```
15760        SUBROUTINE WELTEM(T,XMU)
15770        DIMENSION LFTYPE(5)
15780        COMMON/C10/ WORK(2,9),H,RINJ,C,FM,FK,TIME,PHI,LENGTH,TEMP,WX,TRES
15790        COMMON/VJ10/CZERO,C1,C2,RHO,HKF
15800        COMMON/CAUG1/TINIT,TMAX,TINCR
15810        COMMON/ROCT11/DTI,DTE,DCI,DCE,GE,SFT,TES,TFS
15820        COMMON/INTTAB/NR,TEMINT(10),VISINT(10)
15830        COMMON/C40/LFTYPE,DEPTH,PERM,PRESS,WIDTH
15840        DELTZ = 500.
15850        GAMMA = RHO / 62.4
15860        WRITE(6,5)
15870      5 FORMAT(/,8X,'WELTEM CALCULATIONS',//,5X,'DEPTH',8X,'TEMPERATURE'/
15880 C      NR > 0  IF VISCOSITY TABLE IS TO BE READ IN.
15890        IF (NR.LE.0) GO TO 10
15900        FMU = VISINT(1)
15910        GO TO 15
15920     10 CALL TERP(TFS,FMU)
15930     15 PVN = C * FMU / HKF
15940        HH=(10.29*HKF*(RINJ*GAMMA*1440.)**0.8)/((DTI**1.8)*(FMU**0.8))*
15950       ?   PVN**0.4
15960        U =1./(1./HH+(DCE+DTE-DCI-DTI)/14400.+(DCI-DTE)/226.4)
15970        THOURS = TMAX / 3600.
15980        F = 1.18333 + 0.2119*THOURS - 0.09693 * DCE
15990        W = RINJ * 350. * 1440.
16000        RTI = DTI/2.
16010        FKDAY = FK * 86400.
16020        A = (W*C*(FKDAY+RTI*U*F))/(2.*3.14159*RTI*FKDAY*U)
16060        Z = 0.0
16070        WRITE(6,25) Z,TES
16080     20 Z = Z + DELTZ
16090        IF (Z.GE.DEPTH) GO TO 13
16100        T = GE * Z + TES - GE *·A + (TFS+GE*A-TES) * EXP(-Z/A)
16110        WRITE(6,25) Z,T
16120     25 FORMAT(5X,F6.0,6X,E14.6)
16130        GO TO 20
16140     13 IF ( (Z-DEPTH).LT.1.0) GO TO 31
16141        T = GE * DEPTH + TES - GE * A + (TFS+GE*A-TES) * EXP(-DEPTH/A)
16142        WRITE(6,25) DEPTH,T
16150     31 IF (NR.GT.0) GO TO 37
16160        CALL TERP(T,XMU)
16170        GO TO 39
16180     37 CALL INTERP(T,XMU)
16190     39 CONTINUE
16200        WRITE(6,26)
16210     26 FORMAT(//)
16220        RETURN
16230        END
```

Gertsm

```
11650       SUBROUTINE GERTSM(T,TINJ)
11660       COMMON/C10/WORK(2,9),H,RINJ,COLD,FM,FK,OLDTIM,PHI,LENGTH,TEMPV
11670      ?  OLDW,TRES
11680       COMMON/C20/IN,OUT,X,DX
11690       COMMON/C40/FLTYPE,DEPTH,PERM,PRESS,WIDTH
11700       COMMON/CLAIR/Q,MU,FH,G,C,SP
11710       COMMON/C60/KURVE
11720       COMMON/CMG/MODELS
11730       COMMON/FRACV/WS(10),XLS(10),VOLS(10),EFFS(10),TIM(10)
11740       INTEGER YES/'Y'/
11750       REAL LENGTH,MU
11760       REAL MT,MU
11770 C      NO EXIT FROM HERE UNTIL SUCCESSIVE XL'S CONVERGE.
11780       TIME = T/60.
11790       PI = 3.14159
11800       SAVXL = -1.
11810       TROOT = SQRT(TIME)
11820       WRITE(6,1) KURVE
11830     1 FORMAT(//,5X,'*****  CURVE  # ',I1,'  *****',//)
11840     2 ZAP1 = FH * (C*C)
11850       ZAP2 = .00561 * Q / ZAP1
11860       ZAP3 = ZAP2 * ZAP2 * ZAP2
11870       WRITE(6,3) MU
11880     3 FORMAT(/,5X,'IN  GERTSM:  MU =',F8.2 ,/)
11890       DKML = 8.724 * ZAP3 * (145. * MU / (G*60.* TIME))
11900       DKU = 1
11910       DKUP = DKU
11920       KIT = 0
11930    50 CONTINUE
11940       KIT = KIT + 1
11950       IF (KIT.LT.500) GO TO 52
11960       WRITE(3,53) KURVE
11970    53 FORMAT(/,5X,'%-',I1).
11980       GO TO 100
11990    52 CONTINUE
12000       IF (SP.NE.0.0) GO TO 34
12010       A = PI
12020       GO TO 5
12030    34 DKS = C * TROOT / SP
12040       A = PI + 8. * DKU / DKS
12050     5 CONTINUE
12060       ARG = 8.* SQRT(PI) * DKU / A
12070       IF (ARG.LT.2.) GO TO 10
12080       NUM = 1
12090       EAE = 1
12100       DO 40 N=1,8
12110       NUM = (2 * N - 1) * NUM
12120       EAE = EAE + (-1) ** N * NUM/(2*(ARG*ARG))**N
12130    40 CONTINUE
12140       EAE = EAE/ARG/SQRT(PI)
12150       DKL = (1.-(A/16./DKU)*(1.-EAE))/2./PI
```

```
12160         GO TO 11
12170      10 CONTINUE
12180         ARG2 = ARG * ARG
12190         CX = ERFC(ARG)
12200         DKL = (1.-(A/16./DKU) * (1.-EXP(ARG2)*CX))/2./PI
12210      11 CONTINUE
12220         DKU =(1./DKML/DKL/DKL) ** .25
12230         DDKU = DKU - DKUP
12240         DDKU = ABS(DDKU)
12250         IF(DDKU.LT..0001) GO TO 100
12260         DKUP = DKU
12270         GO TO 50
12280     100 CONTINUE
12290         W = 12.*C*TROOT/DKU
12300         XL = 5.61 * Q * TROOT * DKL/C/FH
12310         VOL = 2. * W * XL * FH / 12.
12320         EFF = VOL * 100. / (Q*5.61*TIME)
12330         WRITE(6,21)
12340      21 FORMAT(//,5X,'WIDTH',4X,'LENGTH',4X,'VOLUME',5X,'EFF.',
12350        ?  7X,'TIME' ,/)
12360         WRITE(6,22) W,XL,VOL,EFF,TIME
12370      22 FORMAT( F10.3,2F10.1,F9.1,F11.1)
12380         VERG = ABS(XL-SAVXL) / XL
12390         SAVXL = XL
12400         IF (VERG.LT.0.01) GO TO 300
12410         IF (MODELS.NE.YES) GO TO 24
12420         ALTRES = TRES
12430 C       TINJ, RETURNED FROM WELTEM, IS INPUT TO SINCLR.
12440         CALL SINCLR(RINJ,ALTRES,TINJ,W,H,TIME,FK,XL,MU,FM,EFF)
12450         GO TO 2
12460      24 CONTINUE
12470         CALL DYSART(T,XL,W,EFF,MU)
12480         GO TO 2
12490     300 CONTINUE
12500         WRITE(6,38)
12510      38 FORMAT(//,5X,'CONVERGENCE REACHED IN SUBROUTINE GERTSM. ',//)
12520 C       NOW INCREMENT POINTER TO NEXT CURVE. (SECOND DIMENSION OF
12530 C       ARRAYS XP,YP,VISCOS IN SUBROUTINE FRAC.
12540         KURVE = KURVE + 1
12550         KU = KURVE
12560         WS(KU) = W
12570          XLS(KU) = XL
12580          VOLS(KU) = VOL
12590          EFFS(KU) = EFF
12600          TIM(KU) = TIME
12610         RETURN
12620         END
```

Plotv

```
      SUBROUTINE PLOTV( NUMPTS)
      DIMENSION XA(202),VA(202),LUMA(9),NUMPTS(9),DIF(9),DIFV(9)
      COMMON/PLAY/ XD(202,9),YD(202,9),VISCOS(202,9)
      COMMON/C20/IN,OUT,XXDUM,DXDUM
      INTEGER OUT
      COMMON/C50/ SAVAVT(10), NDUMMY(9),NPASS
      DATA MAX/200/,LUMA/0,1,2,5,6,10,14,36,37/,PLOTHT/6.5/,PLOTWD/9.5
      SMALL = .1E+10
      BIG   = .1E-10
      SMLV = .1E+10
      BIGV = .1E-10
      DO 5 K=1,NPASS
      NCR = NUMPTS(K)
      NCRLIM = NCR
      IF (NCRLIM.GT.200) NCRLIM = 200
      DO 8 L=1,NCRLIM
      XPL = XD(L,K)
      YPL = VISCOS(L,K)
      IF (XPL.LT.SMALL) SMALL = XPL
      IF (XPL.GT.BIG  )  BIG  = XPL
      IF (YPL.LT.SMLV) SMLV = YPL
      IF (YPL.GT.BIGV) BIGV = YPL
    8 CONTINUE
      DIF(K) = BIG - SMALL
    5 DIFV(K) = BIGV - SMLV
      BIGDIF = .1E-10
      IUSE = 0
      DO 9 K=1,NPASS
      IF (DIF(K).LE.BIGDIF) GO TO 9
      BIGDIF = DIF(K)
      IUSE = K
    9 CONTINUE
      BIGDV = .1E-10
      IUSEV = 0
      DO 14 K=1,NPASS
      IF (DIFV(K).LE.BIGDV) GO TO 14
      BIGDV = DIFV(K)
      IUSEV = K
   14 CONTINUE
C     IUSE & IUSEV INDICATE WHICH CURVES HAVE LARGEST MAX & MIN VALUES
      IF (IUSE.GT.0.AND.IUSEV.GT.0) GO TO 11
      WRITE(OUT,12)
   12 FORMAT(//,2X,'*** ERROR IN SUB.PLOTV. VALUE OF IUSE IS ',
     ?  'INVALID. JOB TERMINATED. ')
      STOP
   11 CONTINUE
      LPTS = NUMPTS(IUSE)
      IF (LPTS.GT.200) LPTS = 200
      DO 10 K=1,LPTS
      VA(K) = VISCOS(K,IUSE)
   10 XA(K) = XD(K,IUSE)
```

```
      CALL PLOT(0.,0.,-3)
      CALL PLOT(11.5,0.,2)
      CALL PLOT(11.5,8.5,2)
      CALL PLOT(0.,8.5,2)
      CALL PLOT(0.,0.,2)
      CALL PLOT(1.,1.,-3)
      CALL SCALE(XA,PLOTWD,LPTS,1)
      CALL SCALE(VA,PLOTHT,LPTS,1)
      BEGINX = XA(LPTS+1)
      DELTX  = XA(LPTS+2)
C     BEGINV = VA(LPTS+1)
      BEGINV = VA(LPTS+1) - ( DIFV(IUSEV)*.1)
      DELTV  = VA(LPTS+2)
      CALL AXIS(0.,0.,' ',-1,PLOTWD,0.,BEGINX,DELTX )
      CALL SYMBOL(3.,-0.75,0.175,'FRACTURE DISTANCE - FEET',
     ?  0.,24)
      CALL AXIS(0.,0.,' ',1,PLOTHT,90.,BEGINV,DELTV )
      CALL SYMBOL(-.5,2.5,0.175,'VISCOSITY  -  CP.',90.,17)
      CALL SYMBOL(1.3,7.0,0.175,
     ? 'FLUID VISCOSITY VS DISTANCE IN FRACTURE',0.0,39)
   20 CONTINUE
      DO 30 KEG=1,NPASS
      KPTS = NUMPTS(KEG)
      IF (KPTS.GT.200) KPTS = 200
      DO 25 K=1,KPTS
      XA(K) = XD(K,KEG)
   25 VA(K)  = VISCOS(K,KEG)
      XA(KPTS+1) = BEGINX
      XA(KPTS+2) = DELTX
      VA(KPTS+1) = BEGINV
      VA(KPTS+2) = DELTV
   30 CALL LINE(XA,VA,KPTS,1,10,LUMA(KEG))
      RETURN
   77 WRITE(6,84) KNT,MAX
   84 FORMAT(/,'  **** ERROR. KNT=',I3,' IS GREATER THAN MAX. (',I3,')'
     ?  '  PROGRAM TERMINATED.')
      STOP
      END
```

Terp

```
10710       SUBROUTINE TERP(TEMP,VIS)
10720       COMMON/TERCON/A,B,TLOW,THIGH,VLOW,VHIGH
10730       VIS = B * 10.**(A*TEMP)
10740       RETURN
10750       END
```

Dverk

```
      SUBROUTINE DVERK  (N,FCN,X,Y,XEND,TOL,IND,C,NW,W,IER)
C
      INTEGER           N,IND,NW,K
      INTEGER           IER
C1    DOUBLE PRECISION  X,Y(N),XEND,TOL,C(1),W(NW,9),TEMP
      REAL              X,Y(N),XEND,TOL,C(1),W(NW,9),TEMP
C1    DOUBLE PRECISION  ZERO,ONE,TWO,THREE,FOUR,FIVE,SEVEN,TEN,HALF,P
      REAL              ZERO,ONE,TWO,THREE,FOUR,FIVE,SEVEN,TEN,HALF,P
     1                  C4D15,C2D3,C5D6,C1D6,C1D15,C2D96
C1    DOUBLE PRECISION  RK(39),REPS,RTOL
      REAL              RK(39),REPS,RTOL
C1    DATA              ZERO/0.0D0/,ONE/1.0D0/,TWO/2.0D0/,THREE/3.0D0
      DATA              ZERO/0.0/,ONE/1.0/,TWO/2.0/,THREE/3.0/
C1    DATA              FOUR/4.0D0/,FIVE/5.0D0/,SEVEN/7.0D0/
      DATA              FOUR/4.0/,FIVE/5.0/,SEVEN/7.0/
C1    DATA              TEN/10.0D0/,HALF/0.5D0/,P9/0.9D0/
      DATA              TEN/10.0/,HALF/0.5/,P9/0.9/
C1    DATA              C4D15/.26666666666666 7D0/
      DATA              C4D15/.2666667/
C1    DATA              C2D3/.66666666666666 7D0/
      DATA              C2D3/.6666667/
C1    DATA              C5D6/.83333333333333 3D0/
      DATA              C5D6/.8333333/
C1    DATA              C1D6/.16666666666666 7D0/
      DATA              C1D6/.1666667/
C1    DATA              C1D15/.66666666666666 7D-1/
      DATA              C1D15/.6666667E-1/
C1    DATA              C2D96/120.4272910821709D0/
      DATA              C2D96/120.4273/
C1    DATA              REPS/Z3410000000000000/
      DATA              REPS/Z3C100000/
C1    DATA              RTOL/Z0D10000000000000/
      DATA              RTOL/Z05100000/
C1    DATA              RK( 1)/.16666666666666 7D+00/
      DATA              RK( 1)/.1666667E+00/
C1    DATA              RK( 2)/.53333333333333 3D-01/
      DATA              RK( 2)/.5333333E-01/
C1    DATA              RK( 3)/.21333333333333 3D+00/
      DATA              RK( 3)/.2133333E+00/
C1    DATA              RK( 4)/.83333333333333 3D+00/
      DATA              RK( 4)/.8333333E+00/
C1    DATA              RK( 5)/.26666666666666 7D+01/
      DATA              RK( 5)/.2666667E+01/
C1    DATA              RK( 6)/.25000000000000 0D+01/
      DATA              RK( 6)/.2500000E+01/
C1    DATA              RK( 7)/.25781250000000 0D+01/
      DATA              RK( 7)/.2578125E+01/
C1    DATA              RK( 8)/.91666666666666 7D+01/
      DATA              RK( 8)/.9166667E+01/
C1    DATA              RK( 9)/.66406250000000 0D+01/
      DATA              RK( 9)/.6640625E+01/
C1    DATA              RK(10)/.88541666666666 7D+00/
      DATA              RK(10)/.8854167E+00/
C1    DATA              RK(11)/.24000000000000 0D+01/
      DATA              RK(11)/.2400000E+01/
C1    DATA              RK(12)/.80000000000000 0D+01/
```

```
      DATA  RK(12)/.8000000E+01/
C1    DATA  RK(13)/.6560457516339869D+01/
      DATA  RK(13)/.6560458E+01/
C1    DATA  RK(14)/.3055555555555556D+00/
      DATA  RK(14)/.3055556E+00/
C1    DATA  RK(15)/.3450980392156863D+00/
      DATA  RK(15)/.3450980E+00/
C1    DATA  RK(16)/.5508666666666667D+00/
      DATA  RK(16)/.5508667E+00/
C1    DATA  RK(17)/.1653333333333333D+01/
      DATA  RK(17)/.1653333E+01/
C1    DATA  RK(18)/.9455882352941176D+00/
      DATA  RK(18)/.9455882E+00/
C1    DATA  RK(19)/.3240000000000000D+00/
      DATA  RK(19)/.3240000E+00/
C1    DATA  RK(20)/.2337882352941176D+00/
      DATA  RK(20)/.2337882E+00/
C1    DATA  RK(21)/.2035465116279070D+01/
      DATA  RK(21)/.2035465E+01/
C1    DATA  RK(22)/.6976744186046512D+01/
      DATA  RK(22)/.6976744E+01/
C1    DATA  RK(23)/.5648179814561484D+01/
      DATA  RK(23)/.5648180E+01/
C1    DATA  RK(24)/.1373815676141258D+00/
      DATA  RK(24)/.1373816E+00/
C1    DATA  RK(25)/.2863022661036103D+00/
      DATA  RK(25)/.2863023E+00/
C1    DATA  RK(26)/.1441785567164738D+00/
      DATA  RK(26)/.1441786E+00/
C1    DATA  RK(27)/.7500000000000000D-01/
      DATA  RK(27)/.7500000E-01/
C1    DATA  RK(28)/.3899286987522282D+00/
      DATA  RK(28)/.3899287E+00/
C1    DATA  RK(29)/.3194444444444444D+00/
      DATA  RK(29)/.3194444E+00/
C1    DATA  RK(30)/.1350383631713555D+00/
      DATA  RK(30)/.1350384E+00/
C1    DATA  RK(31)/.1078329882677709D-01/
      DATA  RK(31)/.1078330E-01/
C1    DATA  RK(32)/.6980519480519481D-01/
      DATA  RK(32)/.6980519E-01/
C1    DATA  RK(33)/.6250000000000000D-02/
      DATA  RK(33)/.6250000E-02/
C1    DATA  RK(34)/.6963012477718360D-02/
      DATA  RK(34)/.6963012E-02/
C1    DATA  RK(35)/.6944444444444444D-02/
      DATA  RK(35)/.6944444E-02/
C1    DATA  RK(36)/.6138107416879795D-02/
      DATA  RK(36)/.6138107E-02/
C1    DATA  RK(37)/.6818181818181818D-01/
      DATA  RK(37)/.6818182E-01/
C1    DATA  RK(38)/.1078329882677709D-01/
      DATA  RK(38)/.1078330E-01/
C1    DATA  RK(39)/.6980519480519481D-01/
      DATA  RK(39)/.6980519E-01/
C
```

```
C                                       BEGIN INITIALIZATION, PARAMETER
C                                         CHECKING, INTERRUPT RE-ENTRIES
      IER = 0
C                                       ABORT IF IND OUT OF RANGE 1 TO 6
      IF (IND.LT.1.OR.IND.GT.6) GO TO 290
C                                       CASES - INITIAL ENTRY, NORMAL
C                                         RE-ENTRY, INTERRUPT RE-ENTRIES
      GO TO (5,5,40,145,265,265), IND
C                                     . CASE 1 - INITIAL ENTRY (IND .EQ. 1
C                                         OR 2) ABORT IF N.GT.NW OR TOL.LE.
C
    5 IF (N.GT.NW.OR.TOL.LE.ZERO) GO TO 295
      IF (IND.EQ.2) GO TO 15
C                                       INITIAL ENTRY WITHOUT OPTIONS (IND
C                                         .EQ. 1) SET C(1) TO C(9) EQUAL TO
C                                         0
      DO 10 K=1,9
         C(K) = ZERO
   10 CONTINUE
      GO TO 30
C                                       SUMMARY OF THE COMPONENTS OF THE
C                                         COMMUNICATIONS VECTOR
C                                         PRESCRIBED AT THE OPTION
C                                             OF THE USER
C
C                                         C(1) ERROR CONTROL INDICATOR
C                                         C(2) FLOOR VALUE
C                                         C(3) HMIN SPECIFICATION
C                                         C(4) HSTART SPECIFICATION
C                                         C(5) SCALE SPECIFICATION
C                                         C(6) HMAX SPECIFICATION
C                                         C(7) MAX NO OF FCN EVALS
C                                         C(8) INTERRUPT NO 1
C                                         C(9) INTERRUPT NO 2
C
C                                         DETERMINED BY THE PROGRAM
C
C                                         C(10) RREB(REL ROUNDOFF ERROR BND
C                                         C(11) DWARF (VERY SMALL MACH NO)
C                                         C(12) WEIGHTED NORM Y
C                                         C(13) HMIN
C                                         C(14) HMAG
C                                         C(15) SCALE
C                                         C(16) HMAX
C                                         C(17) XTRIAL
C                                         C(18) HTRIAL
C                                         C(19) EST
C                                         C(20) PREVIOUS XEND
C                                         C(21) FLAG FOR XEND
C                                         C(22) NO OF SUCCESSFUL STEPS
C                                         C(23) NO OF SUCCESSIVE FAILURES
C                                         C(24) NO OF FCN EVALS
C                                         IF C(1) = 4 OR 5, C(31),C(32),...
C                                           C(N+30) ARE FLOOR VALUES
   15 CONTINUE
C                                       INITIAL ENTRY WITH OPTIONS (IND .EQ.
```

```
C                                          2) MAKE C(1) TO C(9) NON-NEGATIVE
      DO 20 K=1,9
C1       C(K) = DABS(C(K))
         C(K) = ABS(C(K))
   20 CONTINUE
C                                        MAKE FLOOR VALUES NON-NEGATIVE IF
C                                          THEY ARE TO BE USED
C
      IF (C(1).NE.FOUR.AND.C(1).NE.FIVE) GO TO 30
      DO 25 K=1,N
C1       C(K+30) = DABS(C(K+30))
         C(K+30) = ABS(C(K+30))
   25 CONTINUE
   30 CONTINUE
C                                        INITIALIZE RREB, DWARF, PREV XEND,
C                                          FLAG, COUNTS
      C(10) = REPS
      C(11) = RTOL
C                                        SET PREVIOUS XEND INITIALLY TO
C                                          INITIAL VALUE OF X
      C(20) = X
      DO 35 K=21,24
         C(K) = ZERO
   35 CONTINUE
      GO TO 45
C                                        CASE 2 - NORMAL RE-ENTRY (IND .EQ.
C                                          3) ABORT IF XEND REACHED, AND
C                                          EITHER X CHANGED OR XEND NOT
   40 IF (C(21).NE.ZERO.AND.(X.NE.C(20).OR.XEND.EQ.C(20))) GO TO 285
C
C                                        RE-INITIALIZE FLAG
      C(21) = ZERO
C                                        CASE 3 - RE-ENTRY FOLLOWING AN
C                                          INTERRUPT (IND .EQ. 4 TO 6)
C                                          TRANSFER CONTROL TO THE
C                                          APPROPRIATE RE-ENTRY POINT. THIS
C                                          HAS ALREADY BEEN HANDLED BY THE
C                                          COMPUTED GO TO.
   45 CONTINUE
C                                        LOOP THROUGH THE FOLLOWING 4 STAGES
C                                          ONCE FOR EACH TRIAL STEP UNTIL TH
C                                          OCCURRENCE OF ONE OF THE FOLLOWIN
C                                          (A) THE NORMAL RETURN (WITH IND
C                                          .EQ. 3) ON REACHING XEND IN STAGE
C                                          4 (B) AN ERROR RETURN (WITH IND
C                                          .LT. 0) IN STAGE 1 OR STAGE 4 (C)
C                                          AN INTERRUPT RETURN (WITH IND .EQ
C                                          4, 5 OR 6), IF REQUESTED, IN STAG
C                                          1 OR STAGE 4
   50 CONTINUE
C                                        STAGE 1 - PREPARE - DO CALCULATIONS
C                                          OF HMIN, HMAX, ETC., AND SOME
C                                          PARAMETER CHECKING, AND END UP
C                                          WITH SUITABLE VALUES OF HMAG,
C                                          XTRIAL AND HTRIAL IN PREPARATION
C                                          FOR TAKING AN INTEGRATION STEP.
```

```
C                                          ERROR RETURN (WITH IND=-1) IF NO
C                                          OF FCN EVALS TOO GREAT
C
      IF (C(7).EQ.ZERO.OR.C(24).LT.C(7)) GO TO 55
      IND = -1
      GO TO 9005
   55 CONTINUE
C                                        CALCULATE SLOPE (ADDING 1 TO NO OF
C                                          FCN EVALS) IF IND .NE. 6
      IF (IND.EQ.6) GO TO 60
      CALL FCN (N,X,Y,W(1,1))
      C(24) = C(24)+ONE
   60 CONTINUE
C                                        CALCULATE HMIN - USE DEFAULT UNLESS
C                                          VALUE PRESCRIBED
      C(13) = C(3)
      IF (C(3).NE.ZERO) GO TO 120
C                                        CALCULATE DEFAULT VALUE OF HMIN
C                                          FIRST CALCULATE WEIGHTED NORM Y -
C                                          C(12) - AS SPECIFIED BY THE ERROR
C                                          CONTROL INDICATOR C(1)
      TEMP = ZERO
      IF (C(1).NE.ONE) GO TO 70
C                                        ABSOLUTE ERROR CONTROL - WEIGHTS AR
C                                          1
      DO 65 K=1,N
C1       TEMP = DMAX1(TEMP,DABS(Y(K)))
         TEMP = AMAX1(TEMP,ABS(Y(K)))
   65 CONTINUE
      C(12) = TEMP
      GO TO 115
   70 IF (C(1).NE.TWO) GO TO 75
C                                        RELATIVE ERROR CONTROL - WEIGHTS AR
C                                          1/DABS(Y(K)) SO WEIGHTED NORM Y I
C                                          1
      C(12) = ONE
      GO TO 115
   75 IF (C(1).NE.THREE) GO TO 85
C                                        WEIGHTS ARE 1/MAX(C(2),ABS(Y(K)))
      DO 80 K=1,N
C1       TEMP = DMAX1(TEMP,DABS(Y(K))/C(2))
         TEMP = AMAX1(TEMP,ABS(Y(K))/C(2))
   80 CONTINUE
C1    C(12) = DMIN1(TEMP,ONE)
      C(12) = AMIN1(TEMP,ONE)
      GO TO 115
   85 IF (C(1).NE.FOUR) GO TO 95
C                                        WEIGHTS ARE 1/MAX(C(K+30),ABS(Y(K))
      DO 90 K=1,N
C1       TEMP = DMAX1(TEMP,DABS(Y(K))/C(K+30))
         TEMP = AMAX1(TEMP,ABS(Y(K))/C(K+30))
   90 CONTINUE
C1    C(12) = DMIN1(TEMP,ONE)
      C(12) = AMIN1(TEMP,ONE)
      GO TO 115
   95 IF (C(1).NE.FIVE) GO TO 105
```

```
C                                       WEIGHTS ARE 1/C(K+30)
      DO 100 K=1,N
C1       TEMP = DMAX1(TEMP,DABS(Y(K))/C(K+30))
         TEMP = AMAX1(TEMP,ABS(Y(K))/C(K+30))
  100 CONTINUE
      C(12) = TEMP
      GO TO 115
  105 CONTINUE
C                                     . DEFAULT CASE - WEIGHTS ARE
C                                         1/MAX(1,ABS(Y(K)))
      DO 110 K=1,N
C1       TEMP = DMAX1(TEMP,DABS(Y(K)))
         TEMP = AMAX1(TEMP,ABS(Y(K)))
  110 CONTINUE
C1    C(12) = DMIN1(TEMP,ONE)
      C(12) = AMIN1(TEMP,ONE)
  115 CONTINUE
C1    C(13) = TEN*DMAX1(C(11),C(10)*DMAX1(C(12)/TOL,DABS(X)))
      C(13) = TEN*AMAX1(C(11),C(10)*AMAX1(C(12)/TOL,ABS(X)))
  120 CONTINUE
C                                       CALCULATE SCALE - USE DEFAULT UNLESS
C                                         VALUE PRESCRIBED
      C(15) = C(5)
      IF (C(5).EQ.ZERO) C(15) = ONE
C                                       CALCULATE HMAX - CONSIDER 4 CASES
C                                         CASE 1 - BOTH HMAX AND SCALE
C                                         PRESCRIBED
C
C1    IF (C(6).NE.ZERO.AND.C(5).NE.ZERO) C(16) = DMIN1(C(6),TWO/C(5))
      IF (C(6).NE.ZERO.AND.C(5).NE.ZERO) C(16) = AMIN1(C(6),TWO/C(5))
C
C                                       CASE 2 - HMAX PRESCRIBED, BUT SCALE
C                                         NOT
C
      IF (C(6).NE.ZERO.AND.C(5).EQ.ZERO) C(16) = C(6)
C
C                                       CASE 3 - HMAX NOT PRESCRIBED, BUT
C                                         SCALE IS
C
      IF (C(6).EQ.ZERO.AND.C(5).NE.ZERO) C(16) = TWO/C(5)
C
C                                       CASE 4 - NEITHER HMAX NOR SCALE IS
C                                         PROVIDED
C
      IF (C(6).EQ.ZERO.AND.C(5).EQ.ZERO) C(16) = TWO
C
C                                       ERROR RETURN (WITH IND=-2) IF HMIN
C                                         .GT. HMAX
      IF (C(13).LE.C(16)) GO TO 125
      IND = -2
      GO TO 9005
  125 CONTINUE
C                                       CALCULATE PRELIMINARY HMAG -
C                                         CONSIDER 3 CASES
      IF (IND.GT.2) GO TO 130
C                                       CASE 1 - INITIAL ENTRY - USE
```

```
C                                       PRESCRIBED VALUE OF HSTART, IF
C                                       ANY, ELSE DEFAULT
      C(14) = C(4)
      IF (C(4).EQ.ZERO) C(14) = C(16)*TOL**C1D6
      GO TO 140
  130 IF (C(23).GT.ONE) GO TO 135
C                                     CASE 2 - AFTER A SUCCESSFUL STEP, (
C                                       AT MOST ONE FAILURE, USE MIN(2,
C                                       .9*(TOL/EST)**(1/6))*HMAG, BUT
C                                       AVOID POSSIBLE OVERFLOW. THEN
C                                       AVOID REDUCTION BY MORE THAN HALF
      TEMP = TWO*C(14)
      IF (TOL.LT.C2D96*C(19)) TEMP = P9*(TOL/C(19))**C1D6*C(14)
C1    C(14) = DMAX1(TEMP,HALF*C(14))
      C(14) = AMAX1(TEMP,HALF*C(14))
      GO TO 140
  135 CONTINUE
C                                     CASE 3 - AFTER TWO OR MORE
C                                       SUCCESSIVE FAILURES
      C(14) = HALF*C(14)
  140 CONTINUE
C                                     CHECK AGAINST HMAX
C1    C(14) = DMIN1(C(14),C(16))
      C(14) = AMIN1(C(14),C(16))
C                                     CHECK AGAINST HMIN
C1    C(14) = DMAX1(C(14),C(13))
      C(14) = AMAX1(C(14),C(13))
C                                     INTERRUPT NO 1 (WITH IND=4) IF
C                                       REQUESTED
      IF (C(8).EQ.ZERO) GO TO 145
      IND = 4
      GO TO 9005
C                                     RESUME HERE ON RE-ENTRY WITH IND
C                                       .EQ. 4
  145 CONTINUE
C                                     CALCULATE HMAG, XTRIAL - DEPENDING
C                                       ON PRELIMINARY HMAG, XEND
C
C1    IF (C(14).GE.DABS(XEND-X)) GO TO 150
      IF (C(14).GE.ABS(XEND-X)) GO TO 150
C
C                                     DO NOT STEP MORE THAN HALF WAY TO
C                                       XEND
C
C1    C(14) = DMIN1(C(14),HALF*DABS(XEND-X))
      C(14) = AMIN1(C(14),HALF*ABS(XEND-X))
C1    C(17) = X+DSIGN(C(14),XEND-X)
      C(17) = X+SIGN(C(14),XEND-X)
      GO TO 155
  150 CONTINUE
C                                     HIT XEND EXACTLY
C1    C(14) = DABS(XEND-X)
      C(14) = ABS(XEND-X)
      C(17) = XEND
  155 CONTINUE
C                                     CALCULATE HTRIAL
```

```
C                                       VECTOR (PER UNIT STEP) FOR THE
C                                       UNEXTRAPOLATED APPROXIMATION AND
C                                       STORE IT IN W(*,2). THEN CALCULAT
C                                       THE WEIGHTED MAX NORM OF W(*,2) A
C                                       SPECIFIED BY THE ERROR CONTROL
C                                       INDICATOR C(1). FINALLY, MODIFY
C                                       THIS RESULT TO PRODUCE EST, THE
C                                       ERROR ESTIMATE (PER UNIT STEP) FO
C                                       THE EXTRAPOLATED APPROXIMATION
C                                       YTRIAL.
C
C                                     CALCULATE THE UNWEIGHTED ABSOLUTE
C                                       ERROR ESTIMATE VECTOR.
      DO 200 K=1,N
         W(K,2) = W(K,1)*RK(33)+W(K,3)*RK(34)-W(K,4)*RK(35)+W(K,5)
     1   *RK(36)+W(K,6)*RK(37)-W(K,7)*RK(38)-W(K,8)*RK(39)
  200 CONTINUE
C                                     CALCULATE THE WEIGHTED MAX NORM OF
C                                       W(*,2) AS SPECIFIED BY THE ERROR
C                                       CONTROL INDICATOR C(1)
      TEMP = ZERO
      IF (C(1).NE.ONE) GO TO 210
C                                     ABSOLUTE ERROR CONTROL
      DO 205 K=1,N
C1       TEMP = DMAX1(TEMP,DABS(W(K,2)))
         TEMP = AMAX1(TEMP,ABS(W(K,2)))
  205 CONTINUE
      GO TO 260
  210 IF (C(1).NE.TWO) GO TO 220
C                                     RELATIVE ERROR CONTROL
      DO 215 K=1,N
         IF (Y(K).EQ.ZERO) GO TO 280
C1       TEMP = DMAX1(TEMP,DABS(W(K,2)/Y(K)))
         TEMP = AMAX1(TEMP,ABS(W(K,2)/Y(K)))
  215 CONTINUE
      GO TO 260
  220 IF (C(1).NE.THREE) GO TO 230
C                                     WEIGHTS ARE 1/MAX(C(2),ABS(Y(K)))
      DO 225 K=1,N
C1       TEMP = DMAX1(TEMP,DABS(W(K,2))/DMAX1(C(2),DABS(Y(K))))
         TEMP = AMAX1(TEMP,ABS(W(K,2))/AMAX1(C(2),ABS(Y(K))))
  225 CONTINUE
      GO TO 260
  230 IF (C(1).NE.FOUR) GO TO 240
C                                     WEIGHTS ARE 1/MAX(C(K+30),ABS(Y(K))
      DO 235 K=1,N
C1       TEMP = DMAX1(TEMP,DABS(W(K,2))/DMAX1(C(K+30),DABS(Y(K))))
         TEMP = AMAX1(TEMP,ABS(W(K,2))/AMAX1(C(K+30),ABS(Y(K))))
  235 CONTINUE
      GO TO 260
  240 IF (C(1).NE.FIVE) GO TO 250
C                                     WEIGHTS ARE 1/C(K+30)
      DO 245 K=1,N
C1       TEMP = DMAX1(TEMP,DABS(W(K,2)/C(K+30)))
         TEMP = AMAX1(TEMP,ABS(W(K,2)/C(K+30)))
  245 CONTINUE
```

```
      C(18) = C(17)-X
C                                        STAGE 2 - CALCULATE YTRIAL (ADDING
C                                          TO NO OF FCN EVALS). W(*,2), ...
C                                          W(*,8) HOLD INTERMEDIATE RESULTS
C                                          NEEDED IN STAGE 3. W(*,9) IS
C                                          TEMPORARY STORAGE UNTIL FINALLY I
C                                          HOLDS YTRIAL.
      DO 160 K=1,N
         W(K,9) = Y(K)+C(18)*W(K,1)*RK(1)
  160 CONTINUE
      CALL FCN (N,X+C(18)*C1D6,W(1,9),W(1,2))
C
      DO 165 K=1,N
         W(K,9) = Y(K)+C(18)*(W(K,1)*RK(2)+W(K,2)*RK(3))
  165 CONTINUE
      CALL FCN (N,X+C(18)*C4D15,W(1,9),W(1,3))
C
      DO 170 K=1,N
         W(K,9) = Y(K)+C(18)*(W(K,1)*RK(4)-W(K,2)*RK(5)+W(K,3)*RK(6))
  170 CONTINUE
      CALL FCN (N,X+C(18)*C2D3,W(1,9),W(1,4))
C
      DO 175 K=1,N
         W(K,9) = Y(K)+C(18)*(-W(K,1)*RK(7)+W(K,2)*RK(8)-W(K,3)*RK(9)
     1   +W(K,4)*RK(10))
  175 CONTINUE
      CALL FCN (N,X+C(18)*C5D6,W(1,9),W(1,5))
C
      DO 180 K=1,N
         W(K,9) = Y(K)+C(18)*(W(K,1)*RK(11)-W(K,2)*RK(12)+W(K,3)*RK(13
     1   -W(K,4)*RK(14)+W(K,5)*RK(15))
  180 CONTINUE
      CALL FCN (N,X+C(18),W(1,9),W(1,6))
C
      DO 185 K=1,N
         W(K,9) = Y(K)+C(18)*(-W(K,1)*RK(16)+W(K,2)*RK(17)-W(K,3)
     1   *RK(18)-W(K,4)*RK(19)+W(K,5)*RK(20))
  185 CONTINUE
      CALL FCN (N,X+C(18)*C1D15,W(1,9),W(1,7))
C
      DO 190 K=1,N
         W(K,9) = Y(K)+C(18)*(W(K,1)*RK(21)-W(K,2)*RK(22)+W(K,3)*RK(23
     1   -W(K,4)*RK(24)+W(K,5)*RK(25)+W(K,7)*RK(26))
  190 CONTINUE
      CALL FCN (N,X+C(18),W(1,9),W(1,8))
C                                        CALCULATE YTRIAL, THE EXTRAPOLATED
C                                          APPROXIMATION AND STORE IN W(*,9)
      DO 195 K=1,N
         W(K,9) = Y(K)+C(18)*(W(K,1)*RK(27)+W(K,3)*RK(28)+W(K,4)*RK(29
     1   +W(K,5)*RK(30)+W(K,7)*RK(31)+W(K,8)*RK(32))
  195 CONTINUE
C                                        ADD 7 TO THE NO OF FCN EVALS
      C(24) = C(24)+SEVEN
C                                        STAGE 3 - CALCULATE THE ERROR
C                                          ESTIMATE EST. FIRST CALCULATE THE
C                                          UNWEIGHTED ABSOLUTE ERROR ESTIMATI
```

```
      GO TO 260
  250 CONTINUE
C                                       DEFAULT CASE - WEIGHTS ARE
C                                         1/MAX(1,ABS(Y(K)))
      DO 255 K=1,N
C1       TEMP = DMAX1(TEMP,DABS(W(K,2))/DMAX1(ONE,DABS(Y(K))))
         TEMP = AMAX1(TEMP,ABS(W(K,2))/AMAX1(ONE,ABS(Y(K))))
  255 CONTINUE
  260 CONTINUE
C                                       CALCULATE EST - (THE WEIGHTED MAX
C                                         NORM OF W(*,2))*HMAG*SCALE - EST
C                                         IS INTENDED TO BE A MEASURE OF TH
C                                         ERROR PER UNIT STEP IN YTRIAL
      C(19) = TEMP*C(14)*C(15)
C                                       STAGE 4 - MAKE DECISIONS. SET IND=5
C                                         IF STEP ACCEPTABLE, ELSE SET IND=
      IND = 5
      IF (C(19).GT.TOL) IND = 6
C                                       INTERRUPT NO 2 IF REQUESTED
      IF (C(9).NE.ZERO) GO TO 9005
C                                       RESUME HERE ON RE-ENTRY WITH IND
C                                         .EQ. 5 OR 6
  265 CONTINUE
C
      IF (IND.EQ.6) GO TO 275
C                                       STEP ACCEPTED (IND .EQ. 5), SO
C                                         UPDATE X, Y FROM XTRIAL, YTRIAL,
C                                         ADD 1 TO THE NO OF SUCCESSFUL
C                                         STEPS, AND SET THE NO OF
C                                         SUCCESSIVE FAILURES TO ZERO
      X = C(17)
      DO 270 K=1,N
         Y(K) = W(K,9)
  270 CONTINUE
      C(22) = C(22)+ONE
      C(23) = ZERO
C                                       RETURN(WITH IND=3, XEND SAVED, FLAG
C                                         SET) IF X .EQ. XEND
      IF (X.NE.XEND) GO TO 50
      IND = 3
      C(20) = XEND
      C(21) = ONE
      GO TO 9005
  275 CONTINUE
C                                       STEP NOT ACCEPTED (IND .EQ. 6), SO
C                                         ADD 1 TO THE NO OF SUCCESSIVE
C                                         FAILURES
      C(23) = C(23)+ONE
C                                       ERROR RETURN (WITH IND=-3) IF HMAG
C                                         .LE. HMIN
      IF (C(14).GT.C(13)) GO TO 50
      IND = -3
      GO TO 9005
C                                       END STAGE 4
C
C                                       END LOOP
```

```
  280 CONTINUE
C                                       RELATIVE ERROR OPTION SELECTED AND
C                                         Y(K) IS ZERO
      IER = 132
      GO TO 9000
  285 CONTINUE
C                                       X OR XEND WAS NOT CHANGED FROM
C                                         PREVIOUS CALL
      IER = 131
      GO TO 9000
C
  290 CONTINUE
C                                       IND OUT OF RANGE
      IER = 130
      GO TO 9000
  295 CONTINUE
C                                       N.GT.NW OR TOL.LE.0
      IER = 129
C                                       BEGIN ABORT ACTION
 9000 CONTINUE
      CALL UERTST (IER,6HDVERK )
 9005 CONTINUE
      RETURN
      END
```

Bxdata

```
02810       SUBROUTINE BXDATA
02820       DIMENSION FLTYPE(5),LUMA(9)
02830       INTEGER FLTYPE
02840       COMMON/C10/WORK(2,9),H,RINJ,C,FM,FK,TIME,PHI,XLEN,TEMP,W,TRES
02850       COMMON/C40/FLTYPE,DEPTH,PERM,PRESS,WIDTH
02860       COMMON/C50/ SAVAVT(10),NDUMMY(9),NPASS
02870       COMMON/CAUG1/TINIT,TMAX,TINCR
02880       COMMON/BXOCT/ BXLEN
02890       DATA LUMA/0,1,2,5,6,10,14,36,37/
02900       TIMEM = TIME / 60.
02910       THOURN = TINCR / 3600.
02920       TIMLEG = TINIT / 3600.
02930       THOURM = TMAX / 3600.
02940       CALL PLOT(10.5,-1.,-3)
02950       CALL PLOT(2.5,0.0,2)
02960       CALL PLOT(2.5,8.5,2)
02970       CALL PLOT(0.0,8.5,2)
02980       CALL SYMBOL(0.2,8.0,0.15,'FRACTURE DATA',0.,13)
02990       CALL SYMBOL(0.2,7.6,0.1,'FLUID TYPE:',0.,11)
03000       CALL SYMBOL(1.35,7.6,.1,FLTYPE,0.,20)
03010       CALL SYMBOL(.2,7.2,.1,'RATE:',0.,5)
03020       CALL NUMBER(1.25,7.2,.1,RINJ,0.,2)
03030       CALL SYMBOL(2.,7.2,.1,'BPM',0.,3)
03040       CALL SYMBOL(.2,6.8,.1,'MAX TIME:',0.,9)
03050       CALL NUMBER(1.25,6.8,.1,THOURM,0.,2)
03060       CALL SYMBOL(2.,6.8,.1,'HR. ',0.,4)
03070       CALL SYMBOL(.2,6.4,.1,'FRAC. WIDTH:',0.,12)
03080       CALL NUMBER(1.5,6.4,.1,WIDTH,0.,2)
03090       CALL SYMBOL(2.,6.4,.1,'IN.',0.,3)
03100       CALL SYMBOL(.2,6.0,.1,'FRAC.LENGTH:',0.,12)
03110       CALL NUMBER(1.5,6.0,.1,BXLEN,0.,0)
03120       CALL SYMBOL(2.1,6.0,.1,'FT.',0.,3)
03130       CALL SYMBOL(.2,5.6,.1,'INJ. TEMP.:',0.,11)
03140       CALL NUMBER(1.5,5.6,.1,TEMP,0.,1)
03150       CALL SYMBOL(2.0,5.68,.1,75,0.,-1)
03160       CALL SYMBOL(2.1,5.6,.1,'F',0.,1)
03170       CALL SYMBOL(.2,5.1,.15,'RESERVOIR DATA',0.,14)
03180       CALL SYMBOL(.2,4.7,.1,'DEPTH:',0.,6)
03190       CALL NUMBER(1.25,4.7,.1,DEPTH,0.,1)
03200       CALL SYMBOL(2.,4.7,.1,'FT.',0.,3)
03210       CALL SYMBOL(.2,4.35,.1,'HEIGHT:',0.,7)
03220       CALL NUMBER(1.25,4.35,.1,H,0.,1)
03230       CALL SYMBOL(2.,4.35,.1,'FT.',0.,3)
03240       CALL SYMBOL(.2,4.0,.1,'PRESSURE:',0.,9)
03250       CALL NUMBER(1.25,4.0,.1,PRESS,0.,1)
03260       CALL SYMBOL(2.,4.0,.1,'PSI',0.,3)
03270       CALL SYMBOL(.2,3.65,.1,'TEMP:',0.,5)
03280       CALL NUMBER(1.25,3.65,.1,TRES,0.,1)
03290       CALL SYMBOL(2.,3.73,.1,75,0.,-1)
03300       CALL SYMBOL(2.1,3.65,.1,'F',0.,1)
03310       CALL SYMBOL(.2,3.3,.1,'PERM:',0.,5)
```

```
03320         CALL NUMBER(1.25,3.3,.1,PERM,0.,3)
03330         CALL SYMBOL(2.,3.3,.1,'MD',0.,2)
03340         CALL SYMBOL(.8,2.85,.15,'LEGEND',0.,6)
03350         YPS = 2.5
03360         DO 18 K=1,NPASS
03370         CALL SYMBOL(.3,YPS+.05,.1,LUMA(K),0.,-1)
03380         CALL SYMBOL(.67,YPS,.1,'TIME= ',0.,6)
03390         TIMLEG = TIMLEG + THOURN
03400         CALL NUMBER(1.5,YPS,.1,TIMLEG,0.,2)
03410         CALL SYMBOL(2.1,YPS,.1,'HRS',0.,3)
03420      18 YPS = YPS - .24
03430         CALL PLOT(-10.5,1.,-3)
03440         RETURN
03450         END
```

Plott

```
01930        SUBROUTINE PLOTT( NUMPTS)
01940        INTEGER OUT
01950        DIMENSION XA(202),YA(202),LUMA(9),NUMPTS(9),DIF(9)
01960        COMMON/PLAY/ XD(202,9),YD(202,9),VISCOS(202,9)
01970        COMMON/C10/WORK(2,9),H,RINJ,C,FM,FK,TIME,PHI,LENGTH,TEMP,W,TRES
01980        COMMON/C50/ SAVAVT(10),NDUMMY(9),NPASS
01990        COMMON/C20/IN,OUT,XDUM,DXDUM.
02000        DATA MAX/200/,LUMA/0,1,2,5,6,10,14,36,37/,PLOTHT/6.5/,PLOTWD/9.5/
02010 C       PLOTHT & PLOTWD ARE PLOT FRAME HEIGHT & WIDTH.
02020 C    FIRST,FIND OUT WHICH OF THE NPASS CURVES TO USE TO CALL AXIS.
02030 C    (I.E.,ONE FOR WHICH MAX X VALUE MINUS MIN X VALUE IS GREATEST)
02040        SMALL = .1E+10
02050        BIG   = .1E-10
02060        DO 5 K=1,NPASS
02070        NCR = NUMPTS(K)
02080        NCRLIM = NCR
02090        IF (NCRLIM.GT.200) NCRLIM = 200
02100        DO 8 L=1,NCRLIM
02110        XPL = XD(L,K)
02120        IF (XPL.LT.SMALL) SMALL = XPL
02130        IF (XPL.GT.BIG  )  BIG  = XPL
02140      8 CONTINUE
02150        DIF(K) = BIG - SMALL
02160      5 CONTINUE
02170        BIGDIF = .1E-10
02180        IUSE = 0
02190        DO 9 K=1,NPASS
02200        IF (DIF(K).LE.BIGDIF) GO TO 9
02210        IUSE = K
02220      9 CONTINUE
02230 C      IUSE INDICATES WHICH CURVE TO USE IN CALLING AXIS.
02240        IF (IUSE.GT.0) GO TO 11
02250        WRITE(OUT,12)
02260     12 FORMAT(//,2X,'*** ERROR IN SUB.PLOTT. VALUE OF IUSE IS ',
02270       ?  'INVALID. JOB TERMINATED. ')
02280        STOP
02290     11 CONTINUE
02300        LPTS = NUMPTS(IUSE)
02310        IF (LPTS.GT.200) LPTS=200
02320        DO 10 K=1,LPTS
02330 C      YA(K) = YD(K,IUSE)
02340     10 XA(K) = XD(K,IUSE)
02350        CALL PLOT(-1.,-1.,3)
02360        CALL PLOT(10.5,-1.,2)
02370        CALL PLOT(10.5,7.5,2)
02380        CALL PLOT(-1.,7.5,2)
02390        CALL PLOT(-1.,-1.,2)
02400        CALL PLOT(1.,1.,3)
02410        CALL SCALE(XA,PLOTWD,LPTS,1)
02420 C      CALL SCALE(YA,PLOTHT,LPTS,1)
02430        BEGINX = XA(LPTS+1)
```

```
02440        DELTX  = XA(LPTS+2)
02450 C      BEGINY = YA(LPTS+1)
02460 C      DELTY  = YA(LPTS+2)
02470        INDELT = (TRES+20.-TEMP) / PLOTHT
02480        DELTY = INDELT
02490        BEGINY = TEMP
02500        CALL AXIS(0.,0.,' ',-1,PLOTWD,0.,BEGINX,DELTX)
02510        CALL SYMBOL(3.,-0.75,0.175,'FRACTURE DISTANCE - FEET',
02520       ?  0.,24)
02530        CALL AXIS(0.,0.,' ',1,PLOTHT,90.,BEGINY,DELTY)
02540        CALL SYMBOL(-.5,2.5,0.175,'TEMPERATURE - F',90.,15)
02550        CALL SYMBOL(-.69,4.8,.2,75,0.0,-1)
02560        CALL SYMBOL(1.3,7.0,0.175,'FLUID TEMPERATURE VS DISTANCE IN FRACTU
02570       ?RE',0.0,41)
02580        CALL BXDATA
02590     20 CONTINUE
02600        DO 30 KEG=1,NPASS
02610        KPTS = NUMPTS(KEG)
02620        IF (KPTS.GT.200) KPTS = 200
02630        DO 25 K=1,KPTS
02640        XA(K) = XD(K,KEG)
02650     25 YA(K)  = YD(K,KEG)
02660        XA(KPTS+1) = BEGINX
02670        XA(KPTS+2) = DELTX
02680        YA(KPTS+1) = BEGINY
02690        YA(KPTS+2) = DELTY
02700        NUMSYM = KPTS / 20
02710        CALL LINE(XA,YA,KPTS,1,NUMSYM,LUMA(KEG))
02720     30 CONTINUE
02730        CALL PLOT(0.,0.,-3)
02740        CALL PLOT(15.,-1.,-3)
02750        RETURN
02760     77 WRITE(6,84) KNT,MAX
02770     84 FORMAT(/,'  **** ERROR. KNT=',I3,' IS GREATER THAN MAX. (',I3,')',
02780       ? '  PROGRAM TERMINATED.')
02790        STOP
02800        END
```

Block Data

```
01830       BLOCK DATA
01840       INTEGER OUT
01850       REAL LENGTH
01860       COMMON/C10/ WORK(2,9),H,RINJ,C,FM,FK,TIME,PHI,LENGTH,TEMP,W,TRES
01870       COMMON/C20/IN,OUT,X,DX
01880       COMMON/PLAY/ XP(202,9),YP(202,9),VISCOS(202,9)
01890       COMMON/C60/KURVE
01900       DATA XP/1818*0./,YP/1818*0./,VISCOS/1818*0./
01910       DATA IN/8/,DX/5.0/,X/0.0/,OUT/6/,KURVE/1/
01920       END
```

MATHEMATICAL TREATMENT OF TRACER BEHAVIOR IN A FRACTURE

Ottomar Vetter
Vetter Research

Paper not submitted for publication.

SESSION THREE

ACTIVE AND PASSIVE SEISMIC TECHNIQUES
IN MAPPING FRACTURES

James Albright
LOS ALAMOS SCIENTIFIC LABORATORY

STIMULATION CASE HISTORIES:

(I) RAFT RIVER: MECHANICAL DESIGN AND OPERATIONS

(II) RAFT RIVER EVALUATION

(III) EAST MESA STIMULATION

Charles Morris
Robert Verity
REPUBLIC GEOTHERMAL, INC.

Robert Nicholson
TERRA SERVICES
Scott Keys
UNITED STATES GEOLOGICAL SURVEY

ACTIVE AND PASSIVE SEISMIC TECHNIQUES IN MAPPING FRACTURES

James Albright
Los Alamos Scientific Laboratory

Paper not submitted for publication.

RAFT RIVER STIMULATION TREATMENT RESULTS

by C. W. Morris

ABSTRACT

The Geothermal Reservoir Well Stimulation Program (GRWSP) group planned and executed two field experiments at the Raft River KGRA during 1979. Well RRGP-4 was stimulated using a dendritic or "Kiel" hydraulic fracture technique, and Well RRGP-5 was stimulated using a conventional massive hydraulic fracture technique. This presentation summarizes the analyses and results of these stimulation treatments.

Both stimulation experiments at Raft River were technically successful; however, the post-stimulation productivity of the wells was disappointing. The productivity indices (PI) of Wells RRGP-4 and RRGP-5 were found to be 0.6 gpm/psi and 2.0 gpm/psi, respectively.

Well RRGP-4 productivity was greatly increased over its pre-stimulation condition, but the artificially created fracture and/or the natural fracture system did not provide a high transmissivity connection with the source of the geothermal fluid. The artesian flow rate was 60 gpm. The artificially created fracture in Well RRGP-5 apparently connected with existing natural fractures very near the wellbore. This connection did not significantly affect the already high transmissivity of these fractured zones (artesian production rate about 200 gpm). The low temperature of the produced fluids from RRGP-5 suggests that these fractures extend upward to cooler zones of the reservoir.

Pressure transient data indicate an area of reduced transmissivity or limited entry near these wells and an area of high transmissivity (greater than 500,000 md-ft/cp) located at some distance which acts as a constant pressure boundary. The major fault lines near these wells are suspected of being the major source of the geothermal fluids. Further long-term testing is needed to confirm this fact.

INTRODUCTION

The purpose of this presentation is to summarize the results of the Raft River stimulation experiments. Discussion of the general well selection process, mechanical preparation of the wells, and the specific fracture stimulation procedures at Raft River were presented earlier and therefore, will not be repeated here.

The operator of the Raft River geothermal field, EG&G, completed and tested the Wells RRGP-4 and RRGP-5 as part of the normal field development program. Figure 1 shows the Raft River KGRA and the well locations. The pre-stimulation well conditions are discussed herein and compared with the post-stimulation test results. It should be remembered, however, that a large portion of the original open-hole completion interval was cased off ("Planning and Execution of Raft River Stimulation Treatments," R. V. Verity) prior to the fracture treatments and the direct comparison may not necessarily be an accurate representation.

PRE-STIMULATION WELL CONDITIONS

All the Raft River production wells are completed within the naturally fractured zone from about 3,400 feet to 6,543 feet. The formation producing intervals are comprised primarily of siltstone, sandstone, metamorphosed quartz, quartz schist, elba quartzite, and quartz monzonite. Pre-stimulation borehole televiewer surveys, discussed previously ("Application of Acoustic Televiewer to the Characterization of Hydraulic Fractures in Geothermal Wells," Scott Keys), indicated that both Wells RRGP-4 and RRGP-5 have natural fractures intersecting their wellbores; however, RRGP-4 showed much less fracturing in the entire well (open-hole interval 3,526 feet to 5,115 feet) as compared to other Raft River wells. Well RRGP-5 had numerous horizontal and vertical fractures throughout the open-hole section from 3,408 feet to 4,925 feet.

After leg B of Well RRGP-4 was deepened to 5,115 feet, an attempt was made by EG&G to flow test the well. The well was found to be non-commercial and would not sustain an artesian flow rate greater than approximately 10 gpm. The maximum bottom-hole temperature was measured by borehole geophysical logs at 254 degrees F.

Well RRGP-5 (leg B) productivity was tested by EG&G several times after completion. The well was artesian flow tested for 72 hours at a rate of 140 gpm in November 1978. Short-term flow periods (approximately 1 hour) prior to this test obtained rates in excess of 280 gpm; however, the wellhead pressure was declining very rapidly and the well could not sustain this rate. No downhole transient pressure data were obtained during these tests with which to calculate a

productivity index. A maximum bottom-hole temperature of 274 degrees F was measured in the well. As discussed previously (paper by R. V. Verity), leg B is believed to have penetrated a zone extensively damaged by cement during the workover of leg A. Sufficient volume of cement had been injected into leg A to fill the wellbore and the near-well natural fractures. Some confusion remains as to the actual productive potential of RRGP-5 after it was completed. Flow test results vary from over 1,000 gpm to 140 gpm. It should be stated that several very short-term production tests were attempted during the drilling operations and shortly thereafter. These tests were not fully documented and no downhole transient pressure data were obtained. It seems clear that for a number of reasons, mostly related to the drilling operations or the test procedures, the well data might indicate these rates were observed for short periods of time. However, pressure data obtained during later tests indicate that the bottom-hole pressure must have been decreasing rapidly during these early flow tests and that the well would not have continued to sustain anywhere near the high flow rates originally ascribed to this well. None of the current Raft River wells are capable of very high artesian flow rates. The most likely maximum flow rate of Well RRGP-5 prior to the stimulation treatment was about 140-200 gpm.

As described above, these wells originally had long open-hole intervals. A 7-inch casing liner was cemented in the hole such that a 200-foot open-hole interval was isolated for stimulation treatment. With the liner in place, both wells were essentially non-productive as the formation natural fractures feeding the wellbore were cased-off. Therefore, no production tests were performed under these conditions prior to the fracture experiments.

POST-STIMULATION PRODUCTION TEST INSTRUMENTATION

Both Wells RRGP-4 and RRGP-5 were production tested following the fracture stimulation treatments. EG&G assisted in this test program and provided the surface equipment required to monitor the flow conditions. The general procedure was to construct a flow line from the wellhead to the nearby holding pond. The flow line was instrumented with an orifice plate and a differential pressure gauge to monitor the single phase fluid flow rate. The flow line was also instrumented to measure wellhead pressure and temperature, and ports were provided for fluid sampling capability. In some cases the wellhead pressure was measured with a conventional Bourdon guage and, in others, with a digiquartz pressure transducer. The deep geothermal wells and the shallow water wells in the Raft River area were monitored continuously by EG&G for possible interference pressure data.

Downhole pressure (and temperature) instrumentation was utilized during the flow tests to obtain the transient pressure drawdown and buildup response. In most instances, the downhole pressure equipment was a quartz crystal pressure gauge provided by either EG&G or Lawrence Berkeley Laboratory (LBL). However, several instrument failures occurred during these tests. In the case of the September 1979 flow test of Well RRGP-4, a conventional Amerada type downhole pressure gauge was used to obtain the pressure buildup data. Downhole temperature measurements were obtained to aid in the analysis of the pressure data, which can be significantly affected by a change in the fluid temperature, and to document the flowing temperature of the well.

Fluid samples were taken periodically during all post-stimulation flow tests. These samples were analyzed for fracture fluid and tracer material returns by Vetter Research. Also, the U.S. Geological Survey ran borehole televiewer surveys in each of the wells to determine the extent of the newly created vertical fracture at the wellbore.

TEST RESULTS AND ANALYSIS

The pressure testing of the Wells RRGP-4 and RRGP-5 under the GRWSP will be discussed in chronological order. The pressure data were analyzed using conventional pressure analysis techniques, type curve (log-log) matching techniques, and numerical simulation methods.

1. RRGP-4

Well RRGP-4 was stimulated with a dendritic hydraulic fracture treatment in August 1979. A 20-hour flow test was run on August 25-26, 1979. The flow rate declined from an initial 250 gpm to about 60 gpm; however, at that point two-phase flow began to occur at the orifice meter used to measure the flow rate. The test was terminated and plans were made to re-test the well for a longer period with improved flow control equipment. A borehole televiewer survey confirmed the existence of a 200 foot vertical fracture created by the stimulation treatment. The fracture was oriented in an east-west direction which would parallel the Narrows Fault.

The September 1979 production test of Well RRGP-4 was similar to the first test in flow rates and the rapid downhole pressure response. Figure 2 gives the production data and Figures 3 through 6 show the pressure data plots. The downhole instrumentation failed about 8 hours into the drawdown phase. The test continued until September 12, 1979, at which point Amerada type downhole pressure and temperature instruments were utilized to obtain the reservoir buildup data given in Figure 3. The well was flowed at a

rate of about 60 gpm for 150 hours before shut-in. The fracture flow effects are indicated to last about 6 hours by the early-time pressure versus square root of time plot in Figure 6. The bottom-hole pressure apparently reached the initial reservoir pressure after approximately 15 hours of buildup time. The data show a very flat pressure curve from 15 hours to 47 hours. The significance of this is discussed later. The conventional fracture type curve analysis (log-log plot) yields a fracture length of approximately 335 feet and a permeability-thickness (kh) of 800 md-ft. The Horner plot indicated the presence of two straight line segments, one early-time (less than 15 hours) and one late-time (greater than 15 hours) segment. These two data segments give kh values of 1070 md-ft and 85,000 md-ft, respectively, and suggest the possibility of more than one permeable zone near the wellbore. Also a negative skin factor (-6.0) indicates a stimulated zone close to the wellbore. This is further confirmed by the fact that the buildup curve approaches the Horner straight line from above. Table I summarizes the calculations of reservoir properties derived from this test. Wellbore temperature changes were small during the reservoir buildup period and did not significantly affect the pressure data.

The maximum bottom-hole temperature recorded during the September 1979 flow test was 270 degrees F. This temperature is significantly higher than past measurements have shown, i.e., about 240 degrees F before stimulation. This fact suggests that the new artificial fracture is producing fluid from a deep reservoir zone not open in the original hole.

2. RRGP-5

Well RRGP-5 was stimulated on November 12, 1979. The post-stimulation production test was performed during November 25-26, 1979 after the well had been produced several times to clean out sand. Figure 7 illustrates the production data obtained during the 6 hour flow period. The wellhead and downhole pressure and temperature conditions stabilized very rapidly (about 2 minutes). An average flow rate of about 200 gpm was maintained with a wellhead pressure of about 30 psia. The pressure drawdown of 100 psi was extremely rapid (less than 1 minute) and no early-time data were obtained. A plot of the pressure buildup data versus square root of time, shown in Figure 3, indicates the fracture flow effect near the wellbore persists for only about 38 seconds. This short linear flow period and the resulting calculated fracture length value is so small that no single fracture flow exists. The Horner plot and type curve plot of the pressure data, in Figures 9 and 10, show only a short transition phase between the fracture dominated period and the late-time constant pressure period. The results indicate a higher transmissivity than was found in RRGP-4.

Estimates of the late-time formation kh are large, i.e., greater than 100,000 md-ft.

Thus, the hydraulic fracture stimulation treatment may have reopened existing natural fractures near the wellbore and/or intersected leg A which dissipated the injected frac fluid and energy. The borehole televiewer survey did indicate a newly created vertical fracture at the wellbore of about 140 feet in length and oriented in a northeast-southwest direction which is parallel to the Bridge Fault. These reopened natural fractures did not significantly affect the already high permeability of this fractured zone. The Horner analysis indicated a very large positive skin factor; however, this skin factor is not due to any formation damage but to the limited entry nature of the completion. A limited entry, theoretical skin effect calculation yields a skin factor of the same order of magnitude.

The maximum flowing bottom-hole temperature was measured at 264 degrees F at the shoe of the 7-inch liner. Figure 11 illustrates three separate temperature surveys made in Well RRGP-5.

In March 1980, Well RRGP-5 was flow tested again using a downhole submersible pump. The maximum rate obtained during this test was 650 gpm. The productivity index obtained from the artesian flow test (2 gpm/psi) is in close agreement with the values observed during this pumped flow test. Table 2 summarizes the reservoir property calculations derived from these tests.

Pressure Interference Data

The deep exploration wells and shallow water wells in the area were monitored for wellhead pressure changes during both stimulation treatments and subsequent production tests. No interference was indicated during the RRGP-4 fracture job or its two production tests; however, the RRGP-5 fracture treatment apparently did cause a pressure spike at RRGE-1 during the injection of the frac materials. The first flow tests of RRGP-5 did not cause any pressure changes at the observation wells.

Reservoir Model

Both Wells RRGP-4 and RRGP-5 show remarkably similar pressure response following the fracture treatments. Well RRGP-4 is apparently in a less fractured, tighter area of the reservoir compared to all the other production wells. The transient pressure data indicate three distinct flow response periods:

(1)fracture flow (2)early-time low effective kh flow (near wellbore); and (3)late-time high effective kh flow (some distance from wellbore).

The late-time pressure results suggest the presence of a constant pressure boundary. It is possible to satisfy the observed pressure results of both wells with two types of reservoir models:

1. A fractured reservoir with low transmissivity near the wellbore and a constant pressure boundary (or very high transmissivity area some relatively short distance from the wellbore) or

2. A reservoir with high effective transmissivity but with a large skin at the wellbore.

The second model does not conform to the known reservoir physical characteristics and, therefore was not considered a valid model. Numerical simulations were performed using the fractured reservoir model to confirm the first hypothesis. It was possible to reproduce the pressure transient data for both RRGP-4 and RRGP-5 with essentially the same model (RRGP-4 was given a lower near-wellbore transmissivity). The single layer model consisted of a vertical fracture through the wellbore, a relatively low transmissivity near the wellbore, and a constant pressure boundary located along one short side of a two-to-one rectangular drainage area. Figure 12 illustrates the model geometry. Obviously, the numerical simulation approach does not yield a unique solution to the transient reservoir pressure response, but it does provide a confirmation of the conventional and type curve pressure analysis results. Tables 3 and 4 summarize the pre- and post-stimulation well characteristics.

It is interesting to note that the well distance from the known or suspected faults in the Raft River area are close to the distance indicated in the reservoir model calculations for the constant pressure boundary. The results discussed herein suggest that the naturally fractured rock formation, at some distance from a fault, is not sufficiently permeable to support a high productivity well. Also, hydraulic fracture stimulation does not appear to be an economic alternative to recompletion of a well since the risk of not communicating effectively with the high transmissivity zones is great.

Chemical Aspects of Field Experiments

1. RRGP-4

In addition to the conventional chemical analyses, several analytical methods were developed and applied by Vetter Research to the characterization of the produced fluids from post-stimulation flow tests at RRGP-4. These methods included total organic carbon and carbonate analysis. Wellbore and near-wellbore cooling was indicated by the lack of polymer degradation in samples collected during the clean-up flow period conducted soon after the fracture treatment had been completed. Significant polymer degradation was observed during the two production tests, but the products of degradation appear to be water soluble and were observed in the produced fluid. Of the frac polymer injected, only 45 percent can be accounted for with certainty (see Figure 13). Some of the frac material as well as water soluble degradation products were still being produced back when the flow tests were terminated.

2. RRGP-5

Similar analytical methods were utilized to characterize the fluids produced from post-stimulation flow at RRGP-5. In addition, a chemical tracer (ammonium nitrate), which was co-injected with the frac fluid, was analyzed for during the flow tests. Based upon all the chemical work, it appears that a major portion of the frac fluid entered a cold zone of limited productivity. This conclusion is based on two facts: (1) there was little thermal degradation of the polymer after a one-month period in the reservoir; and (2) less than 50 percent of either polymer or tracer was produced back even after a cumulative volume of 2.5 times the injected volume had been produced from the well. The analytical results are illustrated is Figures 14 and 15.

CONCLUSION

Well RRGP-4 was successfully stimulated using the dendritic fracture treatment method. The productivity index was increased from essentially zero to 0.6 gpm/psi and the produced fluid temperature increased approximately 20 degrees F.

Well RRGP-5 was successfully stimulated using a conventional massive hydraulic fracture treatment technique; however, the artificially created fracture probably intersected existing natural fractures near the wellbore and/or intersected leg A. No significant increase in productivity was achieved. The post-stimulation PI was 2.0 gpm/psi.

With the exception of low material return in both field experiments, there were no striking similarities between the chemical behavior of the post-stimulation fluids produced at

RRGP-4 and RRGP-5. The frac fluid injected at RRGP-4 entered a hotter zone than at RRGP-5. While the temperature at the top of the producing interval in RRGP-4 is slightly warmer than in RRGP-5 (i.e., 270 degrees F. vs. 264 degrees F. respectively), this temperature difference is not large enough to account for the extensive differences in polymer degradation that were observed.

REFERENCES

1 Kiel, Othar, Kiel Fracturing Process, U.S. Patent No. 3,933,205

2 Unpublished data reports on the Raft River Project, prepared by EG&G, 1979.

TABLE I

RAFT RIVER RRGP-4

TEST 2 - SEPTEMBER 6-14, 1979

Flow Rate = 50 gpm

Production Time = 150 hrs

Maximum Bottom-Hole Temperature = 270 degrees F.

BUILDUP DATA

A. FRACTURE TYPE CURVE ANALYSIS:

L = 335 ft

KH = 300 md-ft

B. HORNER PLOT ANALYSIS:

KH = 1,070 md-ft (Early Time)

KH = 85,000 md-ft (Late Time) (1)

S = 5.0

(1) Constant Pressure Boundary Effect

TABLE 2

RAFT RIVER RRGP -5

TEST 1 - NOVEMBER 25-26, 1979

Flow Rate = 200 gpm

Production Time = 6 hrs

Maximum Bottom-Hole Temperature - 264 degrees F.

BUILDUP DATA (1)

A. HORNER PLOT ANALYSIS:(1)

KH > 100,000 md-ft (Late Time) (2)

TEST 2 - EG&G: USING DOWNHOLE REDA PUMP (March 1980)

Flow Rate = 650 gpm

Production Time = 61.3 hrs

Productivity Index = 2.05 gpm/psi

Maximum Temperature = 257 degrees F. (Wellhead)

(1) No transition or steady-state data before constant pressure boundary effects

(2) Constant pressure boundary effect

TABLE 3

RAFT RIVER RRGP -4

PRE-STIMULATION WELL CONDITION:

Open-hole Interval 3526 ft - 5115 ft

Maximum Bottom-hole Temperature = 254 degrees F. from geophysical logs

Flow Rate = Well Would Not Sustain Flow

Natural Fractures in Wellbore

POST-STIMULATION WELL CONDITION:

Open-hole Interval 4705 ft - 4900 ft

Vertical Fracture in Wellbore (200 ft height)

Flow Rate = 60 gpm (artesian)

Maximum Bottom-hole Temperature = 270 degrees F. at 3200 ft

Fracture Effects Show L = 335 ft

Near Wellbore Effective KH = 800-1,000 md-ft

Constant Pressure Boundary
with High Effective KH > 100,000 md-ft

Communicates with natural fractures or matrix permeability in area. Did not communicate effectively with major source of reservoir fluids

TABLE 4

RAFT RIVER RRGP-5

PRE-STIMULATION WELL CONDITION:

Open-hole Interval 3403 ft - 4925 ft

Maximum Bottom-hole Temperature = 274 degrees F.

Flow Rate = 140 gpm (artesian)

Near Wellbore Cement Damage

Natural Fractures in Wellbore

POST-STIMULATION WELL CONDITION:

Open-hole Interval 4537 ft - 4803 ft

Maximum Bottom-hole Temperature = 264 degrees F. at 4,600 ft

Flow Rate = 200 gpm (artesian)

Near Wellbore Effective KH > 100,000 md-ft with Limited Entry

Constant Pressure Boundary with
High Effective KH > 100,000 md-ft

Vertical Fracture in Wellbore (100 ft height)

Communicates with natural fractures or matrix permeability in area. Did not communicate effectively with major source of reservoir fluids

Appears to have limited pressure communication with RRGE-1

FIGURE 1

RAFT RIVER FACILITY WITH GEOLOGIC STRUCTURE AND WELL LOCATION.

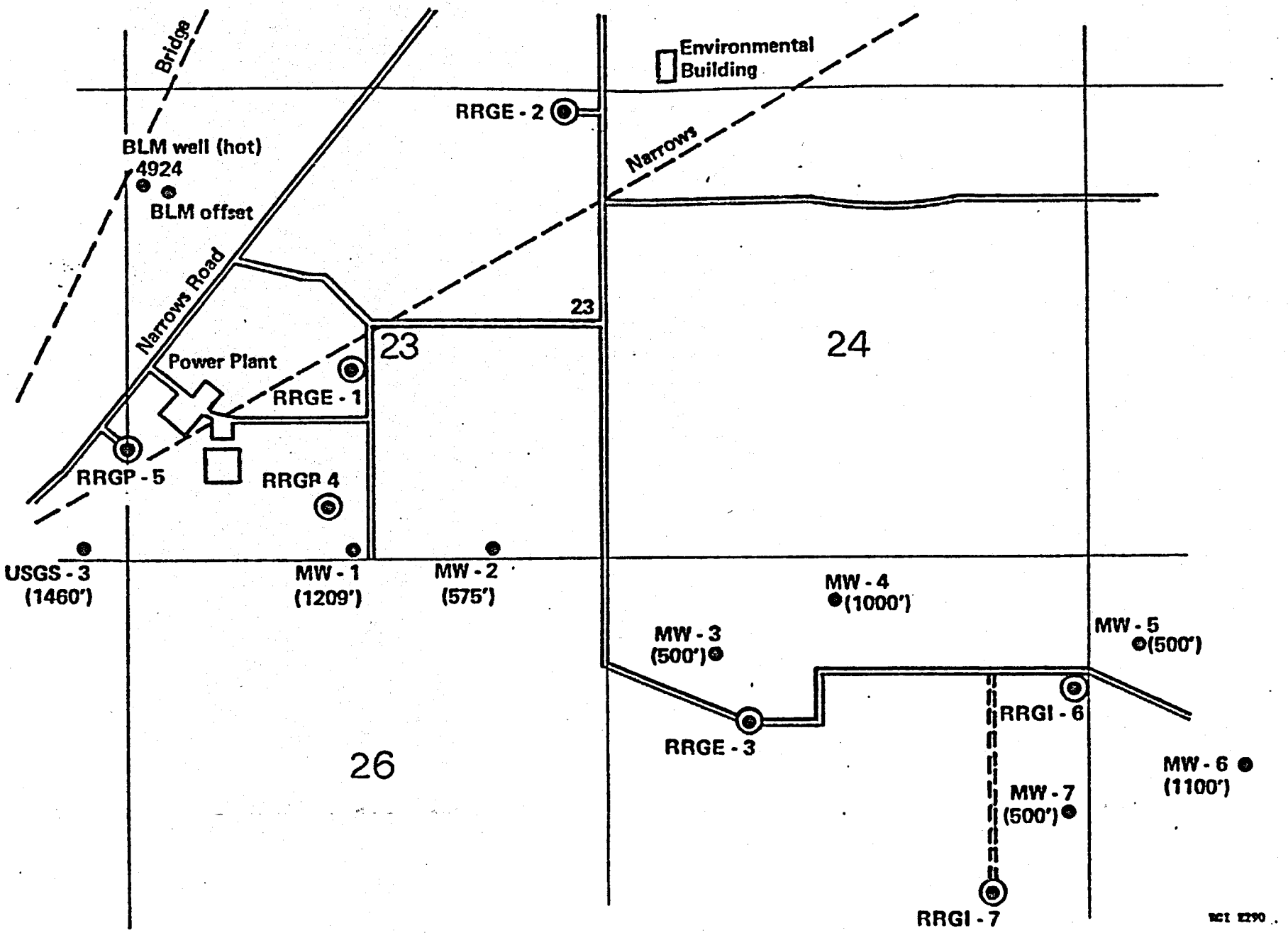

FIGURE 2

RRGP-4 PRODUCTION DATA

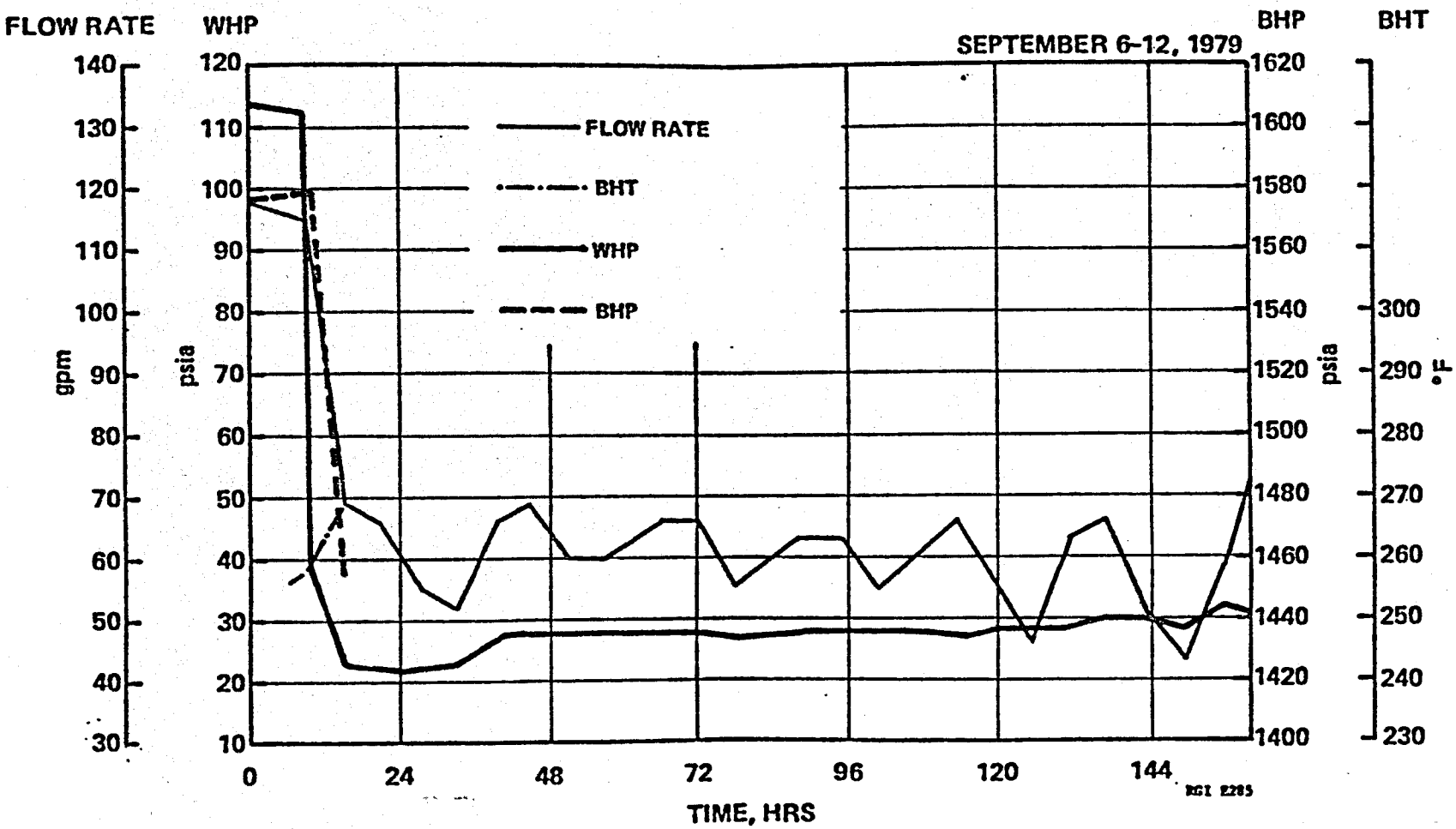

FIGURE 3

RAFT RIVER RRGP - 4
BOTTOM-HOLE DATA

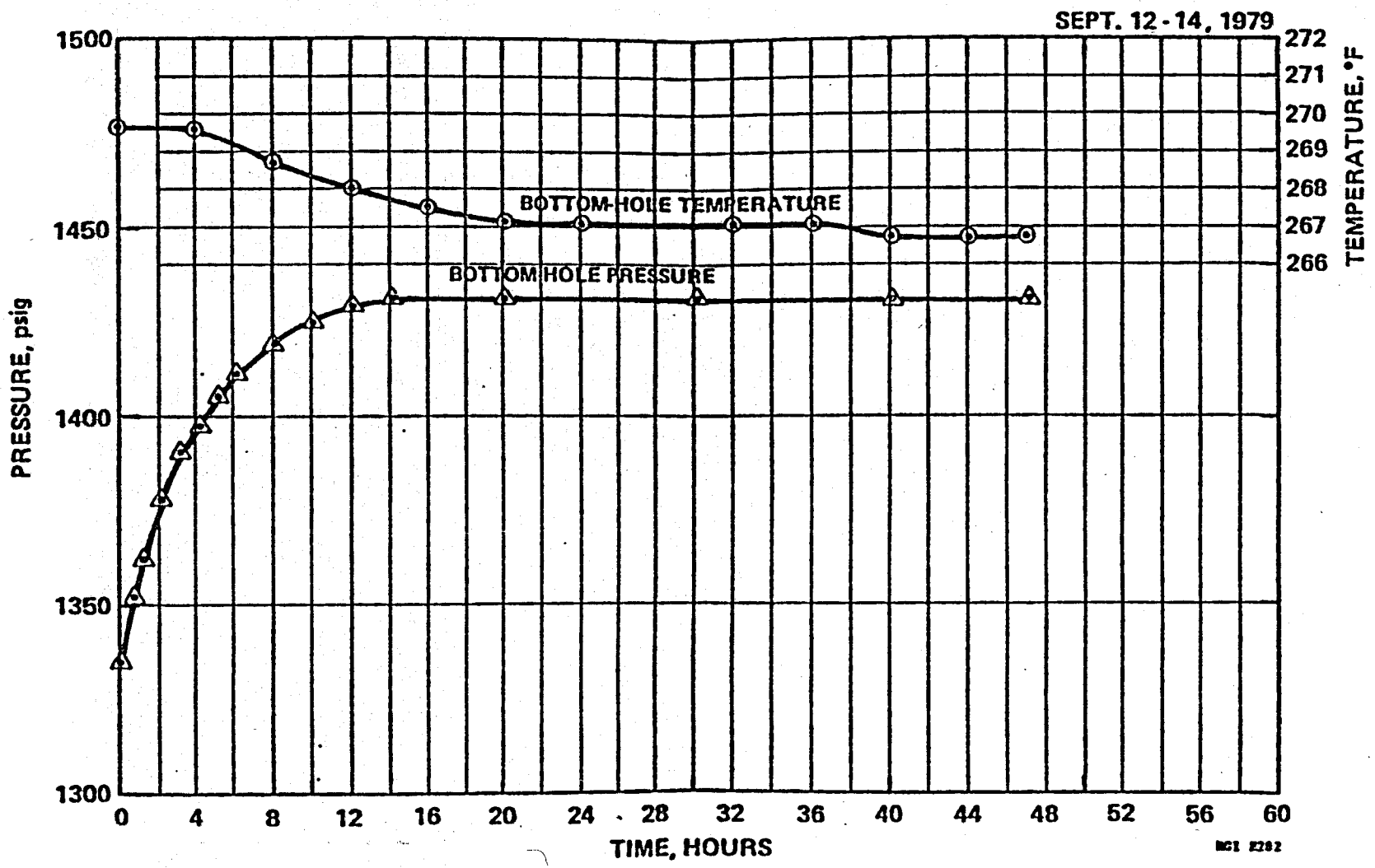

FIGURE 4

RRGP–4 BUILDUP DATA

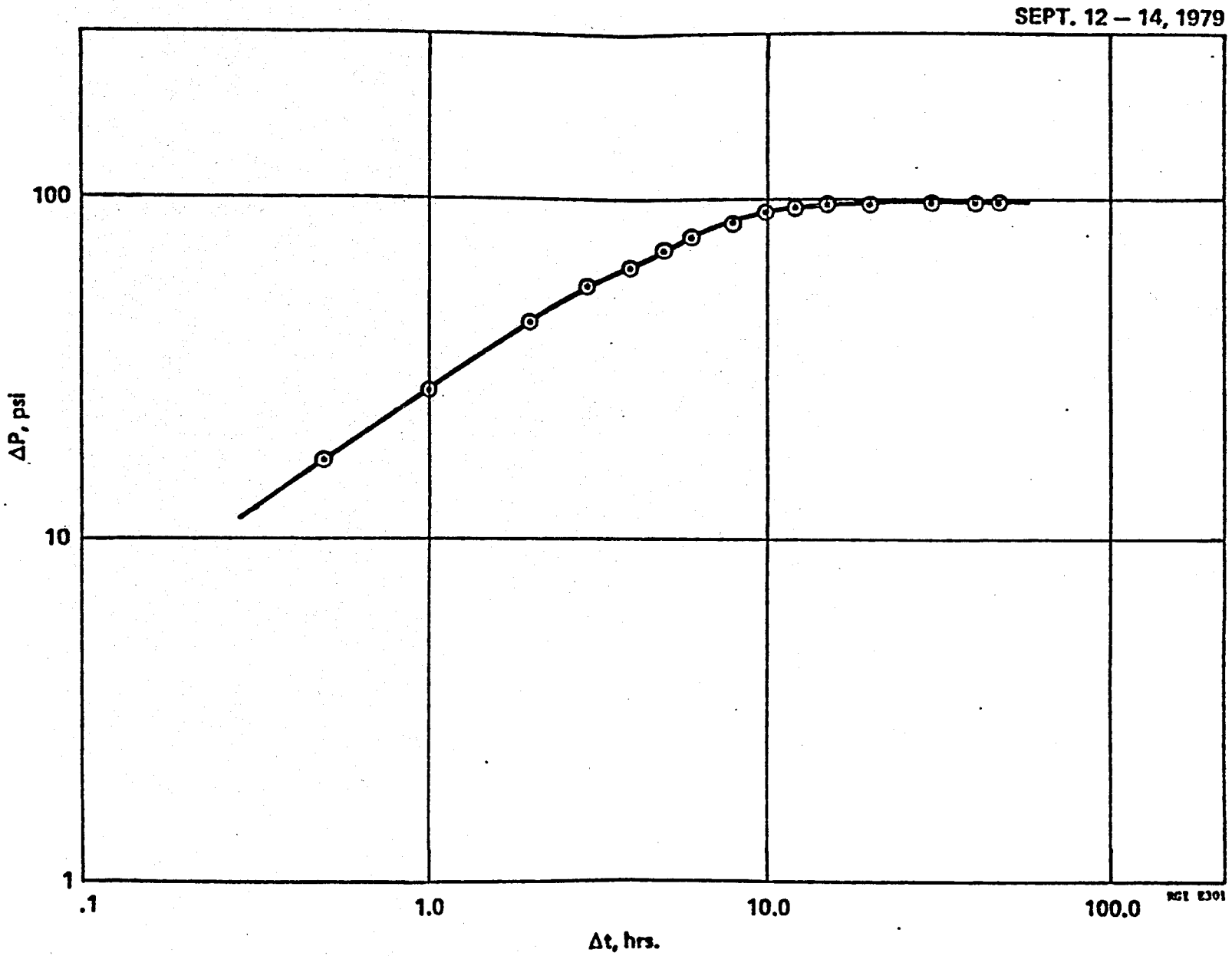

FIGURE 5

RRGP-4 BUILDUP DATA

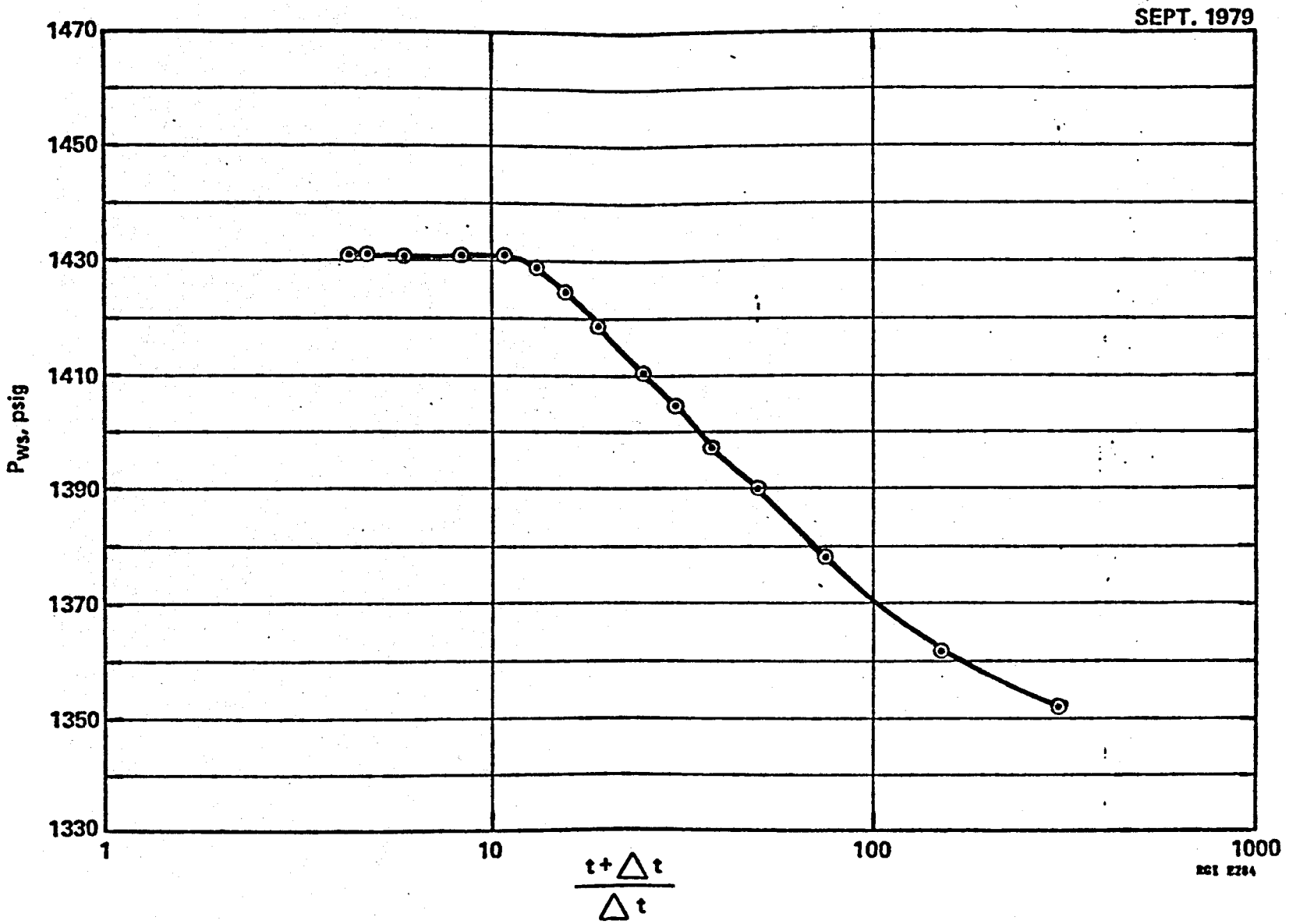

FIGURE 6

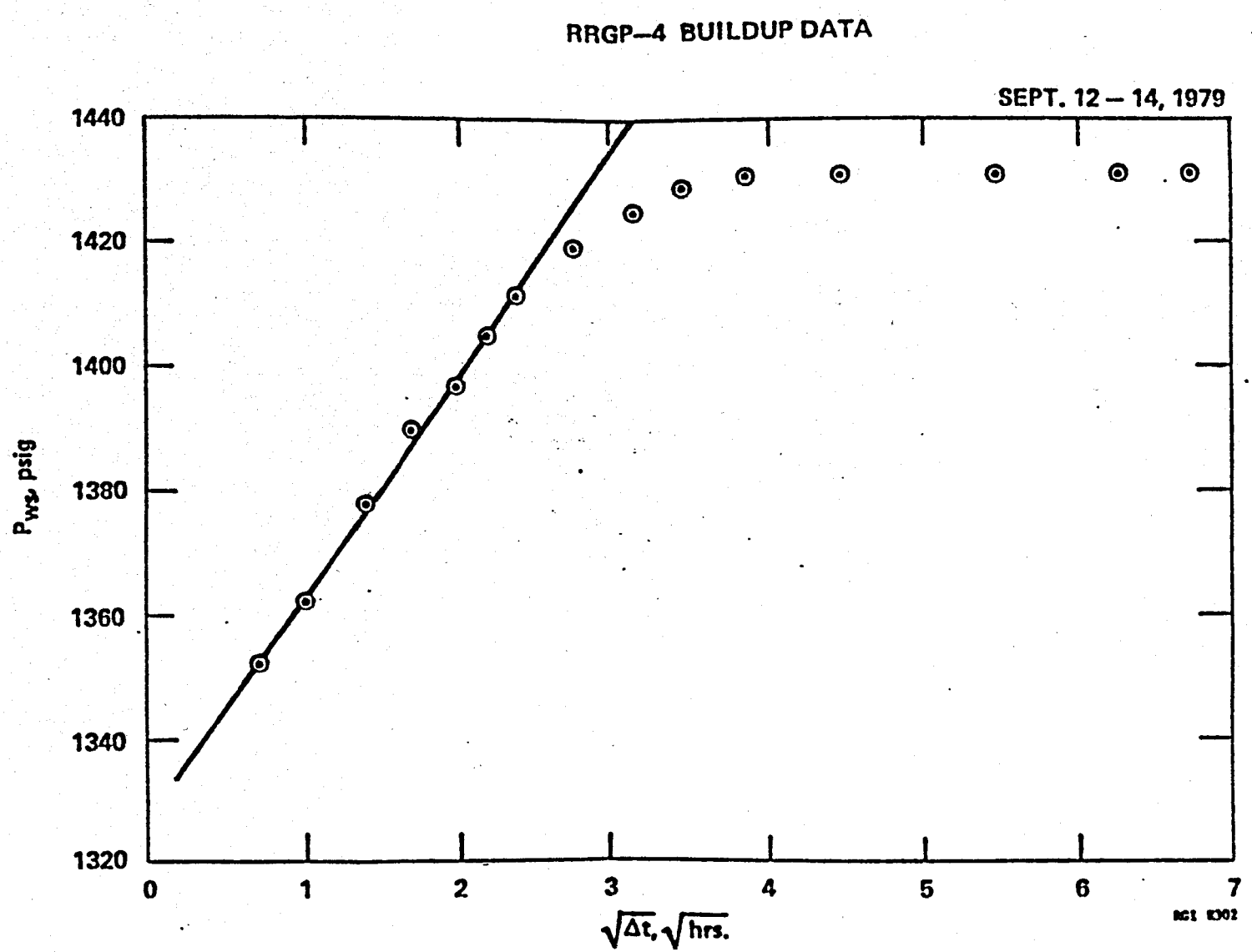
RRGP–4 BUILDUP DATA
SEPT. 12 – 14, 1979
1440
1420
1400
1380
1360
1340
1320
P_{ws}, psig
0
1
2
3
4
5
6
7
$\sqrt{\Delta t}, \sqrt{\text{hrs.}}$

FIGURE 7

RRGP-5 PRODUCTION DATA

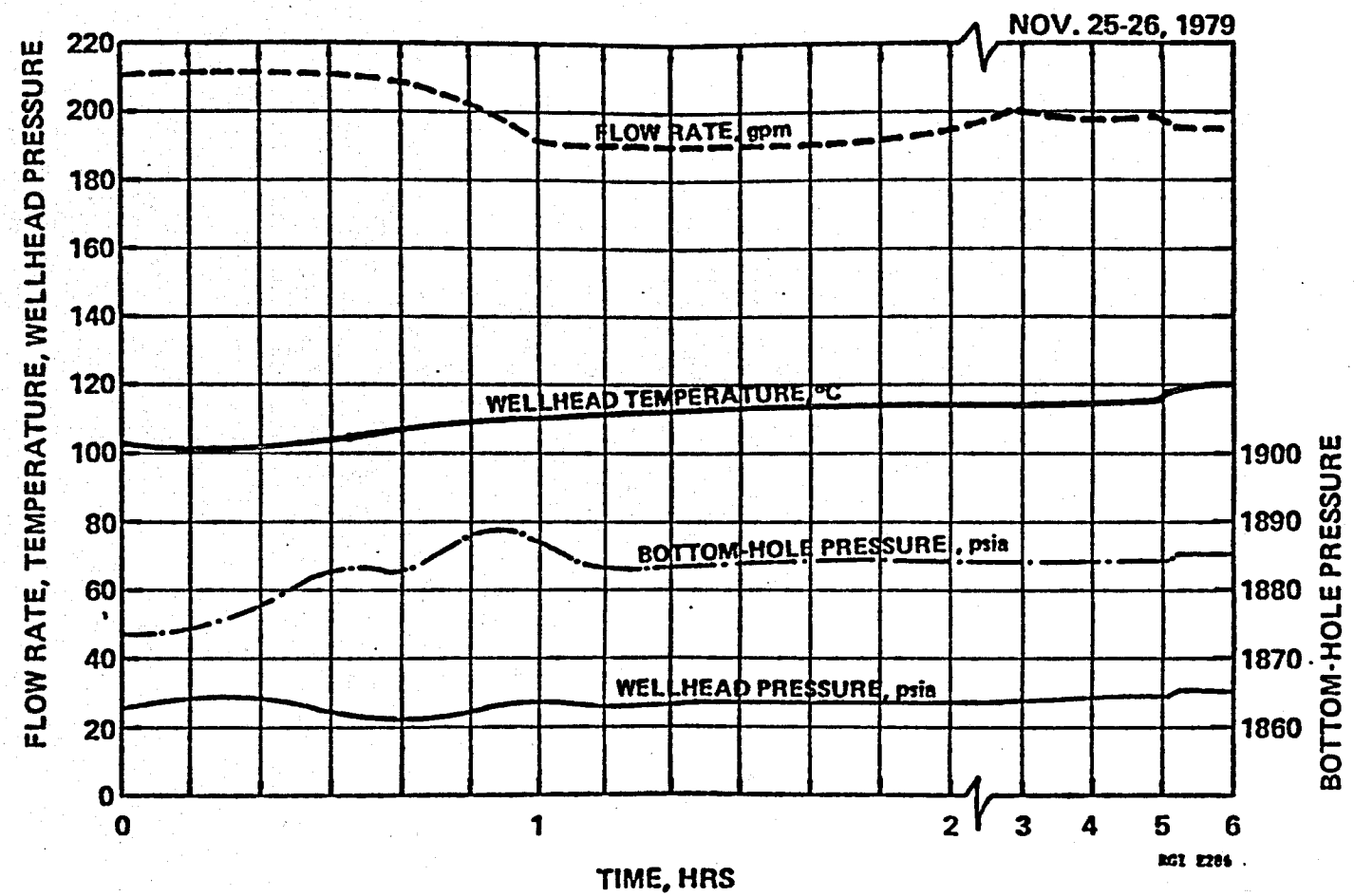

FIGURE 8

RRGP–5 BUILDUP DATA

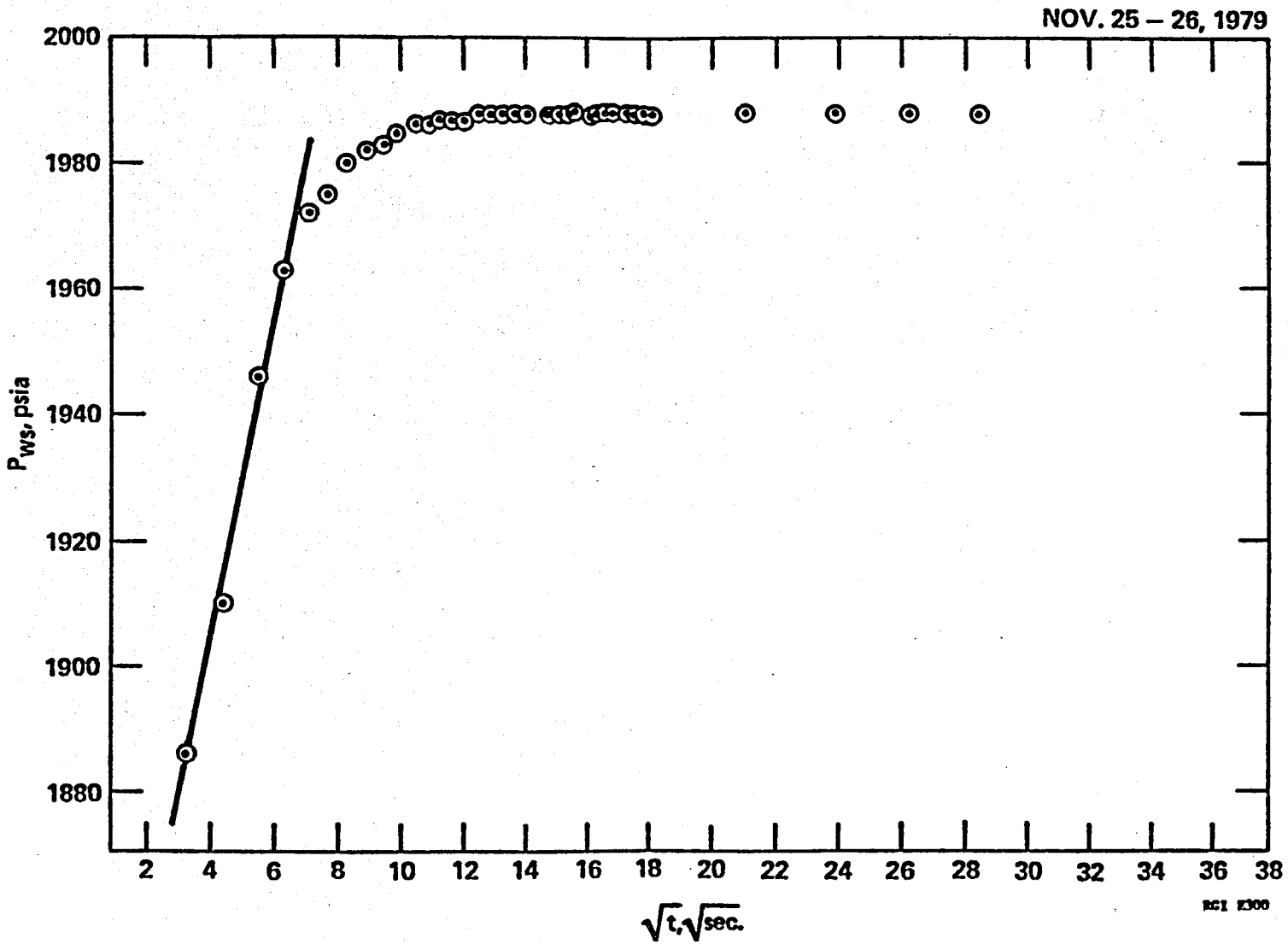

FIGURE 9

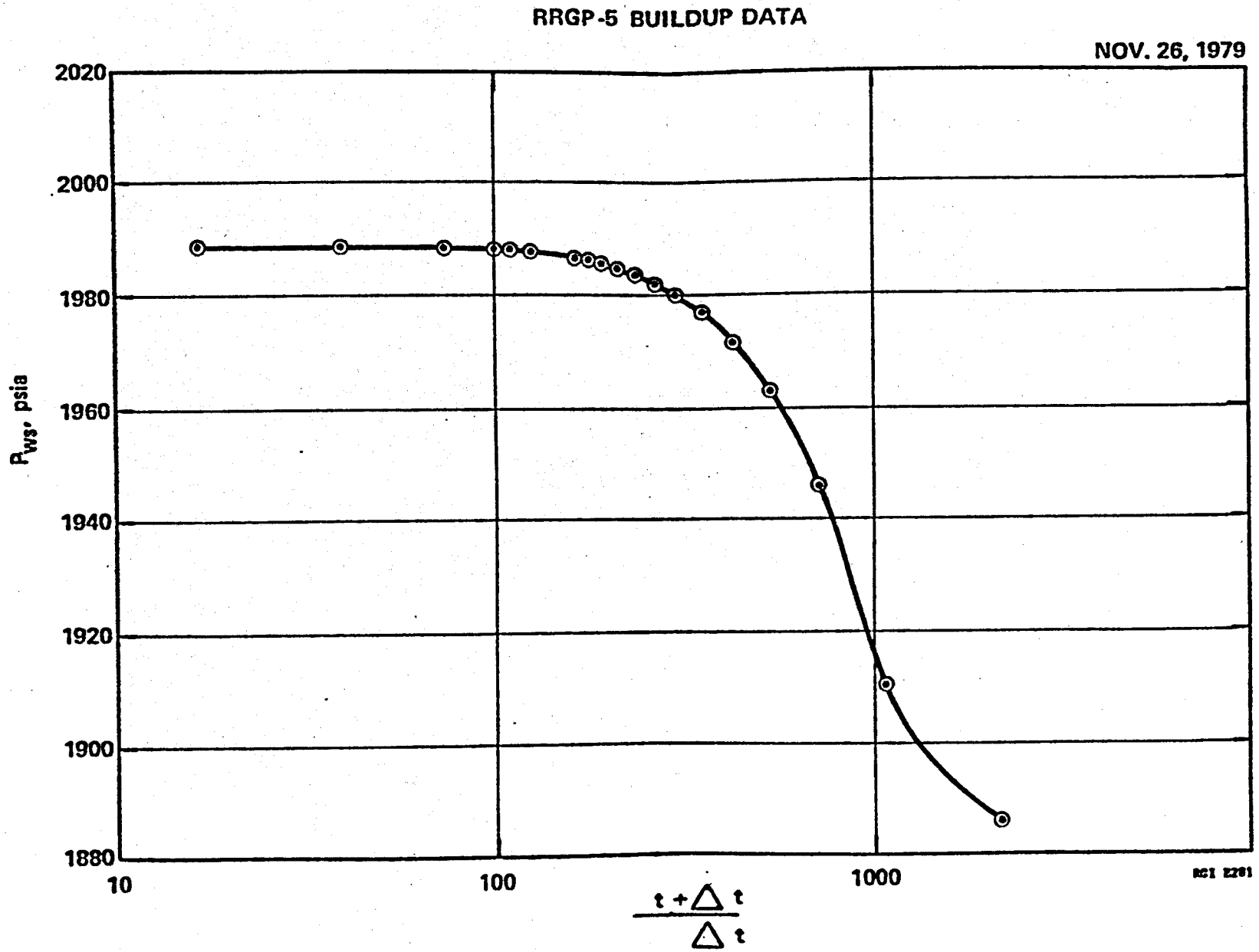
RRGP-5 BUILDUP DATA
NOV. 26, 1979
2020
2000
1980
1960
1940
1920
1900
1880
P_{ws}, psia
10
100
1000
$\frac{t+\Delta t}{\Delta t}$
RCI 2261

FIGURE 10

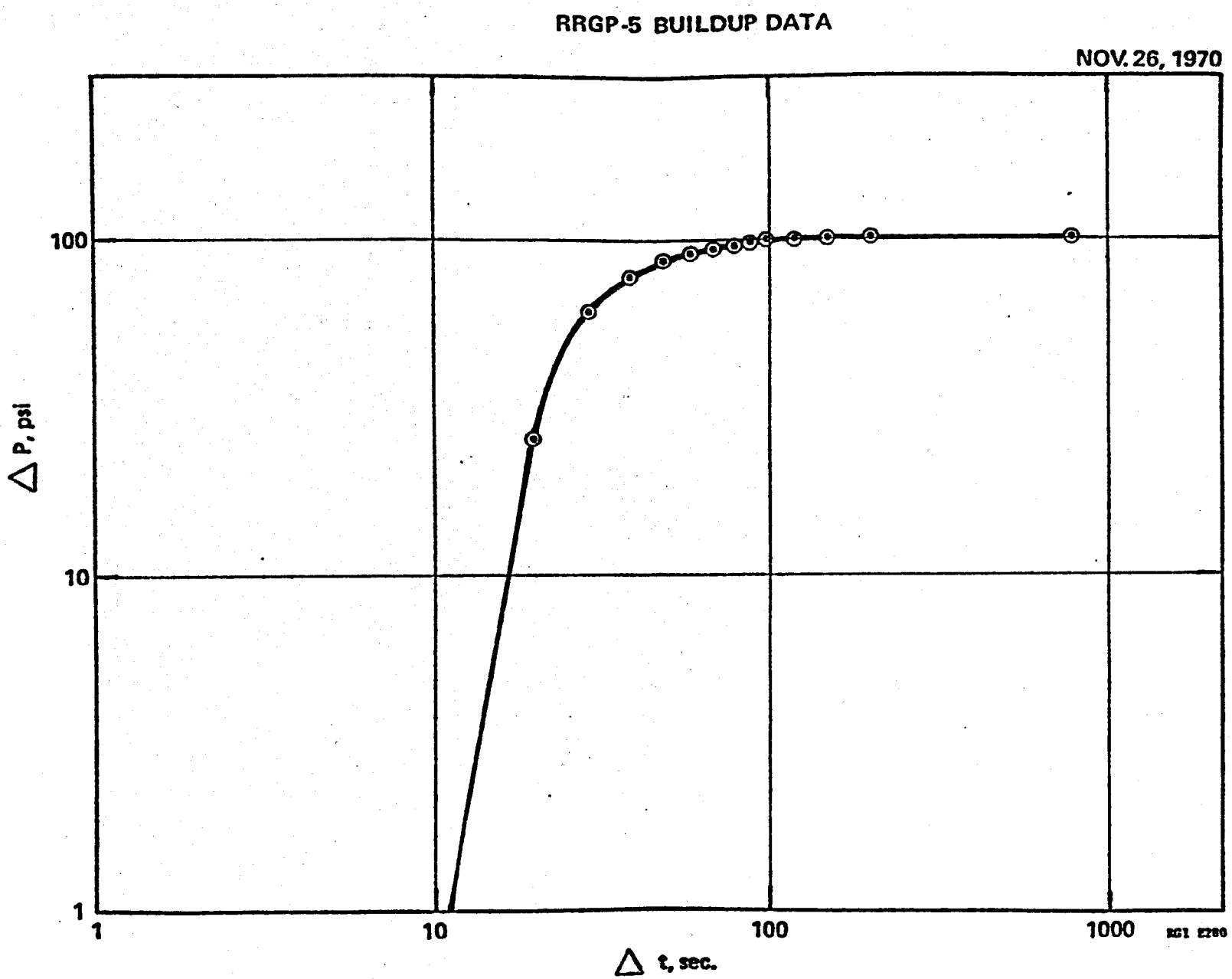
RRGP-5 BUILDUP DATA
NOV. 26, 1970
100
10
1
Δ P, psi
1
10
100
1000
Δ t, sec.

FIGURE 11

RRGP - 5
TEMPERATURE SURVEYS
RAFT RIVER, IDAHO

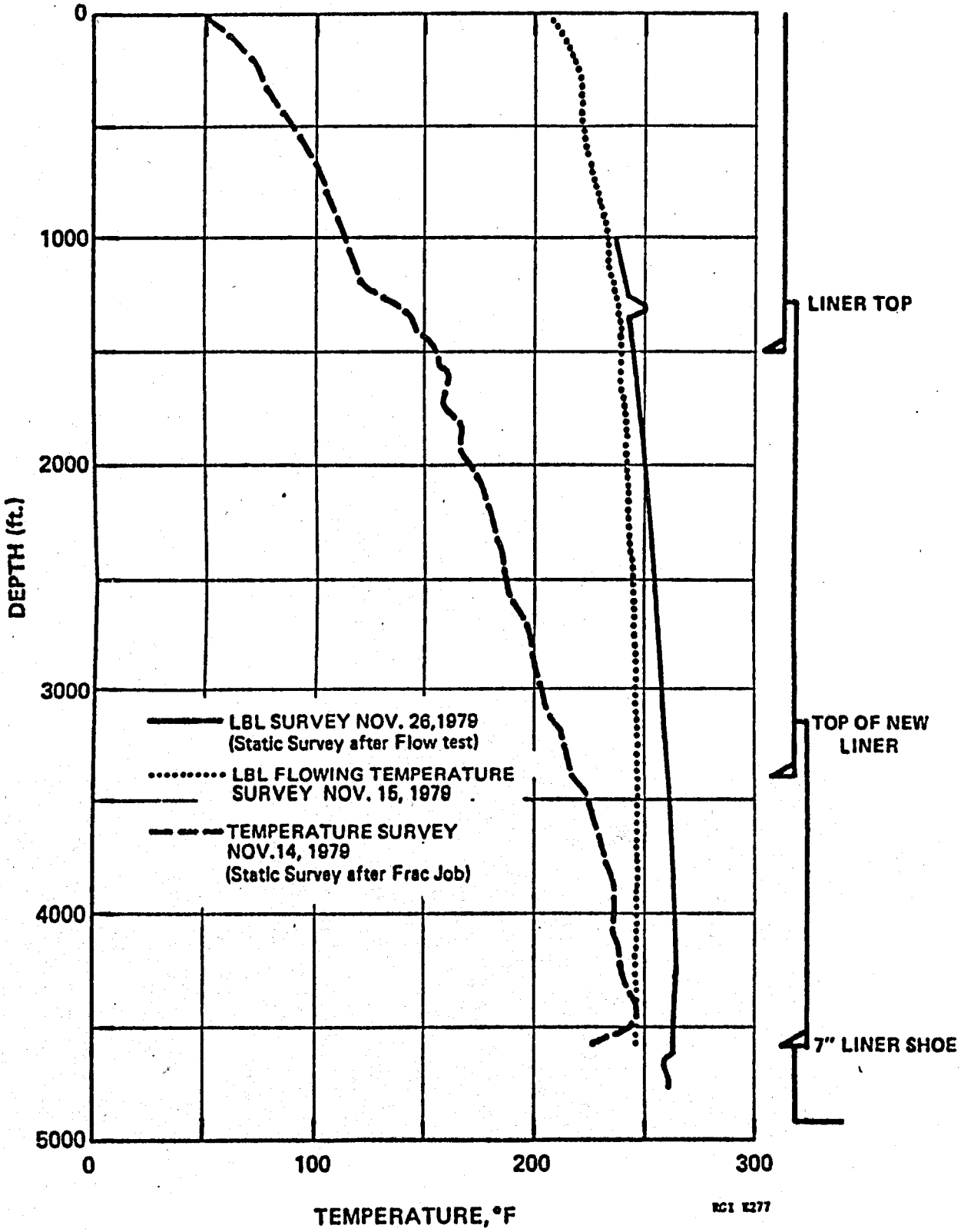

FIGURE 12

RESERVOIR SIMULATION

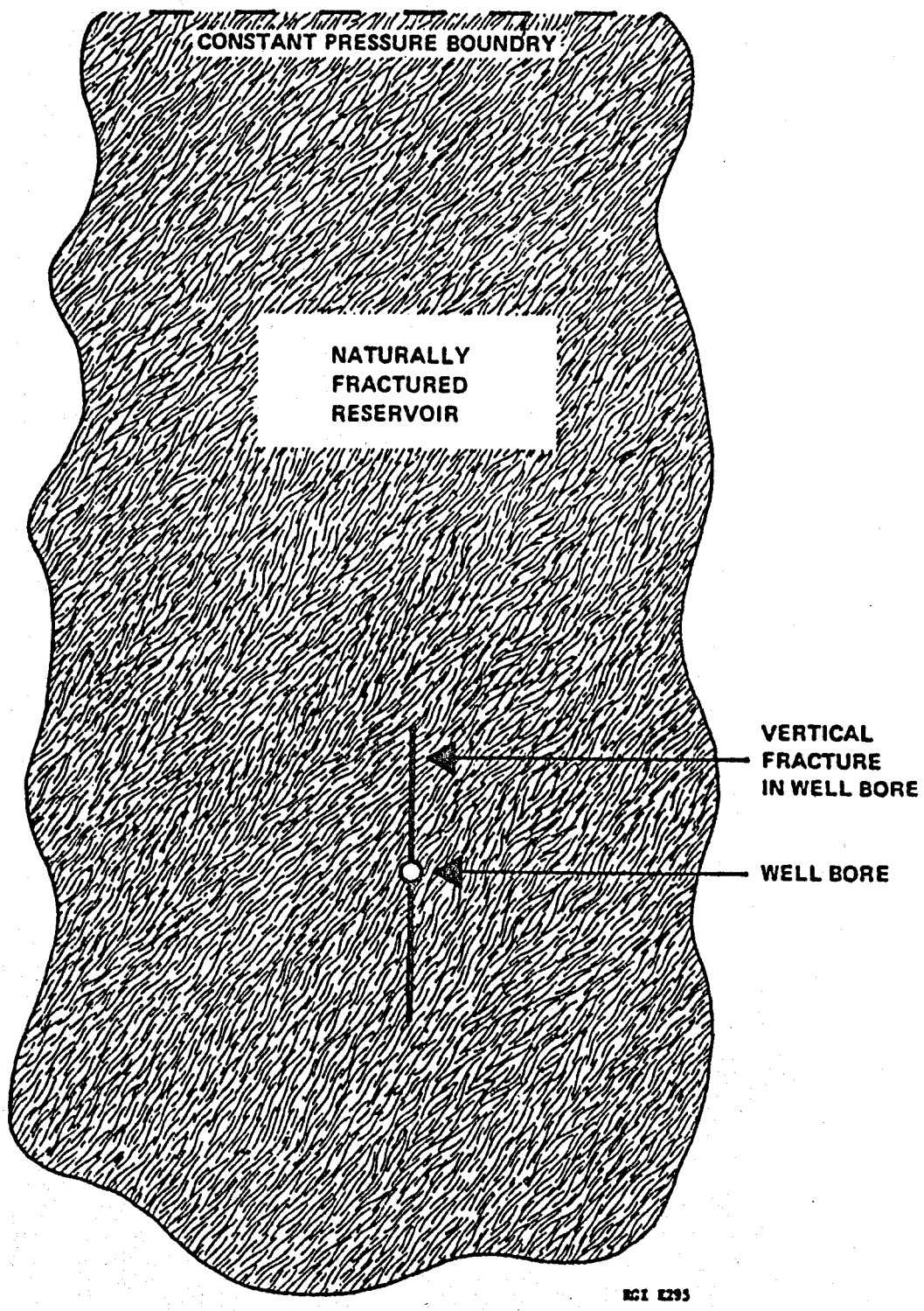

FIGURE 13

TOTAL ORGANIC CARBON AND CARBOHYDRATE CONCENTRATION OF RRGP-4 PRODUCED FLUID

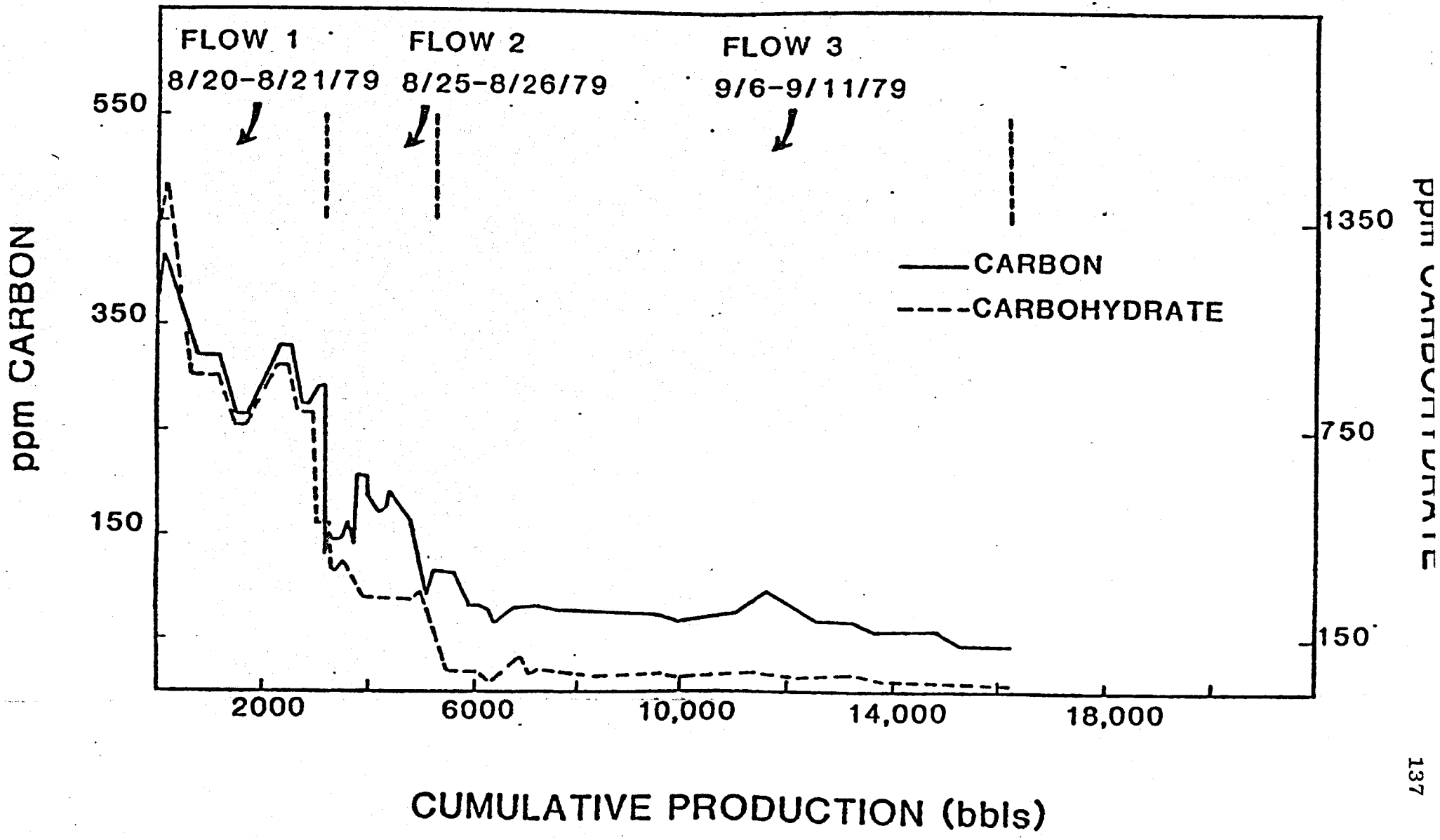

FIGURE 14

AMMONIUM AND NITRATE TRACER CONCENTRATION IN RRGP-5 PRODUCED FLUID

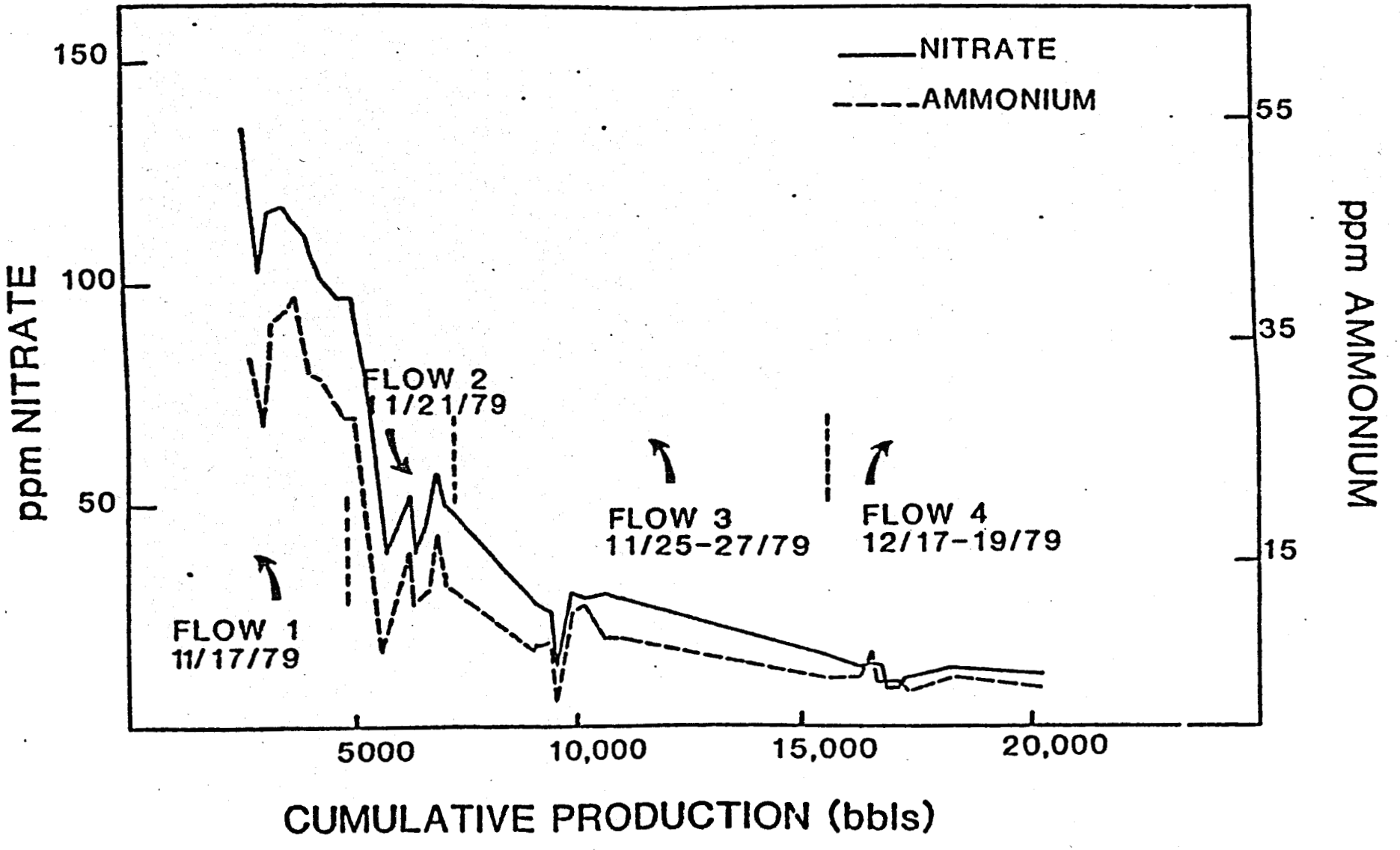

FIGURE 15

TOTAL ORGANIC CARBON AND CARBOHYDRATE CONCENTRATION OF RRGP-5 PRODUCED FLUID

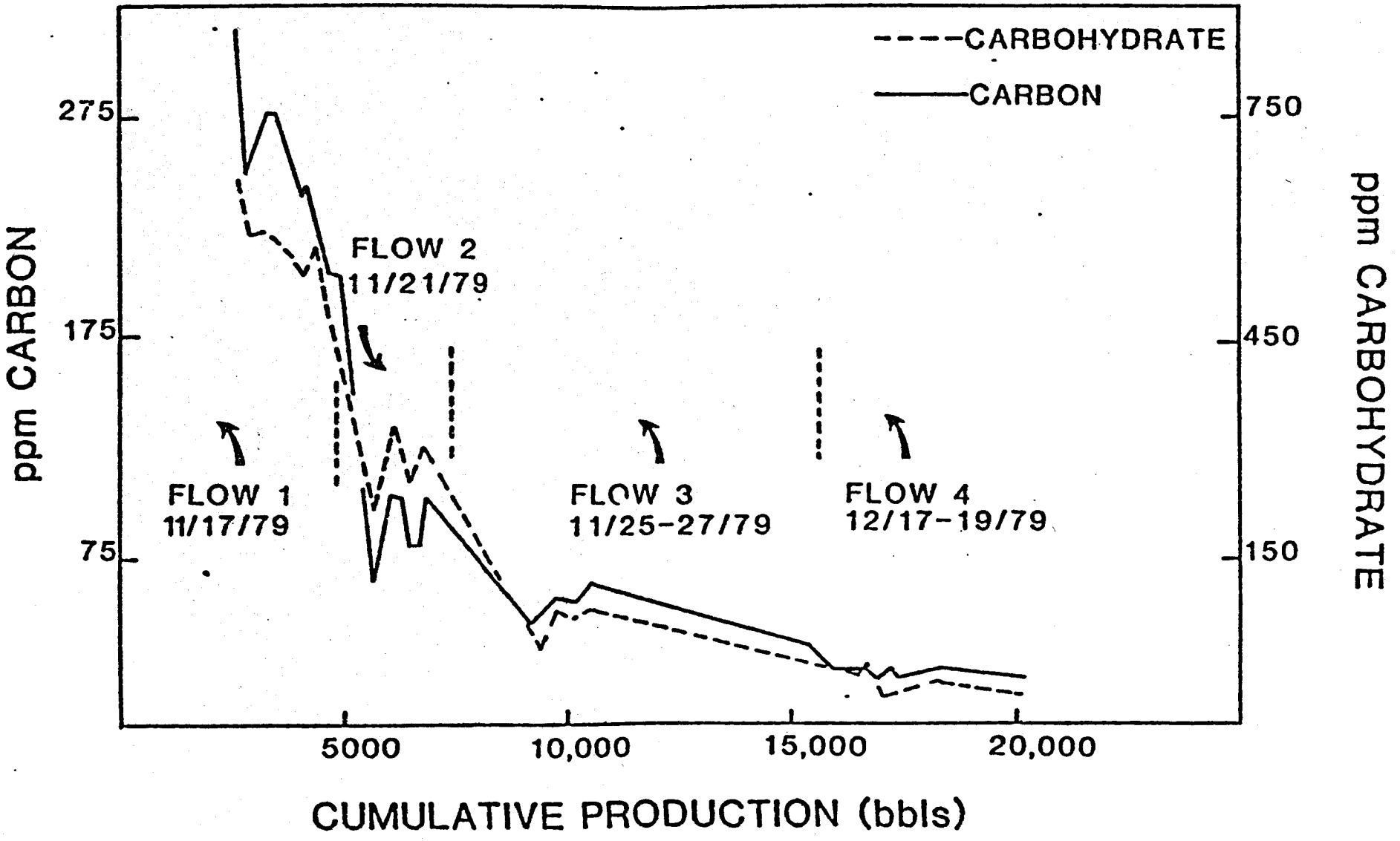

PLANNING AND EXECUTION OF RAFT RIVER STIMULATION TREATMENTS

Robert V. Verity
Republic Geothermal, Inc.
Santa Fe Springs, Ca

1. RRGP-4 Well Characteristics and Treatment Objective

Raft River Well RRGP-4 was the first stimulation candidate under the Geothermal Reservoir Well Stimulation Program (GRWSP). Prior to the stimulation treatment, the well produced at a stabilized artesian flow rate of only about 10 gpm, compared to rates of more than 200 gpm for the better producing wells in the field. An acoustic borehole televiewer log (1) run previously by the U.S. Geological Survey indicated the well had less natural fracturing in the wellbore than other wells in the field. Since the other wells had encountered a better developed and more productive fracture system, it was not unreasonable to believe that major productive fractures could exist near RRGP-4. Therefore, it was considered likely that a fracture stimulation treatment in the well could create fractures which would intercept major natural fractures and therefore make the well comparable in productivity to the better producing wells in the field.

A producing temperature of 270 degrees F. or higher was required for efficient use in the power plant. Since only the lower portion of the well had sufficient temperature to meet the minimum temperature requirement, a 7-inch liner was installed and cemented which excluded all of the upper portion of the original open-hole interval (Figure 1). Only the interval from 4705' to 4900' was left open for the fracture treatment. The 200-ft. interval was selected as a length which could be effectively fracture treated.

2. Treatment Selection and Design

Maurer Engineering and RGI evaluated several different fracturing processes for use in RRGP-4. The Kiel (dendritic) Fracturing Process (2) was selected primarily because it appeared to offer the best opportunity of intersecting the major natural fractures in the area. Our concern with a conventional planar fracturing treatment was that the created fracture would only parallel major natural fractures in the area.

The Kiel frac treatment was designed for five stages of 1,975 bbl per stage. Each stage included two pumping periods, each of which was followed by a brief flow-back period. The pumping and flow-back sequence for a typical stage is shown in Table 1. The alternating pump-in and flow-back periods are designed to stress and restress the rock, rearranging the stresses to achieve a change in

fracture direction. Therefore, on the second and succeeding stages of a Kiel dendritic fracturing program, it can be expected that branched or dendritic fracturing will occur. Figure 2 is an idealized diagram of a dendritic fracturing pattern. Each stage, as shown in Table 1, included three slugs of 100 mesh sand for fluid loss control followed by four slugs of 20/40 proppant sand. Each stage was designed to achieve a fracture 200 ft high by about 1,500 ft. long assuming a fluid efficiency of 30%. The frac fluid was a low viscosity gel containing 10 pounds of hydroxypropyl guar plus two pounds of XC polymer per thousand gallons of water. As discussed below the treatment was terminated after 4 stages. A total of 7,900 bbls of frac fluid was injected with 108,400 lbs of sand at an average rate of 50 bbls/min.

3. Treatment History

Figure 3 is a pressure-rate history of the treatment. There are three major items of interest to notice in the figure. The erratic behavior in the first two stages is a result of some unscheduled shutdowns caused by minor equipment problems and leaks. One advantage of the Kiel process is that such shutdowns do not normally have an adverse effect on the treatment results. Such a shut-down in the advanced stages of a conventional fracturing treatment would likely result in a sand-out and failure of the job. Stages 3 and 4 proceeded with no difficulty. As shown in the figure, there is little character to the pressure curve in the last two stages except for a minor decline in pressure in the final stage. It is also important to notice the trend of instantaneous shut-in pressures (ISIP's) following each pumping period. After the first stage, there is very little change in the ISIP, and that is an indication that dendritic fracturing was not actually occurring. In a normal dendritic fracturing job, changes in the rock stresses which result in dendritic fracturing would also be evidenced by a change in the ISIP from stage to stage. Since there were no apparent results other than the probable extension of the natural fractures, the job was terminated after four stages.

4. Mechanical Arrangement

The frac job was pumped through a 4-1/2" frac string with a packer set in the 7" liner. The frac string was used because of pressure limitations on the casing and liner laps above the 7" liner. Figure 4 is a schematic diagram of the surface fracturing equipment layout. B-J Hughes provided all surface fracturing equipment and treatment materials. The selection of B-J Hughes was based on competitive bids and equipment availability. Because of the large volume of the treatment, the frac fluid was mixed and pumped in a continuous process. A new 24,000 bbl lined pond was filled with geothermal fluid from RRGP-5 prior to the job. A Model 607 45 bbl/min blender pumped water from the pond, added the

two polymers and a small amount of hydrochloric acid to lower the pH of the water slightly and enhance the jelling of the polymers. The fluid then was pumped into the four 500-barrel frac tanks which provided surge capacity and residence time for gelation to occur. A Model 611 120 bbl/min blender pumped frac fluid from the tanks, added proppant sand, and fed the frac units. Sand was delivered to the blender by dump trucks. The frac units pumped through two 3" frac lines to the well. A branch line from one of these frac lines to the pit provided a means of back-flowing the well between pumping stages. A pump truck was connected to the well annulus to hold pressure on the annulus in anticipation of fracturing pressures higher than the capability of the frac string and packer. However, fracturing pressures were lower than anticipated, and this truck was not actually needed. There were four Model 133 semi-trailer frac units and four Model 139 truck-mounted frac units on location for a total of 8,000 hydraulic horsepower. Because the fracturing pressures were lower than anticipated, only 4,000 hp was actually used. B-J Hughes also provided a mobile laboratory for final checks of water chemistry and gelation. Although the polymers had been pretested in Raft River water, a final check on the location was done.

5. RRGP-5 Well Characteristics and Treatment Objective

RRGP-5 was chosen for the second stimulation treatment under the GRWSP. This well was already capable of producing 600 gal/min or more with a pump, which is considered an adequate rate for a Raft River well. However, the producing temperature of 255 degrees F was lower than desired for the Raft River power plant. The USGS borehole televiewer log of this well showed extensive natural fracturing in the wellbore. The producing interval was in a cooler, more shallow interval of the well. The deeper, hotter portion of the well, which was our stimulation target, also had extensive fracturing, but the fractures appeared to be very tight. It was also noted that the fractures ran in many different directions in this lower portion of the hole. Because of this observation and because RRGP-5 is near the intersection of two major faults, i.e., the Narrows and Bridge Faults, it appeared likely that a single planar fracture in the deeper portion of the well would intercept major natural fractures. The objective of the treatment was to achieve a producing rate at least comparable to the existing rate, but from a deeper, hotter interval.

6. Treatment Design

Maurer Engineering designed a conventional planar fracture treatment to achieve a 200 ft high by 1,000 ft long fracture with a 14% fluid efficiency. The treatment was designed for a total of 7,250 bbl as shown in the pumping

schedule (Table 2). A total of 7,600 bbl of frac fluid was actually pumped because the job was restarted after some early unscheduled shutdowns. The frac fluid was a relatively low viscosity gel containing 30 lb of hydroxypropyl guar per thousand gallons of water. Eighty-four thousand pounds of 100 mesh sand was used for fluid loss control and 347,000 lb of proppant included 42,000 lb of 20/40 Supersand (a resin-coated sand) which was tailed in at the end of the job. It was intended that the Supersand would bond together in the fracture near the wellbore and prevent the other proppant sand from being produced into the wellbore after the frac job. The relatively low viscosity frac fluid was designed specifically to allow settling of the sand within the fracture at a controlled rate. As the sand settles, it is believed to settle in banks, as shown in Figure 5, which props the lower portion of the fracture at nearly the full dynamic width, leaving the upper portion of the fracture open. The flow capacity of this open portion of the fracture is many times that of a sand-filled fracture.

6. Treatment History

Figure 6 is a pressure-rate history of the treatment. During the first 700 bbl of the treatment, there were several unscheduled shutdowns for leaks and it was observed that the ISIP at that time was 500 psi. As the job progressed, there were substantial pressure breaks between the 800 and 1,500 bbl points, and at the time about 2,800 bbl were pumped. As the job progressed past the 5,000 bbl point, the pressure began to increase steadily. This is probably a result of leak-off into adjoining fractures and a narrowing of the fracture which resulted in a higher friction loss there. At the end of the job, the rate was gradually reduced in an attempt to sand out the well and leave a fully propped fracture at the wellbore. As the rate was reduced and finally pumping was stopped, it was noted that the ISIP was near zero. This change in ISIP from 500 psi near the beginning the job to near zero at the end indicated that communication with major fractures had been achieved.

8. Mechanical Arrangements

Figure 7 is a diagram of the well with the frac string in place. As in the case of RRGP-4, a 7" liner was installed to exclude all but the lower portion of the original completion interval. The interval below the liner, from 4,587' to 4,803', was open at the time of the fracture treatment. A 4-1/2-inch frac string with a packer in the 7" liner was also used for this job. The surface equipment layout for this job was very similar to that for RRGP-4. B-J Hughes provided all surface fracturing equipment and all treatment materials except for the resin-coated proppant sand. The selection of B-J Hughes was based on competitive bid. Because of the large volume of the treatment, the frac

fluid was mixed and pumped in a continuous process. A Model 608 120 bbl/min blender located at the pit added polymer, a small quantity of acid, and ammonium nitrate as a chemical tracer. The fluid was then pumped through a 10" steel line to four 500 bbl frac tanks which provided gelation time for the polymers. A Model 611 120 bbl/min blender fed by a Sand King drew frac fluid from the tanks and pumped to the frac units. The Sand King is a four-compartment field storage unit which stores up to 475,000 lb of proppant sand. It incorporates a conveyor belt delivery system to the blender. These units are especially useful where large volumes of sand and high delivery rates are required. A total of 6,000 hydraulic horsepower was on location, consisting of seven Model 139 truck-mounted frac units and one Model 133 semi-trailer frac unit. Frac fluid was pumped through two 3" lines to the well.

Following the frac job, the well produced substantial quantities of proppant sand, a common occurrence following a massive frac job. Approximately ten days of flowing and circulating were necessary before sand production diminished to a sufficiently low concentration to reinstall the electric submersible pump.

9. Job Costs

The total cost of rig work and fracturing in RRGP-4 was $340,000. Of this amount $64,000 was for fracturing service and materials. The remainder was spent for recompletion of the well as described above. The total cost of rig work and fracturing of RRGP-5 was $460,000. Of this total, $132,000 was for fracturing service and materials. The remainder was spent on pulling and rerunning the pump and permanent packer, and recompleting the well with 7" liner. Costs incurred by EG&G Idaho, Inc., for testing the well and providing support to the rig operation are not included in the above cost figures.

REFERENCES

1 Keys, W. Scott.
The Application of the Acoustic Televiewer to the characterization of Hydraulic Fractures in Geothermal Wells. Proceedings of the First Geothermal Reservoir Well Stimulation Symposium, San Francisco, California, February 7, 1980.

2 Kiel, Othar.
Kiel Fracturing Process, U.S. Patent No. 3,933,205.

Figure 1

SCHEMATIC OF RAFT RIVER RRGP-4
WITH 7"LINER IN PLACE

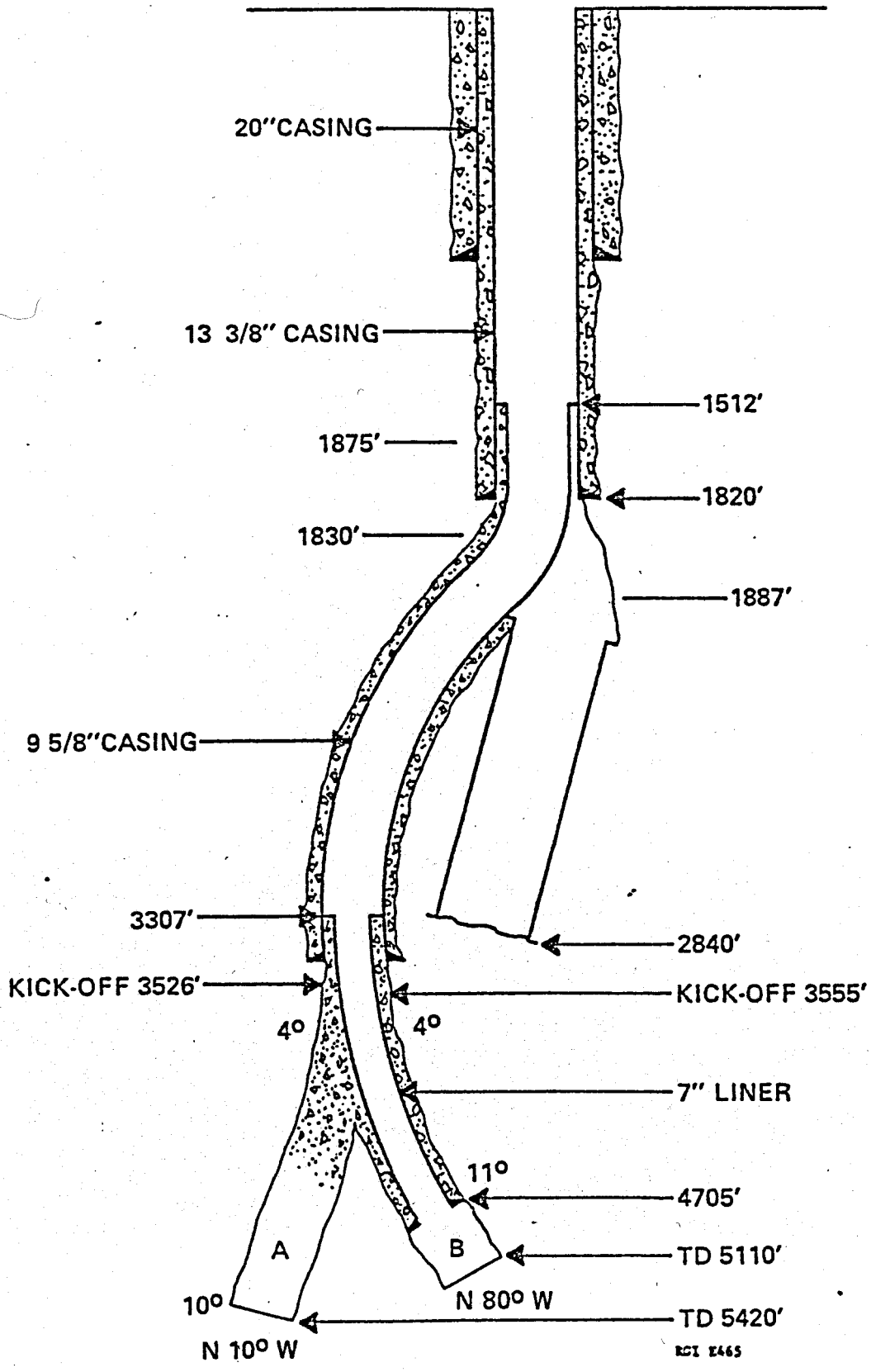

Figure 2

SCHEMATIC OF A DENDRITIC FRACTURE (AFTER KIEL)

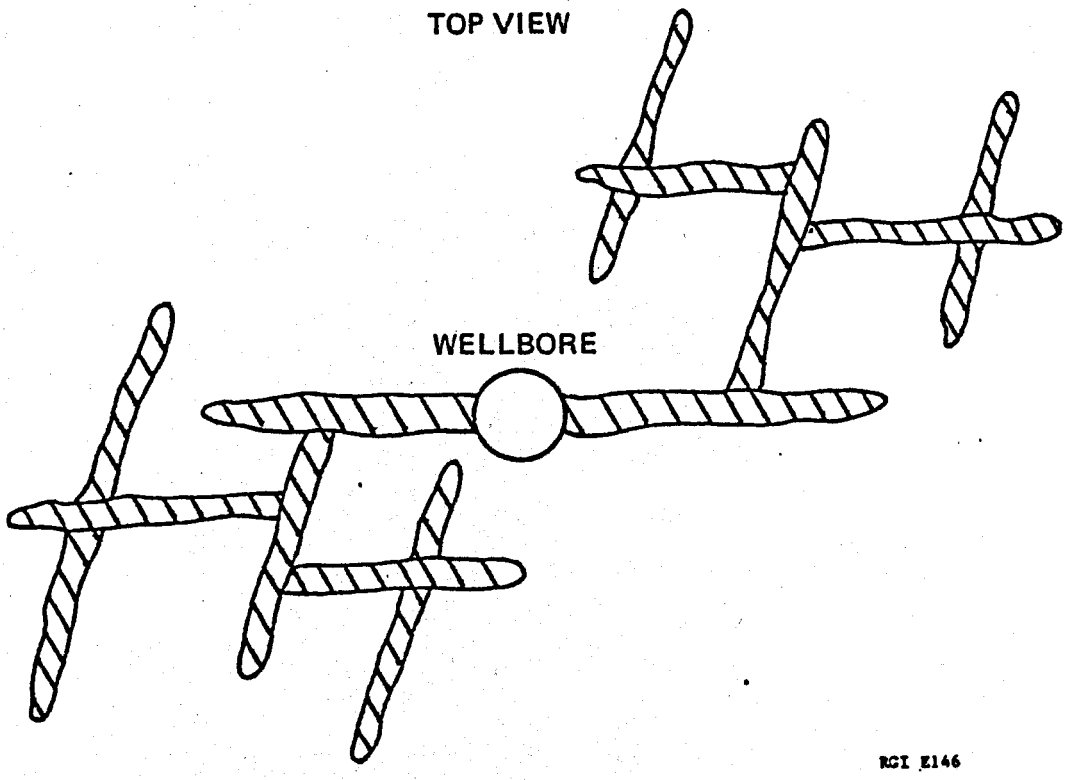

Figure 3

RRGP–4 KIEL FRAC

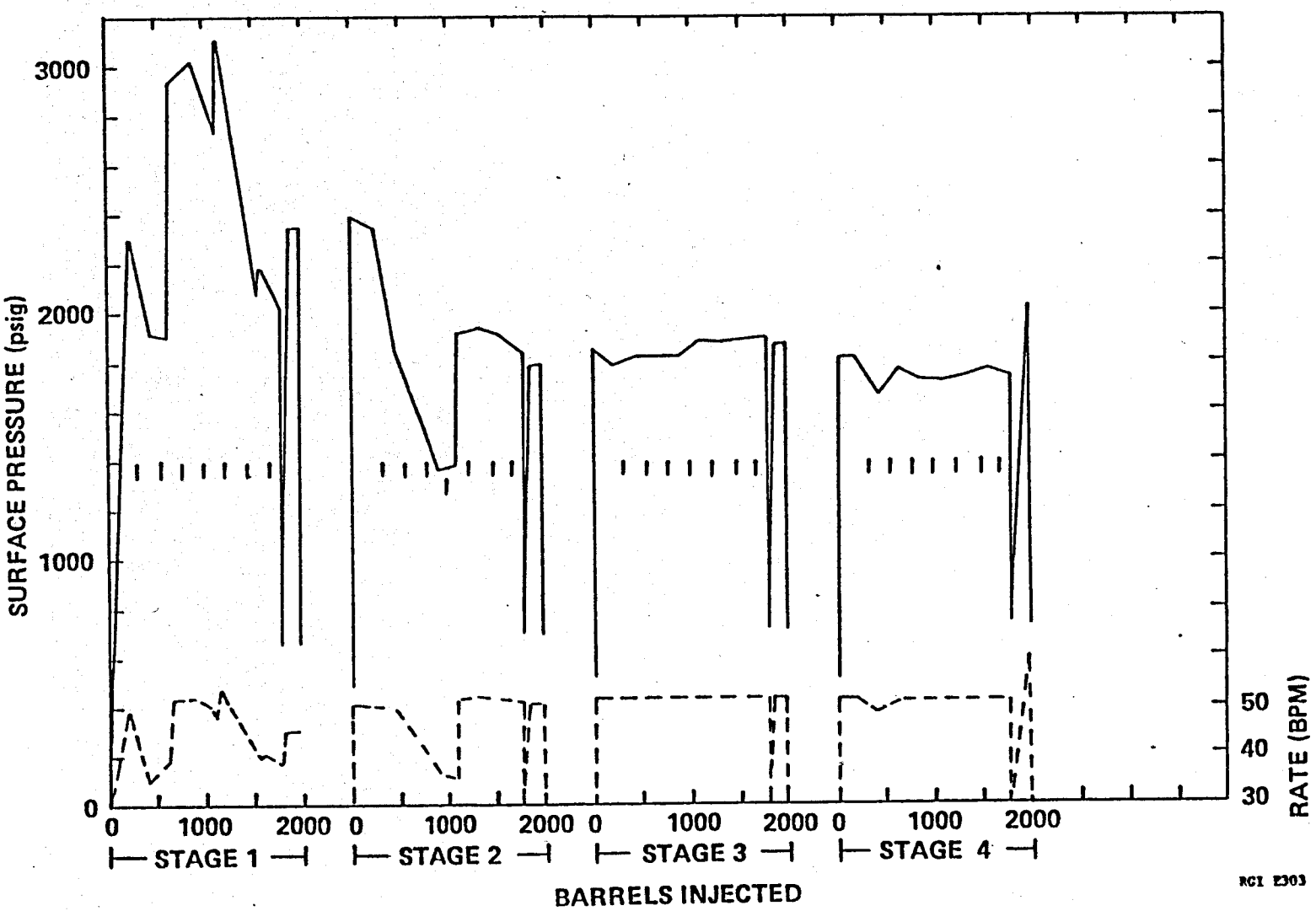

Figure 4

EQUIPMENT LAYOUT FOR RRGP-4 FRAC TREATMENT

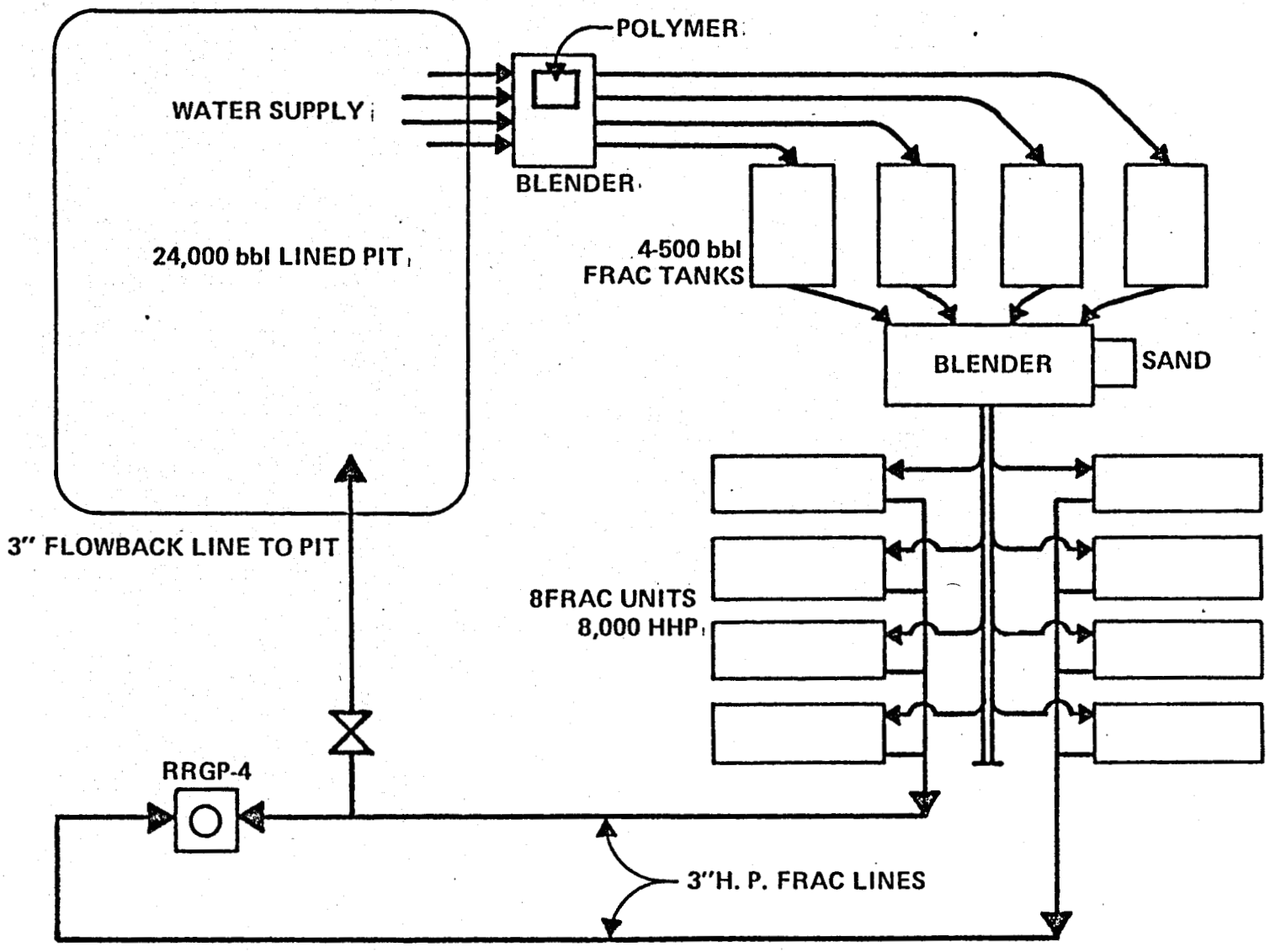

Figure 5

SCHEMATIC SIDEVIEW OF PLANNER FRACTURE
SHOWING SAND SETTLING IN LAYERS

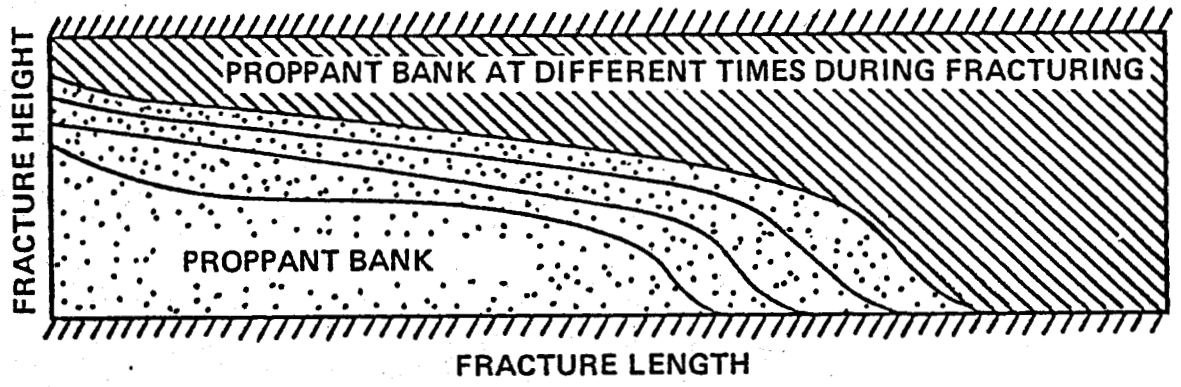

EQUILIBRIUM SAND BANK IS FORMED WHEN PROPPANT SETTLES THRU FLUID

RGI E145

Figure 6

RRFP–5 FRAC JOB

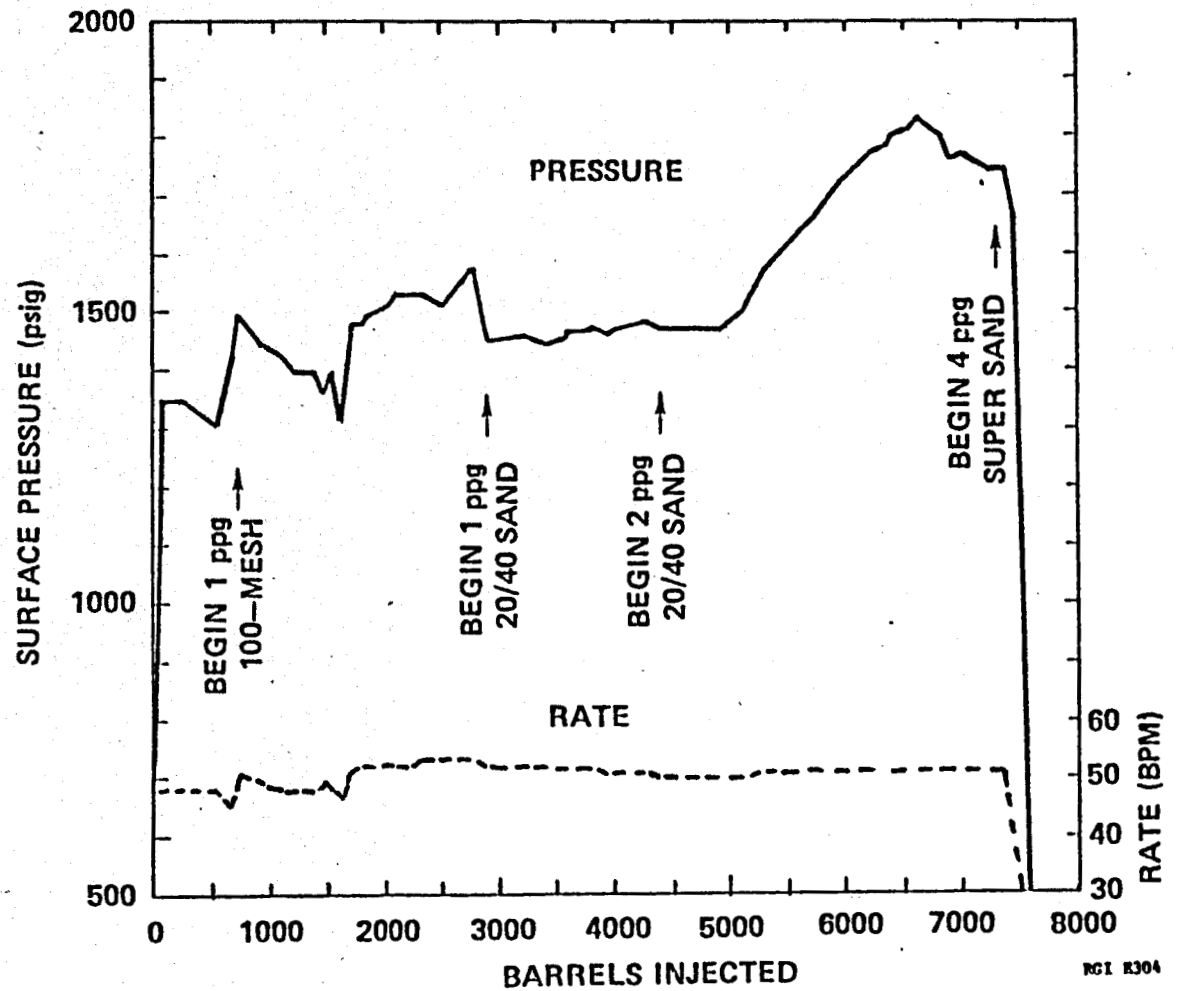

Figure 7

SCHEMATIC OF RAFT RIVER WELL RRGP-5
WITH LINER AND FRAC STRING IN PLACE

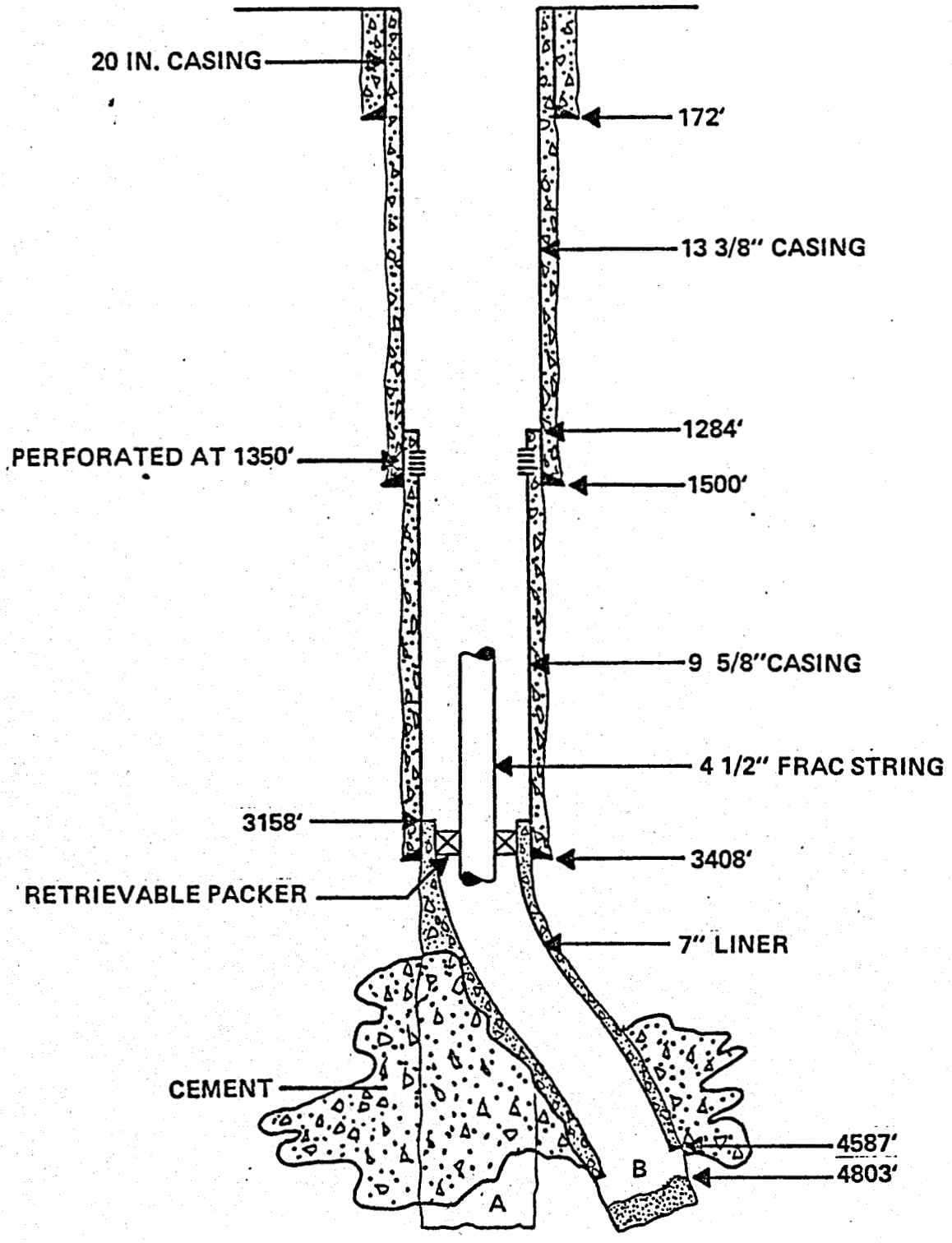

RGI 8476

TABLE 1

Pumping Schedule For One Stage
Of Kiel Frac, RRGP-4

Event No.	Fluid Volume (bbl) Incr.	Fluid Volume (bbl) Cum.	Sand lb/gal	Sand Size	Fluid
1	200	200			10 lb H.P. guar + 2 lb XC polymer per 1,000 gal
2	25	225	4	80/100	"
3	200	425			"
4	25	450	4	80/100	"
5	200	650			"
6	25	675	4	80/100	"
7	200	875			"
8	25	900	2	20/40	"
9	200	1,100			"
10	25	1,125	4	20/40	"
11	200	1,325			
12	25	1,350	4	20/40	"
13	200	1,550			"
14	25	1,575	4	20/40	"
15	200	1,775			"
16	Shut down and flow back				"
17	200	1,975			"
18	Shut down and flow back; ready for next stage.				

TABLE 2

RRGP-5 Fracture Treatment
Pumping Schedule

Time (min)	Fluid Volume (bbl) Incr.	Cum.	Sand lb/gal	Size	Comments
0-10	500	500			Pad Stabilize rate and measure ISIP during pad.
10-50	2,000	2,500	1	100	
50-80	1,500	4,000	1	20/40	
80-140	3,000	7,000	2	20/40	
140-145	250	7,250	4	20/40 Supersand	Slow rate if possible at the end. Displace Supersand to below liner and stop. Measure ISIP.

RAFT RIVER: MECHANICAL DESIGN AND OPERATIONS

by Robert W. Nicholson
Terra Services, Inc.

Robert Emslie: Now, I would like to introduce four gentlemen who have been working on the Raft River project. The first speaker is Robert Nicholson, who will talk on the mechanical preparation of the wells for the project.

Robert Nicholson: Thank you very much. Most of the information we have heard today has been concerned about the engineering activities that go on when you do, or plan, a fracturing job. But one of the real problems in geothermal well stimulation, is how to actually mechanically accomplish the stimulation job. In geothermal wells, we have some very difficult mechanical problems: No. 1 is the wellbores are very large; No. 2 is producing zones are very long; and No. 3 is the producing rates are very high. Isolation of any zone for any type of stimulation method is absolutely necessary but is very difficult to accomplish.

First slide, please. I would like to tell you some of the problems we face when considering fracture stimulation, or any chemical stimulation, in geothermal wells. In geothermal wells, the primary problem is they produce at very high rates (30,000 to 60,000 BED). These rates are necessary for economic operation. Such rates require large diameter casing in the wells because of small drawdown pressures you can normally induce because of low reservoir pressure. Also, the necessity for high rates requires the long completion intervals of geothermal wells. Slide 2, please.

Most of the geothermal wells are completed in some manner similar to those we are looking at here. The surface pipe is 13 3/8-inches or 16-inches at the top. The 9 5/8-inch, 10 3/4-inch, or 11 3/4-inch are some of the sizes of intermediate casing set down to the top of the producing interval. The bottom of this string is usually at depths of 2500 feet to 10,000 feet. The very long (2000 feet to 3000 feet) openhole completion interval is difficult to stimulate. We are looking at an even worse situation in which we have slotted liners in the wells over these very long completion intervals. Then, hopefully, in some of the wells we

do have some jet perforated, cemented casing completions. Although, this completion can also be a problem because the cement jobs are usually not very good. If the wells have been producing, or have been in existence for any length of time, cement deterioration due to the high temperature is a serious problem which develops. Zonal isolation is still a problem where we have this cemented, jet perforated liner completion.

We have completions with liners and long casing strings or just the single casing all the way down through thr completion interval with some slots down at the bottom of the casing. This type of completion, slotted casing, has become the rule in areas where severe scale problems occur because of pressure changes between the two sizes of pipe at a liner top. This problem is accentuated at high flow rates. In Raft River, the wells are primarily completed now in this fashion (open hole). That is, casing set to the top of the completion interval with open hole through the producing zone. We have a very difficult problem of how to isolate a single zone in any of these wells. Thus, we have this problem of how to place the fracture stimulation fluid or chemical stimulation fluid in the desired zone. Our normal methods we are familiar with for zone isolation from the oil industry do not work. We must come up with some methods that can be used in geothermal wells to make stimulation activity economical.

For open-hole completions, we have isolation techniques available using packers of combination liners and sand plugs. In completions where we have cemented casing, we can use packers also, but different types of packers than for openhole. We can also, selectively perforate or plug off zones, put cement plugs, or sand plugs. There are a number of things you can do if you have a jet perforated, cemented casing in the well. We face a real bad problem with slotted liners. You just really cannot accomplish isolation in any type of slotted liner. Several attempts by a number of people have been made at zone isolation in slotted liners using cement plugs or chemical plugs. At times, these are semi-successful, but generally not.

A problem you also encounter in geothermal wells is having such long slotted liner intervals which have been produced, injected into or treated, etc. You cannot pull those slotted liners back out of the well. This is usually because of formation falling around the casing which packs around those liners. If you run another string of pipe inside the slotted liner you have to get a cement job. There is no possibility of getting any good cement job behind the slotted liner to effectively isolate the entire interval. Slide 3, please.

Here are some slides to show those people who are not

informed about the mechanical problems that exist or how you go about accomplishing zone isolation. Slide 4, please. In geothermal wells, if you have a good cemented casing in the well, you can use permanent packers, or drillable packers. These have not been too bad in a number of cases because the clearance between the packer elements and the casing wells is small. Even though the elastomers cannot withstand very high temperature, this clearance is very small and you can often get a pretty good seal. A number of failures do occur. Of course, you cannot then inject the stimulation fluid in the desired zone. Slide 5, please.

Then open-hole packers have been tried and used. They have been tried at the hot dry rock project a number of times. However, the following problem is very common. What happens is fluids bypass through, or around the packer through the natural fracture system around the wellbore. In wellbores where you have a lot of production, injection temperature cycling, the wellbore is very torn up. This happens to be the case in Raft River. Slide 6, please.

Thus, one of the things you can do if you have a long open-hole interval is to run a liner through part of the interval and sandplug back a lower zone. This effectively isolates the interval you want to treat. The big problem with this, of course, is you are then limited to only one zone. You cannot treat this zone down below. You can wash the plug out of the well, but then you cannot isolate the previously treated zone above. Of course, if you have this cement job, you could possibly now do some stimulation up above in the cemented liner you now have installed in the well. Next slide, please.

This is just a picture of the Raft River area. Some of you may or may not be familiar with it. I think Charles Morris will probably have some other pictures of the site. Here is the geothermal plant that is being installed and this is where we were working, over here on Well #5. These are the other wells; the area is fairly large; it is in a nice basin, but in the wintertime it is pretty cold up there. That is another operational problem which influenced the timing of the job. As you can see, this is a desolate looking area and there are not many facilities around. It is very expensive to get equipment in and out of there; and that runs the job cost up substantially. Slide 7, please.

The Raft River field is essentially laid out around the power plant. The two major fault systems around which the original drilling was done is this bridge fault area and this narrows fault area. This was the #1 well, the discovery well in the field, which is also the best producing well in the field. Well, Dr. Morris will get into why we selected the wells #4 and #5 to stimulate. A major reason we selected Well #5 was its location at essentially the

boundary of these two fault systems, the bridge and the narrows fault.

We also selected Well #4. Some of the reasons we did select well #4 was that it was a very poor producer. Also, we did not want to damage one of the good producing wells because of mechanical failure. Right now the field production rate is just sufficient to feed the power plant and do the other experiments. Thus, because well #4 was a poor well, the project would not be in jeopardy because of a mechanical failure. If we were very successful there, then we would have significantly contributed to the total project. Well #5 was also not a very good well, but we went into well #4 first. Slide 3, please.

Our operational problems in designing the job were primarily downhole, and we had the problem of zone isolation which we discussed already. Another big problem especially in agricultural areas, which is not limited to the Raft River project, but common to almost all the geothermal areas, is how do you contain these geothermal fluids, or saltwater fluids at the surface. We tried working with the well flowing. However, then we had some additional problems such as how to get the tools down into the ground, and how to confine the cement placement job. The primary surface problem, of course, is the disposal of the fluids.

I talked about the problem of containment of geothermal fluids; I also want to imply the problem of containment of fracturing fluid. The shallower groundwater zones appeared to be in contact with some of the deeper fracture zones and so we knew if we could not isolate the intervals, at least at the wellbore, we would run a very high risk of actually a fracture penetrating from the geothermal zones into the surface water zones. So this was a real concern of ours during the planning of each project and analyzing pressure responses in some of the offset wells-both shallow surface wells and deeper wells, also.

Some of the surface problems included safety or working with the well flowing under geothermal conditions. People who have not worked with geothermal wells will find out there is one bad thing about them. They do not burn, i.e., catch on fire, which is good, but they are very hot. When working with the well flowing at a pretty high rate, it becomes tricky at times. We were also concerned about safety because we were planning some radioactive work. Next slide, please.

Here is a typical scene around the work site when we were cleaning out sand after the frac job. We were working with the well under pressure. You can see it is kind of warm around the well and you have to pay attention to what you are doing, otherwise someone can be burned. Next slide,

please.

This is the Grant rotating head which was on the well at all times to help prevent boiling or splashing hot water on the rig floor. And as you can see, it is very hot on the floor. However, the weather was getting very cold out here towards the end of the job on #5 which actually concluded sometime in November. Slide 7 (repeat) please.

Here are the wells and the fault system. Wells #4, #5, #1, and #2 are on the northwest side of the field up here. The injection wells and well #3 are really in a completely different environment. I will let the geologist explain about that; I do not want to do into those details myself. Next slide. (See Dr. Charles Morris' talk).

Here are some of the things we were concerned about. These are the data EG&G had run in the field and there appears to be some connection between the shallower wells and the deeper wells. As you can see, there are concurrent pressure responses in certain wells indicating subterranean connection. Slide 9, please.

Here is a schematic of Raft River #4 well. They had some problems drilling the well. They lost some pipe here after the surface pipe was cemented. That section of hole was sidetracked and they eventually drilled down to this point here; I do not have the depth written down here, but it is around 3500 feet. They then drilled one leg, the A leg, which went off in this direction. The problem with the A leg was it did not have any production. Thus, they did what we commonly call in the oil and gas industry, a low hole sidetrack. The hole went off in another direction which was called Leg B. They did get some production in this leg where they had almost none in the first leg. Slide 10, please.

Here is a plan view of the well from the directional survey. Now, these two legs gave us a bad problem. We were concerned about fracturing into Leg A while we were working in Leg B, which was the second leg. We wanted to plug Leg A; however, we knew we could not easily enter Leg A. We tried to enter Leg A, but we could not because we did not have the right type of tools. Acquisition of proper tools is a very difficult job especially if no pre-planning to selectively re-enter certain legs is made during drilling. This was not done at the time they made the sidetrack, they never considered having to re-enter Leg A or stimulate the well. So, at this particular time we were concerned that if we did fracture, we might fracture over this other leg which was probably still open. If the leg were still open, we were concerned about the pressure traveling up this leg and creating a shallow fracture and creating a connection into the shallow groundwater system. Slide 11, please.

We tried to cement off Leg A. We could not re-enter to cement here. What we did do, was to run a 7-inch liner into the well and cement the bottom of it. We left the liner uncemented at the top. We then came in and squeezed a considerable amount of cement on the top of that liner. We were hoping to get some cement down into this leg here. We may or may not have done that. We did get a good fracture across this interval which we did isolate. We had a 200-foot interval isolated between the sand fill and the 7-inch liner. Scott Keys will show you some of the results of his logging of that interval before and after we did the frac job. We just used a normal Baker Retriev-a-Matic Packer here at the top of the liner. We used a 4 1/2-inch frac string which was fine for the injection rates we were interested in.

Bob Verity will talk about the rates in a little while. One of the problems we did have which was not anticipated occurred when we dropped our ball to pressure test this tubing string. We pressured it up to 5000 psi and held the pressure there about a minute, and all of a sudden we lost all of the pressure. We were concerned about whether we parted the frac string or not. We made checks of two or three things, and decided the frac string looked pretty good, so we dropped another ball. We pressured it up again in stages, and the string held good at 2500 psi, 3000 psi, 4000 psi; we got up to 5000 psi again and the pressure immediately went to zero again. We made some checks and the string still looked good. What was happening was the drop balls Baker supplied to use in this tubing tester were just pumping right through. Of course, Baker swears their balls had been used under all types of conditions and they always held and that would never occur under any type of circumstances, but under those temperature environments, those types of things would occur. So, mechanically we did the job with really no problems at all. Slide 12, please.

This shows Well #5. These other slides show well #5 before we worked on the well. We also put the 7-inch liner in the well since we were successful before in well #4. We plugged back agagin with the sandplug on the bottom. (Slide 13). This effectively isolated the interval. We again also, apparently got interval isolation since we did have fracturing in all the open interval, at least at the wellbore interface. This is the wellbore face here. Now, as you can see, what we did was a very costly operation. That is, run a liner, cement and then plug the well back and do all that pre-work. As a matter of fact, well preparation was about half the cost of the job.

We looked at the possibilities of trying to do open-hole packers. But when we looked at the economics, if you have a single failure, the cost is higher than going this way. If we have a single packer failure, we start counting

up the standby time for the frac trucks and possibility of sanding up your drill string and all the other things that can go wrong down there when you are doing a job like this, the open-hole packers did not look good at all. So, retrievable open-hole packers you run on a drill string was used inside cemented liner. What is available from the oil and gas industry is really completely inadequate for what we need to do in geothermal work.

So, in conclusion, we were mechanically successful at Raft River. I think we can mechanically be successful in other areas. Although in geothermal work, the cost is very high. We need to have some better downhole tools. For surface tools, we do not feel like we have difficult problems to overcome. There has been some development in some of the elastomers and some of the other tools for geothermal work. These were developed through some of the DOE-funded work. However, because of the limited sales volume available, the service industry really has not jumped on the bandwagon and developed the commercial tools we really need.

That is all I have to say -- any questions?

Q: Are the other speakers going to tell us the improvement to the well and that sort of thing?

A: Right, I was just talking about the mechanical aspects of what we did. Charles Morris will talk about the reservoir work we did before and after; and Bob Verity will tell you about the fracturing design, the fluids and the proppants; and Scott Keys will tell you about some of the logging work done in those wells.

SLIDE NO. 1

GEOTHERMAL WELLS

PRODUCE AT HIGH RATES

NECESSARY FOR ECONOMIC OPERATION

LARGE DIAMETER CASING

SMALL DRAWDOWN PRESSURES

LONG COMPLETION INTERVALS

SLIDE NO. 2

TYPES OF GEOTHERMAL WELL COMPLETIONS

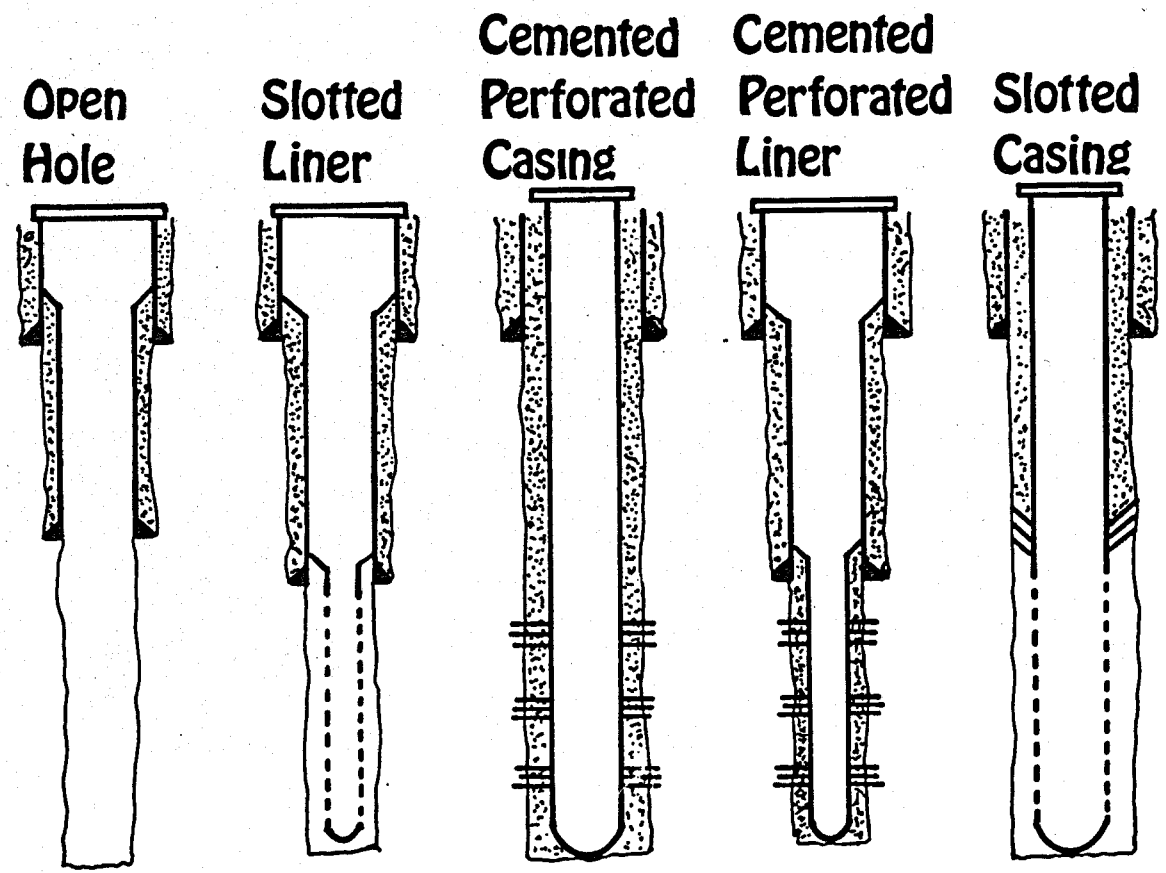

SLIDE NO. 3

METHODS FOR DOWNHOLE ZONAL ISOLATION

OPENHOLE

- PACKERS
- COMBINATION LINER AND SAND PLUG

CASING

- PACKERS
- SELECTIVE PERFORATION AND BRIDGE PLUGS

SLOTTED LINERS

- GENERALLY CANNOT BE ACCOMPLISHED EXCEPT WITH CHEMICAL OR CEMENT PLUGS

SLIDE #4

PERMANENT DRILLABLE CASING PACKER

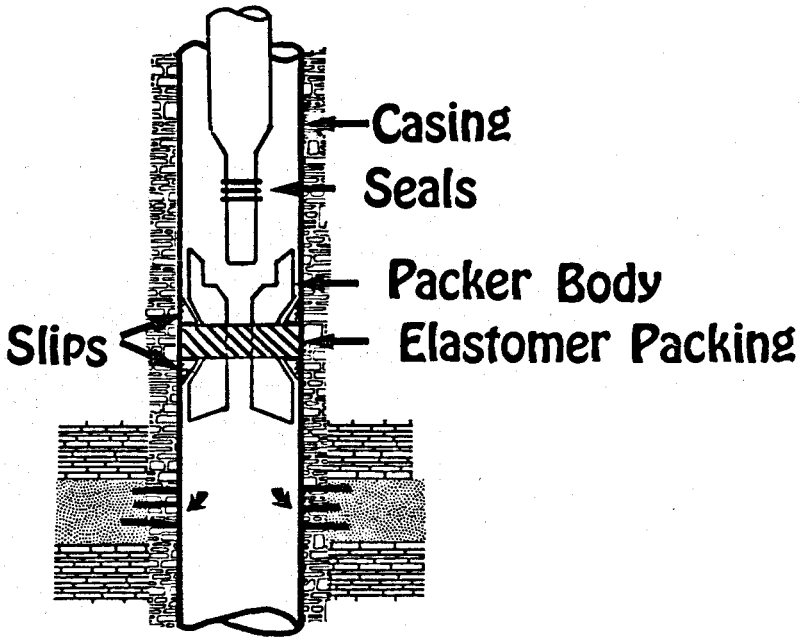

SLIDE NO. 5

CONCEPT OF
OPEN HOLE ELASTOMERIC PACKER

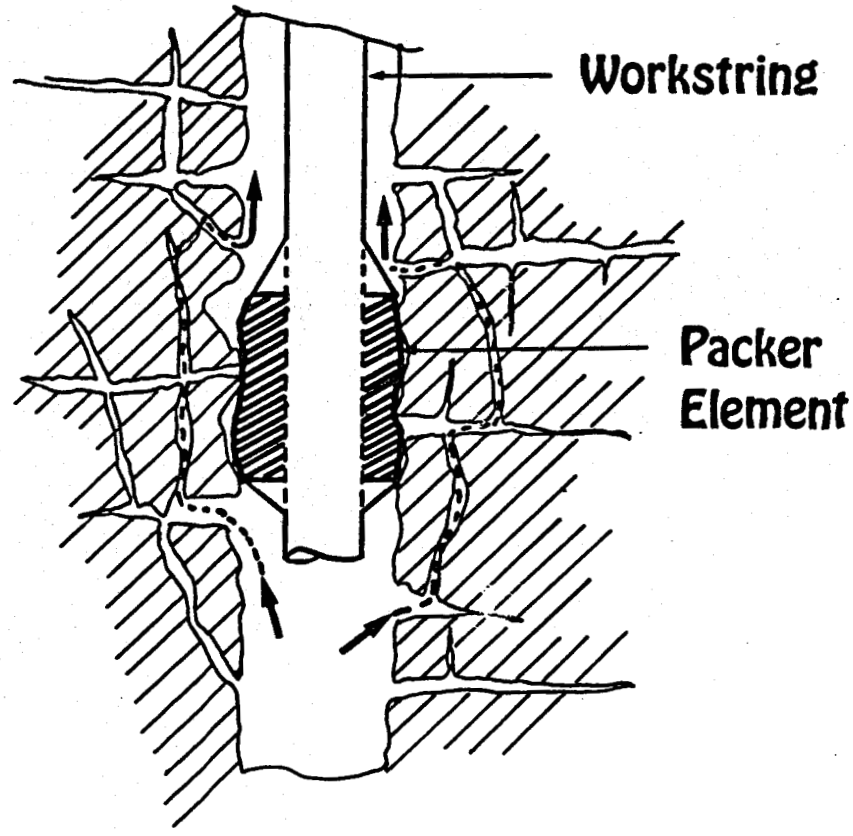

--- Fluid Bypass

SLIDE NO. 6

Zone Isolation with Liner and Sand Plug

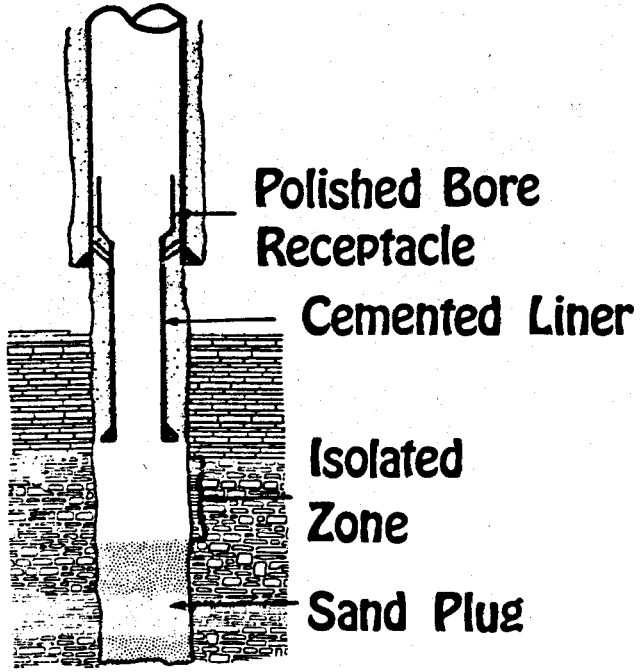

SLIDE NO. 7

SUSPECTED MAJOR FAULT PLANES WITH RESPECT TO WELL LOCATIONS

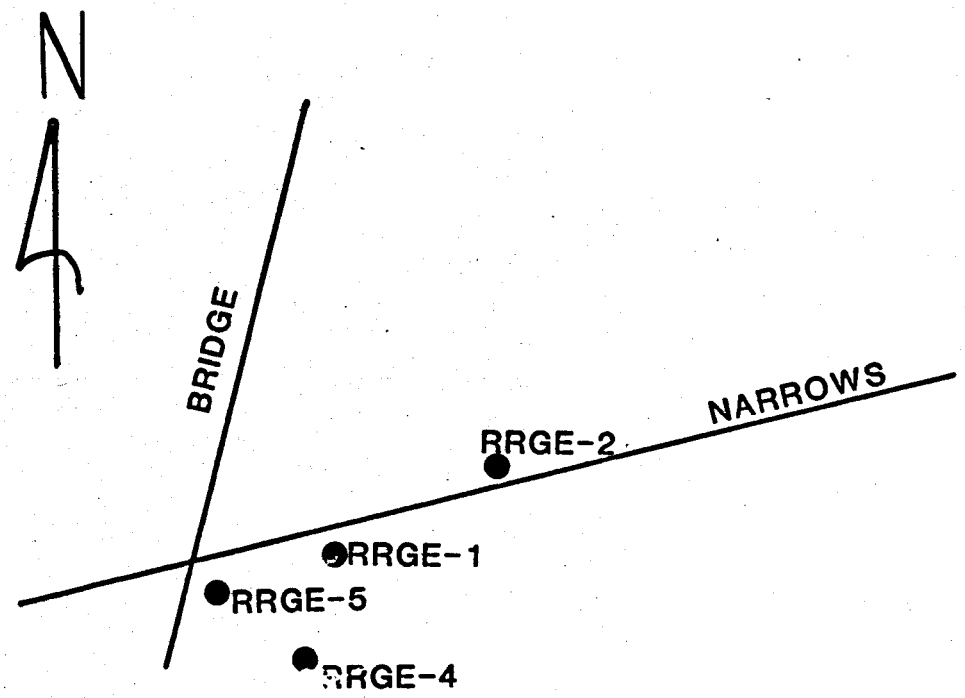

SLIDE NO. 8

OPERATIONAL CONSIDERATIONS FOR STIMULATION IN RAFT RIVER

DOWNHOLE

- ZONAL ISOLATION OF OPENHOLE COMPLETIONS
- CONTAINMENT OF "KILL" FLUIDS
- WORKING WITH THE WELL FLOWING

SURFACE

- DISPOSAL OF CONTAMINATED FLUIDS
- SAFETY WHILE WORKING WITH THE WELL FLOWING
- RA TRACER SAFETY

SLIDE NO. 9

SCHEMATIC OF RAFT RIVER RRGP 4A

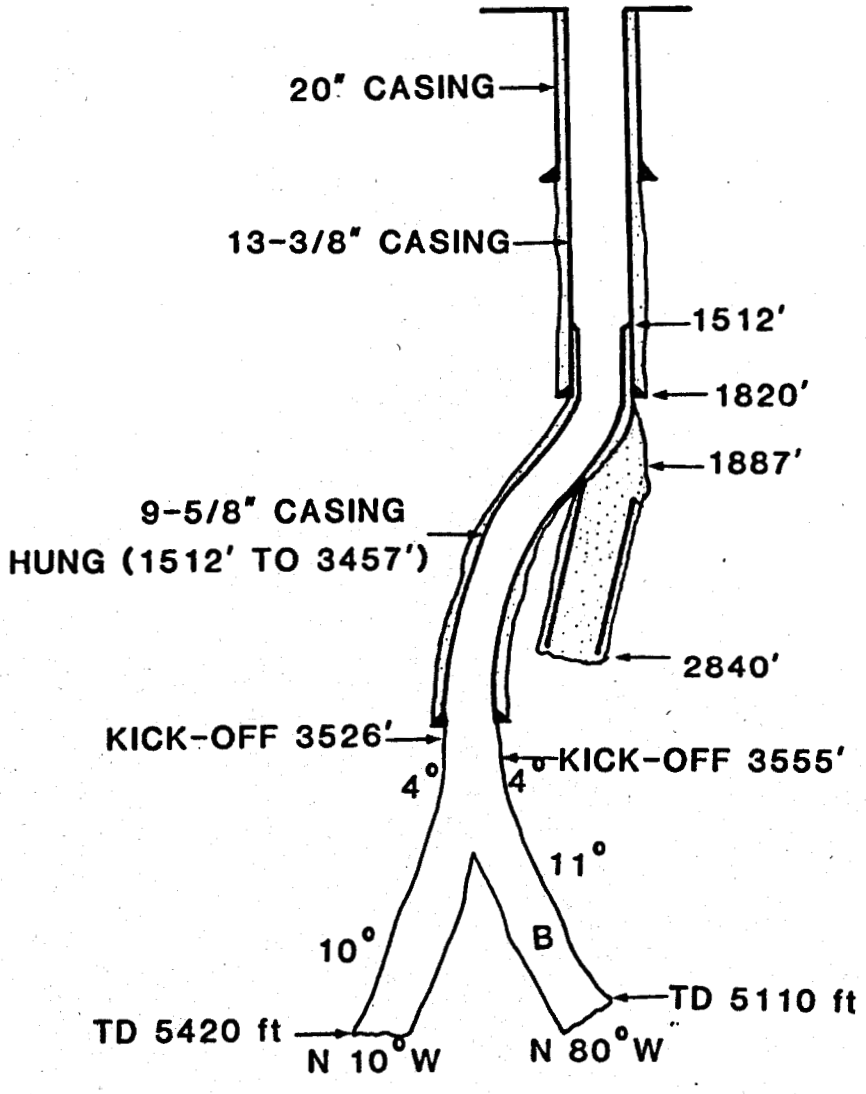

SLIDE NO. 10

RAFT RIVER WELL RRGP-4
DIRECTIONAL DRILLING SURVEY SUMMARY

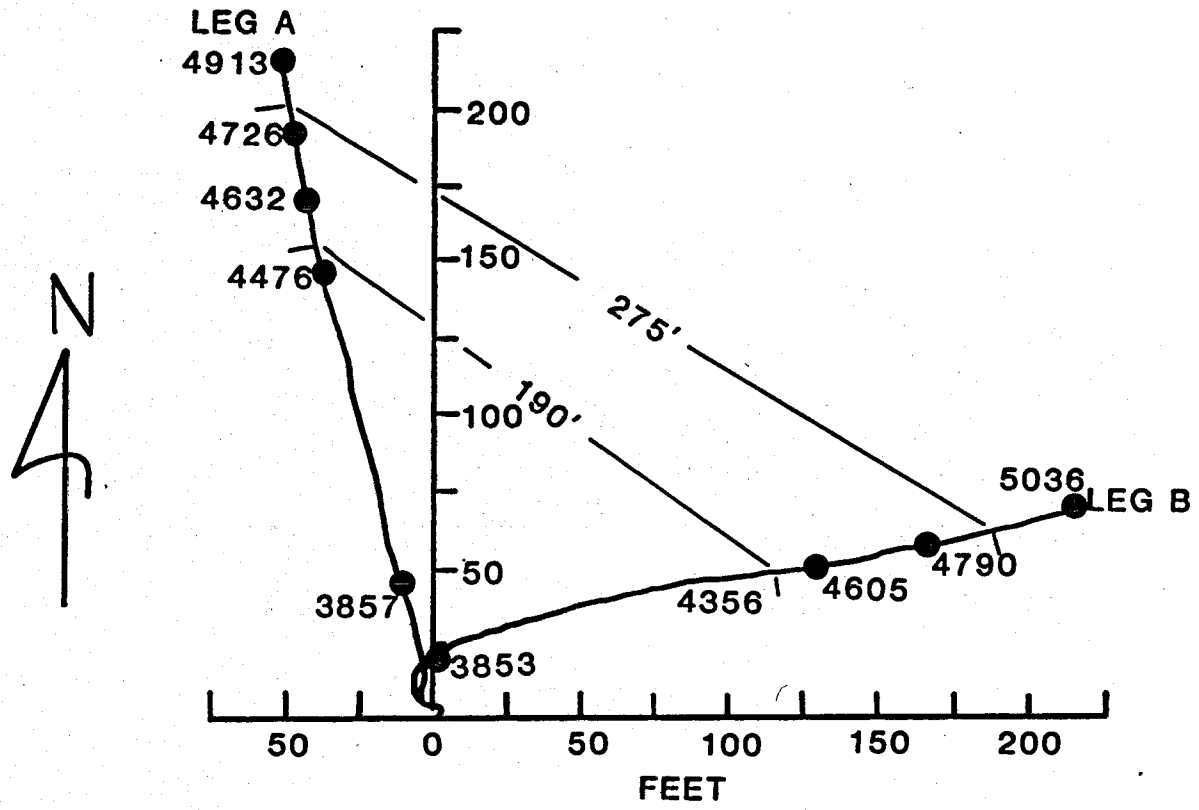

NOTE: HOLE ASSUMED VERTICAL FROM SURFACE TO 1036 M (3400 FT.)

SLIDE NO. 11

SCHEMATIC OF RAFT RIVER RRGP-4

WITH WORKSTRING AND RETRIEVABLE PACKER

PACKED-OFF IN THE 7" CASING

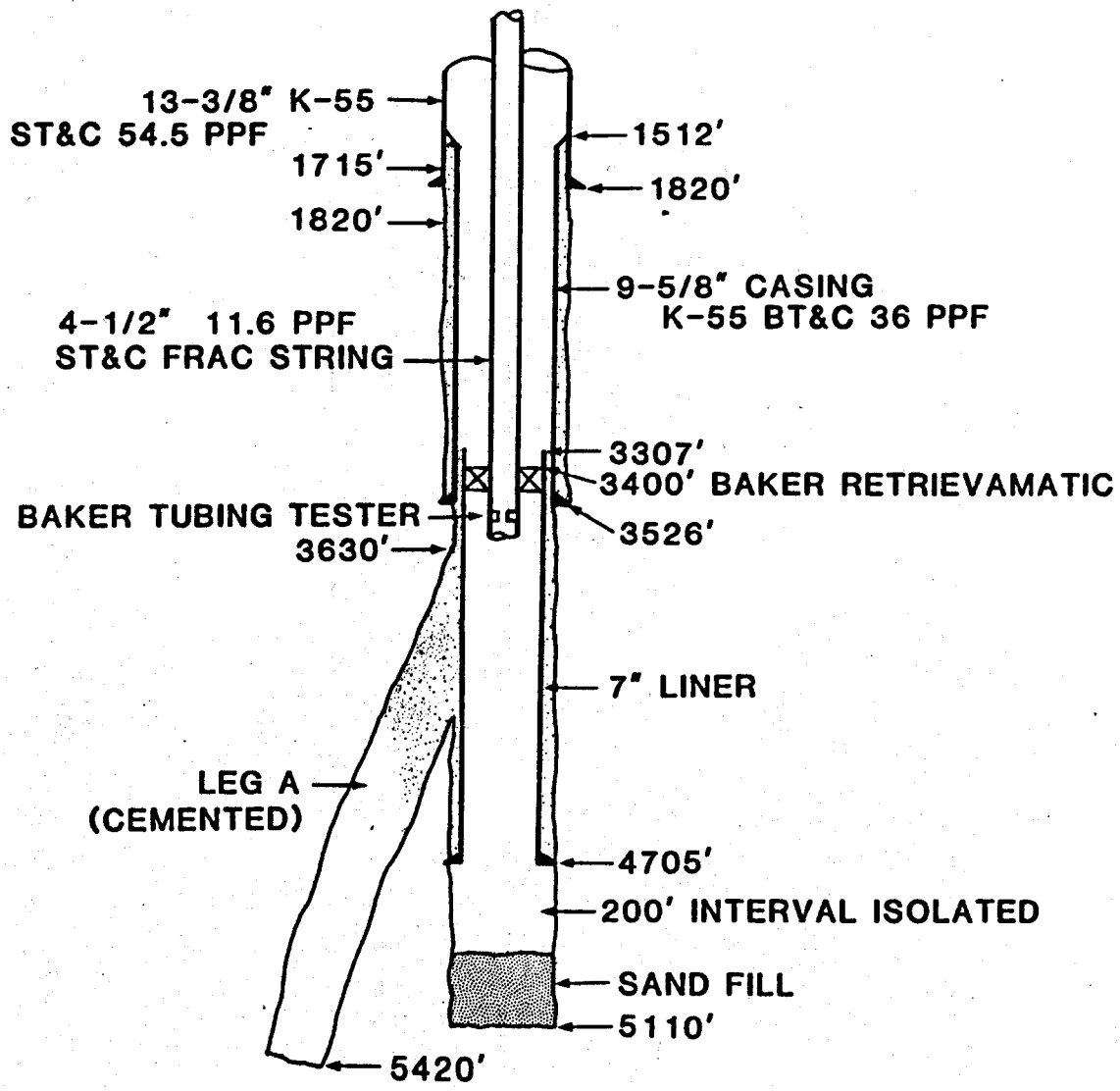

SLIDE NO. 12

SCHEMATIC OF RAFT RIVER WELL RRGP-5

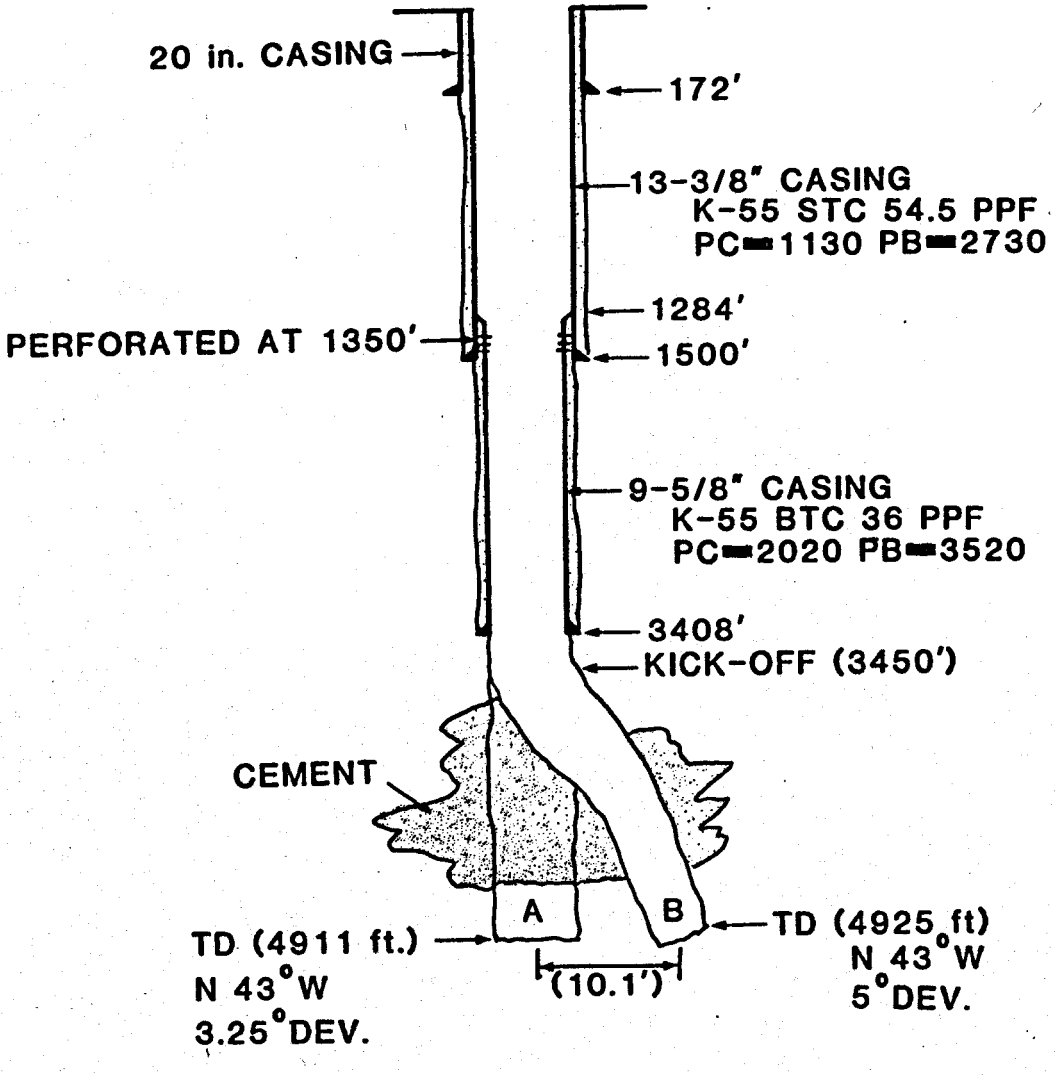

SLIDE NO.13

SCHEMATIC OF RAFT RIVER RRGP-5

WITH WORKSTRING AND RETRIEVABLE PACKER

PACKED-OFF IN THE 7" CASING

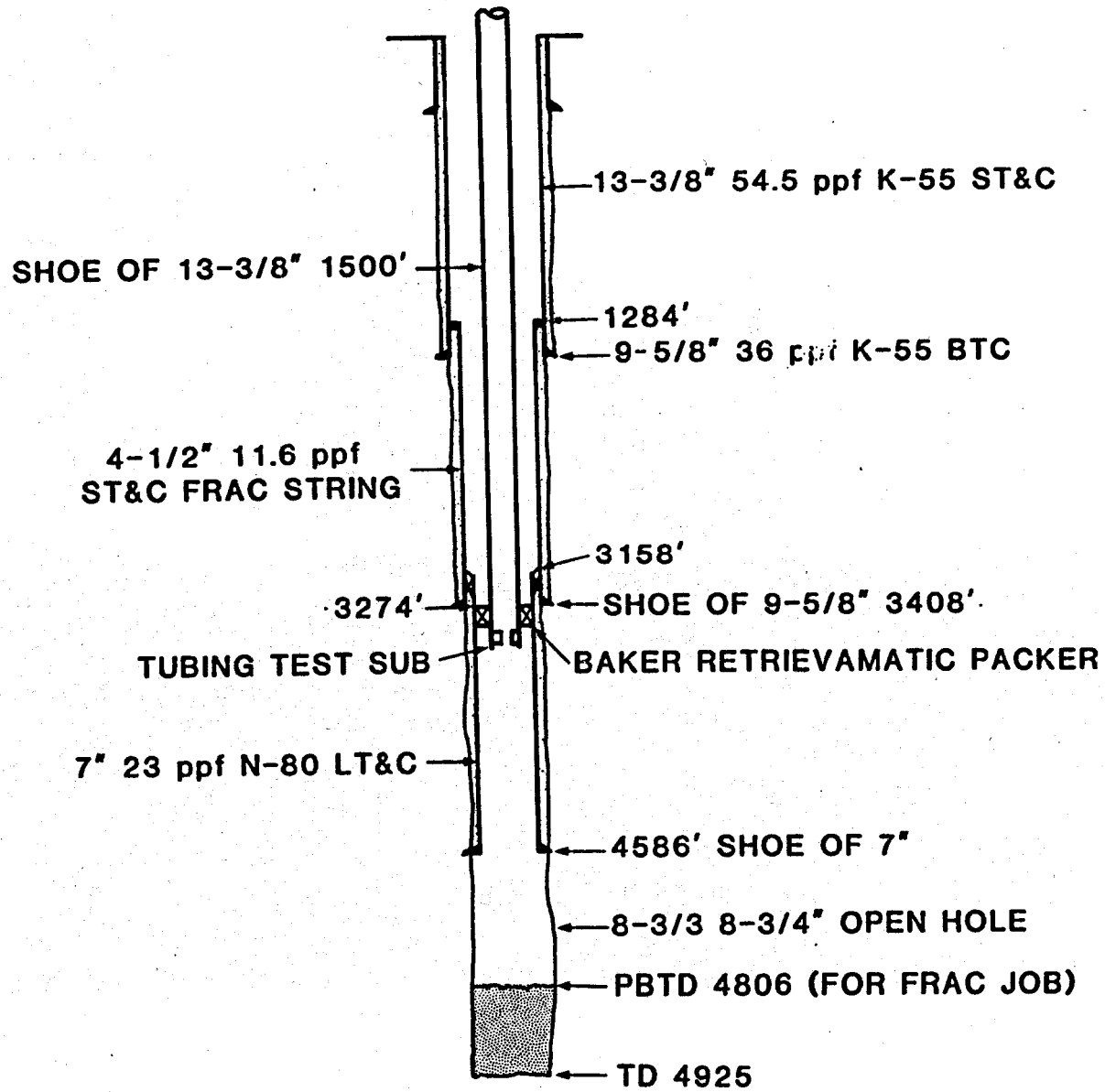

THE APPLICATION OF THE ACOUSTIC TELEVIEWER TO THE CHARACTERIZATION OF HYDRAULIC FRACTURES IN GEOTHERMAL WELLS

by

W. Scott Keys
United States Geological Survey

THE APPLICATION OF THE ACOUSTIC TELEVIEWER TO THE CHARACTERIZATION OF HYDRAULIC FRACTURES IN GEOTHERMAL WELLS

by

W. Scott Keys

ABSTRACT

Two wells in the Raft River geothermal reservoir, Idaho, were hydraulically fractured in an attempt to increase productivity. The U.S. Geological Survey made geophysical logs of these wells both before and after fracturing. A high temperature version of the acoustic televiewer was the most useful tool for obtaining data on the location, orientation, and character of the fractures produced.

In RR-4 (Raft River well 4), a hydraulic fracture was logged with the televiewer from a depth of 4,682.5 to 4,873.9 feet, a total of 191.4 feet. This fracture was largely due to the propping and possible extending of a previously logged fracture which is thought to have been accidentally induced during drilling or testing. The fracture is essentially vertical, strikes an average of N. 72 degrees E., and has an average apparent maximum width of 0.4 inch. The fracture is complex, branching, or en echelon, and in one place curves to parallel a natural fracture.

In RR-5 (Raft River well 5), a new hydraulic fracture was logged from a depth of 4,562 feet to approximately 4,705 feet, a vertical extent of approximately 143 feet. There is no evidence that this fracture follows a pre-existing break except for intervals where the orientation is affected by natural fractures. The hydraulic fracture is nearly vertical, strikes an average of N. 29 degrees E., and has an average apparent maximum width of 0.6 inch. The character of this fracture is apparently affected by a change in lithology.

The influence of natural fractures and lithology on these two hydraulically induced fractures suggests that propagation away from a well may be significantly affected by these two parameters. Consideration should be given to such effects in future fracturing. Recommendations are presented to improve the logging program for future hydraulic well stimulation efforts.

INTRODUCTION

The U.S. Geological Survey has a research program on borehole geophysics as applied to geohydrology. One of the main thrusts of this program for the past 9 years has been the development of logging equipment, and log interpretation techniques for geothermal wells. The Survey has been involved in studies of the hydrology, geology, and geophysics of the Raft River geothermal reservoir since the first shallow test holes were drilled in 1974. Experimental Geophysical well logging has been carried out by the Survey in many of the test holes and wells (Keys, 1979), and the logging described in this report is a continuation of that effort. It is also a logical extension of state of stress studies where hydraulic fracturing was carried out by the Survey (Wolff and other, 1974; and Keys and others, 1979). The logs used in this study were made by high-temperature logging equipment developed as part of the research program on borehole geophysics. Four of these probes have been tested and operated in wells at temperatures of 250 degrees to 260 degerees C., and others at temperatures of 200 degrees C.

The hydraulic fracturing of RR-4 and RR-5 (Raft River wells 4 and 5) was carried out by Republic Geothermal, Inc., under contract to D.O.E. (The Department of Energy). The wells were selected for stimulation because of their inadequate yield. Development of the Raft River geothermal field is implemented by EG&G, Idaho, Inc., under the supervision of the Idaho National Engineering Laboratory of D.O.E. (Fig. 1).

The purpose of this report is to describe the use of geophysical logs to obtain pre and post hydraulic fracture data in geothermal wells. The acoustic televiewer is the most useful device for obtaining these data and improvements were made to both equipment and interpretative techniques in order to better characterize the fractures.

Two papers presented at the Geothermal Reservoir Stimulation Symposium provide background information essential to this report. R. V. Verity of Republic Geothermal described the planning and execution of hydraulic stimulation in RR-4 and RR-5 (1980). C. W. Morris of Republic Geothermal provided an evaluation of the results of treatment (1980).

1. Fracture Characterization Using Acoustic Televiewer Logs

The acoustic televiewer was invented and patented by Mobil Oil Co. (Zemanek and others, 1969). A 1.3 megahertz transducer is rotated at three revolutions per second. The sweep on an oscilloscope is triggered on magnetic north and the amplitude of the signal reflected from the wall of the

borehole is used to intensity modulate the trace. The resulting log shows fractures as dark traces of low reflectivity, whose orientation can be calculated. The U.S. Geological Survey and Simplec Manufacturing, Inc., have cooperated to develop the first high temperature version of this useful probe. It has been used at borehole temperatures of 261 degrees C. A system for recording the televiewer signal on magnetic tape was put into use for the first time on RR-5. Playback of these data provided the opportunity to improve the quality of the televiewer logs (Fig.2).

It would appear that the width of a hydraulic fracture may be measured directly from an acoustic televiewer log, but relative width may only be inferred with significant qualifications. Therefore, the maximum apparent widths listed in tables 1 and 2 should be used with caution. The televiewer log only detects changes in acoustic reflectivity at the face of the borehole. If the edge or angle of intersection of fracture and borehole wall is broken out this surface will not reflect high frequency energy back to the transducer, and the apparent width of the fracture will increase. The most accurate measurement of fracture width can therefore be made where the angle of intersection with the borehole is approximately 90 degrees.

This only occurs where a vertical fracture passes through the center of the borehole. As the fracture approaches a tangential relationship with the borehole the angles of intersection become more obtuse and acute, and the likelihood of the acute edge breaking off is increased (Fig. 3). Furthermore, there is an apparent geometric widening and the obtuse angle does not provide a sharp contact on the log. Figure 3 shows an interval of RR-5 from 4,635 to 4,640 feet that clearly demonstrates this problem. The drawings in figure 3 shows how this portion of the fracture might look in vertical view. Therefore, for the reasons described above, the fractures are likely to be narrower than measurements made from acoustic televiewer logs. The width measurements listed in tables 1 and 2 were made with an optical micrometer and corrected for scale.

The output from an acoustic televiewer probe can also be used to record acoustic caliper logs. The transit time of the acoustic pulse is recorded rather than amplitude of reflected signal. This approach should provide an extremely high resolution log of hole diameter. Furthermore, the signal can be sampled in four directions, NESW, to produce four oriented caliper logs. Recordng the probe output on magnetic tape permits acoustic caliper logs to be plotted after returning to the office. Examples of these logs are shown in the section on RR-5.

All orientations are with respect to magnetic north and

all depths are measured along the inclined borehole from ground level. Corrections of strike and dip for true north, hole inclination, and magnetic declination remain to be done in the computer for the hundreds of natural fractures logged with the televiewer at Raft River. These corrections will then yield the true vertical and horizontal positions, and orientations so that a three dimensional fracture model of the reservoir can be constructed.

2. Selection of Intervals to be Fractured

Data from U.S. Geological Survey logs were made available to D.O.E. and EG&G for the selection of intervals to be fractured in RR-4 and RR-5. Geophysical well logs were utilized to a degree in the selection of the depth intervals to be isolated for pressurization. Gamma, neutron, and resistivity logs distinguish Precambrian schist and quartzite from overlying Tertiary sediments and underlying Precambrian quartz monzonite (Keys, 1979). The depth intervals to be fractured were selected in the metamorphic rock sequence above the quartz monzonite for several reasons. Steep natural fractures that produce significant quantities of hot water occur within this interval in other wells.

Acoustic televiewer logs indicate that fewer open fractures are present in the quartz monzonite. Production water of highest possible temperature was desired, which suggested deep, rather than shallow, fracturing. Logs indicated the presence of open fractures within the intervals selected; however, the low specific yields suggested that these fractures were either not interconnected or they had somehow been plugged. It was definitely important, however, to set the liner below the large open fracture recognized on the televiewer log at a depth of 4,540 to 4,550 feet in RR-5. Nuclear and resistivity logs indicated the presence of both quartzite and schist in the intervals to be fractured. This provided the opportunity to study the behavior of hydraulic fractures in both rock types.

With the advent of the acoustic televiewer it became possible to detect hydraulic fractures accidentally induced by overpressure during drilling (Zemanek and others, 1969). It has also been shown that fracturing is possible at wellbore-face pressures considerably less than the overburden pressure which can be assumed to be 1.0 lb/in**2/ft of depth (Wolff and others, 1975). Some measurements of least principal stress were approximately one-half the assumed overburden pressure. A column of water will produce approximately 0.5 lb/in**2/ft of depth so a column of heavy drilling mud, cement, or pumping or injection pressures may be sufficient to break the rock.

Once it is broken the fracture will continue to

propagate at somewhat lower pressures. Televiewer logs indicate that accidentally induced hydraulic fractures may be more common in oil wells than previously supposed (Zemanek and others, 1970). Drilling induced hydraulic fractures have the same character on televiewer logs as those produced by intentional overpressure. The most diagnostic characteristics of hydraulic fractures are: vertical or follow well bore for many feet, irregular or branching trace and variable width.

Information from acoustic televiewer logs suggested that an accidentally induced hydraulic fracture might already be present in the interval selected in RR-4. Possibly these data should have received more consideration in the selection of an interval to be fractured. A newly induced hydraulic fracture in a different interval would probably have had the same orientation, however. It would be interesting to examine records of operations in RR-4 to determine how this fracture might have been produced.

3. Raft River Well 4

In written communications to the Department of Energy, dated June 1, 1979, the author noted the presence of complex vertical fractures that appeared to be hydraulically induced in RR-4. These fractures appear on the U.S. Geological Survey televiewer log made in March 1979. It is not known at what stage during drilling, reaming, and testing that overpressure may have occurred, but similar fractures that appear to be hydraulically induced have been seen on televiewer logs of other geothermal wells at Raft River, Idaho, and Roosevelt Hot Springs, Utah (Keys, 1979).

The acoustic caliper log indicates that the RR-4 well bore is not round in much of the interval isolated for hydraulic fracturing. Combined with the deviated hole, this accounts for the poor quality of the televiewer log, because the probe must be centered for best results. This problem is particularly severe from the bottom of the liner to a depth of 4,743.5 feet, and accounts for some of the difficulty in locating the fracture on both sides of the hole.

Acoustic televiewer, acoustic caliper, and mechanical caliper logs of RR-4 made prior to hydraulic fracturing substantiate the presence of the vertical fractures to the west (Fig. 4), and indicate that these fractures have a depth of several inches. Although it is possible that these pre-existing fractures are natural in origin, the irregularity of branching and relatively consistent strike over such a great depth interval suggest they are hydraulically induced.

The pre-existing hydraulic fracture system can be traced from the bottom of the liner at 4,682.5 to 4,873.9

feet. The earlier fracture is only visible on the March televiewer logs in the west quadrant of the hole, but this may be due to better acoustic reflection in that direction. The postfracturing logs made in August indicate widening or propping of the fracture to the west, and a detectable fracture in most intervals to the east. Fractures are propped open by the injection of large quantities of sand after the rock is broken hydraulically. The propped fracture follows branches or en echelon traces of the previous fracture, particularly well demonstrated in the interval 4,769 to 4,780 feet (Fig. 5). The hydraulically widened and propped fracture is detectable on the August 1979 acoustic televiewer log from the bottom of the liner at 4,682.5 feet to the top of sand fill up in the hole at 4,873.9 feet. The presence of vertical fractures to a depth of approximately 4,980 feet on the March televiewer log suggests that the widened fracture may extend to at least the sand level that existed prior to pressurization. Thus, the fracture that was expanded and probably extended during intentional hydraulic fracturing, is semicontinuous for at least 191.4 feet along the axis of the well. The well deviates 10.5 degrees from the vertical in the direction N. 80 degrees E. (Miller and Prestwich, 1979).

The hydraulic fracture logged in March appears to extend above the bottom of the liner to a depth of approximately 4,664 feet. This is just below a major open fracture in the schist which has a low angle dip to the southeast. Thus, it appears that the most significant part of the hydraulically-induced fracture may have been limited in upward extent by a natural fracture. Table 1 is a compilation of data and descriptions of the propped hydraulic fracture in RR-4.

The average strike of the nearly vertical hydraulic fracture is N. 72 degrees E. which has been corrected to true north and is shown as a line through RR-4 in Figure 1. Most of the natural fractures in well RR-4 dip from 12 degrees to 50 degrees to the southwest and strike averages N. 45 degrees W. At least one fracture in the pressurized zone is thought to be natural; at 4,820 to 4,822 feet a fracture dips 75 degrees to the north and strikes N. 60 degrees E. (Fig. 6).

It is possible that some of the other pre-existing vertical fractures in the pressurized interval are natural, but that seems unlikely because they follow the well for such a great distance, have the irregular character of hydraulic fractures, and are subparallel and similar to the intentionally produced hydraulic fracture in well RR-5. Furthermore, there are vertical fractures in well RR-2 below 5,000 feet that strike northeast, and have an appearance similar to unpropped hydrofractures.

In areas and at depths where the least principal stress is less than overburden stress, hydraulically induced fractures can be expected to be vertical. In areas of low topographic relief and at sufficient depth, the maximum compressive stress is vertical and the least and intermediate stresses are in the horizontal plane. The depth intervals of the wells intentionally fractured at Raft River are 10.5 degrees and 5 degrees from vertical and this fact, along with interruption of fracture propagation by natural fractures and lithology changes, may encourage the production of complex rather than simple planar fractures.

Most hydraulic fractures logged by the U.S. Geological Survey tend to branch, curve, and split, rather than propagate as simple planar features geologists are used to seeing in outcrop or in core. Actually, these complex characteristics are typical of some hydraulic fractures, produced by pressurizing drill holes, that have been exposed by mining at the Nevada Test Site (Northrup and others, 1978).

The unique opportunity to examine these fractures has proven helpful in the interpretation of televiewer logs. Figure 7 is a photograph of a neat-cement-filled hydraulic fracture exhibiting some of the curving and branching characteristics of the fractures induced at Raft River. The width of this vertical fracture averages 0.1 inch in the sample of tuff illustrated, the same order of magnitude of the hydraulic fractures in RR-4 and RR-5.

4. Raft River Well 5

A new fracture was intentionally produced by pressurization and propping with sand in RR-5. A 200-foot stimulation interval was isolated by a packer set in a cemented liner and sand-filled hole. The fracture is clearly defined on televiewer logs from the bottom of the liner at 4,562 feet to a major natural fracture system at a depth of approximately 4,690 feet (Fig. 8). A relatively tight extension of the hydraulic fracture is poorly defined below the natural fractures to a depth of approximately 4,705 feet, which gives a vertical length of 143 feet. The hydraulic fracture is approximately parallel to leg B of RR-5 which is deviated 5 degrees to 5 1/4 degrees from vertical in a direction N. 56 degrees to 59 degrees S. (Miller and Prestwich, 1979). Therefore, it is nearly vertical. The average strike is N. 29 degrees E., but the fracture curves considerably.

Figure 9 is a tracing of the fractures described from a taped televiewer log, played back at a compressed scale. The scale ratio tends to exaggerate curvature, but it does show the complexity of the hydraulic fracture. The apparent maximum fracture width from the acoustic televiewer log

averaged 0.6 inch. The absolute value of the width is not so meaningful as the relative widths as a function of depth (Table 2). Furthermore, it is likely that the fracture in RR-5 is wider than the fracture in RR-4.

If the lithology is simlar, which appears likely, then the difference in width may be related to fracturing or propping procedures. Test data show that more than four times as much sand was used in propping RR-5 than was used in RR-4, which apparently produced a wider fracture. Furthermore, pumping tests are not complete, but it appears that production may be greater from RR-5.

Figure 10 shows an acoustic caliper log of the depth interval of RR-5 from 4,585 to 4,590 feet compared with an acoustic televiewer log. The caliper was calibrated as shown with a 2-inch change in well diameter equal to a 1-inch change on the radius from the transducer. Note the correspondence between the oriented caliper traces and the televiewer log at the same azimuth. The caliper traces would suggest fracture depths greater than one inch; however, this may be misleading because of the unknown acoustic reflectivity of the epoxy sand used for propping.

Figure 11 shows another type of acoustic caliper presentation for the depth interval 4,665 to 4,670 feet. The X axis still represents a single-transducer sweep around the hole, but the Y axis represents changes in hole diameter or transit time. The eccentricity of the probe or well can be seen along with the two fracture traces. This caliper presentation suggests that fracture widths measured from the televiewer log may be too great.

The hydraulic fracture in RR-5 does not always pass through the center of the well bore. Further, it has a very irregular trace which indicates a varying strike. From a depth of 4,563 to 4,570 feet, the hydraulic fracture is nearly parallel to a pre-existing vertical fracture which is probably natural. There is no strong evidence of a pre-existing hydraulic fracture in RR-5 as was found in RR-4.

There is a significant change in the apparent character of the fracture and direction of strike at a depth of 4,652.6 feet (Fig. 12). This may be primarily due to a change in lithology. Although the interval fractured has been described on the basis of cuttings as all quartzite with minor amounts of feldspar and muscovite, geophysical logs suggest more significant changes in lithology. The natural gamma log indicates that the quartzite may contain layers of schist, possibly biotite. A change in lithology is indicated by several logs at approximately 4,650 feet, which is close to the depth where hole diameter and character of the postfracturing televiewer log changes. A decrease in radioactivity below this depth suggests an

increase in the percentage of quartzite. If this interpretation is correct, then the hydraulic fracture as seen in Figure 12, is better developed in quartzite than in schist.

If measurements of hole deviation are correct, then a northeast-striking, vertical, hydraulic fracture should have intersected leg A of RR-5 in the vicinity of a production zone which was reported to have yielded 1,000 gal/min (Miller and Prestwich, 1979). Unfortunately, this fracture was apparently cemented up so the hydraulic fracture may have intersected cement rather than a producing zone. Cement may have also limited the lateral propagation of the fracture. The hydraulic fracture was also probably limited in vertical propagation between natural fractures at 4,535 to 4,540 feet and 4,690 feet. These major natural fractures are essentially parallel with a dip of 80 degrees with respect to the hole and a strike of N. 20 degrees W. to N. 40 degrees E. The shallower of these two fractures appeared on gamma-gamma, acoustic velocity, neutron, caliper, and acoustic televiewer logs as a major open fracture zone which should have produced significant amounts of water. Production was minimal, and may have been drastically reduced by cement invasion.

The average strike of the hydraulic fracture in RR-5 corrected to true north is shown by a line through the well on Figure 1. The average strike of N. 29 degrees E. appears to be significantly different than the N. 72 degrees E. average strike in RR-4. The averaging technique for such a complex surface may produce an error; however, it is important to note that the hydraulic fractures are subparallels to major faults postulated in the area (Williams and others, 1976). RR-5 is closer to the Bridge fault which trends slightly east of north, and RR-4 is closer to the Narrows structure which trends east-northeast. In many areas, hydraulic fractures have been found to parallel major structures (Wolff and others, 1974). If this is the case at Raft River, then hydraulic fractures may parallel rather than intersect major structures that are probably conduits for the movement of hot water.

5. Recommendations

As a result of this study, a number of suggestions can be made to improve the cost benefit ratio for utilizing borehole geophysics in hydraulic fracturing programs. Well logging can be more beneficial to planning a hydrofracture and understanding the results.

Better results from logging and fracturing in general might be obtained if the interval of the well selected was near vertical rather than deviated. The televiewer can be better centered in a vertical hole, but even more important,

the hole is more likely to be perpendicular to the direction of least principal stress. This may tend to produce a fracture with a more uniform trace that does not change direction away from the well. Under these conditions measurements of fracture orientation in the well are more likely to be related to average orientation. The prefracture logs should be considered carefully from the standpoint of existing fractures or lithologic contacts that may affect the extent and direction of propagation of a hydraulic fracture. Further, favored directions of natural fractures may be followed by induced fractures; that is, the stress field may have the same orientation at the time of hydraulic fracturing as it did when natural fractures were produced. These factors may tend to influence fracture propagation parallel to a producing structure rather than towards it.

After the depth interval to be fractured has been selected, but before pressurizing, a complete suite of porosity sensing logs should be run on a high resolution scale. These can then be compared to the same kind of postfracture logs in an attempt to detect changes in porosity. Resistivity devices, such as micro guard and dipmeter, might be particularly useful. Before and after acoustic waveform logs would improve the understanding of the response of these logs to vertical fractures. A prefracture rerun with the televiewer should be made with maximum attention to log resolution.

Postfracture logging would be greatly enhanced by assuring that the well is clean and free of sand to the bottom. Successive depth measurements may be necessary to determine that no propping agent or other material is entering to fill the well. Under these conditions, it should be possible to determine the lower limit of crack propagation. It would be extremely useful if the well could be made available for temperature and flowmeter logs during postfracture testing. It is very important to determine which part of a fracture is producing and possibly why. An attempt should be made to determine if the apparent fracture width on a televiewer log is related to productivity as our preliminary data suggest.

It has been reported that RR-5 is continuing to produce propping sand. If the pump is pulled to clean out the hole then a third televiewer log should be run in order to determine if intervals of sand loss can be detected and what effect this has on apparent fracture width.

6. Selected References

1 Keys, W. Scott, 1979:
Borehole geophysics in ingeous and metamorphic rocks: Society of Professional Well Log Analysts, 20th Annual Logging Symposium, Tulsa, Okla., June, 26 p.

2 Keys, W. Scott, and Sullivan, James K., 1979:
Role of borehole geophysics in defining the physical characteristics of the Raft River Geothermal Reservoir, Idaho: Geophysics, v. 84, no. 6, p. 1116-1141.

3 Keys, W. S., Wolff, R. G., Bredehoeft, J. D., Shuter, Eugene, and Healy, J. H., 1979:
In-situ stress measurements near the San Andreas Fault in central California: Journal of Geophysical Research, v. 84, no. B4, p. 1583-1591.

4 Miller, L. G., and Prestwich, S. M., 1979:
Completion report: Raft River geothermal production well four: Idaho Operations Office Report 10081 RRGP 4, February, 20 p.

5 -----1979:
Completion report: Raft River geothermal production well five: Idaho Operations Office Report 10082 RRGP 5, February, 19 p.

6 Morris, C. W., 1930:
Raft River stimulation treatment results: Proceedings of the Geothermal Reservoir Well Stimulation Symposium, San Francisco, Calif., February 1930

7 Northrup, D. A., Warpinski8, M. R., Schmidt, R. A., and Smith, C. W., 1978:
Stimulation and Mineback Experiment Project--the direct observation of hydraulic and explosive tests: 2nd Annual Eastern Gas Shales Symposium Tulsa, Okla., October, p. 291-302.

8 Verity, R. V., 1980:
Planning and execution of the Raft River stimulation treatment: Proceedings of the Geothermal Reservoir Well Stimulation Symposium, San Francisco, Calif., February 1980.

9 Williams, P. L., Mabey, D. R., Zohdy, A. R., Ackermann, Hans, Hoover, D. B., Pierce, K. L., and Oriel, S. S., 1976:
Geology and geophysics of the Southern Raft River Valley geothermal area, Idaho, U.S.A.: 2nd United Nations Symposium on the Development and Use of Geothermal Resources, Proceedings, San Francisco, Calif., v. 2, p. 1273-1282.

10 Wolff, R. G., Bredehoeft, J. D., Keys, W. Scott, and Shuter, Eugene, 1974:
Tectonic stress determinations, Northern Piceance Creek Basin, Colorado: Rocky Mountain Association of Geologists--1974 Guidebook, p. 193-198.

11 Zemanek, Joseph, Caldwell, R. L., Glenn, E. E. Jr., Holcomb, S. V., Norton, L. J., and Straus, A. J. D., 1969:
The borehole televiewer--a new concept for fracture location and other types of borehole inspection: Journal of Petroleum Technology, v. 21, p. 762-774.

12 Zemanek, Jodeph, Glenn, E. E., Norton, L. J., and Caldwell, R. L. 1970:
Formation evaluation by inspection with the borehole televiewer: Geophysics, v. 35, no. 2, p. 254-269.

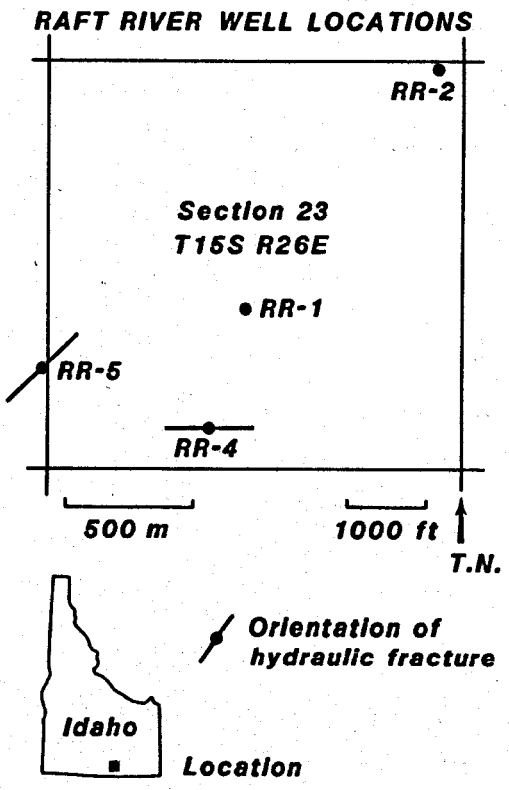

Figure 1 -- Well location map showing average strike of hydraulic fractures.

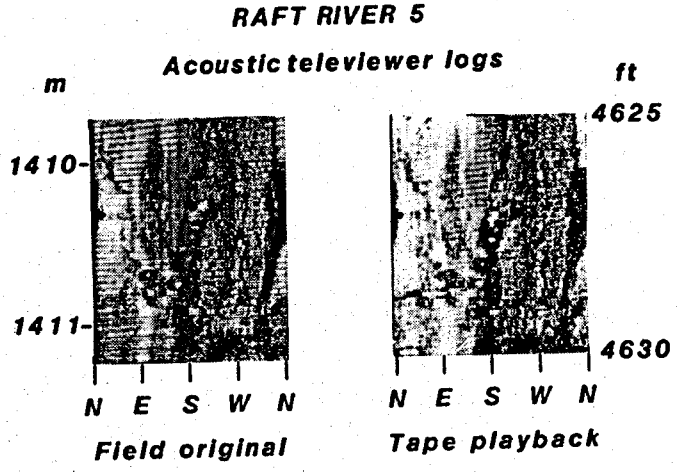

Figure 2 -- Comparison of field log and tape playback log of hydraulic fracture in RR-5.

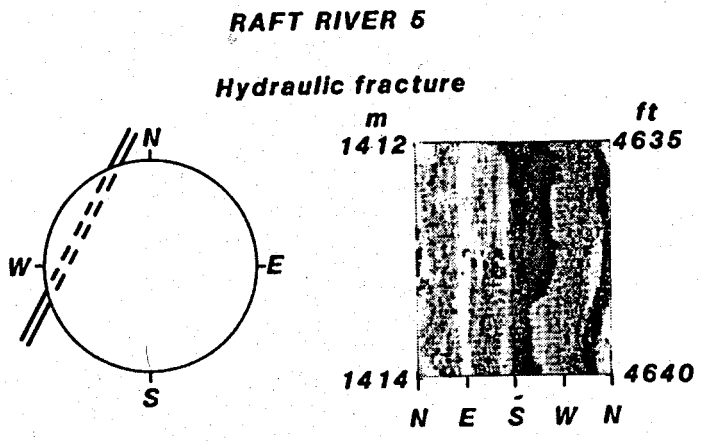

Figure 3 -- Vertical view and televiewer log of hydraulic fracture in RR-5.

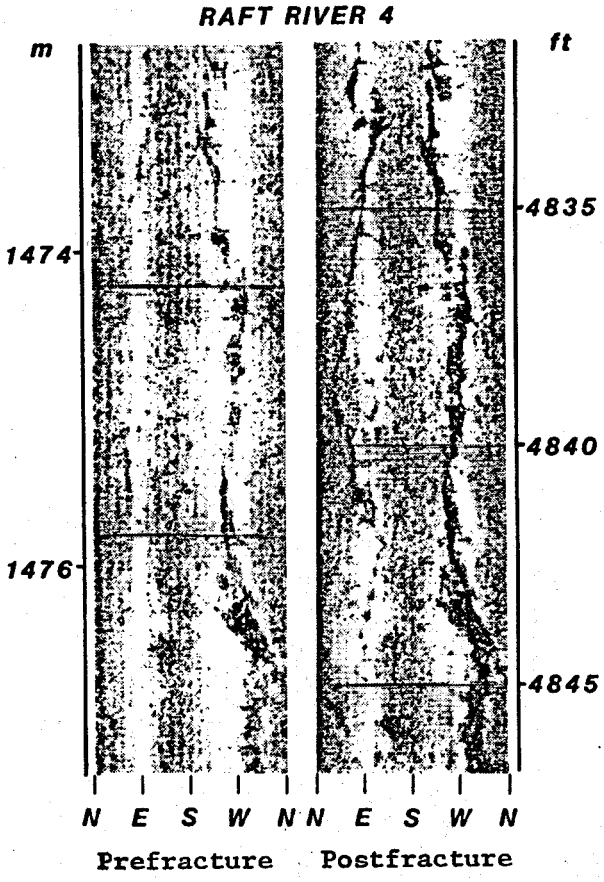

Figure 4 -- Preexisting and propped hydraulic fracture in RR-4.

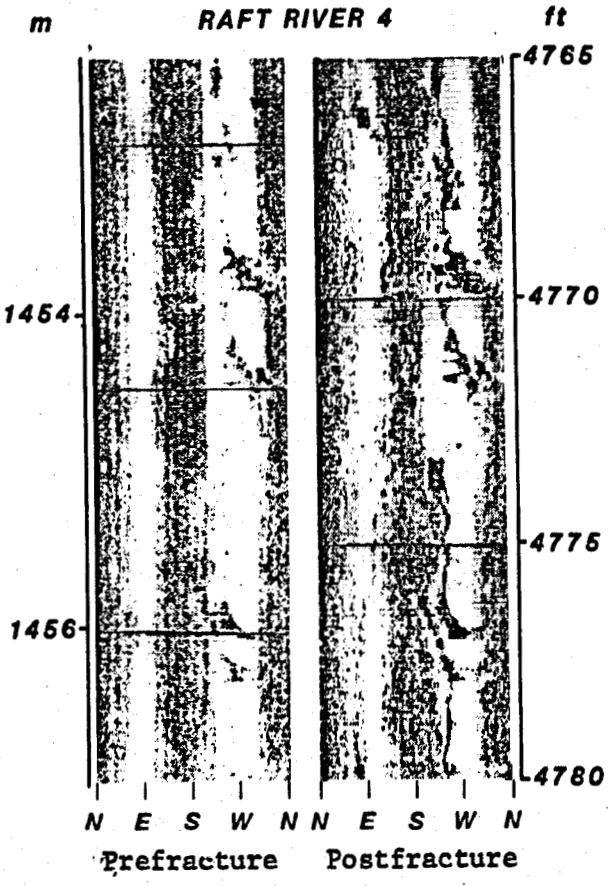

Figure 5 -- Complex preexisting and propped hydraulic fracture in RR-4.

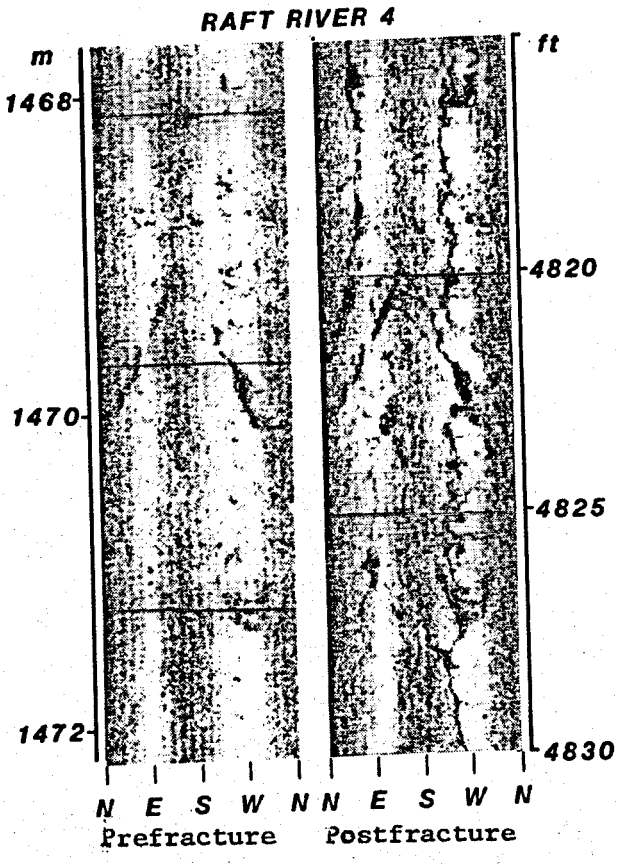

Figure 6 -- Natural fracture in RR-4 causing change in orientation of hydraulic fracture.

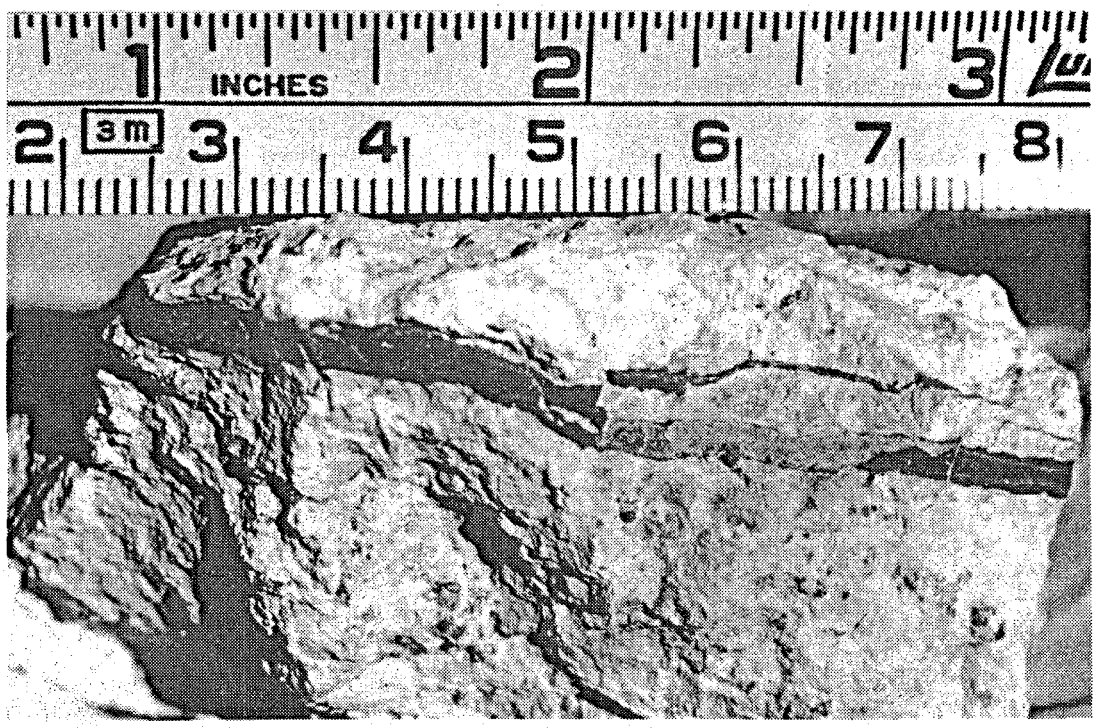

Figure 7 -- Cement-filled hydraulic fracture in tuff from Nevada Test Site.

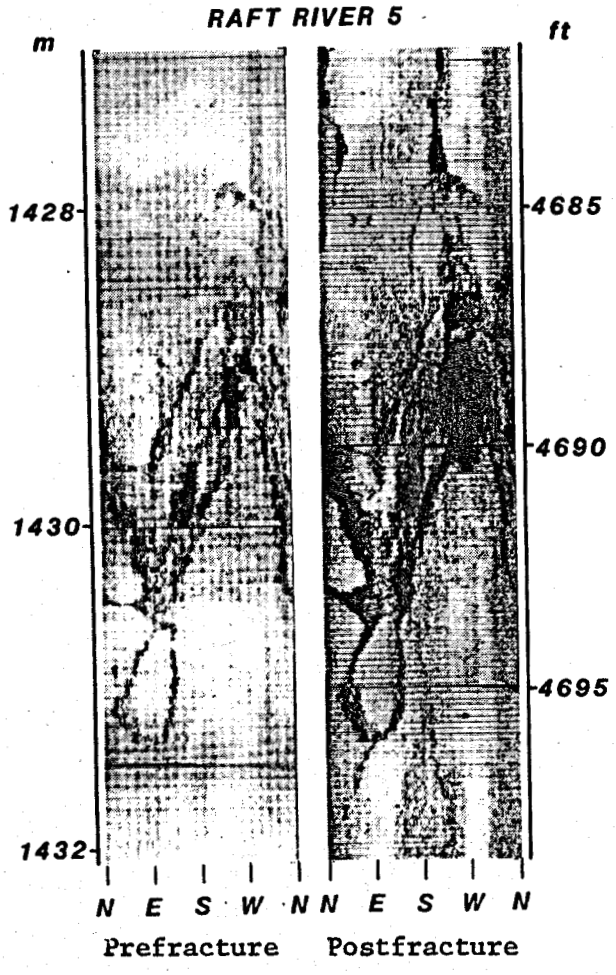

Figure 8 -- Natural fracture system in RR-5 which terminates open interval of hydraulic fracture.

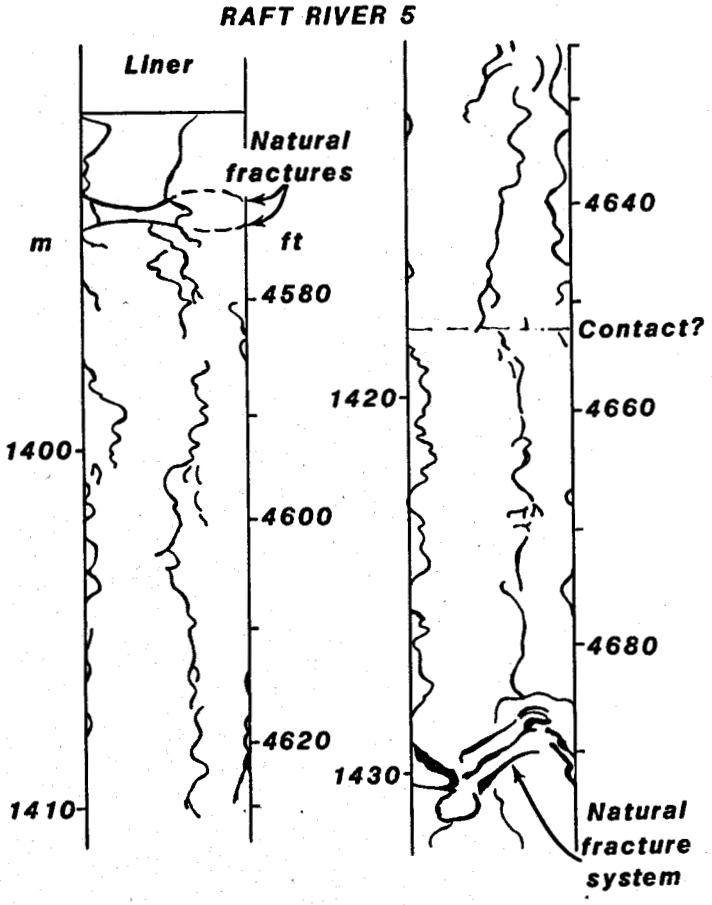

Figure 9 -- Drawing of hydraulic fracture in RR-5 traced from televiewer log.

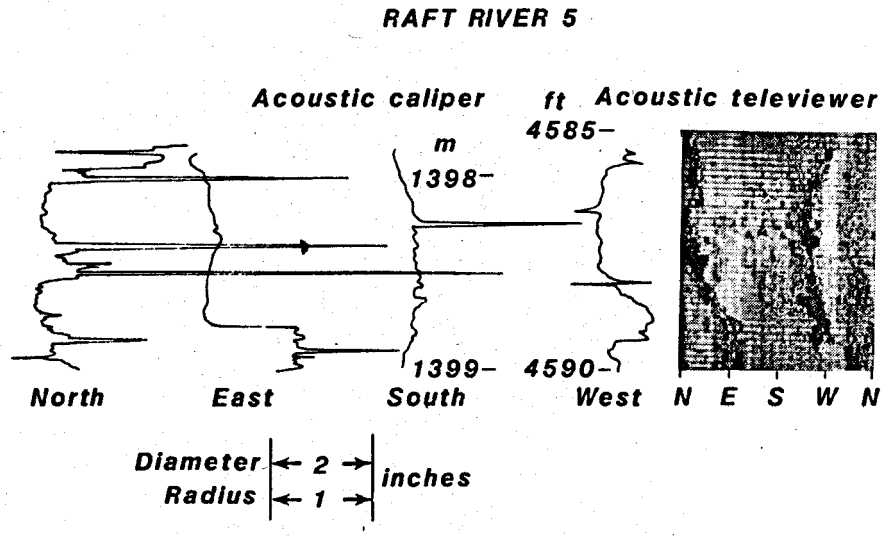

Figure 10 -- Acoustic caliper and acoustic televiewer logs, RR-5.

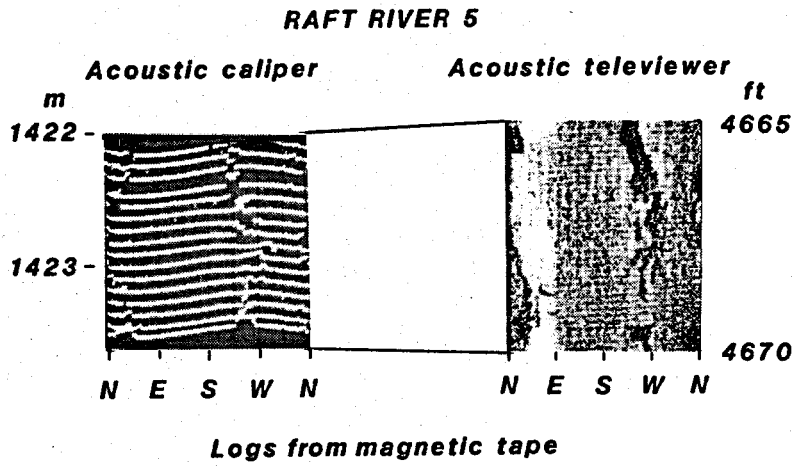

Figure 11 -- Oscilloscope display of acoustic caliper traces compared with televiewer log of same depth interval in RR-5.

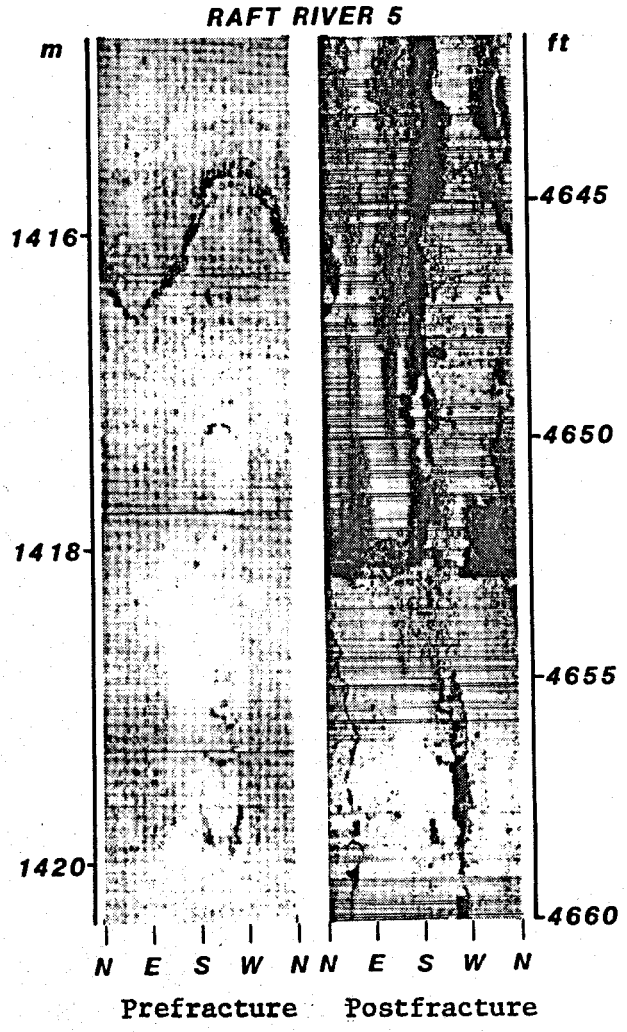

Figure 12 -- Prefracture and postfracture acoustic televiewer logs of RR-5 showing change in character at 4,652 feet.

Table 1

Raft River Well 4

Hydraulic Fracture

DEPTH (feet)	STRIKE (Mag. N) (uncorrected for hole deviation)	APPARENT MAXIMUM WIDTH (inches)	CHARACTER OF THE VERTICAL HYDRAULIC FRACTURE
4682.5-4688	--------	unknown	Poorly defined from bottom of liner at 4682.5 ft to 4688 ft.
4688-4703	N70 to 75E	unknown	Fracture better defined. Parallel to preexisting hydraulic fracture to the west.
4703-4715	N60E to N80E	.7 to 1.1	Still better defined, curving, off-center, best defined to the east.
4715-4743.5	N65E to N75W	unknown	Poorly defined but present. Irregular, well badly out of round. Follows preexisting fracture.
4743.5-4750	N50E to E-W	.3 to 1.1	Better defined. Well rounder. Curving preexisting fracture to west widened.
4750-4769	N65 to 70E	.3 to 1.4 Av. .7	Well defined, best to west. Preexisting fracture widened.
4769-4800	N80E	.1	Branching or en echelon, complex, broken out in spots. Follows older fracture.
4800-4820	N70E	.1 to .3	Well defined, broken out in spots. Older fracture poorly defined or not present.
4820-4822	Natural Fracture Dips 75°N N60E	-------	Hydraulic fracture curves out of well approx. 1 ft above and parallel to natural fracture, returns below.
4822-4831	N65E	.1	Complex, relatively tight and poorly defined.
4831-4846	N65E to E-W	.3 to 1.4	Preexisting vertical fracture widened by propping agent.
4846-4861.5	N80E to E-W	.1 to .7	May follow indistinct preexisting fracture, wider to west.
4861.5-4873.9	N70 to 80E	.1 to .7	Preexisting en echelon vertical fractures widened. Continues to level of sand fill-up in bottom of well.

Table 2

Raft River Well 4
Hydraulic Fracture

DEPTH (feet)	STRIKE (Mag. N) (uncorrected for hole deviation)	APPARENT MAXIMUM WIDTH (inches)	CHARACTER OF THE VERTICAL HYDRAULIC FRACTURE
4566	N13E	1.4	Not through center of hole.
4571.5	N45E	.7	Change in strike between natural fractures.
4575-4578	unknown	.6	Fracture splits - en echelon.
4582	N13E	1.4	Not through center of hole.
4586-4589	N42E to E-W	1.4 to 2.1	Fracture curves, well defined and apparently wider.
4592	N58E	.3	Well defined but narrow.
4593.5-4600	----------	---------	Poorly defined, irregular and branching.
4606	N15E	.6 to 1.4	Apparently wider to south.
4615.5	N7E	---------	Poorly defined and irregular.
4623	N-S	.3+	Apparently wider and more irregular to south.
4626-4632	----------	---------	Complex and splits.
4633-4645	N5W to N10E	---------	Considerably off-center, giving false impression of widening, strike changes.
4652.6	----------	---------	Apparent change in fracture character and direction due to change in hole diameter and lithology.
4655	N25E	.3	More broken out to southwest, nearly centered, well defined, irregular.
4662-4665	N67E to N50E	.3 to .7	Nearly centered, very well defined, curved.
4666.5-4669	----------	---------	Branching, poorly defined due to natural fracture
4669-4684.5	N50E to N10E	.1 to .3	Well defined, irregular, broken out.
4684.5-4687	N-S	---------	Indistinct, curves to parallel natural fracture set.
4694-4705 ?	N35E ?	---------	Very poorly defined, tight, curving due to natural fracture.

SESSION FOUR

THERMAL STABILITY OF FRAC FLUIDS IN AQUEOUS SYSTEMS
Donald Tyssee
VETTER RESEARCH

MASSIVE HYDRAULIC FRACTURING
Ralph Veatch
AMOCO

EXPLOSIVE STIMULATION OF A GEOTHERMAL WELL AT THE GEYSERS
Robert Hanold
LOS ALAMOS SCIENTIFIC LABORATORY

THERMAL STABILITY OF FRAC FLUIDS IN AQUEOUS SYSTEMS

BY

D. A. TYSSEE AND O. J. VETTER
VETTER RESEARCH

1. INTRODUCTION

Many factors have to be taken into consideration in designing a stimulation involving the use of frac polymers - particularly when the high temperature of a geothermal reservoir are taken into consideration. While productivity enhancement is the desired end result, other factors such as economics, material availability, potential formation damage, etc. have an influence on the decision regarding the type of frac polymer to be used. The majority of the papers given during the symposium have been concerned with the physical and engineering aspects of fracture stimulation. This paper focuses on that property that directly determines the physical behavior of a frac polymer - namely, the inherent chemistry of the polymer.

Two general types of polymer classes are normally encountered in the field. The first class of polymers are known as synthetic polymers (Figure 1). They tend to be made up of very simple molecules (acrylamides, polacrylates, etc.) and give relatively short-chained molecules with molecular weights on the order of 100,000 or so. These synthetic polymers (man-made polymers) generally are structurally much less complex than the biopolymers. A typical example of these polymers is shown in Figure 2. This biopolymer (Xanthan gum) is typical of biopolymers used in the field. Xanthan gum, with its sugar back bone, has a molecular weight of several million.

Much of the preliminary laboratory work has been done on xanthan gum which was one of the frac polymers used in the Raft River field experiments. Because of the general similarity in structure among the biopolymers, the chemical technology developed for xanthan gum should also be applicable to other frac polymers.

When dealing with a fracture, one is really dealing with a closed system under dynamic conditions. That is, the frac polymer introduced is eventually produced back and all of the chemistry that has taken place in the reservoir should be observable. Thus, if one has complete control of the materials, the total amount of organic materials that

goes in - either in the laboratory under simulated conditions or in the field under actual conditions - should be accounted for when the return fluids are analyzed. The carbohydrate concentration is an indication of the total amount of carbohydrate present in the solution. As mentioned above, the biopolymers are derived from carbohydrates (i.e., sugars). Simple breaking of the chain still leaves carbohydrate molecules. In the case of gross degradation (for example, pyrolysis), the carbohydrate content is lost. Thus, the carbohydrate concentration in the fluid is at least an indication of the integrity of the polymer. Finally, in the laboratory some preliminary work has been done using high pressure liquid chromatography (HPLC) as a means of attempting to unravel the details of polymer degradation.

The final section of the paper describes the results of return fluid analyses from the Raft River field experimients. Special emphasis is placed on what information can be obtained by chemically analyzing the fluids.

2. LABORATORY STUDIES

Several areas have been investigated in order to identify techniques that could be usefully applied to the analysis of frac polymer solutions. Because the polymers tend to be used at high dilution in brine solutions, efforts have been directed to techniques that are applicable to these kinds of solutions. Of the numerous methods considered, three were selected for intensive study. These three methods were directed towards characterization of the solutions by:

1 Total organic carbon content (TOC)

2 Total carbohydrate content

3 High pressure liquid chromatography

The rationale for selecting these methods have been briefly referred to earlier.

One of the biggest problems encountered in unraveling the chemistry of these complex molecules is general analytical methodology. In other words, how does one quantitatively and qualitatively characterize complex organic compounds in an aqueous solution at a very high dilution? Typically, the polymers go in at a half a percent or less in concentration and they are produced back at concentrations on the order of 0.025%. Additional problems are introduced by the high TDS content of the geothermal fluid.

A great deal of preliminary information can be obtained by measuring the injected and produced fluid for simply the total organic carbon (TOC) content of the fluid. In this way, a good indication of material balance (i.e., organic material injected and produced) can be obtained. This measurement can be done on a routine basis using present day analytical instrumentation. This TOC value, while monitoring material balance, provides little useful information as to the fate of the polymer. For example, if the polymer degrades to water soluble non-polymeric products, the TOC value remains unchanged. These changes, however, can be detected by monitoring the fluid for total carbohydrates - a value that is a direct measure of the amount of polymer dissolved in solution. Information provided by this analytical procedure is illustrated in Figure 3 where the carbohydrate concentration of a xanthan gum solution containing various calcium ion concentrations is shown as a function of time when being heated at 150 degrees C. Note the stabilizing effect of the calcium at concentrations up to and including 800 ppm Ca. Above this concentration, calcium accelerates the degradation of the polymer.

The degradation of the polymer is accompanied by a drop in the TOC content of the solution and, after an extended period, by the formation of particulate matter suspended in the aqueous phase. A typical micrograph of these particles is shown in Figure 4. Whether or not this particle matter has an adverse effect on the productivity after the stimulation must be determined by laboratory flow tests and actual field data.

As discussed above, the TOC content and total carbohydrate content of the fluids are an indication of gross chemical properties of the polymer under reaction conditions. While this information is of value, it is desirable to develop methods that allow more detailed information to be obtained. One of the most promising methods is that of high pressure liquid chromatography (HPLC). This technique can be used to identify relatively complex organic structures in a dilute aqueous solution. For example, Figure 5 shows the HPLC of xanthan gum heated for various periods of time in deionized water. The response along the ordinate is an indication of the amount of material eluting at a given retention time. In general, under the conditions of this analysis, the retention time can be related to the molecular weight of the component being eluted.

As a rule of thumb, lower molecular weight fragments elute at longer retention times. This is shown in Figure 5 where the formation of lower molecular weight fragments is indicated by the increasing amounts of materials eluting at longer retention times. Presently, work is being directed towards chemically characterizing these fragments in order to elucidate the pathway by which the polymer degrades.

3. FIELD STUDIES

Heavy emphasis has been placed in the laboratory on developing a body of knowledge and techniques that will ultimately be transferred to the field. Although as discussed earlier, the laboratory results are somewhat preliminary, sufficient work has been done to indicate that valuable field information can be obtained. The field experiment at Raft River 4 is a case in point. The chemical work done on the fluids from this field experiment was concentrated in two areas:

1 Material balance as determined by TOC.

2 Polymer degradation as determined by comparing the TOC to the total carbohydrate.

The chemical data from the fluids produced during the Raft River 4 field experiment are shown in Figure 6. The injection was completed on August 20, 1979 and immediately produced during the period August 20-21. Note the high ratio of total carbohydrate to organic carbon during this first flow period. This is indicative of little thermal degradation. The well was next produced on August 25, 1979, after having been shut-in for a four-day period. The final flow test took place between September 6 and September 11. During the times between the last two flow periods there has been substantial thermal degradation of the polymer. This is indicated by the decreasing ratio of total carbohydrate to total organic carbon as the well is produced.

The laboratory data can be further used to quantify material returns. According to the field records, 4,032 lbs. of polymer were injected on August 20, 1979. By integrating the data it can be shown that 22% of the injected polymer is produced back during the first flow test with no substantial degradation. By contrast, the fluid produced during the second and third test contains appreciable amounts of degraded polymer as the injected fluid becomes exposed to the higher temperature of the formation for longer periods of time. Of the total frac polymer injected (i.e., 4,032 lbs.) 1,206 lbs. are produced back with little degradation. An additional 613 lbs. of the polymer were converted to soluble organic materials which were produced in the return fluids primarily during the second and third flow test. Approximately 55% or 2,213 lbs. of the frac polymer are not accounted for. At present, the fate of this material is unknown.

4. SUMMARY AND CONCLUSIONS

The work described above is admittedly less than a definitive study of the chemical behavior of frac polymers under both laboratory and field conditions. However, sufficient work has been done to indicate that useful information relevant to field experiments can be obtained. Material balances and thermal degradation of the polymer in the formation are notable examples. While HPLC is a potentially useful technique, the presence of salts in the fluids has caused problems in developing the method to the point where it is directly applicable to field samples. Work to resolve these problems is underway and with continued effort, a method to unravel the complex chemistry of the polymers under actual field conditions will be developed.

GENERALIZED STRUCTURE OF POLYACRYLIC ACID DERIVATIVES

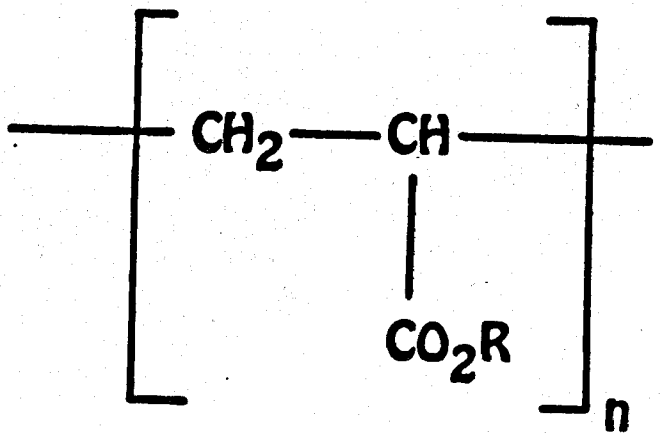

R: H, NH_2, ALKYL

FIGURE 1

CHEMICAL STRUCTURE OF XANTHAN GUM

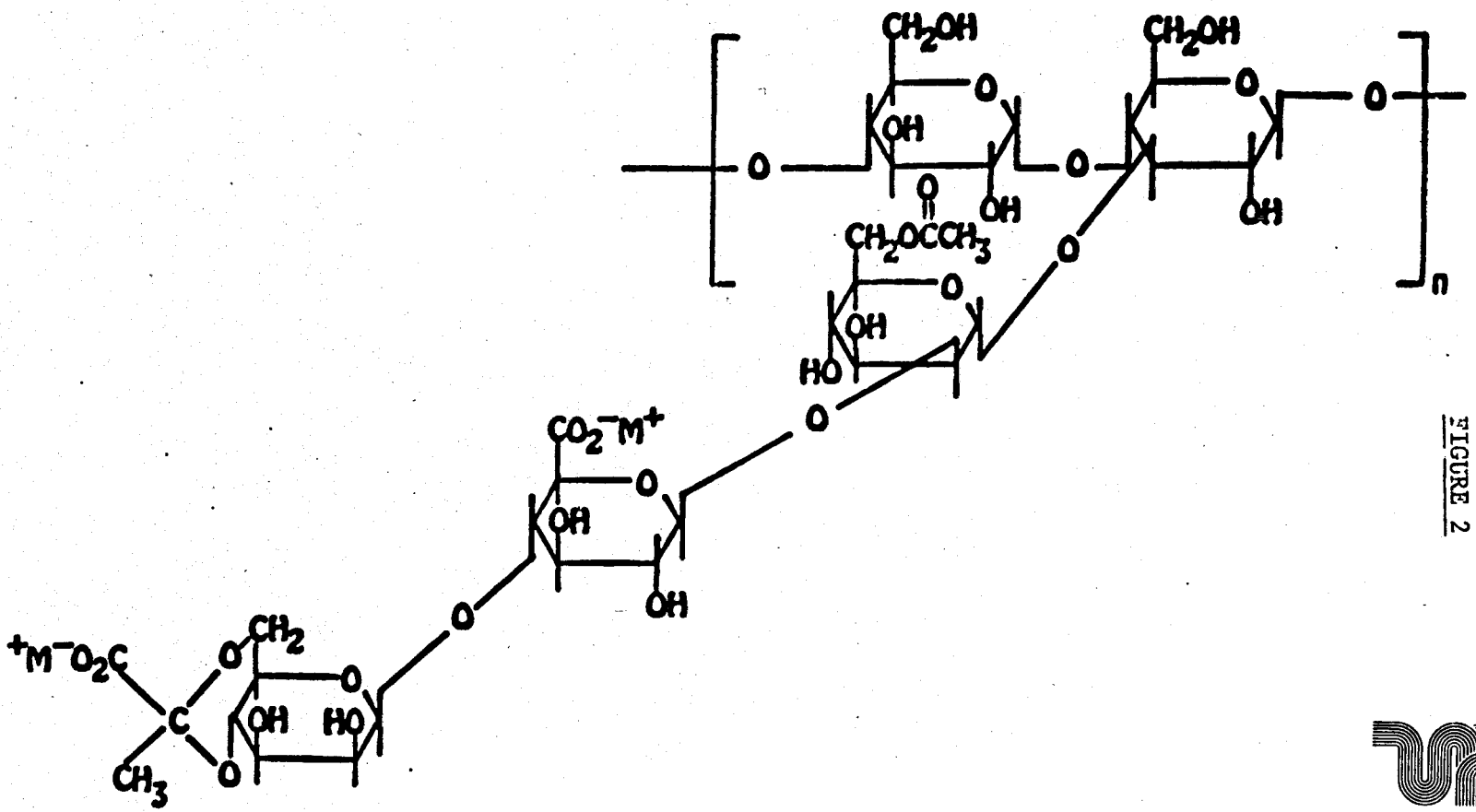

FIGURE 2

THERMAL STABILITY OF XANTHAN GUM AT 150°C IN CALCIUM CHLORIDE

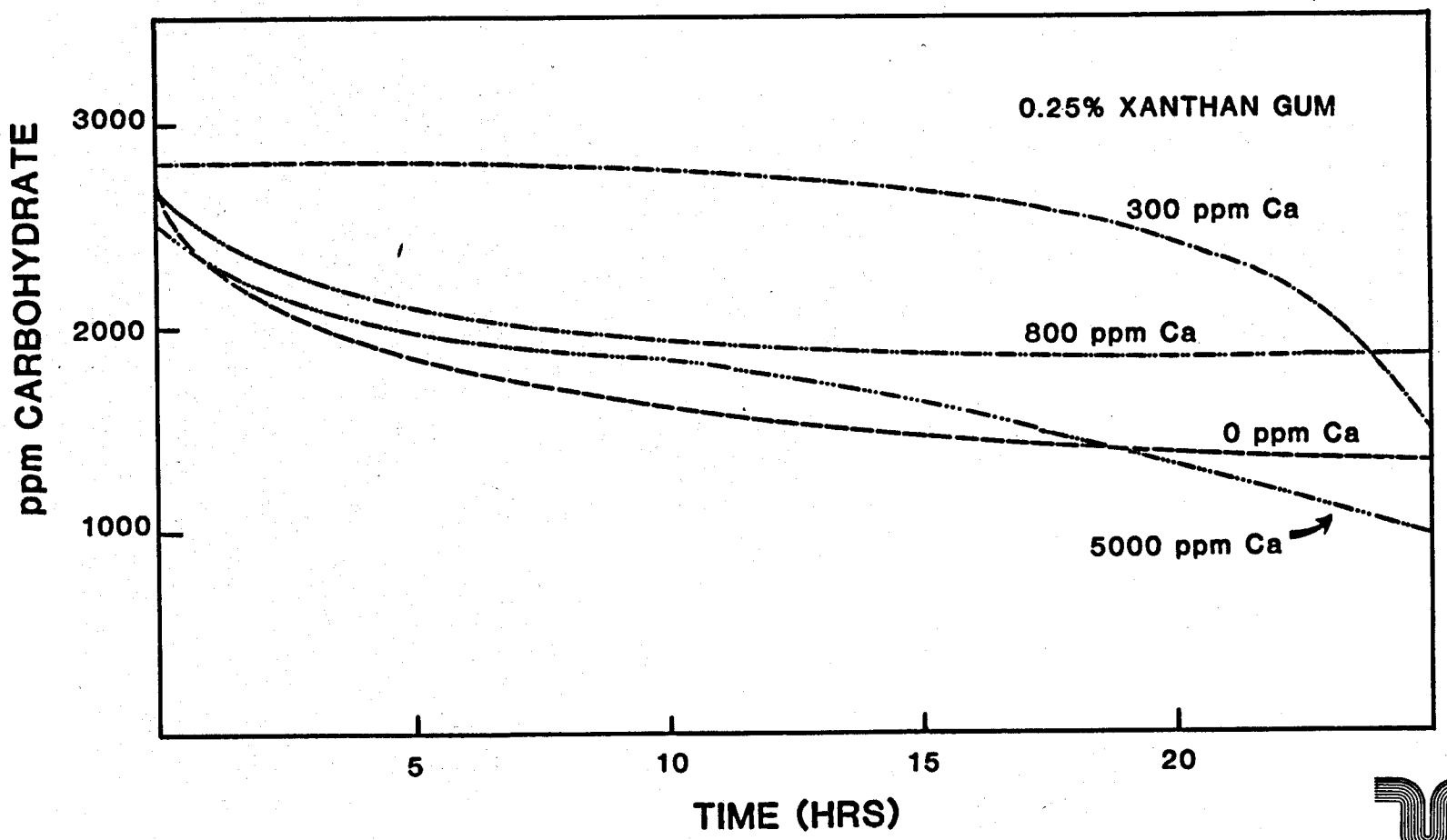

FIGURE 3

FIGURE 4

MICROGRAPH OF PARTICULATE FORMED
UPON THERMAL DEGRADATION OF XANTHAN GUM

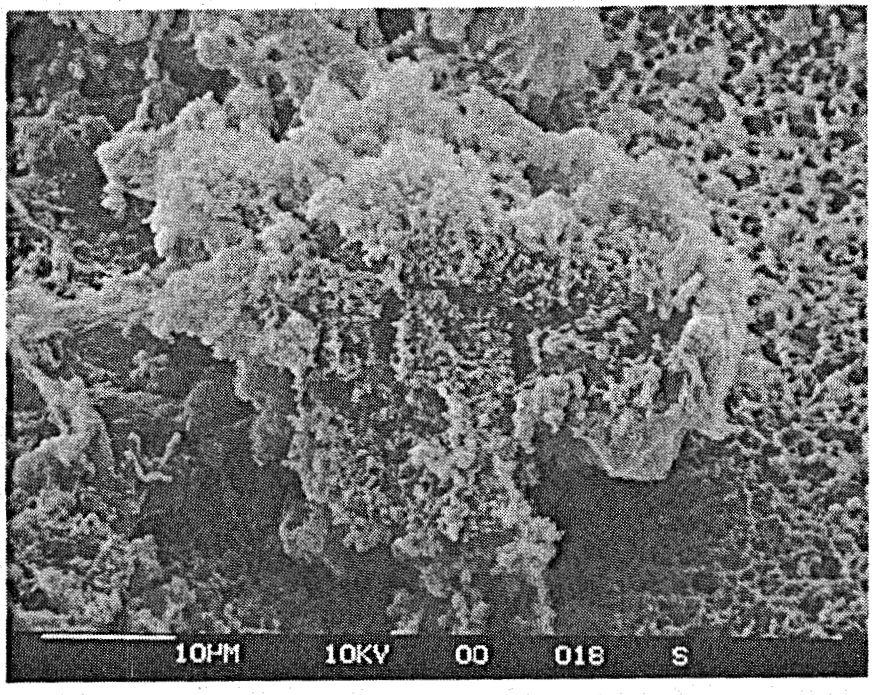

THERMAL DEGRADATION OF XANTHAN GUM AT 150°C IN DEIONIZED WATER

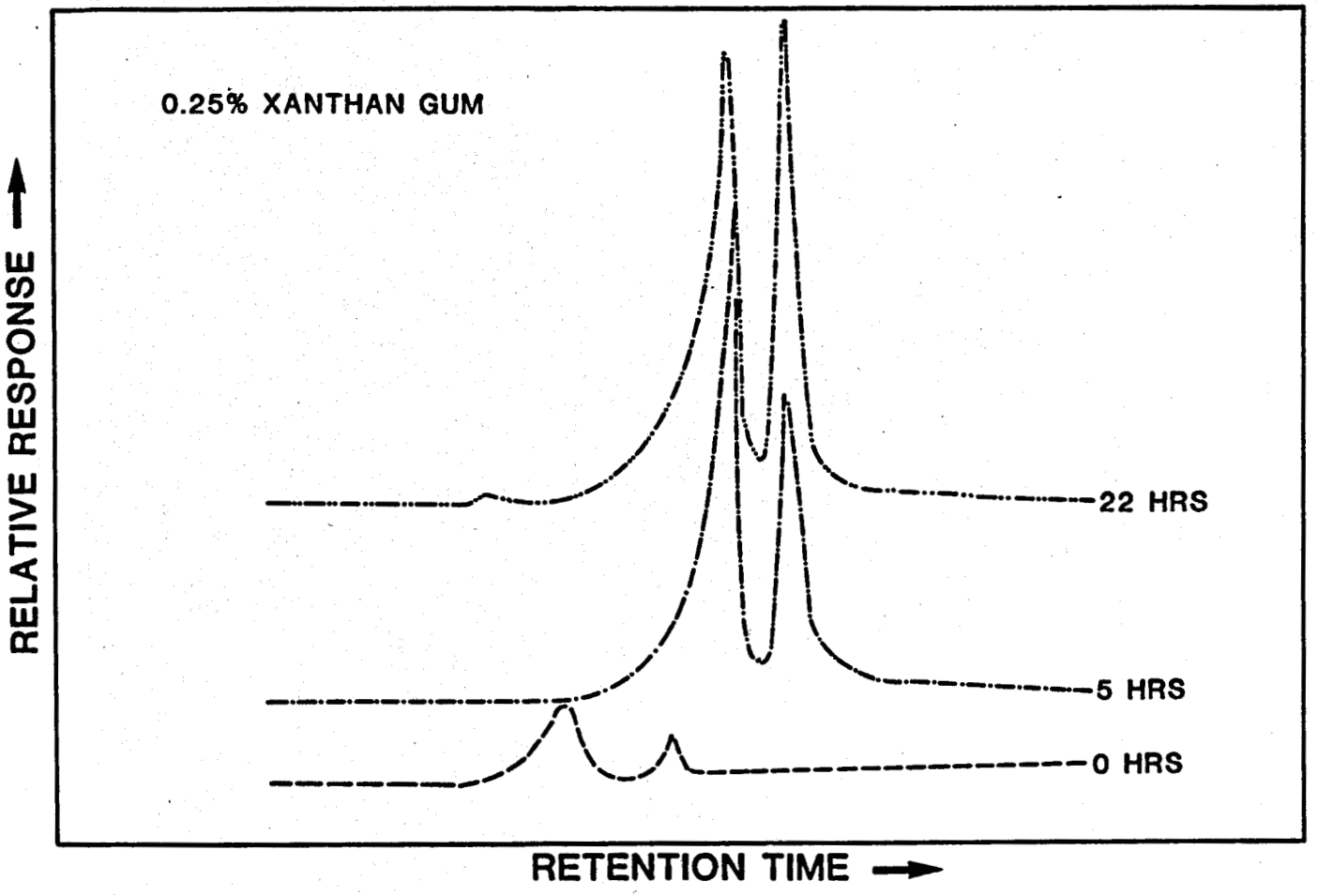

FIGURE 5

TOTAL ORGANIC CARBON AND CARBOHYDRATE CONCENTRATION OF RRGP-4 PRODUCED FLUID

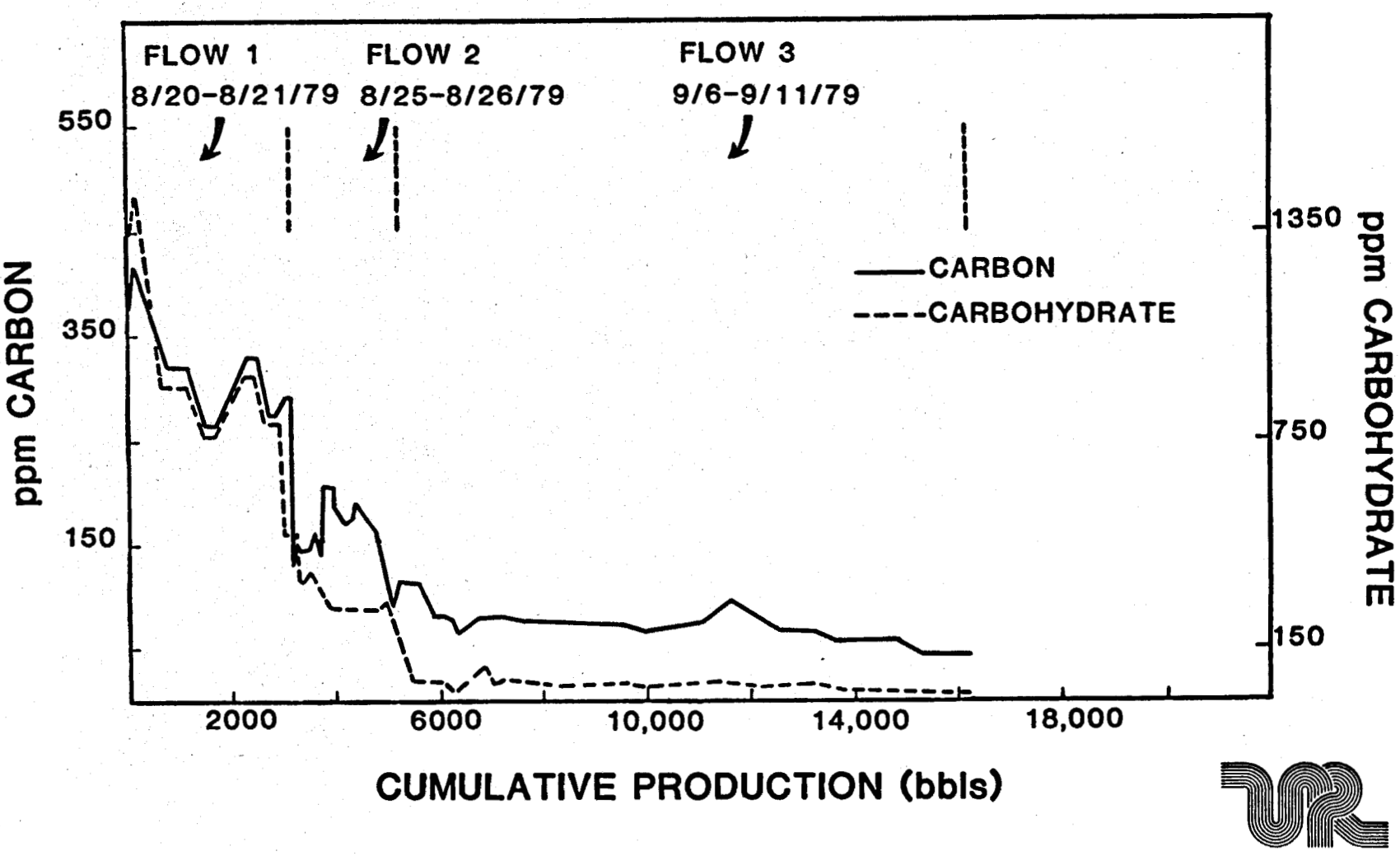

FIGURE 6

MASSIVE HYDRAULIC FRACTURING

Ralph Veatch
AMOCO

Paper not submitted for publication.

Dup

EXPLOSIVE STIMULATION OF A GEOTHERMAL WELL AT THE GEYSERS

R. J. Hanold
Los Alamos Scientific Laboratory
Los Alamos, New Mexico

The well stimulation treatment described in this paper does not come under the domain of Republic Geothermal's Geothermal Well Stimulation Program and is being conducted as a separate entity. Emphasis in the Republic program is on liquid-dominated hydrothermal reservoir stimulation by hydraulic fracturing and/or chemical treatments while this experiment involves the use of an explosive in a vapor-dominated reservoir. This experiment originated as a result of an unsolicited cost-sharing proposal from a number of cooperating industrial organizations. The principal organizations involved are Rocket Research Company, Physics International, Union Oil Company - Geothermal Division, and the Los Alamos Scientific Laboratory. Rocket Research Company, under separate funding, had developed a class of specialized explosives with high-temperature stability characteristics that made them suitable for use in geothermal well conditions. They are providing the explosive for the stimulation treatment along with most of the characterization data on the explosive performance at the anticipated well temperature. Physics International is responsible for designing, testing, and fabricating an explosive detonator system which is hardened to survive the well environment and will provide reliable initiation of the explosive charge. They are also providing assistance in some of the high-temperature explosive characterization tests and will support the field test at the well site. Union Oil Company - Geothermal Division will provide one of their wells at the Geysers and will be responsible for the well-site services associated with preparing the well and conducting the stimulation treatment. The Los Alamos Scientific Laboratory, acting in the capacity of a technical advisor to the Department of Energy (DOE), is funding the subcontracts with Rocket Research Company and Physics International with DOE pass-through

funds provided specifically for this purpose. This experiment is scheduled to take place during the last quarter of 1980.

The relatively inaccessible rolling countryside at the Geysers introduces some special considerations into the selection and preparation of well drilling sites. The preparation of drilling pads is expensive and it has become typical for Union to prepare a pad and then to drill anywhere from 2 to 4 directional wells from that basic developed area. This technique reduces some of the associated preparation costs and also reduces the environmental damage on the surface. With multiple wells drilled from a common site, a situation analagous to that depicted in Fig. 1 can arise.

With reference to Fig. 1, the solid circles denote the surface location of the wells while the heavy bars represent the location of the bottom of the wells. Drilling in the brittle and fractured formations of the Geysers is very difficult and directional control of the wells cannot always be maintained. Of the seven wells depicted, note that five of the wells have unstimulated steam production rates in excess of 200,000 lb/hr with well 2 exceeding 300,000 lb/hr. The only obviously poor well of the group is well 5 with a steam production rate of 65,000 lb/hr. Well 5, drilled as part of a cluster with wells 3 and 4, stands out as an anomoly in this productive portion of the Geysers field. Its proximity to wells 3 and 4 is the interesting feature because 3 and 4 both have very high productivity with 4 being one of the most productive in this section of the field. With the production from well 5 being only approximately 25% of that obtained from the two adjacent wells, it represents an excellent stimulation candidate based on the criteria of established reservoir deliverability from offset well data.

A possible scenario for explaining the low productivity of well 5 is related to the directionality of the well in relation to the major fracture systems in the area. Knowledge of the field indicates that it can be characterized as consisting of a number of large major fracture systems which are interspersed among a large number of smaller or secondary fracture systems. With reference to Fig. 2, the solid wellbore curving to the left could represent well 5. The well has missed the major fractures but has intersected a number of the smaller fractures resulting in limited steam

production. This is consistent with the logs for well 5 which indicate steam inflows from the 3,000 ft. horizon clear on down to the 8,000 ft. horizon. The cumulative effect of these steam inflows is not enough, however, to bring the well up to the level of a good commercial producer. If well 5 had kicked-off in the other direction, as depicted by the dashed wellbore in Fig. 2, it might have traversed some of the major fractures and become as productive as the surrounding wells shown in Fig. 1. The task at hand is obviously to find a technique for establishing communication between well 5 and the major fractures which are presumed to exist close-by.

The steam-dominated reservoir at the Geysers has a number of features which make it particularly adaptable for an explosive stimulation treatment. These advantages, listed in Table I, are typically not present in liquid-dominated geothermal reservoirs. Basically we have a field site which is very close to the location of major quaternary and tertiary volcanism. The Franciscan graywacke characteristic of the production horizons is a hard and brittle rock with favorable properties for explosive fracturing. Based on available geophysical information and the drilling and production history of the field, the proximity of a complex natural fracture system is well established. Perhaps the most convincing piece of data in this regard is the fact that 9 out of 10 wells drilled in this location are good commercial producers without the need for any form of stimulation. This data provides the basis for the assumption that this area of the field contains numerous closely spaced productive fracture systems. From an explosive fracturing standpoint the presence of the steam-filled fractures (void volume) in the reservoir is exceedingly important. The effectiveness of explosives in breaking rock in the vicinity of free surfaces has been well documented for a long time. The nearby fractures provide the desirable free surfaces for the explosive stress waves to act against while the associated void volume provides the physical space for relocation of the broken rock masses. This situation should minimize the tendency of the explosive driven stress waves to damage the near-wellbore region through plastic deformation and crushing while maximizing the probability for producing interconnecting fracture paths between the wellbore and the natural fracture systems. The fact that wells at the Geysers have a thick producing interval permits the use of a

stimulation treatment over a substantial length of the wellbore. By extending the treatment length, the probability that a nearby major fracture system can be intersected is considerably enhanced.

For all of the above reasons, the Geysers presents itself as a unique opportunity for a field test using an explosive stimulation treatment. This situation is further enhanced by the fact that wells at the Geysers are not readily amenable to stimulation by other more typical methods. Hydraulic fracturing in the conventional sense is essentially impossible because even the relatively small fractures that allow some steam inflows into the well will allow large amounts of water to percolate away making it very difficult to pressurize the wellbore over a significant length to the formation break-down pressure. Problems associated with setting packers in the high-temperature open-hole formations are also significant.

Under a previous contract from the Department of Energy, Rocket Research Company was investigating the development of explosive formulations which have some very unusual properties including excellent high-temperature stability. This research was directed toward the use of these explosives in geothermal well stimulation treatments but the contract did not contain any provisions for a field test treatment using the new explosives. The present cost-shared joint venture came into existence with the purpose of selecting the most appropriate explosive formulation for a well test at the Geysers, conducting the necessary explosive safety and performance verification tests, and finally designing and fielding a full-scale explosive stimulation treatment in a well specifically selected for this purpose.

The explosive developed and characterized by Rocket Research Company is called HITEX II and some of its noteworthy properties are listed in Table II. The first property, and perhaps the most unusual, is the fact that this explosive is nondetonable as a solid material. I am not aware of any other explosive which has this property. The explosive is fabricated by melting the ingredients in a mold and then cooling it to room temperature. At room temperature HITEX II exists as a solid homogeneous material which, when boosted by any conventional form of explosive booster, will not detonate. This feature lends a certain credibility and safety to the use of HITEX II on a rig floor that has not previously existed in the use of other

conventional explosives. The rules to be complied with in the transportation and storage of the material are also greatly simplified. HITEX II is completely melted at 375°F which is sufficiently below the 500°F temperature of the wells at the Geysers to insure that the explosive will be melted and activated for the treatment after exposure to formation temperature for a number of hours. This means that HITEX II melts and becomes a detonable explosive during its emplacement in the well but you are not handling a detonable explosive on the surface. The explosive will eventually deactivate with time at temperature but its performance has been tested and verified after a 24 hour exposure to conditions analogous to those in a well at the Geysers. Based on these test results we confidently feel that it can withstand 24 hours at 500°F and the experimental plan calls for it being in the well considerably less time than that before it is detonated. If for some reason the HITEX II cannot be detonated and is left in the wellbore, it will deactivate itself with time through the loss of some of the more volatile ingredients. HITEX II is also water soluble and because its components are nitrates they are essentially very much fertilizer-like and do not pose any severe environmental contamination if they are left in the well to deactivate.

The present experimental plan calls for a stimulation interval of 750 ft using approximately 12,500 lbs. of explosive. The explosive will be contained in aluminum drillpipe made up with teflon coated leak-tight joints. To simplify the loading operation, the HITEX II has been cast into 35 lb grains which slip into the 6 inch I.D. aluminium drillpipe which forms the explosive canister. Each length of aluminum drillpipe is loaded with explosive grains on the surface, made-up with rather conventional couplings to the next length of drillpipe, and the operations repeated until the entire canister is filled with solid HITEX II and inserted into the wellbore. When all the explosive has been loaded, the entire canister is lowered into the wellbore on drillpipe to the stimulation interval depth which will be selected on the basis of available geophysical information from Union Oil. It is important to note that the explosive canister is implaced <u>without</u> the detonator package for safety considerations. After final emplacement of the canister, the Physics International developed detonator package is lowered on a wireline through the drillpipe and into the explosive canister. This

technique minimizes the number of surface operations that have to be performed when there is both a live explosive and a detonator package mated in the wellbore. The detontor package is designed to float on the surface of the liquid explosive to provide positive initiation. After releasing the detonator package, the wireline and drillpipe are removed from the hole and the explosive is detonated by preset clock timers.

This is a very ambitious field experiment using concepts and products that have not previously been tested downhole. The potential payoff, however, for developing an explosive stimulation technique applicable to wells at the Geysers could become very significant. Additional technical details on this treatment will be available after the field test is completed.

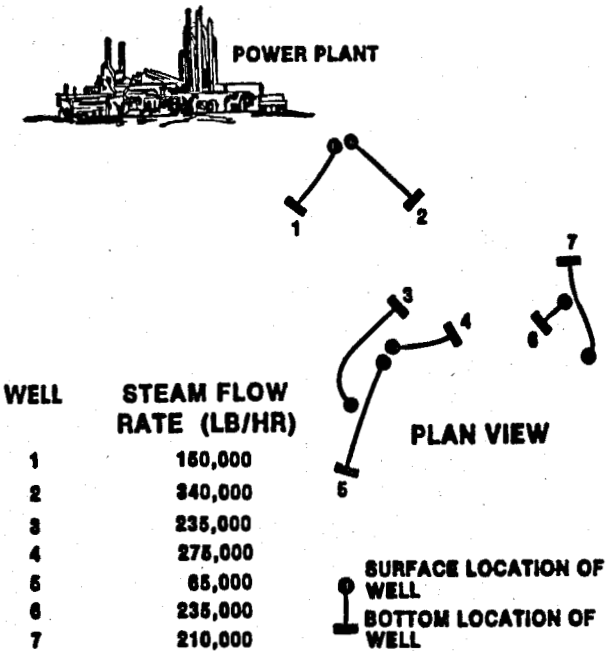

WELL	STEAM FLOW RATE (LB/HR)
1	150,000
2	340,000
3	235,000
4	275,000
5	65,000
6	235,000
7	210,000

Fig. 1. Plan view of a section of the Geysers field. Note the location and productivity of wells 3, 4 and 5.

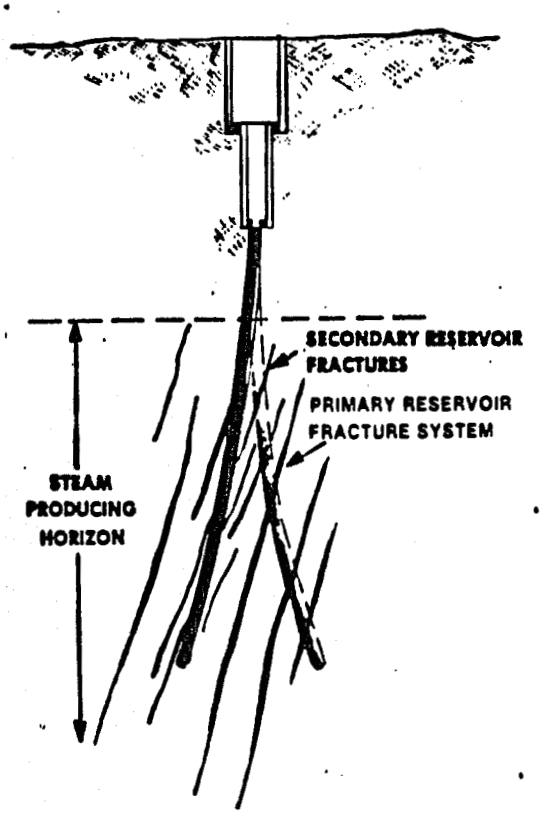

Fig. 2. Possible scenario for well 5 locations in relation to primary and secondary fracture systems.

Table I.

THE GEYSERS

ADVANTAGES FOR A HIGH-TEMPERATURE EXPLOSIVE STIMULATION TREATMENT:

- HARD-BRITTLE ROCK
- PROXIMITY OF NATURAL FRACTURES
- PRESENCE OF VOID VOLUME
- THICK PRODUCING INTERVAL
- NO OTHER AVAILABLE STIMULATION TECHNIQUE

Table II.

HITEX II GEOTHERMAL EXPLOSIVE

- NONDETONABLE AS A SOLID
- MELTS AT 190°C (375°F)
- DEACTIVATES WITH TIME AT TEMPERATURE
- WATER SOLUBLE

SYMPOSIUM PARTICIPANTS

Anthony J. Adduci
United States Department of Energy
Oakland, California

James Albright
Los Alamos Scientific Laboratory
Los Alamos, New Mexico

William C. Allen
Union Oil Company
Brea, California

David N. Anderson
Geothermal Resources Council
Davis, California

Donald Campbell
Republic Geothermal, Inc.
Santa Fe Springs, California

Henry Crichlow
Petroleum Training and Technical Services
Norman, Oklahoma

Ali Daneshy
Halliburton Services
Duncan, Oklahoma

Keith R. Davis
MAPCO Geothermal, Inc.
Tulsa, Oklahoma

Otis L. Day
Global Geothermal Technologies
Santa Rosa, California

M. R. Dolenc
EG&G Idaho, Inc.
Idaho Falls, Idaho

Robert A. Emslie
AMINOIL, USA
Santa Rosa, California

David R. Fielder
LFE Environmental Analysis Labs
Richmond, California

R. T. Forest
Phillips Petroleum Company
Reno, Nevada

B. A. Gillette
Republic Geothermal, Inc.
Santa Fe Springs, California

Ted Glenn
ESL/UURI
Salt Lake City, Utah

Colin Goranson
Lawrence Berkeley Laboratory
Berkeley, California

D. D. Grimlie
MAPCO Geothermal, Inc.
Tulsa, Oklahoma

Robert Hanold
Los Alamos Scientific Laboratory
Los Alamos, New Mexico

Lee Hendershot
Republic Geothermal, Inc.
Santa Fe Springs, California

Al Idrisi
Petroleum Training and Technical Services
Norman, Oklahoma

John V. Janes III
Tretolite
St. Louis, Missouri

Alfred R. Jennings, Jr.
Halliburton Services
Duncan, Oklahoma

Arfon H. Jones
Terra Tek, Inc.
Salt Lake City, Utah

Viv Kandarpa
Vetter Research
Costa Mesa, California

Gerald Katz
United States Department of Energy
Oakland, California

Kenneth Kazmerski
Geothermal Power Corporation
Navato, California

Scott Keys
United States Geological Survey
Denver, Colorado

Roland F. Krueger
Union Oil Company
Brea, California

J. T. Kuwada
GKI
Phoenix, Arizona

Terry Matsumoto
Republic Geothermal, Inc.
Santa Fe Springs, California

Cliff McFarland
United States Department of Energy
Washington, D. C.

William H. McMullen
United States Department of Energy
Albuquerque, New Mexico

Frank G. Metcalfe
Geothermal Power Corporation
Novato, California

Charles Morris
Republic Geothermal, Inc.
Santa Fe Springs, California

Robert Nicholson
Terra Services
Costa Mesa, California

David A. Northrop
Sandia Laboratories
Albuquerque, New Mexico

The Honourable Graeme R. Pirie
New Zealand Consulate General
San Francisco, California

Susan M. Prestwich
United States Department of Energy
Idaho Falls, Idaho

Stephen Pye
Union Oil Company
Santa Rosa, California

Ronda Pyle
Petroleum Training and Technical Services
Norman, Oklahoma

Christopher Rickey
Petroleum Training and Technical Services
Norman, Oklahoma

Stan Shyrock
Halliburton Services
Norwalk, California

Richard Sinclair
Maurer Engineering, Inc.
Houston, Texas

Dan M. Slagel
MAPCO Geothermal, Inc.
Tulsa, Oklahoma

Morton C. Smith
Los Alamos Scientific Laboratory
Los Alamos, New Mexico

Edwin J. Stahl, Jr.
Halliburton Services
Duncan, Oklahoma

Thomas Strickland
Republic Geothermal, Inc.
Santa Fe Springs, California

Kenneth A. Strom
LFE Environmental Analysis Labs
Richmond, California

Donald Tyssee
Vetter Research
Costa Mesa, California

Donna Vanderburg
Petroleum Training and Technical Services
Norman, Oklahoma

Ralph Veatch
AMOCO
Tulsa, Oklahoma

Anthony F. Veneruso
Sandia Laboratories
Albuquerque, New Mexico

Robert Verity
Republic Geothermal, Inc.
Santa Fe Springs, California

Ottomar Vetter
Vetter Research
Costa Mesa, California

A. B. Waters
Halliburton Services
Duncan, Oklahoma

Kenneth Wolgomuth
Terra Tek, Inc.
Salt Lake City, Utah